

Struktur und molekulare Interaktionsanalyse von monoklonalen
Antikörpern in Komplex mit Rezeptor-Tyrosinkinasen

Dissertation
zur Erlangung des Doktorgrades
der Naturwissenschaften

vorgelegt beim Fachbereich 14
Biochemie, Chemie und Pharmazie
der Johann Wolfgang Goethe-Universität
in Frankfurt am Main

von
Judith Schmiedel
aus Berlin

Frankfurt 2009
D30

vom Fachbereich 14 „Biochemie, Chemie und Pharmazie“ der Johann Wolfgang Goethe-Universität Frankfurt am Main als Dissertation angenommen.

Dekan: Prof. Dr. Dieter Steinhilber

1. Gutachter: Prof. Dr. Volker Dötsch

2. Gutachter: Prof. Dr. Martin Pos

Datum der Disputation:

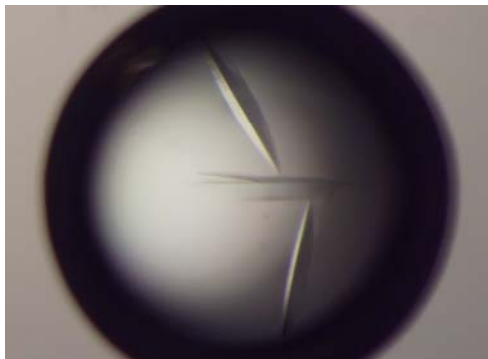


Table of contents

| | | |
|--------|--|----|
| 1. | ZUSAMMENFASSUNG..... | 5 |
| 2. | AIM OF THE THESIS..... | 11 |
| 3. | RECEPTOR TYROSINE KINASES..... | 13 |
| 3.1. | Introduction..... | 13 |
| 3.2. | Structures of RTKs..... | 14 |
| 3.3. | RTK activation..... | 16 |
| 3.4. | Signaling mechanisms downstream of activated RTKs..... | 17 |
| 3.5. | RTKs and cancer..... | 19 |
| 4. | MATERIALS & METHODS..... | 21 |
| 4.1. | Molecular Biology..... | 21 |
| 4.1.1. | EGFR..... | 21 |
| 4.1.2. | sEGFRvIII..... | 22 |
| 4.1.3. | sIGF-1R..... | 23 |
| 4.1.4. | Generation of recombinant baculovirus..... | 23 |
| 4.2. | Protein expression..... | 23 |
| 4.2.1. | sEGFR and sEGFRvIII..... | 23 |
| 4.2.2. | sIGF-1R..... | 24 |
| 4.3. | Protein purification..... | 25 |
| 4.3.1. | sEGFR..... | 25 |
| 4.3.2. | sEGFRvIII, sIGF-1R domain I-III and domain II..... | 25 |
| 4.3.3. | Fab fragments..... | 25 |
| 4.3.4. | Receptor:Fab complexes..... | 26 |
| 4.4. | Molecular interactions and biophysics..... | 27 |
| 4.4.1. | Dynamic light scattering..... | 27 |
| 4.4.2. | Static light scattering..... | 27 |
| 4.4.3. | Surface plasmon resonance..... | 27 |
| 4.4.4. | Analytical ultracentrifugation..... | 29 |
| 4.4.5. | Isothermal titration calorimetry..... | 29 |
| 4.4.6. | Small angle X-ray scattering..... | 30 |
| 4.5. | Protein Crystallography..... | 32 |
| 4.5.1. | sEGFR:Fab72000..... | 32 |
| 4.5.2. | Fab72000..... | 32 |
| 4.5.3. | sEGFRd3:Fab72000..... | 33 |
| 4.5.4. | sEGFRvIII..... | 35 |
| 4.5.5. | Fab1159476..... | 36 |
| 5. | Matuzumab binding to EGFR prevents the conformational rearrangement required for dimerization..... | 37 |
| 5.1. | Introduction..... | 37 |
| 5.1.1. | Ligand-induced EGFR activation..... | 39 |
| 5.1.2. | Structures of ErbB receptor family extracellular domains..... | 40 |
| 5.1.3. | ErbB receptor dimerization at the cell surface..... | 41 |
| 5.1.4. | EGFR and cancer..... | 42 |
| 5.1.5. | Anti-EGFR antibodies..... | 43 |
| 5.2. | Results..... | 46 |
| 5.2.1. | Matuzumab binding to sEGFR..... | 46 |
| 5.2.2. | Ligand competition analysis of matuzumab..... | 47 |
| 5.2.3. | Matuzumab binding prevents receptor dimerization..... | 48 |
| 5.2.4. | The matuzumab epitope..... | 49 |

| | | |
|--------|--|-----|
| 5.2.5. | The matuzumab epitope is distinct from the ligand binding site on domain III of sEGFR..... | 52 |
| 5.3. | Discussion | 54 |
| 5.3.1. | Matuzumab binding characteristics to soluble and cell surface EGFR..... | 54 |
| 5.3.2. | The matuzumab epitope on sEGFR domain III | 55 |
| 5.3.3. | Matuzumab and ligand epitopes do not overlap on sEGFR domain III..... | 56 |
| 5.3.4. | The matuzumab inhibition mechanism | 57 |
| 5.3.5. | Matuzumab binding properties interpreted with structural information | 59 |
| 5.3.6. | Implications for the therapeutic application of matuzumab..... | 60 |
| 5.4. | Conclusion..... | 63 |
| 6. | Antibody binding and dimerization properties of the mutant EGFR variant III ectodomain | 65 |
| 6.1. | Introduction | 65 |
| 6.1.1. | EGFRvIII in-frame deletion | 65 |
| 6.1.2. | EGFRvIII signaling activity | 67 |
| 6.1.3. | EGFRvIII down-regulation | 67 |
| 6.1.4. | Therapeutic strategies against EGFRvIII | 68 |
| 6.2. | Results | 70 |
| 6.2.1. | Expression and purification sEGFRvIII..... | 70 |
| 6.2.2. | sEGFRvIII dimerization properties..... | 71 |
| 6.2.3. | Antibody and ligand binding properties of sEGFRvIII..... | 73 |
| 6.2.4. | The sEGFRvIII structure..... | 74 |
| 6.2.5. | The sEGFRvIII solution structure..... | 76 |
| 6.3. | Discussion | 78 |
| 6.3.1. | Antibody and ligand binding characteristics to soluble EGFRvIII..... | 78 |
| 6.3.2. | The structure of EGFRvIII domain III and IV is unaffected by the mutation .. | 79 |
| 6.3.3. | sEGFRvIII in solution | 80 |
| 6.3.4. | sEGFRvIII dimerization and activation | 80 |
| 6.3.5. | Implications for a therapeutic approach against EGFRvIII driven cancers | 81 |
| 6.4. | Conclusion..... | 83 |
| 7. | Characterization of the antibody EMD1159476 binding to the insulin-like growth factor-1 receptor (IGF-1R)..... | 85 |
| 7.1. | Introduction | 85 |
| 7.1.1. | Structures of IGF-1R and IR extracellular domains..... | 87 |
| 7.1.2. | Ligand-induced IR/IGF-1R activation | 89 |
| 7.1.3. | IGF-1R and cancer | 90 |
| 7.1.4. | Anti-IGF-1R antibodies..... | 92 |
| 7.2. | Results | 94 |
| 7.2.1. | Expression and purification sIGF-1R..... | 94 |
| 7.2.2. | Fab1159476 structure..... | 95 |
| 7.2.3. | Antibody binding to sIGF-1R domain I-III and domain II | 97 |
| 7.3. | Discussion | 101 |
| 8. | OUTLOOK..... | 105 |
| 9. | REFERENCES..... | 107 |
| 10. | GLOSSARY | 123 |
| 11. | APPENDIX | 125 |
| 11.1. | Primer sequences..... | 125 |
| 11.2. | Protein constructs | 126 |
| 11.3. | Supplementary data..... | 130 |

List of figures

| | |
|--|-----|
| Fig. 1: Human receptor tyrosine kinases | 14 |
| Fig. 2: Simplified RTK intracellular signaling pathway overview | 18 |
| Fig. 3: Cloning scheme of <i>sEGFRvIII</i> | 22 |
| Fig. 4: Crystals of the complex sEGFRd3:Fab72000 | 33 |
| Fig. 5: Domain organization of ErbB receptors | 38 |
| Fig. 6: Ligand induced EGF receptor dimerization..... | 39 |
| Fig. 7: ErbB family extracellular domain structures without ligand..... | 41 |
| Fig. 8: Antibody receptor co-structures..... | 45 |
| Fig. 9: Characterization of matuzumab binding to sEGFR..... | 46 |
| Fig. 10: ITC sEGFR and Fab72000 | 47 |
| Fig. 11: Ligand competition properties of matuzumab | 48 |
| Fig. 12: Does the sEGFR:Fab72000 complex dimerize? Analysis by AUC | 49 |
| Fig. 13: Structure of the complex between the matuzumab Fab fragment and domain III of sEGFR | 50 |
| Fig. 14: The epitope of matuzumab in detail | 50 |
| Fig. 15: Electron density at the sEGFRd3:Fab72000 interface..... | 51 |
| Fig. 16: The matuzumab epitope is distinct from the ligand binding site on domain III of sEGFR | 52 |
| Fig. 17: Effects of sEGFR mutant binding to matuzumab or EGF | 53 |
| Fig. 18: Implications for the mechanism of inhibition of EGFR by matuzumab..... | 58 |
| Fig. 19: The matuzumab and cetuximab epitopes do not overlap..... | 61 |
| Fig. 20: Matuzumab and cetuximab use different mechanisms to block ligand induced EGFR dimerization..... | 63 |
| Fig. 21: Domain organization of EGFR and EGFRvIII in comparison | 66 |
| Fig. 22: SDS-PAGE sEGFRvIII purification..... | 70 |
| Fig. 23: sEGFR and sEGFRvIII dimerization properties analysed by static light scattering... | 72 |
| Fig. 24: Characterization of cetuximab and matuzumab binding to sEGFRvIII | 73 |
| Fig. 25: Characterization of EGF binding to sEGFRvIII | 74 |
| Fig. 26: Structure of sEGFRvIII..... | 75 |
| Fig. 27: Electron density of sEGFRvIII domain III | 75 |
| Fig. 28: Experimental and calculated SAXS scattering curves sEGFRvIII..... | 76 |
| Fig. 29: Model of the disordered sEGFRvIII regions calculated by BUNCH | 77 |
| Fig. 30: <i>Ab initio</i> solution structure of sEGFRvIII calculated by DAMMIN | 77 |
| Fig. 31: sEGFRvIII and sEGFR wild type in comparison | 79 |
| Fig. 32: Domain organization of IGF-1R..... | 86 |
| Fig. 33: Comparison of the domain I-III structures of IR and IGF-1R..... | 87 |
| Fig. 34: Structure of the insulin receptor ectodomain monomer..... | 88 |
| Fig. 35: Insulin receptor ligand binding model..... | 89 |
| Fig. 36: SDS-PAGE sIGF-1R domain I-III and domain II purification..... | 95 |
| Fig. 37: Fab1159476 structure | 95 |
| Fig. 38: Fab1159476 electron density | 96 |
| Fig. 39: Characterization of EMD1159476 binding to sIGF-1R | 97 |
| Fig. 40: ITC sIGF-1R domain I-III and Fab1159476..... | 98 |
| Fig. 41: ITC sIGF-1R domain II and Fab1159476..... | 99 |
| Fig. 42: Preliminary ligand competition properties of EMD1159476 | 100 |
| Fig. 43: Thermodynamic characteristics of Fab binding to IGF-1R | 102 |
| Fig. 44: sEGFR in complex with matuzumab binding to EGF | 130 |
| Fig. 45: sEGFR binding to mAb72000 immobilized by protein A..... | 131 |

List of tables

| | |
|---|-----|
| Table 1: Overview structural information of RTK extracellular domains | 15 |
| Table 2: Data collection and refinement statistics Fab72000 and sEGFRd3:Fab72000..... | 34 |
| Table 3: Data collection and refinement statistics sEGFRvIII..... | 35 |
| Table 4: Data collection and refinement statistics Fab1159476 | 36 |
| Table 5: Affinities of Fab72000, FabC225 and EGF to different sEGFR constructs | 78 |
| Table 6: ITC-derived characteristics of antibody binding to IGF-1R at 25°C..... | 130 |

1. ZUSAMMENFASSUNG

Rezeptor-Tyrosinkinasen (RTKs) sind essentielle Bestandteile der inter- und intrazellulären Kommunikation und der Signaltransduktion in Metazoen. Sie sind involviert in die Steuerung wichtiger zellulärer Prozesse wie Zellteilung, Zellwachstum, Zelldifferenzierung und Zelltod (Hubbard and Miller, 2007). RTKs gehören zu der Enzymfamilie der Protein-Tyrosinkinasen, die den Transfer einer Phosphatgruppe von ATP auf Tyrosinreste des Substrates katalysieren. Im menschlichen Genom sind 58 RTKs und 32 nicht-Rezeptor Protein-Tyrosinkinasen kodiert. Die Rezeptoren sind Typ I Transmembranproteine mit einer extrazellulären Liganden-Bindungsdomäne und einer intrazellulären Tyrosinkinasedomäne. Der extrazelluläre Bereich ist mit der intrazellulären Kinasedomäne durch eine einfache Transmembranhelix verbunden (Schlessinger, 2000).

Generell werden RTKs durch Liganden-induzierte Dimerisierung aktiviert, die die intrazellulären Kinasedomänen nahe genug zueinander bringt um eine Autophosphorylierung *in trans* zu ermöglichen. Die phosphorylierten Proteinsequenzen rekrutieren Proteinsubstrate, die eine Signalkaskade in das Zellinnere und in den Zellkern initiieren. Letztendlich werden so Transkriptionsfaktoren reguliert, die in Prozesse involviert sind wie zum Beispiel die Zelldifferenzierung oder das Zellüberleben (Hunter, 2000).

Ausgehend von ersten Untersuchungen in den 1980er Jahren zeigte sich, dass viele RTKs an der Entstehung verschiedener Neoplasien beteiligt sind und sogar Malignome hervorrufen können, wenn Störungen in der normalen Regulation der Rezeptoren vorliegen. Missregulierungen dieser Art können u.a. durch Genamplifikationen oder durch Mutationen verursacht werden, die eine konstitutive Aktivierung der Rezeptoren zur Folge haben (Weinberg, 2007).

In der Klinik werden verschiedene Therapieansätze gegen Neoplasien, die durch RTKs hervorgerufen werden, genutzt (Mendelsohn and Baselga, 2006). Unter anderem können einerseits Tyrosinkinase-Inhibitoren intrazellulär die Signaltransduktionskaskaden blockieren, die zu einer weiteren Zellteilung und –amplifikation führen würden. Andererseits werden monoklonale Antikörper eingesetzt, die die Rezeptoren extrazellulär binden. Hierdurch wird das Immunsystem des Körpers gegen Zellen aktiviert, die eine große Anzahl der Rezeptoren an der Oberfläche tragen. Zusätzlich können Antikörper die Aktivierung der RKTs verhindern, indem sie das Binden von Liganden oder die Rezeptordimerisierung blockieren.

Verschiedene Studien über die Anwendung von monoklonalen Antikörpern in der Krebstherapie haben gezeigt, dass aktivierende Mutationen in Mediatoren der Signalkaskaden (zum Beispiel K-ras), Kompensationsmechanismen bzw. Resistenzen der Zelle und sich gegenseitig beeinflussende Signaltransduktionswege von verschiedenen RTKs Einfluss auf die Wirksamkeit der Therapie haben (Dempke and Heinemann, 2009). Eine für jeden Patienten individuell angepasste Kombination von Chemotherapie, Strahlentherapie und Antikörpern bzw. Inhibitoren könnte ein Weg sein um die Effektivität der Behandlung zu steigern und Nebenwirkungen zu minimieren (Friedman *et al.*, 2005).

In dieser Arbeit wurde mit zwei verschiedenen RTKs gearbeitet: der Epidermale Wachstumsfaktorrezeptor EGFR und der Insulin-ähnliche Wachstumsfaktorrezeptor 1 IGF-1R. Beide Rezeptoren können bei Missregulation Tumoren hervorrufen, u.a. epitheliale Neoplasien wie Bronchialkarzinome oder Kolonkarzinome. Eine ansteigende Anzahl von Antikörpern gegen EGFR and IGF-1R ist in der klinischen Untersuchungsphase oder schon in der Klinik in Anwendung. Gegen EGFR sind die Antikörper Cetuximab/Erbitux[®] und Panitumumab/Vectibix[®] seit 2004 beziehungsweise 2006 zugelassen. Des Weiteren ist der monoklonale Antikörper Trastuzumab/Herceptin[®] seit 1998 in der klinischen Anwendung gegen Mammkarzinome, die das zweite Familienmitglied der EGFR Familie ErbB2 überexprimieren.

Das Ziel dieser Arbeit war die Charakterisierung der Interaktionen von löslichen RTK extrazellulären Domänen mit Antikörper Fab-Fragmenten sowie der Inhibitionsmechanismen von verschiedenen Antikörpern. Ein besseres Verständnis der Epitope der Antikörper, ihrer Affinitäten und Liganden-Kompetitionscharakteristiken könnte dazu beitragen die klinische Anwendung der Antikörper in der Krebstherapie zu verbessern. Es wurden die folgenden Fragestellungen untersucht:

1. an welcher Stelle der extrazellulären Domäne bindet der Antikörper?
2. welche Affinität hat der Antikörper zum löslichen Rezeptor?
3. wie beeinflusst die Bindung des Antikörpers die Aktivierung des Rezeptors?
4. ist es den natürlichen Liganden des Rezeptors noch möglich zu binden, wenn der Antikörper vorhanden ist?
5. welchen Effekt hat der gebundene Antikörper auf die Rezeptordimerisierung?
6. ist die strukturelle Reorganisation, die Voraussetzung für die Rezeptoraktivierung ist, noch möglich mit gebundenem Antikörper?

Die Arbeit wurde in drei Abschnitte gegliedert. Im ersten Abschnitt (Kapitel 5) werden die Interaktionen von EGFR mit dem monoklonalen Antikörper Matuzumab (EMD72000) beschrieben. Der zweite Abschnitt (Kapitel 6) zeigt Untersuchungen zu einer EGFR Mutante (EGFR Variante III oder EGFRvIII), die bisher ausschließlich auf neoplastischen Zellen nachgewiesen werden konnte. Im dritten Abschnitt wird die Bindung des monoklonalen Antikörpers EMD1159476 an den Insulin-ähnlichen Wachstumsfaktor-rezeptor 1 IGF-1R beschrieben (Kapitel 7).

(1) EGFR – Antikörper Interaktionen (Kapitel 5)

In diesem Teil der Arbeit wurden die Eigenschaften des gegen EGFR gerichteten monoklonalen Antikörpers Matuzumab (EMD72000) untersucht. Matuzumab ist die humanisierte Form des murinen anti-EGFR Antikörpers 425 und hat die Phase II der klinischen Studien erreicht. Es konnte die Komplexkristallstruktur des Matuzumab Fab-Fragments mit der Domäne III des Rezeptors gelöst und so erstmals das Epitop des Antikörpers identifiziert werden. Das Epitop wurde durch Rezeptor-Mutationsstudien in Lösung bestätigt. Interessanterweise überlappt die Matuzumab Bindestelle nicht mit dem Epitop des natürlichen Liganden EGF. Das Gegenteil wurde zuvor für den bereits in der Klinik eingesetzten Antikörper Cetuximab beobachtet, dessen Bindungsstelle sich mit dem Epitop von EGF überschneidet. Zudem sind die Epitope der beiden Antikörper Matuzumab und Cetuximab unterschiedlich und nicht überlappend. Während Cetuximab direkt das Binden des aktivierenden Liganden an EGFR verhindert, konnte für Matuzumab in dieser Arbeit ein anderer indirekter Inhibitionsmechanismus vorgeschlagen werden: Matuzumab verhindert sterisch die Konformationsänderungen des Rezeptors, die für die Dimerisierung der Rezeptormonomeren stattfinden müssen. Ein solcher nicht-kompetitiver Inhibitionsmechanismus eines Antikörpers gegen EGFR konnte in dieser Arbeit erstmals beschrieben werden.

Basierend auf den Rezeptor-Antikörper Komplex-Strukturmodellen erscheint eine simultane Bindung beider Antikörper an EGFR möglich. Tatsächlich konnte *in vitro* eine parallele Bindung beider Antikörper an Zelloberflächen-EGFR beobachtet werden. Diese Ergebnisse haben wichtige Konsequenzen für den klinischen Einsatz der Antikörper in der Krebstherapie, da sie implizieren, dass eine Kombinationstherapie mit beiden Antikörpern möglich ist. Präklinisch konnte bereits ein synergistischer Effekt von Cetuximab und Matuzumab in Kombination nachgewiesen werden (Dechant *et al.*, 2008; Kamat *et al.*, 2008). Ob eine solche Therapie allerdings für Patienten Vorteile bringt, müsste erst noch gezeigt werden.

(2) EGFRvIII (Kapitel 6)

Im zweiten Teil dieser Arbeit wurde eine Mutation des EGF Rezeptors untersucht, die durch die Deletion eines Teils der extrazellulären Domäne entsteht: die EGFR Variante III (EGFRvIII). Diese Mutante wurde bisher nur auf neoplastischen Zellen nachgewiesen und tritt gehäuft auf Gliomazellen auf. EGFRvIII ist konstitutiv aktiv und hat eine reduzierte Abbaurate im Vergleich zum Wildtyp-Rezeptor. Es ist bisher nicht klar, auf welche Weise die konstitutive Aktivierung der Rezeptormutante hervorgerufen wird. Daher wurde in dieser Arbeit erstmals die lösliche extrazelluläre Domäne von EGFRvIII strukturell und auf ihre Dimerisierungseigenschaften hin untersucht. Es konnte gezeigt werden, dass die Domänen III und IV des extrazellulären Bereichs strukturell durch die Deletion nicht beeinträchtigt sind und denen des Wildtyp-Rezeptors entsprechen. Des Weiteren konnte nachgewiesen werden, dass die monoklonalen Antikörper Matuzumab und Cetuximab mit einer ähnlichen Affinität an die löslichen extrazellulären Domänen der EGFRvIII und des Wildtyp-Rezeptors binden. Es ist bereits bekannt, dass die Ektodomänen des Wildtyp-Rezeptors bei Zugabe des natürlichen Liganden EGF dimerisieren (Ferguson *et al.*, 2000). In dieser Arbeit konnte erstmals nachgewiesen werden, dass EGF zwar an die Domäne III-Bindungsstelle von EGFRvIII bindet, aber keine Dimerisierung des mutierten Rezeptors hervorruft. Diese Ergebnisse beantworten Teilfragen der EGFRvIII Biologie unter anderem zur Struktur der Ektodomäne, können allerdings nicht die transformierenden Eigenschaften der Mutante an der Zelloberfläche erklären. Dies unterstreicht die Notwendigkeit in diesem Fall den gesamten Transmembran-Rezeptor in zellulären Experimenten zu untersuchen.

(3) IGF-1R – Antikörper Interaktionen (Kapitel 7)

Im dritten Teil dieser Arbeit wurde die Bindung eines weiteren monoklonalen Antikörpers EMD1159476 an den Insulin-ähnlichen Wachstumsfaktorrezeptor 1 IGF-1R untersucht. EMD1159476 hat die letzte Phase der präklinischen Entwicklung erreicht. Ein transientes Säugerzellexpressionssystem wurde für verschiedene Konstrukte der extrazellulären IGF-1R Domäne etabliert. Die Struktur des Fab-Fragments wurde gelöst; eine Komplexstruktur von Rezeptor und Fab-Fragment konnte jedoch trotz intensiven Screenings von Kristallisationsbedingungen bisher noch nicht erhalten werden. Die Bindung des Fab-Fragments an die verschiedenen Konstrukte der löslichen Ektodomäne konnte erstmals biophysikalisch nachgewiesen und die Affinität bestimmt werden. Es konnte gezeigt werden, dass das Epitop von EMD1159476 innerhalb der Domäne II von IGF-1R liegt und dass der gebundene Antikörper die Bindung des natürlichen Liganden IGF-1 beeinträchtigt. Diese Ergebnisse könnten die präklinische Entwicklung unterstützen.



2. AIM OF THE THESIS

Cancer patients often suffer from serious side effects of chemo- and radiotherapy treatment to fight the uncontrolled proliferation in malignant tumors. Targeted therapy, such as therapeutic antibodies against specific cancer related cell surface proteins, might offer a more efficient treatment. An increasing number of therapeutic antibodies targeting tumors that express cell surface receptor tyrosine kinases (RTKs) are in clinical use or late stages of clinical development. The aim of this thesis is to investigate the molecular basis of inhibition of two receptor tyrosine kinases – the epidermal growth factor receptor EGFR and the insulin-like growth factor receptor IGF-1R - by therapeutic antibodies.

The thesis covers investigations about the interactions between antibody Fab fragments and soluble receptor extracellular domains. Several biophysical methods were applied to analyze the mode of receptor inhibition and to address the following questions:

7. which part of the receptor extracellular domain does the antibody bind to?
8. what affinity does the antibody have to the receptor?
9. how does antibody binding influence receptor activation?
10. are the natural ligands that are involved in receptor activation still able to bind to the receptor?
11. which effects does antibody binding have on receptor dimerization?
12. is the structural reorganization of the receptor required for activation still possible with antibody bound?

Based on the results of the biophysical assays questions can be answered about allosteric/competitive receptor inhibition, the antibody epitope and implications of antibody binding on normal receptor activation. Cell surface assays and clinical investigations were beyond the scope of this thesis and results are discussed based on literature.

The thesis is structured in three separate parts representing the receptor types that were investigated.

1. EGFR – antibody interactions (chapter 5)
2. the cancer related mutant variant III of EGFR (EGFRvIII) (chapter 6)
3. IGF-1R – antibody interactions (chapter 7)



3. RECEPTOR TYROSINE KINASES

3.1. Introduction

Receptor tyrosine kinases (RTKs) are essential components of the signal transduction pathways in inter- and intracellular communication in metazoans (Hubbard and Miller, 2007). They belong to the enzyme family of protein tyrosine kinases, which catalyze phosphoryl transfer to tyrosine residues in protein substrates, using ATP as a phosphate donor (Hunter, 1998). The human genome encodes 58 RTKs and 32 non-receptor protein tyrosine kinases (Robinson *et al.*, 2000). The receptor kinases are type I transmembrane-spanning proteins (N-terminus in the extracellular region, C-terminus intracellular) and contain an extracellular ligand binding domain that is usually glycosylated. The extracellular domain is connected to the intracellular kinase domain via a single transmembrane helix (Schlessinger, 2000). The kinase domain contains additional regulatory sequences that are controlled by autophosphorylation or phosphorylation by heterologous protein kinases (Hubbard *et al.*, 1998). RTKs play an important role in the control of most fundamental cellular processes such as cell cycle regulation, cell migration and survival as well as cell proliferation and differentiation (Hubbard and Miller, 2007).

The family of RTKs (Fig. 1) includes, among others, the epidermal growth factor receptor (EGFR), platelet-derived growth factor receptors (PDGFRs), fibroblast growth factor receptors (FGFRs), vascular endothelial growth factor receptors (VEGFRs), Met (hepatocyte growth factor/scatter factor [HGF/SF] receptor), Ephrin receptors (Ephs) as well as insulin receptor (IR) and insulin-like growth factor receptor (IGFR) (Schlessinger, 2000; Blume-Jensen and Hunter, 2001).

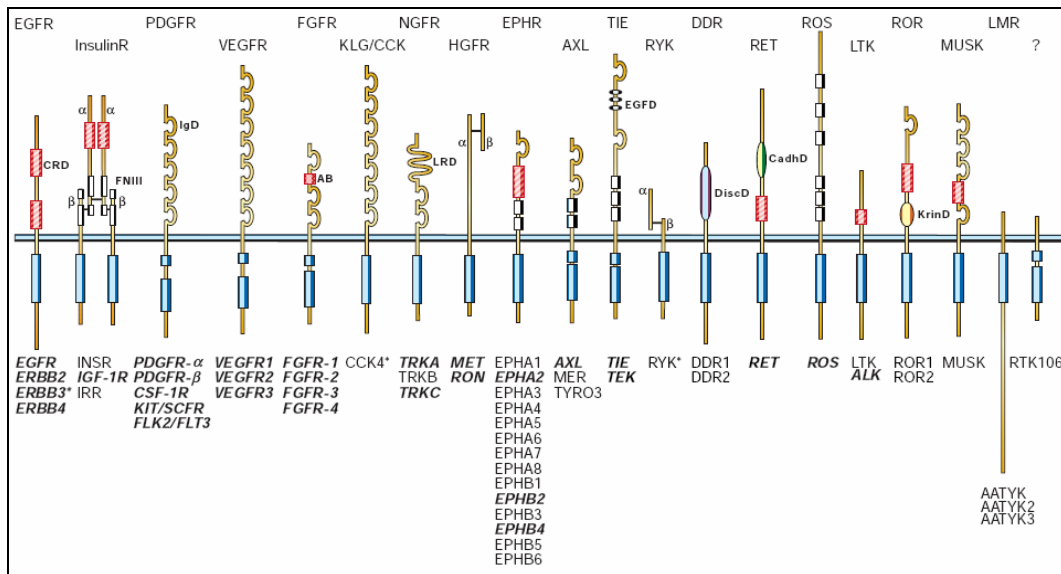


Fig. 1: Human receptor tyrosine kinases

The prototype of each receptor family is shown with the known members listed below. The symbols α and β denote distinct receptor subunits. Members in bold and italic type are implicated in human cancers. An asterisk indicates that the member is devoid of intrinsic kinase activity. Abbreviations: EGFR, epidermal growth factor receptor; InsR, insulin receptor; PDGFR, platelet-derived growth factor receptor; VEGFR, vascular endothelial growth factor receptor; FGFR, fibroblast growth factor receptor; KLG/CCK, colon carcinoma kinase; NGFR, nerve growth factor receptor; HGFR, hepatocyte growth factor receptor; EphR, ephrin receptor; Axl, a Tyro3 protein tyrosine kinase, TIE, tyrosine kinase receptor in endothelial cells; RYK, receptor related to tyrosine kinases; DDR, discoidin domain receptor; Ret, rearranged during transfection; ROS, receptor tyrosine kinase expressed in some epithelial cell types; LTK, leukocyte tyrosine kinase; ROR, receptor orphan; MuSK, muscle-specific kinase; LMR, Lemur; AB, acidic box; CadhD, cadherin-like domain; CRD, cysteine-rich domain; DiscD, discoidin-like domain; EGFD, epidermal growth factor-like domain; FNIII, fibronectin type III-like domain; IgD, immunoglobulin-like domain; KinD, kringle-like domain; LRD, leucine-rich domain (figure taken from Blume-Jensen and Hunter, 2001).

3.2. Structures of RTKs

During the last 10 years crystal structures of the extracellular domains of most RTK family members were solved (Table 1). These include structures of all human EGFR family members without ligand and EGFR with bound ligand (see 5.1.2). In the IR family structures of IR domain I-III and the whole IR ectodomain as well as IGF-1R domain I-III are available (see 7.1.1).

Table 1: Overview structural information of RTK extracellular domains

| Structural information available | |
|-------------------------------------|---|
| Receptor | Structures of parts or the full extracellular domain solved |
| EGFR | all family members, EGFR with ligands EGF and TGF- α (Cho and Leahy, 2002; Ogiso <i>et al.</i> , 2002; Garrett <i>et al.</i> , 2002; Ferguson <i>et al.</i> , 2003; Cho <i>et al.</i> , 2003; Garrett <i>et al.</i> , 2003; Franklin <i>et al.</i> , 2004; Bouyain <i>et al.</i> , 2005) |
| IR family | IR domain I-III and IR ectodomain, IGF-1R domain I-III (Garrett <i>et al.</i> , 1998; McKern <i>et al.</i> , 2006; Lou <i>et al.</i> , 2006) |
| PDGFR | KIT with and without ligand (Yuzawa <i>et al.</i> , 2007) |
| VEGFR1 | domain II (Christinger <i>et al.</i> , 2004) |
| FGFR | parts of the extracellular domain in complex with different ligands (Plotnikov <i>et al.</i> , 1999; Stauber <i>et al.</i> , 2000; Plotnikov <i>et al.</i> , 2000; Yeh <i>et al.</i> , 2003; Olsen <i>et al.</i> , 2004; Olsen <i>et al.</i> , 2006) |
| NGFR | full and fragmented ectodomains with and without ligand (Wiesmann <i>et al.</i> , 1999; Ultsch <i>et al.</i> , 1999; Robertson <i>et al.</i> , 2001; Banfield <i>et al.</i> , 2001; Wehrman <i>et al.</i> , 2007) |
| HGFR | partial ectodomain with ligand bound (Stamos <i>et al.</i> , 2004) |
| EPHR | several extracellular domains with and without ligand (Himanen <i>et al.</i> , 2001; Himanen <i>et al.</i> , 2004; Chrencik <i>et al.</i> , 2006; Qin <i>et al.</i> , 2008; Goldgur <i>et al.</i> , 2009) |
| AXL | two family members alone and in complex with ligand (Heiring <i>et al.</i> , 2004; Sasaki <i>et al.</i> , 2006) |
| TIE | partial ectodomain alone and in complex with ligand (Barton <i>et al.</i> , 2006) |
| DDR | discoidin domain of DDR2 (Ichikawa <i>et al.</i> , 2007) |
| MuSK | first and second immunoglobulin-like domain (Stiegler <i>et al.</i> , 2006) |
| No structural information available | |
| KLG/CCK, RYK, RET, ROS, LTK, ROR | |

3.3. RTK activation

Generally, RTKs are activated through ligand induced receptor dimerization, which brings the tyrosine kinase domains into close proximity promoting the allosteric activation of the kinase domains (Zhang *et al.*, 2006a; Hubbard and Miller, 2007). The phosphorylated tyrosine residues are located in the kinase activation loop or juxtamembrane region, inducing conformational changes that stabilize the active state of the kinase (Hubbard, 2004). Induced by the phosphorylation event, the activated kinase domains recruit downstream substrate molecules which initiate an intracellular signal cascade (see 3.4). The signaling pathways regulate transcription factors involved in cell survival or cell differentiation (Blume-Jensen and Hunter, 2001; Murphy and Blenis, 2006).

Within the RTK family different ligands employ varying modes for inducing the active dimeric state of the receptors. The following mechanisms have been described:

1. The simplest mechanism is represented by bivalent ligands, binding simultaneously to two receptor molecules (1:2 ligand:receptor complex). This binding mode has been observed e.g. in structural studies investigating the growth hormone receptor (GHR, not included in Fig. 1) in complex with growth hormone (GH) (Kossiakoff and de Vos, 1998).
2. A 2:2 ligand:receptor complex was described for homodimeric growth factors, e.g. VEGF, FGF or PDGF (Wiesmann *et al.*, 1997; Plotnikov *et al.*, 1999). Using electron microscopy and small-angle x-ray scattering also the RTK Met was described to be activated in a similar 2:2 ligand:receptor mode with no direct receptor contact in the complex (Gherardi *et al.*, 2006). In case of FGF receptor activation it was shown in crystallographic studies that the receptor requires heparin sulfate proteoglycans in addition to the ligands to stabilize the dimeric complex (Mohammadi *et al.*, 2005).
3. The structures of complexes of EGFR and its ligands EGF and TGF- α (Ogiso *et al.*, 2002; Garrett *et al.*, 2002) also showed a 2:2 ligand:receptor complex. But in contrast to the complexes mentioned above the dimer interface is entirely receptor mediated and the ligands do not touch each other (see 5.1 and Fig. 6).
4. Unlike the majority of RTKs the insulin receptor family is not a single-chain receptor, but a $\alpha_2\beta_2$ homodimer (see 7.1). Recently, the structure of the entire disulfide-linked ectodomain of the insulin receptor has been solved (McKern *et al.*, 2006) (Fig. 34). The current activation model suggests a 2:1 ligand:receptor dimer complex with the ligands mediating the contact between the two halves of the homodimer.

5. A subset of RTKs, including Ret (rearranged during transfection) and MuSK (muscle-specific kinase), do not bind their ligands directly, but require co-receptors for ligand-induced activation. Ret dimerizes as 1:2:2 ligand:receptor:co-receptor complex (Schlee *et al.*, 2006). Ligand and co-receptor of MuSK were recently identified as the heparan sulfate proteoglycan agrin and the low density lipoprotein receptor (LDLR) family member Lrp4 (Stiegler *et al.*, 2006; Kim *et al.*, 2008).

3.4. Signaling mechanisms downstream of activated RTKs

The phosphotyrosine residues in RTKs are bound by cytoplasmic enzymes and adapter/scaffolding proteins containing SRC homology-2 (SH2) or phosphotyrosine-binding (PTB) domains (Hubbard and Miller, 2007). SH2 domain-containing enzymes (SHC) are e.g. protein tyrosine kinases (SRC kinases), protein tyrosine phosphatases (SHP2), phospholipase C (PLC γ) or guanine exchange factors (Ras-GAP). With their SH2 and SH3 domains adapter proteins (e.g. GRB2, NCK, CRK, SHC) form scaffolds that link different proteins involved in signal transduction.

Simplified, there are three main intracellular signal transduction pathways that are activated through RTK phosphorylation (Fig. 2).

1. The Ras/MAP kinase (mitogen-activated protein kinase) signaling cascade (Schlessinger, 2000). The adapter protein GRB2 forms a complex with the guanine nucleotide exchange factor mSOS (mammalian son of sevenless). The GRB2:SOS complex binds to RTK phosphotyrosine residues thus translocating SOS to the plasma membrane and close to Ras. Here it stimulates the exchange of GTP for GDP (Gureasko *et al.*, 2008). Once in the active GTP-bound state, Ras interacts with several effector proteins such as Raf and phosphatidylinositol 3-kinase (PI-3K) to trigger numerous intracellular processes. Activated Ras stimulates MAP-kinase-kinase (MAPKK, MEK1); which in turn phosphorylates MAP-kinase (MAPK, extracellular signal-regulated kinase ERK). MAPK is rapidly translocated into the nucleus where it activates transcription factors (Hunter, 2000; Papin *et al.*, 2005; Murphy and Blenis, 2006; Weinberg, 2007).
2. Activation of PLC γ with subsequent release of the second messengers diacylglycerol (DAG) and inositol-3,4,5-trisphosphate (IP $_3$). Further downstream events comprise Ca $^{2+}$ release, Ca $^{2+}$ /calmodulin-dependent protein kinase and protein kinase C (PKC) activation and finally transcription factor phosphorylation (Hunter, 2000).

3. The phospholipid kinase PI-3K pathway. PI-3K is activated by virtually all RTKs. It generates the second messengers phosphatidylinositol-3,4-bisphosphate (PtdIns(3,4)P₂) and PtdIns-3,4,5-P₃, which lead to the activation of Akt (PKB) and PDK1, two kinases that regulate various metabolic processes including activation of mTOR (mammalian target of rapamycin) and prevent apoptotic death (Baselga, 2008; Maira *et al.*, 2009).

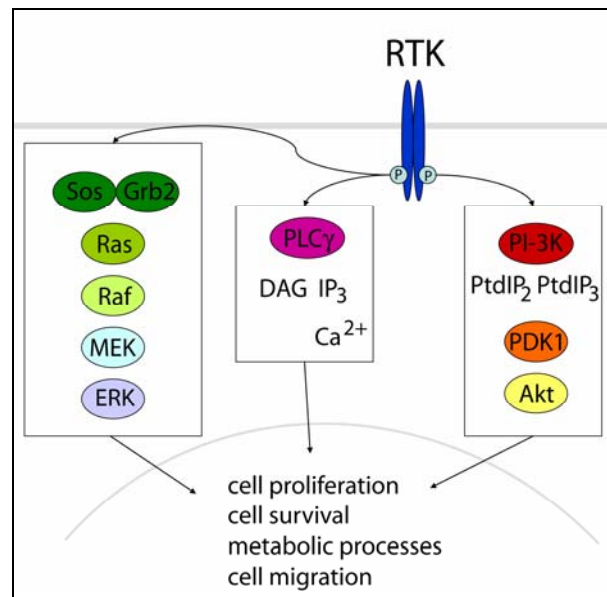


Fig. 2: Simplified RTK intracellular signaling pathway overview

Upon extracellular ligand binding and receptor dimerization, tyrosine trans-autophosphorylation occurs. This triggers the binding of downstream effectors, such as Grb2. Subsequently the recruitment of son-of-sevenless (SOS) and Ras, Raf, MEK leads to the activation of the entire mitogen-activated protein kinase (MAPK) cascade (MEK stands for ‘MAPK and extracellular signal-regulated kinase (ERK) kinase’). Other signaling pathways include the activation of phosphatidylinositol 3-kinase (PI-3K) and Akt or phospholipase C (PLC γ). RTK signaling leads to enhanced cell survival, growth and differentiation through the activation of transcription factors (e.g. ELK, FOS, STAT, not shown here).

The phosphorylation events downstream of RTK activation involve many proteins and expand quickly in the cell. Phosphotyrosine studies in the EGFR signaling network showed significant changes in the phosphorylation state of 81 proteins within 20 min after EGF stimulation (Blagoev *et al.*, 2004; Zhang *et al.*, 2005).

The signaling pathways are subjected to multiple negative feedback mechanisms at the level of the receptor itself by inhibitory protein tyrosine phosphatases and by receptor endocytosis and degradation (Schlessinger, 2000; Le Roy and Wrana, 2005). In addition, the specific activity of downstream effector proteins can be negatively regulated by inhibitory signals, e.g. through MAPK specific phosphatases. The strength and duration of the signals that are transmitted through the networks of signaling cascades are modulated through factors such as cell-surface receptor density, expression levels of scaffolding proteins, the

surrounding extracellular matrix and the balance between kinases and phosphatases (Murphy and Blenis, 2006).

Taken together, the downstream signaling pathways are not linear but consist of multilayered and cross-connected networks. This allows for horizontal interactions and permits multiple combinatorial and integrated responses (Mendelsohn and Baselga, 2006). The complexity of this network makes it especially difficult to treat RTK misregulation in cancer (see next section).

3.5. RTKs and cancer

When mutated or altered structurally, RKTs can become potent oncoproteins. More than half of the known receptors tyrosine kinases (marked in bold in Fig. 1) have been repeatedly found to be either mutated or overexpressed in human malignancies (Blume-Jensen and Hunter, 2001). Once their normal tight regulation is impaired, RTKs can cause deregulated autonomous cell growth and support the capacity to invade other tissues.

This oncogenic transformation can be induced by four main principles: retroviral transduction of a proto-oncogene corresponding to a RTK with deregulating structural changes (commonly found in rodents and chicken); genomic re-arrangement, i.e. chromosomal translocations, resulting in oncogenic fusion proteins; gain-of-function mutations or small deletions; or receptor/ligand overexpression resulting from gene amplification. In general, the transforming effects are based upon enhanced or constitutive kinase activity with quantitatively or qualitatively altered downstream signaling (Murphy and Blenis, 2006; Weinberg, 2007).

In consequence much effort has gone into designing and identifying potent and specific RTK inhibitors. Targeted therapeutics were developed both to the extracellular regions of RTKs using e.g. monoclonal antibodies, and to the cytoplasmic (kinase) domains using small-molecule inhibitors (Mendelsohn and Baselga, 2006).



4. MATERIALS & METHODS

4.1. Molecular Biology

4.1.1. EGFR

The vector constructs of the full length extracellular domain of the epidermal growth factor receptor sEGFR (pFastBac_ *sEGFR_His₆*) and the isolated domain III with the amino acids 310-500 of mature sEGFR (sEGFRd3, pFastBac_ *sEGFRd3_His₆*) were provided by K. M. Ferguson, University of Pennsylvania. These constructs were used for all experiments presented in section 5 beside the mutational studies. The same construct sEGFR (pFastBac_ *sEGFR_His₆*) was cloned by standard PCR and molecular biology procedures for the experiments described in section 6 (primer, DNA and protein sequences in the Appendix in 11.1 and 11.2). Human *EGFR* cDNA was provided by Merck KGaA, Germany.

Site-directed mutagenesis to introduce alanine mutation into *sEGFR* was carried out using the QuikChange Kit (Stratagene) following a two-stage PCR protocol (Wang and Malcolm, 2002). To generate the mutant sEGFR K454A the primers K454 up and K454 rev were used, for the mutant sEGFR K463A the primers K463 up and K463 rev were used and for the double mutant sEGFR T459A/S460A the primers T459A/S460A up and T459A/S460A rev were used (sequences in 11.1).

The residues K454 or K463 for the triple mutants are sequentially close to the double mutant residues T459A and S460A. To prevent back-mutation of already introduced alterations the mutagenesis was carried out in two PCR stages: a first round with the primers of the T459A/S460A mutation (see above) and a second stage performed with the primers tripleK454A up and tripleK454A rev to generate the mutant sEGFR T459A/S460A/K454A or the primers tripleK463A up and tripleK463A rev for the mutant sEGFR T459A/S460A/K463A (sequences in 11.1). The successful introduction of the mutations was verified by DNA sequencing of the respective pFastBac constructs.

Protein of the mutant sEGFR D355T/F357A was provided by K. M. Ferguson, University of Pennsylvania. Protein of the mutant sEGFR Y251A/R285S was a donation of J. Dawson, University of Pennsylvania.

4.1.2. sEGFRvIII

The deletion mutant *sEGFR variant III* (*sEGFRvIII*) was amplified by PCR in two fragments from *EGFR* cDNA (provided by Merck KGaA, Germany). Both fragments were generated with a complementary base pair overlap resulting in a novel glycine residue at the fusion junction (Fig. 3).

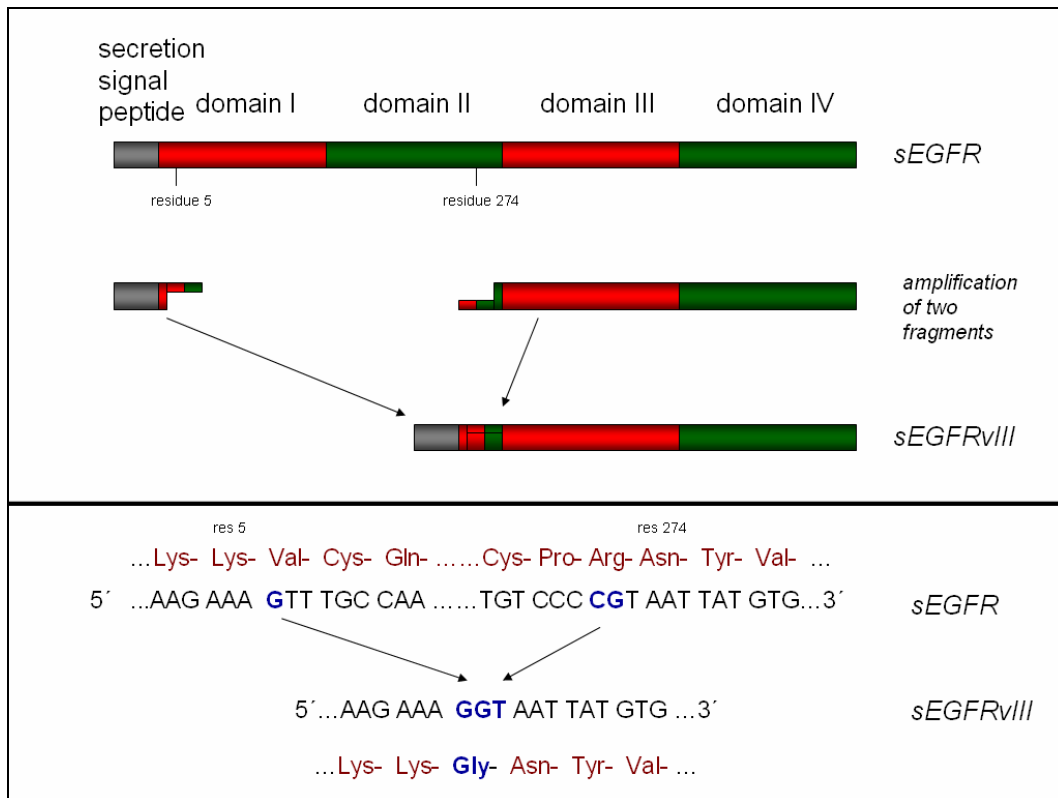


Fig. 3: Cloning scheme of *sEGFRvIII*

sEGFR variant III consists of two fragments of the wild type *EGFR* gene, which are fused by a complementary overlap at the fusion junction introduced by the primers. Thus residue 5 of domain I is directly connected to residue 274 of domain II via a novel glycine residue.

The DNA of *sEGFRvIII* was amplified and purified using standard PCR and molecular biology procedures. The construct was cloned with the N-terminal native secretion signal peptide and a C-terminal hexa-histidine tag. In addition *attB*-sequences were introduced at the start and the end of the PCR product to enable the fusion of the gene into a Gateway[®] entry vector (Invitrogen, 2003). The primers *sEGFRvIII* f1 up and *sEGFRvIII* f1 rev were used to generate the *sEGFRvIII_His₆* N-terminal fragment and the primers *sEGFRvIII* f2 up and *sEGFRvIII* f2 rev for the C-terminal fragment (sequences in 11.1). The sequence of the construct *sEGFRvIII_His₆* was confirmed by DNA sequencing (DNA and protein sequences in 11.2).

4.1.3. sIGF-1R

Based on *IGF-1R* cDNA provided by Merck KGaA, Germany the domains I-III of the extracellular domain (amino acids 31-492 of mature IGF-1R) as well as the isolated domain II (amino acids 180-329 of mature IGF-1R) were amplified by standard PCR techniques. Both constructs were cloned with the N-terminal native secretion signal peptide and a C-terminal hexa-histidine tag. The constructs were transferred into the expression vectors of the respective insect cell or mammalian expression system using the Gateway[®] technology (Invitrogen, 2003). The native secretion signal peptide was directly fused to the domain II by blunt end ligation. The primers sIGF-1Rd1-3 up and sIGF-1Rd1-3 rev were used for the generation of the *sIGF-1Rd1-3* entry vector, the primers sIGF-1Rd2 blunt up and sIGF-1Rd2 blunt rev for the *sIGF-1Rd2* blunt end ligation construct and the primers sIGF-1Rd2 up and sIGF-1Rd2 rev for the *sIGF-1Rd2* amplification (sequences in 11.1). The sequences of the constructs were confirmed by DNA sequencing (DNA and protein sequences in 11.2).

4.1.4. Generation of recombinant baculovirus

Recombinant baculoviruses for the expression of sEGFR, sEGFR domain III, sEGFRvIII, the sEGFR mutants, sIGF-1R domain I-III and sIGF-1R domain II were produced as described (Invitrogen, 2009).

4.2. Protein expression

4.2.1. sEGFR and sEGFRvIII

The soluble extracellular part of the EGFR wild type (sEGFR), the isolated domain III of the receptor (sEGFRd3) and the sEGFR mutants (see 4.1.1) were expressed in Sf9 insect cells infected by recombinant baculovirus exactly as described (Ferguson *et al.*, 2000) (see 4.1.4). Briefly, 5-10 L insect cell culture was infected with freshly amplified baculovirus at a density of 2.0×10^6 c/ml (viability > 98%) and incubated for 96 h at 27°C in multiple 1 L spinner flasks that each contained <500 ml (to ensure adequate aeration) The cells were separated from the protein containing medium by centrifugation.

4.2.2. sIGF-1R

Insect cell expression. The isolated domains 1-3 and domain 2 of the IGF-1R extracellular part (sIGF-1Rd1-3 and sIGF-1Rd2, respectively) were expressed both in Sf9 and Hi5 insect cells infected by recombinant baculovirus (see 4.1.4). The cells grew at 27°C in 500 ml shaking flasks in Sf-900 II serum free medium (Invitrogen) or Express Five serum free medium (Invitrogen), respectively,. They were infected with recombinant baculovirus at a density of 2×10^6 cells/ml and incubated for 24-96h at 27°C. The highest yield was obtained with a multiplicity of infection (MOI) 4 and an expression for 48 h, after which protein degradation started to occur. The cells were separated from the protein containing medium by centrifugation.

Mammalian cell expression. Both sIGF-1R constructs sIGF-1Rd1-3 and sIGF-1Rd2 were transiently expressed in human kidney HEK293 Ebna cells. The cells were cultured in suspension in Ex-Cell VPRO Serum Free Medium (SAFC, Sigma Aldrich) with 4 mM glutamine (Invitrogen) and 0.1% Pluronic (Invitrogen) at 37°C, 25% O₂, 75 rpm in a 8 L fermenter. For transfection, cells harvested after 24h cells at 2.5×10^6 cells/ml were resuspended in transfection medium consisting of DMEM F-12 1:1 (Invitrogen) with 8 mM glutamine, 0.2 % glucose, 10mM HEPES (PAN), 0.4 % Insulin-Transferin-Selenium-Supplement (Invitrogen) and 0.1% Pluronic (Invitrogen). The respective DNA (3 µg/ml) (see 4.1.3) dissolved in transfection medium was added with the addition of PEI 25 after 10 min (0.02 mg/ml in transfection medium). The cells were incubated for 2.5h at 37°C and subsequently diluted with FreeStyle 293 Expression Medium (Invitrogen) with 0.1% Pluronic (Invitrogen) in a 1:3 ratio. After 24h at 37°C the fermenter was cooled down to 31°C and incubated for another 96h prior to harvesting the supernatant.

4.3. Protein purification

4.3.1. sEGFR

Purification of the soluble receptor proteins sEGFR wild type, sEGFR domain III and the sEGFR mutants from Sf9 cell culture supernatants (see 4.3.1) was carried out by immobilized metal-ion affinity chromatography (IMAC) and gel filtration exactly as described (Ferguson *et al.*, 2000). The overall yield of sEGFR wild type was about 1 mg/L cell culture and about 0.6 mg/L cell culture of sEGFRd3 depending on the age and condition of the Sf9 cells. For the sEGFR alanine mutants the overall yield was about 0.5 mg/L cell culture.

All proteins were stored in 10 mM HEPES, 50 mM NaCl (pH 7.5) at ~5 mg/ml at 4°C.

4.3.2. sEGFRvIII, sIGF-1R domain I-III and domain II

After centrifugation of the cell culture (see 4.2.1 and 4.2.2) the supernatant was directly applied to a 5 ml HiTrap™ sepharose column (GE Healthcare) and eluted with an imidazole step gradient (each 5 column volumes [CV] 50 mM, 75 mM, 100 mM and 500 mM imidazole). Subsequently the receptor protein containing fractions were pooled, desalted with a HiPrep™ 26/10 column (GE Healthcare) and further purified by a second IMAC step (1 ml HiTrap™ sepharose column) with a imidazole gradient 100 – 500 mM in 50 mM steps each with 7 CV. As a final step the target protein containing fractions were purified by gel filtration using a HiLoad™ Superdex200 16/60 preparation grade column (GE Healthcare) pre-equilibrated with 20 mM HEPES, 100 mM NaCl (pH 7.5). The overall yield was 0.2 mg/L cell culture for sEGFRvIII and 0.5 mg/L cell culture and 1 mg/L cell culture for sIGF-1R domain I-III and domain II, respectively.

All proteins were stored in 10 mM HEPES, 50 mM NaCl (pH 7.5) at ~5 mg/ml at 4°C.

4.3.3. Fab fragments

Antibody cleavage. The antibodies EMD72000 (matuzumab), C225 (cetuximab) and EMD1159476 were provided by Merck KGaA. They were enzymatically cleaved by papain digestion to generate Fab fragments Fab72000, FabC225 and Fab1159476, respectively. The ImmunoPure® Fab Preparation Kit (Pierce) was used according the manufacturer's instructions.

Fab fragment purification. The Fab fragments were purified by protein A affinity chromatography and gel filtration using a Superose6 column (GE Healthcare) or a HiLoadTM Superdex200 16/60 preparation grade column (GE Healthcare) both pre-equilibrated with 20 mM HEPES, 100 mM NaCl (pH 7.5). Preparations of 50 mg yielded about 9 mg pure Fab fragments. Purified Fab fragments were stored in the purification buffer at ~10 mg/ml at 4°C.

4.3.4. Receptor:Fab complexes

The receptor:Fab complexes were generated by mixing purified receptor protein (see 4.3) with purified Fab fragments (see 4.3.3). To ensure a saturation of the receptor constructs with the antibody the respective smaller complex component was added in a 1.2 molar excess. The complexes of each receptor constructs (sEGFR, sEGFRd3, sIGF-1Rd1-3, sIGF-1Rd2) and the Fab fragments of the respective antibodies were purified by size exclusion chromatography (SEC) using a Bio-Silect[®] SEC 250-5 column (Bio-Rad) or a Superdex75 HR column (GE Healthcare) pre-equilibrated with 20 mM HEPES, 100 mM NaCl (pH 7.5).

4.4. Molecular interactions and biophysics

4.4.1. Dynamic light scattering

Dynamic light scattering (DLS) measurements were conducted to investigate the polydispersity of the soluble receptor samples before crystallization. Samples at a concentration of 2 mg/ml were analyzed using a DynaPro Titan instrument (Wyatt Technologies) at 25°C in 10 mM HEPES, 50 mM NaCl (pH 7.5) and evaluated by the Dynamics 6.7.6 software (Wyatt Technologies).

4.4.2. Static light scattering

Analytical SEC/static light scattering (SLS) studies were performed to investigate the homogeneity in samples intended to crystallize or to determine the oligomeric state in receptor samples with and without ligand. 30-40 µl protein solution were injected onto a Superdex75 HR analytical SEC column (GE Healthcare) or TSK SuperSW3000 4.6/30 column (Tosoh Bioscience) equilibrated with 20 mM HEPES, 100 mM NaCl (pH 7.5) using an Agilent 1200 HPLC system. Light scattering data for protein eluting from the SEC column were collected using a DAWN-HELEOS-II static light scattering detector coupled to an in-line refractive index meter (Wyatt Technologies). The data were analyzed using the Astra V software (Wyatt Technologies).

4.4.3. Surface plasmon resonance

Surface Plasmon Resonance (SPR)/Biacore studies were carried out to investigate the binding affinities of the antibody Fab fragments or natural ligands to the soluble receptor constructs. The samples were investigated using a Biacore 3000 instrument at 25°C in 10 mM HEPES, 150 mM NaCl, 3 mM EDTA and 0.005% Tween-20 (pH 8.0). All data were analyzed using Prism 4 (GraphPad Software, Inc.).

Fab surface preparation. Fab antibody fragments (see 4.3.3) were immobilized on a CM5-chip as follows: the CM-dextran matrix was activated with *N*-ethyl-*N'*-(dimethylaminopropyl)-carbodiimide hydrochloride (EDC) and *N*-hydroxysuccinimide (NHS). After Fab immobilization the remaining reactive sites were blocked with 1 M ethanolamine-HCl (pH 8.5). Fab72000 (5 µg/ml) was immobilized in 10 mM sodium acetate (pH 5.0) at a flow rate of 5 µl/min for 20 min with a final immobilization level of 1400 response units (RU). FabC225 (10 µg/ml) was immobilized in 10 mM sodium acetate (pH 5.5) at a flow rate of 10 µl/min for 5 min with a final immobilization level of 1300 RU. Fab1159476 (Fab EMD1159476) (5 µg/ml) was immobilized in 10 mM sodium acetate (pH 4.5) at a flow rate of 10 µl/min for 10 min. The final immobilization level for Fab1159476 was 1400 RU.

The Fab72000 surfaces used in the experiments presented in section 5 were regenerated with 1 M NaCl in 10 mM glycine (pH 2.5). The Fab surfaces used in experiments presented in section 6 and 7 (Fab72000, FabC225, Fab1159476) were regenerated with 1 M NaCl in 10 mM NaOH (pH 11.3).

EGF surface preparation. EGF (200 µg/ml) (R&D Systems) in sodium acetate (pH 4.0) was immobilized at a flow rate of 5 µl/min for 10 min on an activated CM5 chip surface (Ferguson *et al.*, 2000; Li *et al.*, 2005). The final immobilization level was 250 RU. Regeneration of the EGF surface was carried out with 1 M NaCl in 10 mM sodium acetate (pH 5.0).

Titration and competition experiments. sEGFR, sEGFR domain III and sEGFRvIII were flown as twofold serial dilutions covering a concentration range of 0-1000 nM over the Fab72000 or FabC225 surface. sEGFR wild type, sEGFR mutants and EGFRvIII binding to the immobilized ligand EGF was observed with twofold serial dilutions covering a concentration range of 0-20 µM. sIGF-1R domain I-III and domain II binding to immobilized Fab1159476 was observed with twofold serial dilutions in the range of 0-1000 nM.

Competition experiments were carried out with a constant concentration of the receptor protein (600 nM). The binding to a ligand surface was monitored while increasing amounts of Fab fragments ranging from 0-30 µM were added to the receptor sample.

4.4.4. Analytical ultracentrifugation

Analytical ultracentrifugation sedimentation equilibrium (AUC SE) experiments were performed to investigate the dimerization state of sEGFR in the presence of ligand and Fab72000 using an XL-A analytical ultracentrifuge (Beckman, USA). Samples (4 μ M) of wild type or mutated sEGFR protein were analyzed both in the presence and in the absence of a 1.5-fold molar excess of EGF. As control the molecular weight of a dimerization incompetent sEGFR in complex with Fab was obtained with and without EGF. The dimerization incompetent receptor was provided by Jessica Dawson, University of Pennsylvania. Each sample contained 4 μ M of the relevant protein or sEGFR:Fab72000 complex in 20 mM HEPES, 100 mM NaCl (pH 7.5). Samples were loaded in six-channel charcoal-Epon cells with quartz windows at both ends. Radial scans were performed at 20°C at 6,000, 9,000, and 12,000 rpm in an An Ti 60 rotor, with detection over a wavelength range of 236 to 285 nm. Equilibrium was reached in each speed step within 18h. The partial specific volume of sEGFR proteins was estimated as 0.71 ml/g as described before (Ferguson *et al.*, 2000), and solvent density was taken as 1.003 g/ml. Molecular masses were determined by fitting multiple data sets to a simple model for a single species in Sedfit version 9.4c and Sedphat version 4.4b.

4.4.5. Isothermal titration calorimetry

Isothermal titration calorimetry (ITC) was carried out to investigate the binding affinity of the receptor ectodomains to the antibody Fab fragments and the thermodynamics of the interaction. The experiments were carried out using a VP-ITC microcalorimeter (Microcal LLC) and evaluated with the Origin 7 calorimetry software (MicroCal LLC) to calculate the binding constant (K_A) and the binding affinity ($K_D=1/K_A$), the observed binding enthalpy (ΔH^{obs}) as well as the stoichiometry (N) of the formed complex. For all receptor Fab binding experiments a model of one binding site was assumed. ΔH^{obs} values were calculated based on the difference between the heat liberated during the binding phase of the injections and the average heat of dilution found once the receptor was saturated with antibody.

10 μ l Fab solution (16.7-50 μ M) (see 4.3.3) was titrated to 2 ml receptor in the cell (1.7-5 μ M) (see 4.3). More precisely, Fab72000 (20 μ M) in 10 mM HEPES, 50 mM NaCl (pH 7.5) was injected in 10 μ l steps into a cell containing 2 μ M sEGFR. Fab1159476 (16.7 μ M) in PBS was injected in 11 μ l steps into a cell containing 1.7 μ M sIGF-1R domain I-III (sIGF-1Rd1-3). In addition Fab1159476 was investigated for sIGF-1R domain II (sIGF-1Rd2)

binding and was injected at 50 μM in PBS in 11 μl steps into a cell containing 5 μM sIGF-1Rd2. All binding experiments were carried out at 25°C with a spacing time between the injections of 320 sec.

4.4.6. Small angle X-ray scattering

Small angle X-ray scattering (SAXS) experiments were carried out to determine a low resolution shape (Koch *et al.*, 2003) of sEGFRvIII in solution. The scattering data from sEGFRvIII samples (see 4.3.2) were collected at the SAXS beamline EMBL, DESY, Germany. Using a MAR345 image plate detector at a sample-detector distance of 2.7 m and a wavelength of $\lambda = 1.5 \text{ \AA}$ a range of $0.01 < s < 0.5 \text{ \AA}^{-1}$ was covered ($s = 4\pi \sin\theta/\lambda$, where 2θ is the scattering angle and λ the X-ray wavelength). 100 μl samples of three different concentrations (1 mg/ml, 5 mg/ml and 10 mg/ml in 20 mM HEPES, 100 mM NaCl, pH 7.5) were measured at 10°C for 120 sec. To monitor for radiation damage two successive measurements of protein solutions were compared and no significant changes were observed. The scattering intensities of buffer backgrounds were measured both before and after the sample and the averaged background scattering was subtracted from the scattering of the sample.

The low angle data measured at lower protein concentrations were extrapolated to infinite dilution and merged with the higher concentration data to yield the final composite scattering curve. Data processing was performed using the program PRIMUS (Konarev *et al.*, 2003).

The radius of gyration R_g was calculated using the Guinier approximation (Guinier, 1939) and the program GNOM (Svergun, 1992), which also provided the distance distribution function of the particle $p(r)$ and the maximum particle size D_{max} . The molecular mass of the solute was estimated based on the excluded (Porod) volume (Porod, 1982). For globular proteins, the Porod volume in nm^3 is about twice the molecular mass in kDa.

Molecular modeling. The theoretical scattering from the low resolution crystal structure of sEGFRvIII (see 4.5.4) was calculated using the program CRY SOL (Svergun *et al.*, 1995). Given the atomic coordinates, the program uses the scattering amplitudes to calculate the spherically averaged scattering pattern and takes into account the hydration shell of the protein.

Domain I and II of sEGFRvIII, which are disordered in the crystal structure (see 6.2.4), were modeled using the program BUNCH (Petoukhov and Svergun, 2005). The program combines rigid body and *ab initio* modeling of proteins consisting of domains linked by

flexible loops of unknown structure. A simulated annealing protocol is employed to model the probable conformation of the flexible linkers with the structurally known domains kept as rigid bodies. The *ab initio* modeled loops are represented as interconnected chains of dummy residues (Petoukhov *et al.*, 2002). Domain/loop arrangements with steric clashes, dummy residue loops with improper distribution of bond or dihedral angles as well as too extended loops are penalized.

***Ab initio* shape determination.** The scattering curve of sEGFRvIII was further used to model the low resolution *ab initio* shape of solution sEGFRvIII by the program DAMMIN (Svergun, 1999). This program represents the particle shape by a densely packed bead model, which is fitted through simulated annealing procedures to the experimental data $I_{\text{exp}}(s)$. The models of 10 DAMMIN runs were averaged to determine common structural features using the programs DAMAVER (Volkov and Svergun, 2003) and SUPCOMB (Kozin and Svergun, 2001).

4.5. Protein Crystallography

4.5.1. sEGFR:Fab72000

sEGFR in complex with Fab72000 (see 4.3.4) was concentrated and buffer exchanged by gel filtration into 10 mM HEPES, 50 mM NaCl (pH 7.5) and crystallized using the hanging drop vapor diffusion method. The polydispersity of sEGFR:Fab72000 samples as determined by dynamic light scattering was 15.7%. The complex crystallized in several conditions with a low pH value [0.1 M sodium acetate, 1.7 M ammonium sulfate (pH 4.5) at 4°C; 50 mM citrate, 17% PEG-3350, 1.6 M NaCl, 3% ethylene glycol (pH 5.0) at 20°C; 0.1 M phosphate-citrate, 20% PEG-1000, 0.25 M lithium sulfate (pH 4.2) at 20°C], but the crystals proved to be unstable and/or with low diffraction quality.

4.5.2. Fab72000

Freshly purified protein (see 4.3.3) was concentrated and buffer exchanged by gel filtration into 10 mM HEPES, 50 mM NaCl (pH 7.5) and crystallized using the hanging drop vapor diffusion method. Single crystals of Fab72000 (0.1x0.5x0.1 mm) were obtained by mixing equal volumes (1:1) of the Fab (13 mg/ml) with a solution containing 1.8 M ammonium sulfate, 0.1 M MES (pH 6.5) and equilibrating over a reservoir of this buffer at 20°C. Crystals were flash frozen in reservoir solution that was supplemented with 9% sucrose, 2% glucose, 8% glycerol, 8% ethylene glycol. X-ray diffraction data were collected at the Cornell High Energy Synchrotron Source (CHESS) beamline F1, using an ADSC Quantum-210 CCD detector. The data were processed with HKL2000 (Otwinowski and Minor, 1997). Data collection statistics are summarized in Table 2 (see 4.5.3).

The structure of Fab72000 was solved by the method of molecular replacement using the program PHASER (CCP4, 1994). The coordinates for Fab2C4 (PDB ID 1L7I) (Vajdos *et al.*, 2002) were selected as the initial search model based on the sequence identity between Fab2C4 and Fab72000. Coordinates were manually rebuilt in COOT (Emsley and Cowtan, 2004) and refined using CNS (Brünger *et al.*, 1998) and Refmac (CCP4, 1994). New maps were calculated following each iteration of refinement, including solvent flattened maps with minimized model bias calculated using the program DM (CCP4, 1994). Refinement statistics are summarized in Table 2 (see 4.5.3).

Coordinates of the Fab72000 structures have been deposited with the PDB ID code 3C08.

4.5.3. sEGFRd3:Fab72000

Freshly purified sEGFRd3:Fab72000 (see 4.3.4) was crystallized by mixing equal parts (1 μ l) of the SEC purified complex (14 mg/ml) with 1 M NaCl, 16% PEG 3350, 50 mM MES (pH 6.0) and equilibrating over a reservoir of the same buffer at 20°C. Streak seeding was used to produce large single crystals (0.5x0.1x0.15 mm) (Fig. 4) that were cryostabilized by serial transfer to solutions of reservoir containing increasing concentrations of ethylene glycol.

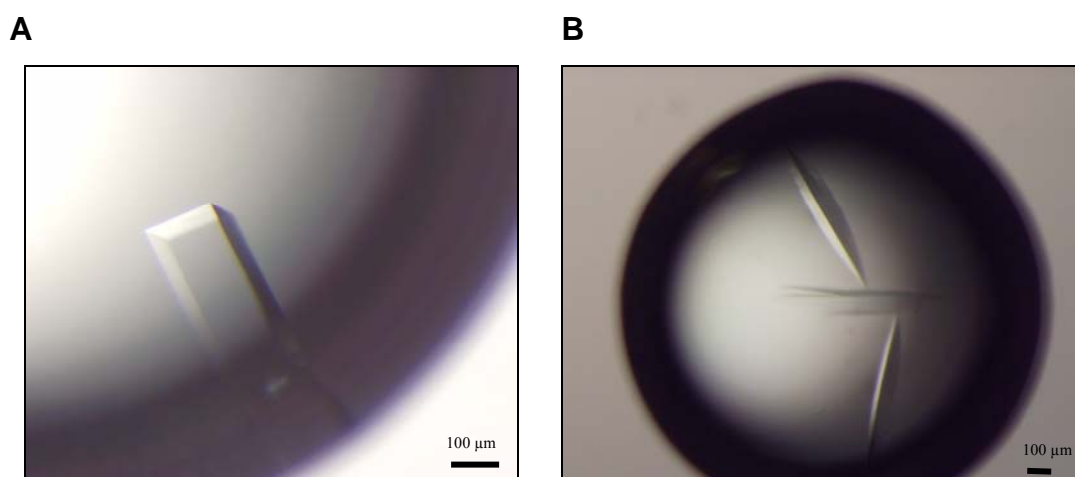


Fig. 4: Crystals of the complex sEGFRd3:Fab72000

The crystals of sEGFRd3:Fab72000 grow after one week at 20°C in 50 mM MES pH 6.0, 1 M NaCl, 16% PEG-3350.

Following transfer to the final cryostabilizer of reservoir plus 15% ethylene glycol, crystals were flash frozen in liquid nitrogen. Data were collected at the Swiss Light Source (SLS) beamline X06SA, using a Mar225 CCD detector. The data were processed with HKL2000 (Otwinowski and Minor, 1997). Data collection statistics are summarized in Table 2.

The structure of sEGFRd3:Fab72000 was solved by methods of molecular replacement using the program PHASER (CCP4, 1994). The Fab fragments in the asymmetric unit were located using the refined Fab72000 coordinates (see 4.5.2) as search model. With the position of the first Fab fragment fixed, a second search using the coordinates of domain III of sEGFR (amino acids 310-500 from PDB ID 1YY9) located one of the sEGFRd3 molecules. Subsequently the second sEGFRd3:Fab72000 complex in the asymmetric unit was found. Refinement was carried out as described in 4.5.2. Refinement statistics are summarized in Table 2.

Coordinates of the sEGFRd3:Fab72000 structures have been deposited with the PDB ID code 3C09.

Table 2: Data collection and refinement statistics Fab72000 and sEGFRd3:Fab72000

| Data collection statistics ^a | | |
|--|---|---|
| | Fab72000 | sEGFRd3:Fab72000 |
| Space group | P2 ₁ 2 ₁ 2 ₁ | C2 |
| Unique cell dimensions | a = 56.8 Å, b = 61.4 Å, c = 102.7 Å | a = 141.1 Å, b = 205.0 Å, c = 81.6 Å β = 117.5° |
| X-ray source | CHESS F1 | SLS X06SA |
| Resolution limit | 2.15 Å | 3.2 Å |
| Observed/unique | 107,297 / 20,191 | 120,206 / 33,886 |
| Completeness (%) | 99.9 (99.9) | 99.7 (98.7) |
| R _{sym} ^b | 0.10 (0.42) | 0.12 (0.35) |
| <I/σ> | 20.7 (3.6) | 11.4 (3.4) |
| Refinement statistics | | |
| Resolution limits | 50 – 2.15 Å | 50 – 3.2 Å |
| No. of reflections/no. test set | 19,098 / 1,029 | 32,028 / 1,709 |
| R factor (R _{free}) ^c | 0.22 (0.26) | 0.24 (0.29) |
| Asymmetric unit | One Fab72000 molecule | Two sEGFRd3:Fab72000 complexes |
| Protein | aa 4-211 of light chain; aa 1-224 of heavy chain | aa 310-500 of mature sEGFR with 13 saccharide units; aa 1-211 of Fab light chain; aa 1-135, 142-222 of Fab heavy chain ^d |
| Water/ions | 99 water molecules; 2 sulfates | - |
| Total number of atoms | 3,209 | 8,517 |
| RMSD bond length (Å) | 0.012 | 0.015 |
| RMSD bond angles (°) | 1.35 | 1.6 |

^aNumbers in parentheses refer to highest resolution shell.

^bR_{sym} = Σ|I_h - <I_h>| / ΣI_h, where <I_h> = average intensity over symmetry equivalent measurements.

^cR factor = Σ|F_o - F_c| / ΣF_o, where summation is over data used in the refinement; R_{free} includes 5% of the data excluded from the refinement.

^dThe number of missing amino acids in the heavy and light chains differs in the two complexes

4.5.4. sEGFRvIII

Freshly purified sEGFRvIII (see 4.3.2) was crystallized using the hanging drop vapor diffusion method. Initial crystals were obtained by mixing equal volumes (1:1) of sEGFRvIII concentrated to 4.5 mg/ml with a solution containing 50 mM acetate (pH 4.8), 22% PEG3350, 10 mM EDTA and equilibrating over a reservoir of this buffer at 20°C. Streak seeding techniques were used to obtain large single crystals that were cryostabilized in reservoir solution supplemented with 25% glycerol. X-ray diffraction data were collected at the Swiss Light Source (SLS) beamline X06SA using a PILATUS 6M detector. The data were processed with XDS (Kabsch, 1993). Data collection statistics are summarized in Table 3.

The structure of sEGFRvIII was solved by molecular replacement using the program PHASER (CCP4, 1994). As search models the domain III and domain IV of sEGFR (amino acids 310-500 and 501-614 from PDB ID 1YY9) were used. Coordinates were manually rebuilt in COOT (Emsley and Cowtan, 2004) and refined with Refmac (CCP4, 1994). Current refinement statistics are summarized in Table 3.

Table 3: Data collection and refinement statistics sEGFRvIII

| Data collection statistics ^a | |
|--|---|
| Space group | P6 ₅ |
| Unique cell dimensions | a = 150 Å, b = 150 Å, c = 44 Å $\alpha = 90^\circ, \beta = 90^\circ, \gamma = 120^\circ$ |
| X-ray source | SLS X06SA |
| Resolution limit | 3.9 Å |
| Observed/unique | 53,719 / 5515 |
| Completeness (%) | 99.2 (95.7) |
| R _{sym} ^b | 0.096 (0.701) |
| $\langle I/\sigma \rangle$ | 20.2 (3.4) |
| Refinement statistics | |
| Resolution limits | 50 – 3.9 Å |
| R factor (R _{free}) ^c | 28.4 (37.6) |
| Asymmetric unit | One sEGFRvIII molecule |
| Protein | aa 300 - 501 of sEGFR wild type with three saccharide units |
| Water/ions | - |
| Total number of atoms | 2,382 |
| RMSD bond length (Å) | 0.032 |
| RMSD bond angles (°) | 3.2 |

^aNumbers in parentheses refer to highest resolution shell.

^bR_{sym} = $\sum |I_h - \langle I_h \rangle| / \sum I_h$, where $\langle I_h \rangle$ = average intensity over symmetry equivalent measurements.

^cR factor = $\sum |F_o - F_c| / \sum F_o$, where summation is over data used in the refinement; R_{free} includes 5% of the data excluded from the refinement.

4.5.5. Fab1159476

Crystals of Fab EMD1159476 (Fab1159476) (see 4.3.3) were obtained by mixing equal volumes (1 μ l) of the Fab (19 mg/ml) with a solution containing 0.1 M Tris, 25% PEG-3350 (pH 8.8) and equilibrating over a reservoir of this buffer at 20°C. Streak seeding was used to produce single crystals. The crystals were flash frozen in reservoir solution that was supplemented with 25% glycerol. X-ray diffraction data were collected at the Swiss Light Source (SLS) beamline X06SA, using a PILATUS 6M detector. The data were processed with XDS (Kabsch, 1993). Data collection statistics are summarized in Table 4.

The structure of the Fab1159476 was solved by molecular replacement using the program PHASER (CCP4, 1994). As initial search model the coordinates of an anti-steroid Fab (PDB ID 1DBA) (Arevalo *et al.*, 1993) was chosen based on similarity of the elbow angle (Stanfield *et al.*, 2006). Refinement was carried out exactly as described in 4.5.2. Data collection and refinement statistics of the EMD1159476 Fab fragment structure are given in Table 4.

Table 4: Data collection and refinement statistics Fab1159476

| Data collection statistics ^a | |
|--|--|
| Space group | P12 ₁ 1 |
| Unique cell dimensions | a = 40.3 Å, b = 140.1 Å, c = 74.3 Å β = 96.7° |
| X-ray source | SLS X06SA |
| Resolution limit | 1.7 Å |
| Observed/unique | 287,820 / 85,024 |
| Completeness (%) | 94.4 (89.4) |
| R _{sym} ^b | 0.07 (0.41) |
| <I/ σ > | 12.8 (2.9) |
| Refinement statistics | |
| Resolution limits | 50 – 1.7 Å |
| R factor (R _{free}) ^c | 0.19 (0.23) |
| Asymmetric unit | One Fab1159476 molecule |
| Protein | aa 1-212 of light chain; aa 1-219 of heavy chain |
| Water/ions | 655 water molecules |
| Total number of atoms | 7,045 |
| RMSD bond length (Å) | 0.014 |
| RMSD bond angles (°) | 1.42 |

^aNumbers in parentheses refer to highest resolution shell.
^bR_{sym} = $\sum |I_h - \langle I_h \rangle| / \sum I_h$, where $\langle I_h \rangle$ = average intensity over symmetry equivalent measurements.
^cR factor = $\sum |F_o - F_c| / \sum F_o$, where summation is over data used in the refinement; R_{free} includes 5% of the data excluded from the refinement.

5. Matuzumab binding to EGFR prevents the conformational rearrangement required for dimerization*

5.1. Introduction

The epidermal growth factor receptor (EGFR) belongs to the best studied receptor tyrosine kinases (RTKs). In mammals, EGFR is one of a family of four RTKs collectively known as the ErbB or HER receptors (Holbro and Hynes, 2004) that is involved in critical cellular processes such as proliferation, differentiation and apoptosis (Schlessinger, 2000; Hubbard and Miller, 2007). Beside EGFR (ErbB1), the family includes ErbB2/HER2/Neu (Citri *et al.*, 2003) as well as the neuregulin receptors ErbB3/HER3 (Citri *et al.*, 2003) and ErbB4/HER4 (Carpenter, 2003). Each has a large extracellular ligand-binding domain (~620 amino acids), a single transmembrane α -helix, and an intracellular region that contains a juxtamembrane region (~45 amino acids), a tyrosine kinase domain (~270 amino acids) and a C-terminal regulatory sequence (~230 amino acids) (Fig. 5).

* The work described in this part of the thesis has been published in Schmiedel *et al.* (2008) *Cancer Cell* **13**, 365-373 and commented in Leahy (2008) *Cancer Cell* **13**, 291-293 (see Appendix 11.3).

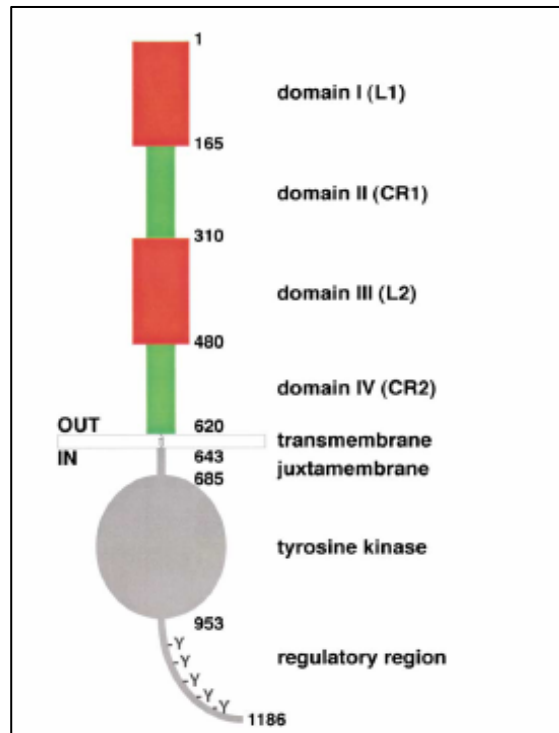


Fig. 5: Domain organization of ErbB receptors

ErbB receptors comprise an extracellular region consisting of domains I-IV, a transmembrane helix and an intracellular region with a juxtamembrane domain, a tyrosine kinase and a regulatory region. Residue numbers of domain boundaries refer to EGFR. L domain, large domain; CR domain, cysteine-rich domain (figure taken from Burgess *et al.*, 2003).

The extracellular region of the ErbB receptors comprises four distinct domains of two different types. There are two homologous large (L) domains (red in Fig. 5), and two cysteine-rich (CR) domains (green in Fig. 5), which occur in the order L1 (I) -CR1 (II) -L2 (III) -CR2 (IV) (Ward *et al.*, 1995). Domains I and III share 37% sequence identity in EGFR (Burgess *et al.*, 2003).

EGFR was one of the first RTKs for which ligand-induced dimerization was described as initial event in transmembrane signaling (Yarden and Schlessinger, 1987a; Yarden and Schlessinger, 1987b; Jorissen *et al.*, 2003). Binding of ligand shifts a monomer-dimer equilibrium to favor the dimeric state (Schlessinger, 2000; Carpenter, 2003). EGFR is regulated by a family of at least seven distinct peptide ligands (Harris *et al.*, 2003), including EGF, transforming growth factor- α (TGF- α), amphiregulin, betacellulin, epigen, epiregulin, and heparin binding EGF-like growth factor (HB-EGF). ErbB2 has no known direct activating ligand (Citri *et al.*, 2003), while ErbB3 and ErbB4 are bound by the four known neuregulins (NRGs) (Falls, 2003).

Upon ligand binding and receptor dimerization the intracellular tyrosine kinase activity is stimulated. In EGFR and ErbB4 homodimers, this occurs through an allosteric mechanism (Zhang *et al.*, 2006b). Kinase autophosphorylation leads to the stimulation of a complex intracellular signaling network (Oda *et al.*, 2005) (see 3.4 and Fig. 2).

5.1.1. Ligand-induced EGFR activation

From 2002 onwards, x-ray crystal structures of the extracellular regions of all human EGFR family members in the absence of ligand were solved (Cho and Leahy, 2002; Ferguson *et al.*, 2003; Cho *et al.*, 2003; Garrett *et al.*, 2003; Franklin *et al.*, 2004; Bouyain *et al.*, 2005). In addition, structures of a large part of the EGFR extracellular region in ligand-induced dimers were published (Ogiso *et al.*, 2002; Garrett *et al.*, 2002). Based on these structures, a model for ligand dependent dimerization and activation of the ErbB receptors has been proposed (Burgess *et al.*, 2003) (Fig. 6).

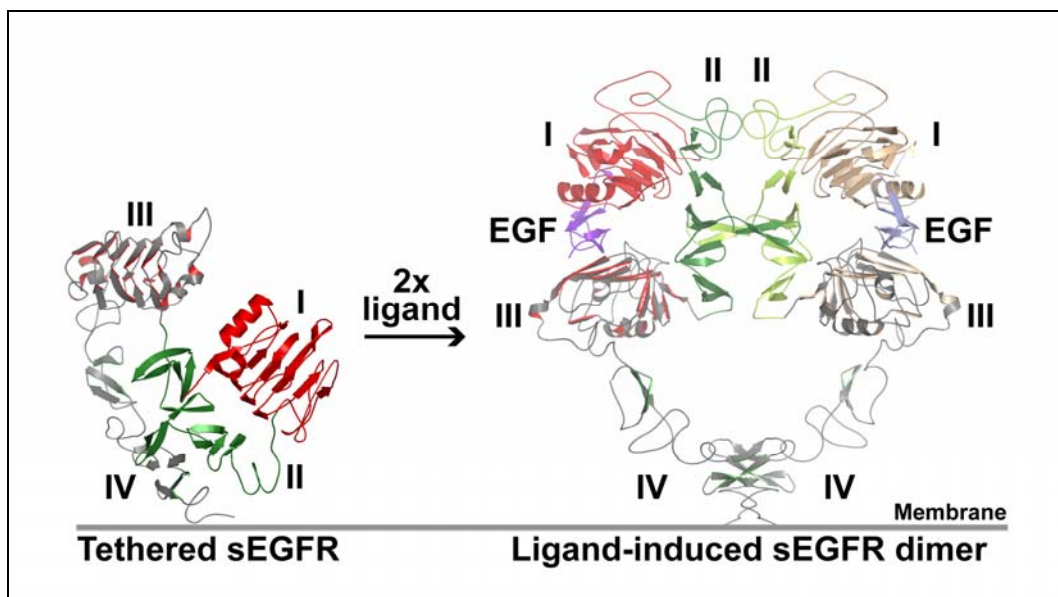


Fig. 6: Ligand induced EGF receptor dimerization

The extracellular region of the EGF receptor (sEGFR) is shown in cartoon representation with domain I in red, domain II in green and domains III and IV in gray with the secondary structure elements highlighted in red and green, respectively. The inactive receptor (left hand view) exists in a tethered, autoinhibited conformation with an intramolecular interaction between the domains II and IV. Upon ligand binding the receptor adopts a very different domain arrangement (right hand view). Ligand (here EGF, shown in purple cartoon) binds between domains I and III of a single EGFR molecule, stabilizing the precise, extended configuration of EGFR that can dimerize. All contacts between the two molecules in the dimer are receptor mediated with domain II providing the primary dimerization contacts. EGF receptor dimerization is ligand induced, but entirely receptor mediated. The colors on the right hand molecule in the sEGFR dimer have been muted for contrast. Coordinates from PDB IDs 1IVO and 1NQL were used to generate this figure. Domain IV in the sEGFR dimer was modeled as previously described (Ferguson *et al.*, 2003).

In a dimer of the EGFR extracellular domains, all intermolecular interactions are contributed by the receptor (Ogiso *et al.*, 2002; Garrett *et al.*, 2002). This entirely receptor mediated dimerization is unique among the RTKs with known ligand-bound structures. In all other ligand RTK complex structures the ligand is located in between the two monomers mediating the dimerization (see 0).

The majority of interactions in the dimer of the EGFR extracellular domains (sEGFR) is contributed by domain II. A ‘dimerization arm’ (Ogiso *et al.*, 2002) protrudes into the dimer interface directly contacting the other receptor monomer. However, it was shown through mutation and deletion studies that simply exposing the dimerization arm is not sufficient to promote sEGFR dimerization in the absence of ligand (Elleman *et al.*, 2001; Ferguson *et al.*, 2003). Additional conformational changes induced by the ligand are required to stabilize the precise conformation of domain II (Dawson *et al.*, 2005; Lemmon, 2009). Further interactions in the sEGFR dimer are contributed by parts of domain IV that are close to or contacting each other as suggested by modeled structures (Ferguson *et al.*, 2003) and biochemical and biophysical data (Berezov *et al.*, 2002; Dawson *et al.*, 2007; Mi *et al.*, 2008).

In the unliganded state the receptor adopts a very different conformation that occludes much of the domain II dimerization interface in an intramolecular interaction or tether with domain IV (Cho and Leahy, 2002; Ferguson *et al.*, 2003) (left hand in Fig. 6). This conformation is thought to be autoinhibited (Burgess *et al.*, 2003). Upon ligand binding both the domain I and domain III are contacting the ligand, which exposes the domain II and domain IV dimerization interface. Thus, promoted by ligand binding the extracellular region of EGFR must undergo a dramatic domain rearrangement to be able to dimerize.

5.1.2. Structures of ErbB receptor family extracellular domains

Interestingly, the EGFR family includes an orphan receptor that nonetheless shows tyrosine kinase activity (ErbB2) and an NRG binding receptor (ErbB3) that lacks tyrosine kinase activity (Burgess *et al.*, 2003). As shown in Fig. 7, the unliganded extracellular regions of EGFR (Ferguson *et al.*, 2003), ErbB3 (Cho and Leahy, 2002) and ErbB4 (Bouyain *et al.*, 2005) adopt the tethered, autoinhibited conformation. Based on solution scattering studies, binding of neuregulins is thought to promote a similar structural reorganization of the receptor as seen for EGF (Dawson *et al.*, 2007). In contrast, structures of the ErbB2 extracellular domain (Cho *et al.*, 2003; Garrett *et al.*, 2003; Franklin *et al.*, 2004) revealed a conformation that is similar to the extended, dimerization competent receptor form. ErbB2 has no known ligand (Citri *et al.*, 2003). Nevertheless this receptor is able to transform cells just by

overexpression (Di Fiore *et al.*, 1987). It was shown that these impaired receptors are signaling at the cell surface through heterodimerization (Wada *et al.*, 1990).

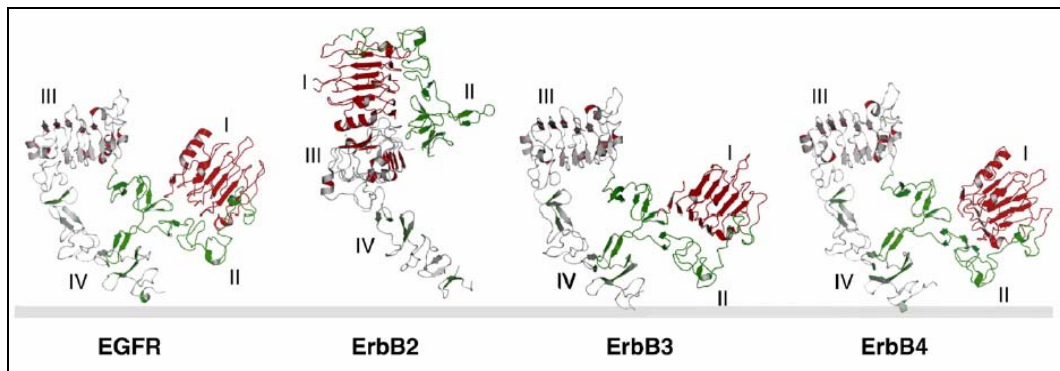


Fig. 7: ErbB family extracellular domain structures without ligand

The structures of the extracellular domains of each ErbB receptor family member in the absence of ligand are shown in cartoon presentation. The coloring is the same as in Fig. 6. EGFR, ErbB3 and ErbB4 adopt the autoinhibited conformation with an intramolecular tether between domain II and IV. ErbB2 in contrast adopts an extended conformation that resembles the ligand-induced dimerization-competent form described in Fig. 6 (structures from Lemmon, 2009).

5.1.3. ErbB receptor dimerization at the cell surface

The model of ligand-induced dimerization (Fig. 6) is in accordance with results for EGFR and ErbB4 receptor homodimerization both at the cell surface and in solution (Lemmon, 2009). However, it fails to answer all questions about ErbB receptor heterodimerization at the cell surface. It is e.g. not clear, why ErbB2 forms heterodimers with all other EGF receptor family members at the cell surface (Graus-Porta *et al.*, 1997; Berger *et al.*, 2004; Wehrman *et al.*, 2006), while it remains monomeric in solution (Horan *et al.*, 1995; Ferguson *et al.*, 2000).

Furthermore, the dimerization model can not explain results from EGF binding studies at the cell surface. Scatchard plots showing a characteristic curvilinear (concave-up) form and ligand competition assays at the cell surface indicate heterogenic ligand binding sites and a negative cooperativity of EGF receptor binding (Shoyab *et al.*, 1979; Magun *et al.*, 1980; Macdonald and Pike, 2008). These findings resulted in the proposal of two different receptor affinity classes at the cell surface, with 2%–5% of receptors binding EGF with high affinity ($K_D < 0.1$ nM) and 92%–95% binding with lower affinity (K_D 6–12 nM) (Hunter *et al.*, 1984; Livneh *et al.*, 1986; Defize *et al.*, 1989; Ullrich and Schlessinger, 1990; Bellot *et al.*, 1990; Burgess *et al.*, 2003). However, the two states can not just be equalized with the tethered and extended conformations of the extracellular domains (Fig. 6). Such a model would lead to positive cooperativity and concave-down Scatchard plots (Wofsy *et al.*, 1992; Lemmon *et al.*, 1997; Özcan *et al.*, 2006). Negative cooperativity requires that the binding of a second EGF to a dimer plus one EGF would need to have a substantially lower affinity than the first EGF

binding event. At the cell surface the receptor dimer with a single EGF bound would be the major species at subsaturating ligand concentrations. This was indeed seen in studies with excess ligand binding to high affinity EGFR and interestingly also for the insulin receptor (Wofsy *et al.*, 1992; Lemmon, 2009). To further complicate interpretation, there is evidence for EGF binding to higher oligomeric EGFR states beside the dimer (Prähl *et al.*, 1991; De Meyts, 1994; Macdonald and Pike, 2008; De Meyts, 2008).

These results imply that additional factors beside the extracellular receptor domains that are responsible for negative cooperativity and heterodimerization at the cell surface (Clayton *et al.*, 2005; Saffarian *et al.*, 2007). It was shown that the transmembrane domains (Holbrook *et al.*, 2000; Domagala *et al.*, 2000; Klein *et al.*, 2004; Mayawala *et al.*, 2005; Lemmon, 2009) as well as the intracellular domains (Mendrola *et al.*, 2002; Duneau *et al.*, 2007) are triggering dimerization and could be crucial for regulating the association of two ErbB receptors. Thus, for a complete picture of ErbB receptor regulation it seems to be necessary to consider the intact EGFR structure and to combine cellular and structural data. This is especially important for the development of anti-cancer drugs that inhibit misregulated ErbB receptors.

5.1.4. EGFR and cancer

In the 1980s EGFR was the first cell-surface receptor to be linked directly to cancer as described in fibroblasts infected with oncogenic viruses (De Larco and Todaro, 1987). It was found that the *neu* oncogene encodes a protein related to EGFR (Schechter *et al.*, 1984; Coussens *et al.*, 1985) and that the product of the *v-erbB* oncogene from avian erythroblastoma virus is a truncated form of EGFR (Downward *et al.*, 1984). These findings revolutionized both the field of growth factors and of cancer biology. It is now known that EGFR is aberrantly activated in a variety of epithelial tumors e.g. metastatic non-small-cell lung cancer, colorectal cancer, squamous-cell carcinoma of head and neck and pancreatic cancer (Mendelsohn and Baselga, 2006). ErbB2/HER2 overexpression is connected to breast cancer (Park *et al.*, 2008). Malignant transformation of the cell in these cancers can be caused through EGFR overexpression or mutation, which leads to constitutive activity or impaired receptor down-regulation (Mendelsohn and Baselga, 2006). Anti-EGFR agents are now approved since the late 1990s in the therapy of non-small cell lung cancer (NSCLC), colon cancer and head and neck cancer, pancreatic cancer and breast cancer, in which they provide significant clinical benefit (Baselga, 2008). The next step in targeted therapy will be the development of predictive markers of response to anti-EGFR agents to identify suitable

patients that will benefit from the treatment. Such markers are downstream effector proteins of the signaling cascade, e.g. Ras and PTEN (phosphatase and tensin homologue) (Nagata *et al.*, 2004; Khambata-Ford *et al.*, 2007; Benvenuti *et al.*, 2007). Increased response rates might be achieved by combination of inhibitors against several members of the same signaling pathway (Zhang *et al.*, 2007; Baselga, 2008) (see also 3.4).

The ErbB regulation mechanism (see 5.1.1 and 5.1.3) suggests a number of ways to inhibit EGFR activation (Baselga, 2002). Intracellularly the kinase domain can be blocked with low molecular weight ATP-competitive tyrosine kinase inhibitors (TKIs), e.g. gefitinib (Iressa[®]), erlotinib (Tarceva[®]) or lapatinib (Tykerp[®]) (Zhang *et al.*, 2007). Gefitinib (AstraZeneca) was approved in 2003 by the US American Food and Drug administration (FDA) for NSCLC; erlotinib (OSI Pharmaceuticals) was approved in 2004 for NSCLC and pancreatic cancer. In 2005 gefitinib failed to show an advantage for patients with NSCLC and was withdrawn from the market (Singer, 2005). After retrospectively studying lung cancer samples from patients enrolled in that studies (Shepherd *et al.*, 2005; Thatcher *et al.*, 2005) it became clear that a part of these patients did not express EGFR at high levels and thus was less gefitinib sensitive from the beginning (Hirsch *et al.*, 2007). This highlights the necessity to develop bio-markers in order to identify patients that will benefit from a targeted therapy. Lapatinib (GlaxoSmithKline), a dual EGFR and ErbB2 inhibitor, was approved in 2007 for HER2 overexpressing breast cancer.

From the extracellular side ErbB family members can be targeted in cancer therapy by monoclonal antibodies as described in the next section.

5.1.5. Anti-EGFR antibodies

The first study with monoclonal antibodies (mAbs) directed against the rat ErbB2 extracellular region were carried out in the early 1980s and found that some mAbs are able to reverse the transformed phenotype of HER2 overexpressing cells (Drebin *et al.*, 1985). Based on this defining study several mAbs to the human extracellular domains of EGFR and ErbB2 were generated with varying effects on the receptor regulation (Hudziak *et al.*, 1989; Lewis *et al.*, 1993). Some induced receptor aggregation thus mimicking ligand activation (Schreiber *et al.*, 1981; Schreiber *et al.*, 1983), while others blocked receptor activation and showed the desired antiproliferative effects (Kawamoto *et al.*, 1983; Sato *et al.*, 1983; Masui *et al.*, 1984; Gill *et al.*, 1984). X-ray crystallographic and biochemical analysis of receptor-antibody complexes have indicated several modes of binding that lead to effective inhibition of ErbB receptor signaling: direct steric blockage of ligand binding or receptor dimerization,

stabilization of the tethered conformation, block of the domain rearrangement required for receptor dimerization, antibody-dependent cellular cytotoxicity (ADCC) and complement-dependent cytotoxicity (CDC), antibody-mediated receptor down-regulation and augmentation of the antitumor effects of chemo- and radiotherapy (Mendelsohn and Baselga, 2006; Leahy, 2008; Schmitz and Ferguson, 2009). Improved efficacy of mAbs in cancer therapy might be achieved by arming the antibodies with radionuclides or toxins (Carter, 2001).

Examples of anti-ErbB receptor antibodies already approved or in clinical trials are listed below.

Cetuximab/Erbitux[®]. The chimeric antibody cetuximab/Erbitux[®] (ImClone/BMS and Merck KGaA) binds to domain III of EGFR, directly blocking ligand binding (Li *et al.*, 2005). Cetuximab was approved by the FDA in 2004 for the treatment of patients with colorectal and head and neck cancer. Clinical trials for cetuximab as a first line treatment are in progress (Bokemeyer *et al.*, 2009; Han *et al.*, 2009).

Panitumumab/Vectibix[®]. The antibody panitumumab/Vectibix[®] (Amgen) was developed from transgenic mice that express fully human antibodies and also binds to EGFR domain III (Yang *et al.*, 2001). Probably it employs a similar ligand binding competition mechanism as cetuximab. As an antibody of the subtype IgG2 it does not stimulate robust antibody dependent ADCC (Schmitz and Ferguson, 2009). In 2006 it was FDA approved for colorectal cancer in combination with chemotherapy and is currently under investigation for first line treatment in colorectal cancer (Stephenson *et al.*, 2008). Recently the addition of panitumumab to the anti-angiogenesis mAb bevacizumab and chemotherapy for the first-line treatment of metastatic colorectal cancer was found to be harmful when compared with bevacizumab and chemotherapy alone (Giusti *et al.*, 2009). Evaluation of this result is still ongoing.

IMC-11F8. The fully human anti-EGFR antibody 11F8 (ImClone) binds to the same epitope on EGFR domain III as cetuximab competing with ligand binding (Li *et al.*, 2008). It has performed well in phase I and is currently investigated in phase II clinical trials.

MAb806, another anti-EGFR antibody, binds to domain II close to the receptor dimerization site (Johns *et al.*, 2004). It was generated using cells expressing EGFR variant III (EGFRvIII, see section 1) as antigen, but also binds to overexpressed wild-type EGFR (Jungbluth *et al.*, 2003). The antibody has performed well in a phase I study (Scott *et al.*, 2007).

Pertuzumab/ Omnitarg[®] (Genentech) binds to the domain II dimerization arm of ErbB2 and directly blocks ligand induced ErbB2 heterodimerization (Franklin *et al.*, 2004). It is a recombinant, humanized mAb and after a phase II study treating breast cancer patients in combination with trastuzumab (Portera *et al.*, 2008) it is currently investigated in a phase III clinical trial (Baselga, 2008).

Trastuzumab/Herceptin[®] (Genentech) binds to the membrane proximal domain IV of ErbB2 (Cho *et al.*, 2003) and likely modulates a cleavage event that leads to ectodomain shedding and kinase activation (Molina *et al.*, 2001). Trastuzumab was FDA approved in 1998 for use in combination with first line chemotherapeutic agents in patients with metastatic breast cancer expressing high levels of ErbB2 (Slamon *et al.*, 2001).

The antibodies with structurally known epitopes are summarized in Fig. 8.

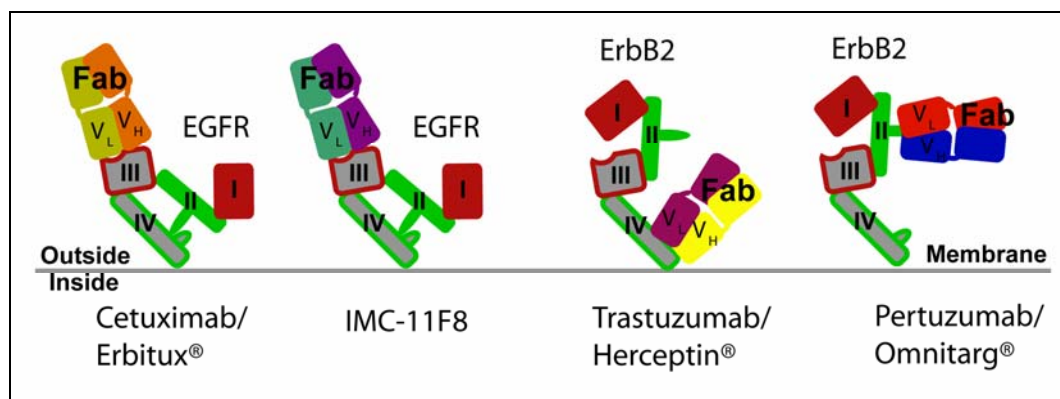


Fig. 8: Antibody receptor co-structures

Cartoon presentation of receptor antibody Fab fragment co-structures. The coloring is the same as in Fig. 6 with the receptor ectodomain in red (domain I) and grey/red (domain III) and green (domain II) and grey/green (domain IV). The antibody Fab fragments of cetuximab/Erbitux[®] is in ocher/orange (Li *et al.*, 2005), of 11F8 in turquoise/violet (Li *et al.*, 2008), of trastuzumab/Herceptin[®] in light violet/yellow (Cho *et al.*, 2003) and of pertuzumab/Omnitarg[®] in red/blue (Franklin *et al.*, 2004). The first two antibodies are directed against EGFR, while the latter two are targeted against ErbB2.

The mode of action of another therapeutic antibody, matuzumab (EMD72000), which targets EGFR expressing tumors, is investigated in this thesis. Matuzumab is the humanized form of the murine mAb 425 (EMD55900) that was produced by immunization of BALB/c mice with human A431 epidermoid carcinoma cells (Murthy *et al.*, 1987; Kettleborough *et al.*, 1991). Matuzumab has performed well in phase I clinical trials against a number of cancers, both alone and in combination with chemotherapy (Bier *et al.*, 2001; Vanhoefer *et al.*, 2004; Graeven *et al.*, 2006; Kollmannsberger *et al.*, 2006; Rao *et al.*, 2008), and has reached phase II trials (Seiden *et al.*, 2007; Socinski, 2007).

5.2. Results

5.2.1. Matuzumab binding to sEGFR

Surface plasmon resonance (SPR)/Biacore experiments were carried out to characterize the binding of Fab72000 (see 4.3.3) to the soluble extracellular domain of the EGF receptor (sEGFR) and the isolated receptor domain III (sEGFRd3) (see 4.3.1). The apparent K_D values obtained were 113 ± 25 nM for sEGFR and 43 ± 13 nM for sEGFRd3 (Fig. 9).

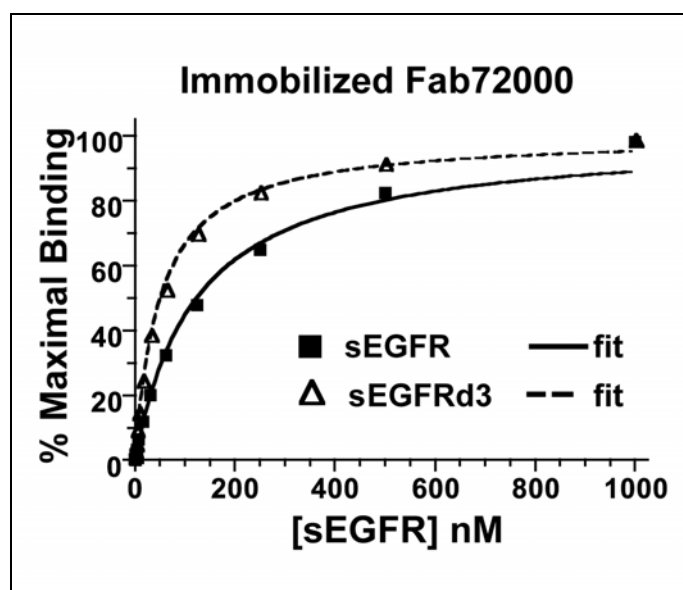


Fig. 9: Characterization of matuzumab binding to sEGFR

Surface plasmon resonance (SPR)/Biacore analysis of the binding of sEGFR and sEGFRd3 to immobilized Fab72000. A series of samples of sEGFR or sEGFRd3, at the indicated concentrations, was passed over a biosensor surface to which Fab72000 had been amine coupled. Data points show the equilibrium SPR response value for a representative set of samples of sEGFR (black squares) and of sEGFRd3 (open triangles), expressed as a percentage of the maximal SPR binding response. The curves represent the fit of these data to a simple one-site Langmuir binding equation. K_D values, based on at least three independent binding experiments, are 113 ± 25 nM for sEGFR and 43 ± 13 nM for sEGFRd3.

The affinity measurement was verified with an ITC experiment, which gave a K_D value of 2.1 ± 0.5 nM for the interaction of Fab72000 with sEGFR (Fig. 10).

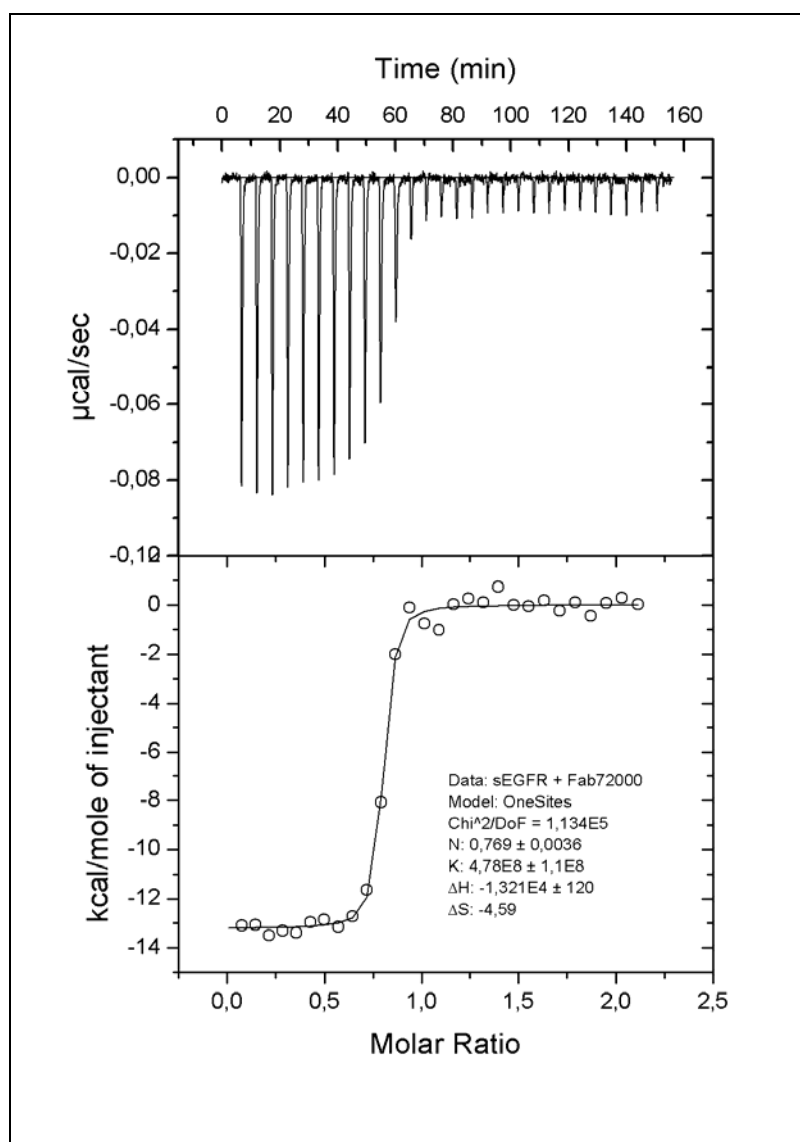


Fig. 10: ITC sEGFR and Fab72000

Fab72000 (20 μM) was injected in 10 μl steps into a cell containing 2 μM sEGFR at 25°C. Each peak represents the heat of binding following one injection (upper plot). The lower plot shows the integrated results, where each point represents the normalized heat change for each injection. The calculated K_D for this interaction is 2.1 ± 0.5 nM.

5.2.2. Ligand competition analysis of matuzumab

Competition assays were carried out to investigate the ability of matuzumab to compete with ligand binding to EGFR. As shown in Fig. 11, there is an initial decrease in the equilibrium SPR response as increasing Fab72000 is added. At a 1:1 molar ratio of Fab72000:sEGFR the SPR response is about 45 % of that obtained with no added Fab. Addition of increasing excesses of Fab72000 does not further reduce this binding level. Even at higher concentration of sEGFR and with up to a 50 fold excess of Fab72000 the equilibrium SPR response does not fall below 40 % of the value in the absence of added Fab.

Equilibrium binding analysis to immobilized EGF for samples of sEGFR containing a 10 fold molar excess of Fab72000 indicates an apparent K_D value that is approximately five fold weaker than for sEGFR alone (see Appendix 11.3 Fig. 44).

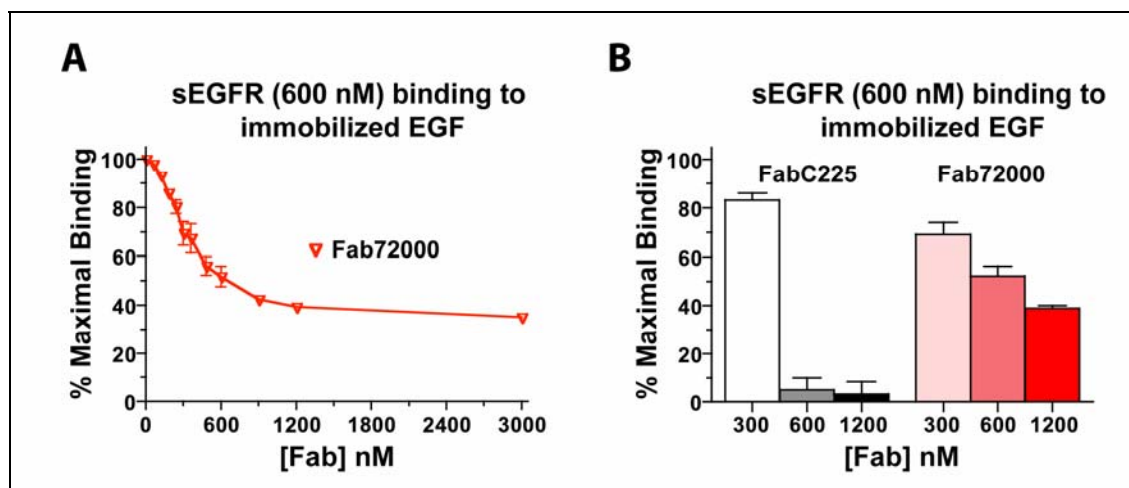


Fig. 11: Ligand competition properties of matuzumab

A: A competition experiment showing the effect of addition of Fab72000 upon the binding of 600 nM sEGFR to immobilized EGF. Mixtures of 600 nM sEGFR plus the indicated concentrations of Fab72000 were passed over a biosensor surface to which EGF had been amine coupled. The equilibrium SPR responses for each mixture is shown, normalized to the response obtained with no added Fab. Error bars indicate the standard deviation on at least three independent measurements. The line simply connects the data points. **B:** The ability of FabC225 (the antigen binding domain of cetuximab; gray shades) and Fab72000 (red shades) to compete for the binding of 600 nM sEGFR to immobilized EGF, determined exactly as described in A. Samples of each Fab alone show no binding to the immobilized EGF (data not shown). Data for FabC225 are taken from Li *et al.*, 2005. Error bars indicate the standard deviation on at least three independent measurements.

5.2.3. Matuzumab binding prevents receptor dimerization

Analytical ultracentrifugation sedimentation equilibrium experiments (SE) were carried out to determine the oligomeric state of sEGFR:Fab72000 (see 4.3.4) in the presence of excess ligand. The control samples show a doubling of the molecular weight for sEGFR in presence of EGF. However, only a slight increase in molecular weight is observed for the complex sEGFR:Fab72000 with added ligand (Fig. 12).

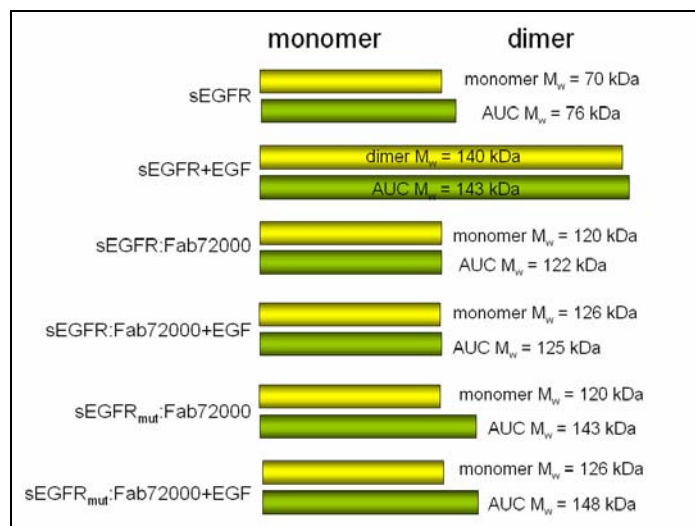


Fig. 12: Does the sEGFR:Fab72000 complex dimerize? Analysis by AUC

Analytical ultracentrifugation sedimentation equilibrium data of the oligomeric state of sEGFR:Fab72000 in the presence of EGF. Depicted are the theoretical molecular weights by sequence of the EGF receptor, the complex sEGFR:Fab72000 and the mutated receptor sEGFR Y251A/R285S:Fab72000 (sEGFR_{mut}:Fab72000) (yellow bars), each alone and in presence of excess EGF. The experimentally determined molecular weights of the respective molecules are shown as green bars. The data represent a fit of 4 μ M samples measured in 20 mM HEPES, 100 mM NaCl (pH 7.5). Equilibrium data after 18 h were obtained at three different speeds 6,000 rpm, 9,000 rpm and 12,000 rpm at 20°C.

The same slight increase in the molecular weight is seen for the dimerization incompetent receptor:antibody complex sEGFR Y251A/R285S:Fab72000 in presence of EGF. This protein has two mutations in the dimerization arm of domain II (Y251A/R285S) that lead to the loss of an inter-receptor hydrogen bond. The mutated receptor binds ligand, albeit with lower affinity, but does not dimerize (Dawson *et al.*, 2005). It is not known why the mutated receptor shows a higher molecular weight than the wild type receptor, but the same was observed in former experiments (personal communication Dr. Dawson).

5.2.4. The matuzumab epitope

The crystal structure of EGFRd3 in complex with Fab72000 (see 4.5.3) reveals that Fab72000 binds primarily to the loop that precedes the most C-terminal strand of the domain III β -helix (amino acids 454-464; highlighted in red in Fig. 13). This loop penetrates into a cleft between the V_L and V_H domains of the Fab. The tip of this loop forms a type I beta turn, with T459 and S460 in this turn protruding the farthest into the cleft. All of the key interactions made by the Fab are from the complementarity determining regions (CDRs), with the major specificity determining contacts coming from CDRs H3 and L3. All CDRs contribute to binding to domain III.

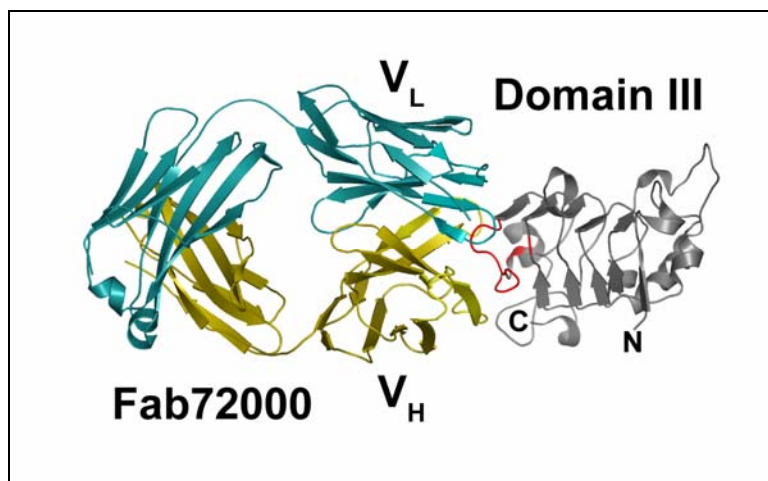


Fig. 13: Structure of the complex between the matuzumab Fab fragment and domain III of sEGFR

Cartoon of the sEGFRd3:Fab72000 complex. Domain III is colored in gray with the epitope highlighted in red. The orientation of domain III is the same as for the tethered sEGFR (left hand view) in Fig. 6. Fab72000 is colored cyan for the light chain and yellow for the heavy chain.

The tip of the buried loop from sEGFR makes interactions with both the heavy and light chain CDRs (Fig. 14); the side chain of T459 interacts with that of H93 from the Fab light chain, while the side chain of S460 contacts the CDR H2 side chain E50. Two lysines, one on either end of the sEGFRd3 epitope loop, form salt bridge interactions with aspartic acids on the Fab (K454 with D100 from CDR H3 and K463 with CDR L2 D49).

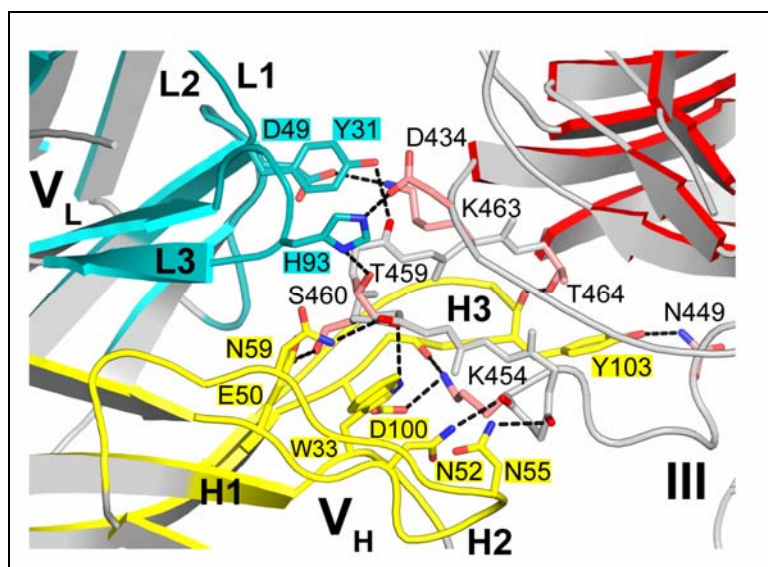


Fig. 14: The epitope of matuzumab in detail

A closeup view of the interactions between Fab72000 and domain III of sEGFR. Domain III is in gray with the secondary structure elements highlighted in red. The V_L and V_H domains of Fab72000 are in gray with cyan and yellow highlights, respectively. The CDRs of Fab72000 are shown in cyan for L1, L2 and L3 of the V_L domain, and in yellow for H1, H2 and H3 of the V_H domain. The side chains of the amino acids participating in key interactions are shown, colored as for the CDRs for the Fab and in pink for domain III. The amino acids are labeled on a cyan background for those from V_L , on a yellow background for V_H and in black for sEGFRd3. Distances corresponding to hydrogen bonds are shown with dashed black lines.

Additional interactions with the buried epitope loop are contributed by side chains in CDRs H1, H2 and L1 that are within hydrogen bonding distance of the main chain of sEGFRd3 (Fig. 14 and Fig. 15). Two important direct interactions are made between the Fab and regions of domain III outside the loop between amino acids 454-464. A histidine from CDR L3 (H93) interacts with D434 on the adjacent loop of the sEGFRd3 β -helix, while on the other side of the binding site Y103 from the apex of CDR H3 extends to interact with N449. These two interactions anchor the Fab over the central binding loop and expand the epitope substantially beyond the single peptide loop.

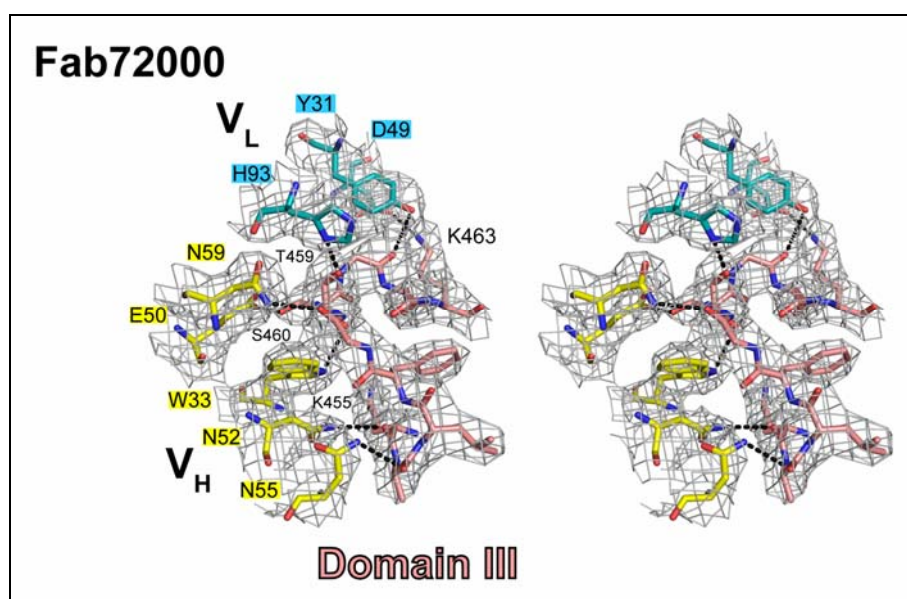


Fig. 15: Electron density at the sEGFRd3:Fab72000 interface

Stereo representation of selected interactions between sEGFR domain III and Fab72000. Amino acids are shown in stick representation and colored pink for domain III, yellow and cyan for Fab72000 V_H and V_L respectively. The gray mesh represents the final $2F_o - F_c$ electron density map contoured at 1.0σ . Distances consistent with hydrogen bonds are shown in dashed black lines.

A total of 2 salt bridges and 11 predicted hydrogen bonds are involved in the interaction between Fab72000 and sEGFRd3, in an interface that buries 758 \AA^2 of solvent accessible surface on domain III (in the complex a total of 1516 \AA^2 of surface is occluded from solvent). The shape complementarity (sc) parameter for the interface of the sEGFRd3: Fab72000 complex is 0.62.

Neither the conformation of sEGFRd3 nor of Fab72000 is significantly altered upon formation of the complex. There are very minor differences in the side chain positions in both the domain III epitope and in the CDRs of the Fab. Most notably Y103 in the V_H domain is disordered in the unbound Fab and becomes ordered on interacting with sEGFR. The elbow angle changes by 4° between the bound and unbound Fab72000.

5.2.5. The matuzumab epitope is distinct from the ligand binding site on domain III of sEGFR

Based on the crystal structures sEGFRd3:Fab72000 (see 4.5.3), sEGFR:FabC225 (PDB ID 1YY9) and sEGFR:EGF (PDB ID 1NQL) the epitopes of matuzumab and EGF were mapped onto sEGFR domain III to investigate the spatial arrangement of their binding sites (Fig. 16A). The same was done with the epitopes of cetuximab and EGF (Fig. 16B). While the binding sites of cetuximab and the ligand clearly overlap, the epitopes of matuzumab and EGF show no overlap.

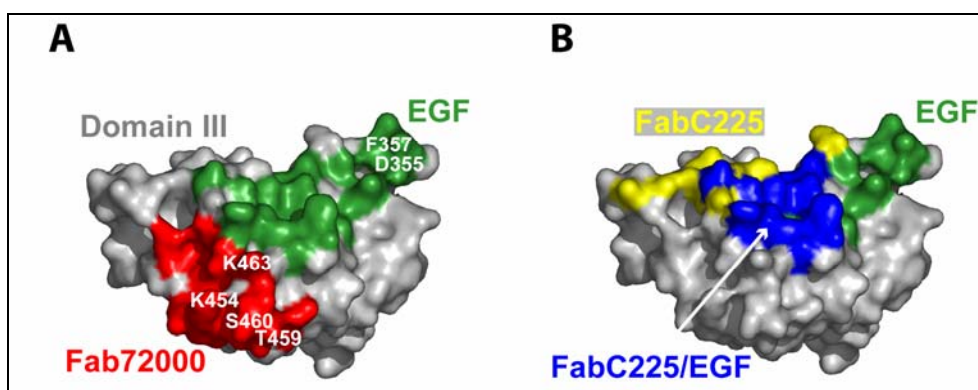


Fig. 16: The matuzumab epitope is distinct from the ligand binding site on domain III of sEGFR

A: surface representation of domain III is shown in gray viewed in approximately the same orientation as in Fig. 13. On the left hand side the amino acids on domain III that are within 4 Å of Fab72000 (red) or of EGF (green) are indicated on this surface. The amino acids that were mutated (Fig. 17) are labeled in white. **B:** the same surface representation of domain III is shown with the contacting amino acids for FabC225 in yellow, for EGF in green and for the region of overlap between FabC225 and EGF in blue.

To confirm that the crystallographically defined epitope for matuzumab precisely represents what is seen in solution, site specific alterations in sEGFR at key amino acids in the domain III matuzumab epitope were generated (Fig. 14) (see 4.1.1). Each purified, altered sEGFR (see 4.3.1) was analyzed for binding to immobilized Fab72000 and to immobilized EGF. Alteration to alanine of either of the two lysines on the epitope loop (K454A or K463A) leads to an approximate 100-fold reduction in the affinity of sEGFR for Fab72000 (Fig. 17). Substitution of alanines at T459 and S460 (T459A/T460A) also dramatically reduces the binding affinity. The combination of either lysine to alanine substitution with T459A/T460A abolishes all detectable interaction between sEGFR and the immobilized Fab72000.

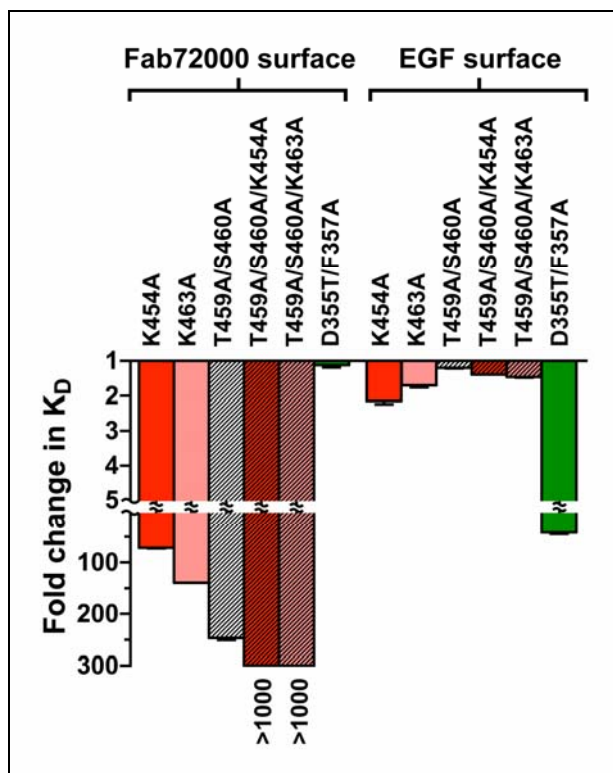


Fig. 17: Effects of sEGFR mutant binding to matuzumab or EGF

Surface plasmon resonance (SPR)/Biacore analysis of the binding of altered sEGFR proteins to immobilized Fab72000 or EGF. The equilibrium binding K_D values for each protein were determined exactly as described in Fig. 9. The fold change in this K_D value for each altered protein relative to that for the binding of wild type sEGFR to each immobilized ligand is plotted. Error bars indicate the standard deviation on at least three independent sets of measurements.

sEGFR proteins with alterations in the Fab72000 epitope bind to immobilized EGF with near wild type affinity (Fig. 17). However, substitution of two amino acids that are known to be critical for EGF binding (D355T/F357A) have negligible effect on binding of sEGFR to Fab72000.

5.3. Discussion

5.3.1. Matuzumab binding characteristics to soluble and cell surface EGFR

The K_D value of 113 ± 25 nM for Fab matuzumab binding to sEGFR obtained by surface plasmon resonance (SPR)/Biacore studies (see 5.2.1) is weaker than observed for the binding of ^{125}I -labeled intact matuzumab to cell surface EGFR with about 1-10 nM, depending on the cell line employed (Schmiedel *et al.*, 2008). The value obtained by ITC with 2.1 ± 0.5 nM corresponds better to the cellular data. However, binding assays with immobilized soluble receptor and with cell surface receptor are not directly comparable. The isolated domain III of sEGFR (sEGFRd3) binds to immobilized Fab72000 with a K_D value of 43.0 ± 12.9 nM. The antigen binding domain of matuzumab, like the ones of the antibodies cetuximab and 11F8 (Li *et al.*, 2005; Li *et al.*, 2008), binds more tightly to sEGFRd3, possibly due to the absence of steric hindrance from the other domains of sEGFR.

It is possible that the immobilization of the Fab72000 could affect the measured affinity in the Biacore experiments. However, essentially the same affinity for sEGFR binding to immobilized (amine coupled or bound via immobilized protein A) mAb matuzumab was obtained (see Appendix 11.3 Fig. 45). The absolute value of the affinity of sEGFR for immobilized Fab72000 obtained from the Biacore experiment is of less significance. This assay is however relevant in comparing the binding of sEGFRd3 and of the sEGFR proteins with alteration in the Fab72000 epitope to this same Biacore surface (see 5.3.3).

It has previously been shown that, in the context of an SPR/Biacore assay, the Fab fragment of cetuximab (FabC225) is able to block all binding of soluble sEGFR to immobilized EGF (Li *et al.*, 2005). Therefore the ability of matuzumab to compete with ligand binding to sEGFR was investigated by SPR. As shown in Fig. 11, matuzumab, in contrast to cetuximab, is not able to completely block the binding of the soluble receptor to immobilized EGF. Instead the equilibrium SPR response plateaus at 40% of the value in the absence of added Fab. One possible explanation for the observed SPR responses in Fig. 11 is that both unbound sEGFR and the sEGFR:Fab72000 complex can interact with the immobilized EGF, but that the complex binds with substantially weaker affinity. Equilibrium binding analysis to immobilized EGF for samples of sEGFR containing a 10 fold molar excess of Fab72000 indicates an apparent K_D value that is approximately five fold weaker than for sEGFR alone.

Still, matuzumab, like cetuximab, competes efficiently for the binding of 3 nM ^{125}I -labeled EGF to the surface of A431 epidermoid carcinoma cells (Schmiedel *et al.*, 2008).

Taken together, these data suggest that there must be something quite different about the mode of binding to sEGFR of the Fab fragment of matuzumab compared to that of cetuximab. Both antibodies are able to compete for binding of low concentrations of EGF to cell surface EGFR, yet the Fab fragments from the two antibodies have very different effects on the ability of soluble EGFR to bind to immobilized EGF in the Biacore assay. This apparent discrepancy can be explained after examining the complex structure of the matuzumab Fab fragment and sEGFRd3 (see 5.3.5).

5.3.2. The matuzumab epitope on sEGFR domain III

The epitope of matuzumab on sEGFR domain III consists of a single loop of 10 amino acids with two additional interactions probably stabilizing the antibody receptor interaction (Fig. 13). Kamat *et al.* identified through mutagenesis experiments the residues S460/G461 to be essential for binding of the murine progenitor of matuzumab 425 (Kamat *et al.*, 2008). These residues comprise exactly the tip of the epitope loop as seen in the crystal structure.

This mode of binding of an antibody to a large protein antigen is unusual. It is more common for the epitope on a large protein antigen to comprise a large flat surface (Sundberg and Mariuzza, 2002), as was observed for the binding of cetuximab and 11F8 to EGFR (Li *et al.*, 2005; Li *et al.*, 2008). The fact that all complementarity determining regions (CDRs) of matuzumab contribute to the binding to sEGFRd3 is also an unusual feature compared to most antigen-antibody complexes (Sundberg and Mariuzza, 2002).

The shape complementarity parameter for the interface of the sEGFRd3:Fab72000 complex of 0.62 is slightly lower than is typically observed for antigen-antibody interfaces (0.64 to 0.68) (Lawrence and Colman, 1993). The sc values reported for cetuximab and 11F8 bound to EGFR (Li *et al.*, 2005; Li *et al.*, 2008) and for the pertuzumab and trastuzumab complexes with the extracellular region ErbB2 (Cho *et al.*, 2003; Franklin *et al.*, 2004) are all somewhat higher, in the range from 0.69 to 0.75. This perhaps reflects the more convex shape of the matuzumab epitope compared to those of these other antibody drugs.

The elbow angle change of only 4° between the bound and unbound Fab72000 is in within the range expected due to dynamic elbow flexibility (Stanfield *et al.*, 2006) and thus probably not induced by the binding event.

Neither the conformation of the domain III and nor that of Fab72000 is significantly altered upon complex formation. Additionally, the binding of Fab72000 would not be expected to disrupt the tethered configuration of sEGFR (Fig. 6, left panel), the preferred solution conformation of the receptor (Dawson *et al.*, 2007) and the likely conformation of the unliganded receptor at the cell surface. Fab72000 can readily be docked onto its epitope on either of the two known structures of tethered sEGFR (PDB IDs 1NQL and 1YY9) without hindrance from any of the other domains of sEGFR.

5.3.3. Matuzumab and ligand epitopes do not overlap on sEGFR domain III

SPR/Biacore experiments showed a dramatically reduced affinity of Fab72000 to sEGFR carrying mutations in the Fab72000 epitope in comparison to wild type receptor (Fig. 17). However, the affinity of EGF to the mutated receptor is only slightly reduced in comparison to the wild type. This confirms that the striking reduction in binding affinity for Fab72000 is not due to a global disruption of the structure of domain III of sEGFR. The reverse effect is seen for receptor protein carrying mutations in the ligand binding site: the affinity of EGF is reduced while the binding to Fab72000 remains unaffected. These results confirm that the epitopes of the ligand and matuzumab are distinct as seen in 5.2.5. Indeed, not only is there no overlap of the epitope for matuzumab and the ligand binding region on domain III (Fig. 16A), but a bound Fab72000 would impose no steric hindrance to the binding of EGF or of TGF- α to domain III. With domain III from the sEGFRd3:Fab72000 complex overlaid on domain III from the sEGFR:EGF complex (PDB ID 1IVO) the closest approach of the Fab and EGF is 9 Å. This is in stark contrast to the situation for cetuximab binding. There is a high degree of overlap between the cetuximab and EGF binding sites on domain III (Fig. 16B). The steric block of this ligand binding site is the primary mechanism of cetuximab mediated inhibition of ligand induced dimerization and activation of EGFR (Li et al., 2005). Clearly the mechanism of inhibition of EGFR activation by matuzumab must be different.

5.3.4. The matuzumab inhibition mechanism

If matuzumab does not directly block access of the ligand to the domain III ligand binding site, how does it prevent high affinity ligand binding, receptor dimerization and activation as seen in ultracentrifugation studies (Fig. 12)? To understand this, the effect of the binding of Fab72000 upon the formation of the ligand induced dimeric form of the receptor is considered.

As shown in Fig. 6, sEGFR undergoes a dramatic domain rearrangement in going from the tethered inactive state to the ligand bound dimeric state (Burgess *et al.*, 2003). Additional local structural changes in domain II are known to be key for high affinity ligand binding, receptor dimerization and activation (Ogiso *et al.*, 2002; Dawson *et al.*, 2005). As shown in Fig. 18 and discussed in detail below, when domain III from the sEGFRd3:Fab72000 complex is overlaid on domain III from the receptor in its extended, dimerization competent conformation (PDB ID 1MOX), there are direct clashes between the bound Fab72000 and both domains I and II of the extended receptor. Thus, with matuzumab bound to domain III of EGFR, the receptor cannot undergo the large scale domain rearrangement that is required for dimerization. Further, the binding of Fab72000 blocks the critical local conformational changes in domain II.

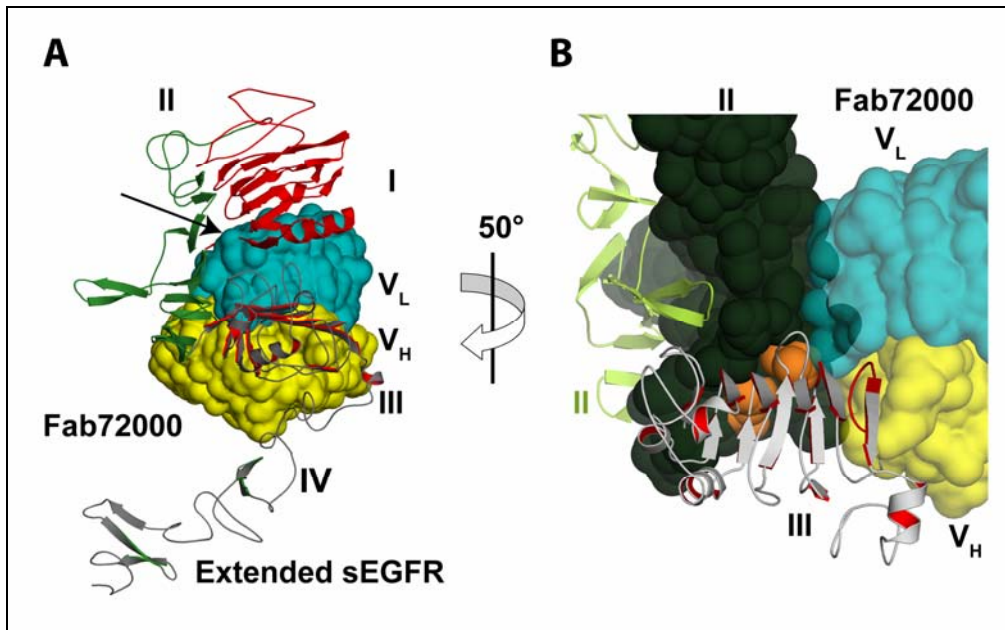


Fig. 18: Implications for the mechanism of inhibition of EGFR by matuzumab

A. Cartoon of the extended sEGFR with Fab72000, in surface representation, docked onto its domain III epitope. The orientation of the receptor is the same as for the right hand protomer in the sEGFR dimer shown in Fig. 6 (with domains colored as for the left hand protomer; EGF is omitted for clarity). Fab72000 is colored as in Fig. 13. The N-terminal region of domain I clashes with the V_L domain (indicated with an arrow). Additional clashes occur along the C-terminal half of domain II (see part B). The C-terminal loop on domain II (D278, H280) that makes critical contacts across the dimer interface is marked with an asterisk.

B. In this view, an approximate 50° rotation about the vertical axis relative to part A, domain II is shown in sphere representation in dark green. A cartoon of domain II of the other molecule in the dimer is shown (light green) for reference. Domain I has been omitted for clarity. The V_L domain of the Fab clashes with domain II in the critical C-terminal region that forms the binding pocket for the dimerization arm and makes important contacts with domain III (from N274 and E293 in domain II, colored orange). These interactions are known to be crucial for stabilizing the dimerization competent conformation of domain II. The Fab72000 epitope loop on domain III is colored in red.

With the receptor in the extended conformation, the N-terminal region of the domain I clashes with the light chain of Fab72000 preventing domain I from reaching the position that is required for high affinity ligand binding (indicated with an arrow in Fig. 18). This is reminiscent in nature and extent to clashes between the antigen-binding fragment of cetuximab (FabC225) and domain I that were previously implicated as part of the mechanism of inhibition of EGFR dimerization by that antibody (Li *et al.*, 2005). In that case, the different orientation of FabC225 on domain III positions the V_H domain such as to occlude the N-terminal portion of domain I from its required position in the receptor dimer.

Clashes between domain II of the extended receptor and the Fab were not seen in the cetuximab complex, and are significant. With Fab72000 bound to domain III of EGFR it would not be possible for the C-terminal portion of domain II to adopt the conformation observed in the ligand bound dimeric form of the receptor. As shown in Fig. 18B, if Fab72000 is docked onto its epitope on domain III of an sEGFR molecule in the extended conformation, there are clashes along the C-terminal half of domain II, predominantly with the V_L domain of

the Fab. This C-terminal half of domain II forms the binding pocket for the dimerization arm from the other molecule in the receptor dimer. Additional interactions across the dimer interface from a C-terminal loop on domain II (D279 and H280, marked with an asterisk in Fig. 18A) contribute substantially to the stability of the EGFR dimer. The conformation of domain II in this region is stabilized by interactions with domain III that have been demonstrated to be critical for EGFR dimerization and activation (Ogiso *et al.*, 2002; Dawson *et al.*, 2005). The binding of Fab72000 to domain III would disrupt all of these interactions.

Thus, Fab72000 binding to domain III of EGFR blocks the global domain rearrangement of EGFR and the local conformational changes in domain II. The blocking both of these key elements in formation of the productive EGFR dimer is critical for the effective inhibition of EGFR activation by matuzumab.

5.3.5. Matuzumab binding properties interpreted with structural information

The steric restriction on EGFR conformation imposed by the binding of matuzumab offers a structural framework to explain the competition data presented in Fig. 11. In binding studies at the cell surface matuzumab and cetuximab are both efficiently competing with EGF to receptor binding, while in SPR/Biacore assays the two antibodies show differing competition characteristics. A major difference between the two competitions assays is the concentrations of the soluble ligands that are used. In the cell based competition assay EGF is present at 3 nM. This concentration is well below the K_D value for the binding of EGF to isolated domain III: between 500 nM (for the Kohda fragment) and 2 μ M (for insect cell expressed sEGFRd3) (Ogiso *et al.*, 2002; Dawson *et al.*, 2005). To observe binding of EGF to cell surface EGFR under these conditions both domains I and III must be engaged to form a high affinity EGF binding site. However, binding of matuzumab to EGFR prevents the receptor from adopting the conformation required to form the high affinity ligand binding site. Thus at this relatively low EGF concentration matuzumab blocks detectable binding of EGF to the cell surface and thus competes as effectively for the binding of EGF as does cetuximab. Any EGF that binds to the exposed ligand binding site on domain III of a matuzumab occupied cell surface EGFR would be so weakly bound that it would be washed out in this assay. By preventing the receptor from adopting the conformation required for the bipartite binding of EGF between domains I and III, matuzumab blocks all detectable binding of EGF to cell surface EGFR in this assay.

By contrast the Biacore assay is performed at a much higher concentration of soluble ligand (in this case sEGFR, which binds to immobilized EGF). The soluble EGFR is passed over this surface at 600 nM, a concentration that is close to the K_D for the binding of isolated domain III of EGFR to immobilized EGF. Under these conditions the monovalent binding of domain III alone to EGF can be detected. There are probably two populations of sEGFR with two different affinities. Unbound sEGFR has a higher affinity for EGF, while the Fab72000 bound sEGFR has a lower affinity. In the Biacore assay, the residual binding to immobilized EGF observed for sEGFR in the presence of excess Fab72000 (Fig. 44) is due, at least in part, to binding to EGF of the exposed domain III in an sEGFR:Fab72000 complex.

5.3.6. Implications for the therapeutic application of matuzumab

As discussed above, the mechanism of inhibition of matuzumab is different from that previously described for cetuximab. Both antibodies effectively block productive binding of EGF to cell surface EGFR, but do so by interacting with distinct epitopes on domain III. Not only are the epitopes of matuzumab and cetuximab non-overlapping, but the structures suggest that both matuzumab and cetuximab could simultaneously bind to EGFR. As shown in Fig. 19, when FabC225 and Fab72000 are simultaneously docked onto their respective epitopes on domain III the two Fab fragments occupy different positions and do not overlap.

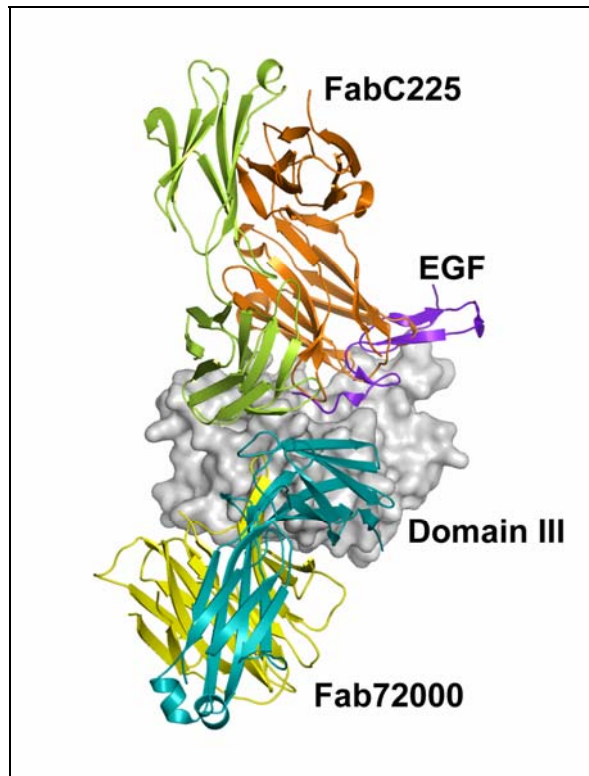


Fig. 19: The matuzumab and cetuximab epitopes do not overlap

A surface representation of the domain III as in Fig. 16 is shown. Cartoons of Fab72000, FabC225 (PDB ID 1YY9) and EGF (PDB ID 1IVO) are shown docked onto their respective binding sites on domain III. Fab72000 is colored as in Fig. 13, FabC225 is shown with the heavy chain in orange and the light chain in light green, and EGF is in purple.

This observation was experimentally confirmed by surface plasmon resonance/Biacore, size exclusion chromatography and analytical ultracentrifugation analysis investigating the simultaneous binding properties of cetuximab and the murine progenitor of matuzumab 425 to soluble and cell surface EGFR (Kamat *et al.*, 2008). Cellular competition assays showed that neither antibody competes with the binding of the other (Schmiedel *et al.*, 2008; Kamat *et al.*, 2008). Further it has been reported that there is an increased number of cell surface antibody binding sites for a mixture of matuzumab and cetuximab compared to either antibody alone (Kreysch and Schmidt, 2004). This suggests that both matuzumab and cetuximab can bind to a single receptor molecule at the cell surface.

Treatment of cells with combinations of antibodies against distinct epitopes on the extracellular domain of EGFR, and on the related family member ErbB2, lead to enhanced receptor internalization and degradation (Ye *et al.*, 1999; Spiridon *et al.*, 2002; Friedman *et al.*, 2005), a factor that contributes to the antitumor activity of many therapeutic antibodies (Logtenberg, 2007). Matuzumab and cetuximab can both bind simultaneously to EGFR and this has the potential to lead to synergistic antitumor effects.

Indeed, a combination of cetuximab and the murine progenitor of matuzumab 425 reduced growth and survival of EGFR overexpressing breast cancer cells more effectively than either antibody alone (Kamat *et al.*, 2008). Furthermore, it was shown that combinations of antibodies binding to different epitopes on EGFR trigger potent complement-dependent cytotoxicity (CDC) (Dechant *et al.*, 2008). The authors particularly emphasized the combination of cetuximab and matuzumab for effectivity. Combination of matuzumab and cetuximab could, thus, be beneficial in cancer therapy.

5.4. Conclusion

EGFR dimerization requires a conformational reorganization of the receptor extracellular region that is promoted by ligand binding to domain I and III (Fig. 6). As shown schematically in Fig. 20, cetuximab acts as a competitive inhibitor, preventing ligand induced dimerization by directly blocking access of ligand to the domain III ligand binding site.

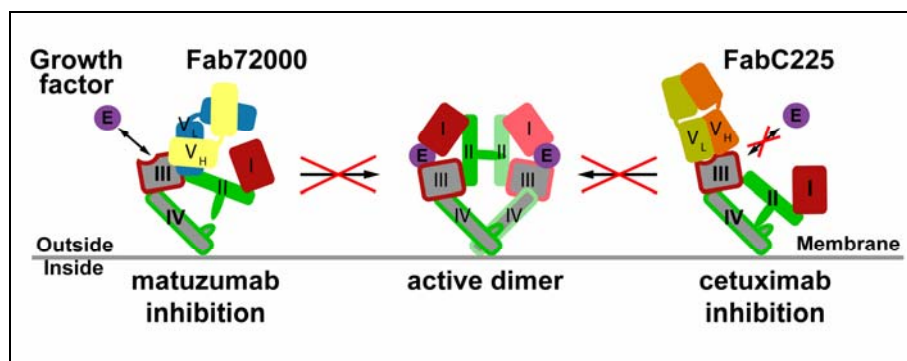


Fig. 20: Matuzumab and cetuximab use different mechanisms to block ligand induced EGFR dimerization
 In the center of the scheme the ligand induced sEGFR dimer is represented, with domain I in red, domain II in green, domain III in gray with red border, domain IV in gray with green border and the ligand (E) in violet. The colors for one protomer are lightened for contrast. On the left hand side a scheme is shown to illustrate the mechanism of inhibition of ligand induced dimerization by matuzumab. Fab72000 binds to domain III of sEGFR and sterically prevents the receptor from adopting the conformation required for dimerization. Importantly, Fab72000 blocks the local conformational changes in domain II that are critical for both high affinity ligand binding and dimerization. The inhibition is non-competitive; the ligand binding site on domain III is not blocked. This contrasts with the mechanism of inhibition previously reported for cetuximab (Li *et al.*, 2005). FabC225 (right hand side) is a competitive inhibitor that blocks the ligand binding site on domain III. This is the primary mechanism of inhibition of ligand mediated dimerization by cetuximab.

By contrast matuzumab does not occlude the ligand binding site on domain III. Rather matuzumab exploits a non-competitive mechanism to inhibit sEGFR dimerization and activation. Inhibition of ligand induced EGFR activation by matuzumab is entirely dependent on sterically blocking the receptor from adopting the conformation that is required for high affinity ligand binding and dimerization. These different mechanisms of inhibition suggest opportunities to exploit multiple EGFR targeting drugs to act synergistically for optimal therapeutic gain.



6. Antibody binding and dimerization properties of the mutant EGFR variant III ectodomain

6.1. Introduction

Beside cancer related mutations in the tyrosine kinase domain of the epidermal growth factor receptor (EGFR), several mutations in the extracellular part of EGFR were described to promote tumorigenesis (Lee *et al.*, 2006). The type III EGFR mutation (EGFRvIII, de2-7 EGFR or Δ EGFR) is the most common one and clinically connected with enhanced tumor aggressivity and chemoresistance (Nishikawa *et al.*, 1994; Huang *et al.*, 1997; Heimberger *et al.*, 2005; Weppeler *et al.*, 2007; Wang *et al.*, 2009). The mutated receptor EGFRvIII is a truncated version of the wild type EGFR showing constitutive signaling activity and impaired down-regulation (Pedersen *et al.*, 2001).

The presence of EGFRvIII was described for many different cancer types, among them lung and prostate cancer as well as gliomas, where the mutation is found in up to 50% of glioblastomas (Moscatello *et al.*, 1995; Frederick *et al.*, 2000; Cavenee, 2002). Expression of EGFRvIII is a negative prognostic indicator in glioblastoma and mediates resistance to TKIs targeted against EGFR (Learn *et al.*, 2004).

6.1.1. EGFRvIII in-frame deletion

EGFRvIII contains a deletion of exons 2-7 of the wild type gene, resulting in the in-frame loss of most of domain I and II including the dimerization arm (Pedersen *et al.*, 2001). At the fusion junction a novel glycine residue is generated. Thus, the protein consists of the residues 1-5 of domain I, the glycine residue and continues with residue 274 of domain II (Fig. 21).

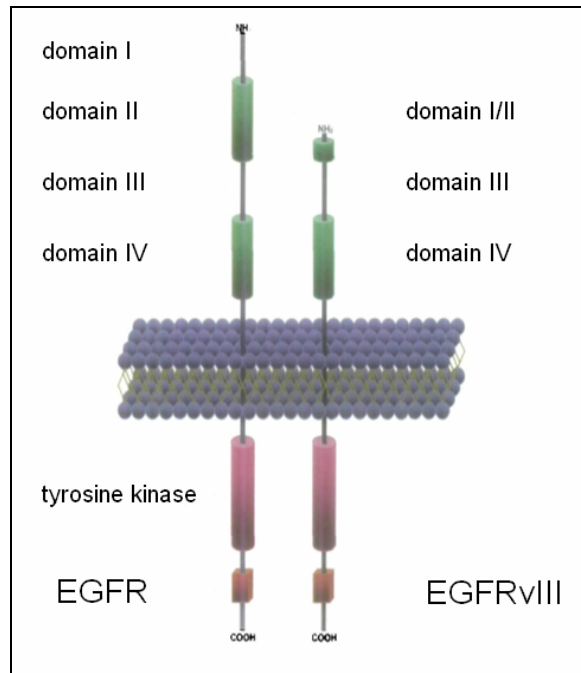


Fig. 21: Domain organization of EGFR and EGFRvIII in comparison

Human EGFR and EGFRvIII comprise an extracellular region consisting of domains I-IV, a transmembrane region and an intracellular tyrosine kinase domain. The truncated EGFRvIII consists of residues 1-5 of domain I of the wild type EGFR, a glycine residue at the fusion junction and continues with residue 274 of domain II. The sequence of domain III and IV are unaltered in mutant EGFRvIII in comparison to full length EGFR (figure adapted from Pedersen *et al.*, 2001).

Based on the sequence the ligand binding site on domain III is unaltered as well as the epitope of the monoclonal antibodies cetuximab (Li *et al.*, 2005) and matuzumab (Schmiedel *et al.*, 2008). However, no ligand binding is observed through the mutated receptor on the cell surface (Wikstrand *et al.*, 1997). It is unclear if the mutant receptor is able to form homodimers at the cell surface upon ligand stimulation since conflicting data were published (Chu *et al.*, 1997; Fernandes *et al.*, 2001). Heterodimerization of the EGFRvIII with the wild type EGFR was shown in murine BaF/3 cells and in human glioblastoma cells (O'Rourke *et al.*, 1998; Luwor *et al.*, 2004). Structural or biophysical investigations of the isolated ectodomain of EGFRvIII are not available so far.

EGFRvIII was so far only shown to be expressed on cancer cells and is therefore an ideal target for anticancer therapy (Wikstrand *et al.*, 1997; Kuan *et al.*, 2000; Li and Wong, 2008). It is unknown if untransfected cells in tumors are able to co-express both the receptor wild type and EGFRvIII within the same cells or if a mixture of cells is present expressing either one or the other receptor controversially discussed in literature (Nishikawa *et al.*, 1994; Aldape *et al.*, 2004; Yang *et al.*, 2008; Zhu *et al.*, 2009).

6.1.2. EGFRvIII signaling activity

In comparison to the wild type receptor, which signals via the phosphatidylinositol 3-kinase (PI3K)/Akt, ras/raf/MEK/ERK, phospholipase C gamma (PLC γ), and signal transducer and activator of transcription (STAT3) signaling pathways (Sebastian *et al.*, 2006) (see 3.4), EGFRvIII seems to activate different signaling pathways (Zhu *et al.*, 2009).

The phosphorylation of the mutant was reported to be lower in comparison to the wild type, but to be constitutive. Recently it was found that tyrosine residue 992 in human EGFRvIII expressed by mouse cells is constitutively phosphorylated (Zhu *et al.*, 2009). Attempts to identify intracellular molecules mediating the mutant signaling have been inconclusive so far. PLC γ was reported not to be phosphorylated in NR6M cells expressing only EGFRvIII (Chu *et al.*, 1997), while it was recently described as persistently activated in mouse glioblastoma cells expressing human EGFRvIII (Zhu *et al.*, 2009). The last group implies a novel MAPK independent signaling pathway for PLC γ in glioblastomas.

Several authors describe elevated PI3K activity in murine fibroblasts and human glioma cells expressing EGFRvIII (Moscatello *et al.*, 1998; Narita *et al.*, 2002; Klingler-Hoffmann *et al.*, 2003). However, both cell lines express endogenous wild type EGFR, which might have influenced the results obtained. In contrast, mouse glioma cells expressing human EGFRvIII were reported to show phosphorylated Akt only on Ser-473, which is not mediated through PI3K but through mTORC2 kinase activity (Zhu *et al.*, 2009).

The activation of the mitogen-activated protein kinase (MAPK) by EGFRvIII also remains controversial. Two groups reported activation of the MAPK pathway in NR6 cells and in U87MG glioma cells (Wu *et al.*, 1999; Lorimer and Lavictoire, 2001). Other groups suggested that there was no MAPK activation in NIH3T3 cells, NR6 cells or in mouse glioma cells (Moscatello *et al.*, 1996; Chu *et al.*, 1997; Zhu *et al.*, 2009). Therefore, it remains unclear so far which pathway contributes significantly to the enhanced tumorigenicity of EGFRvIII *in vivo*.

6.1.3. EGFRvIII down-regulation

There are two main mechanisms described for negative EGF receptor regulation: (1) intracellular binding of the ubiquitin ligase Cbl at phosphorylated tyrosine residues leading to internalization plus lysosomal receptor degradation and (2) extracellular binding of the leucine rich repeat and immunoglobulin-like domain-1 protein (LRIG1), which enhances receptor degradation by a so far unknown mechanism (Davies *et al.*, 2006; Stutz *et al.*, 2008).

The exact mechanism by which EGFRvIII evades down-regulation is not fully understood yet, but it seems that only the first of the two described mechanisms is impaired for EGFRvIII. Studies suggest that the interaction of the mutant receptor with Cbl may be compromised (Davies *et al.*, 2006). Recently it was reported that in spite of the mutation in the extracellular domain of the EGFRvIII the mutual interaction with LRIG1 is not disrupted (Stutz *et al.*, 2008). It was suggested that the loss of LRIG1 might promote EGFRvIII driven oncogenesis. Similar promotion of gliomagenesis especially for EGFRvIII expressing tumors was observed through the loss of the tumor suppressors Ink4a/Arf and PTEN (Zhu *et al.*, 2009).

In addition to inefficient internalization, the EGFRvIII was reported to be efficiently recycled to the plasma membrane resulting in a long half-life of the mutant receptor (Grandal *et al.*, 2007).

6.1.4. Therapeutic strategies against EGFRvIII

Several strategies are under investigation to treat cancer patients with EGFRvIII expressing tumors including active vaccination and monoclonal antibodies.

Vaccination with a peptide containing the EGFRvIII specific mutated junction sequence has now progressed to clinical trial. The efficiency of anti-cancer vaccination was first shown in mice injected with a peptide derived from EGFRvIII. The immunized animals showed a significantly decreased tumor incidence in comparison to control mice (Moscatello *et al.*, 1997). Currently there are five clinical trials evaluating active immunization with exactly the EGFRvIII peptide (now produced under the name CDX-110) described by Moscatello *et al.* (1997) reaching from Phase I to Phase II/III (Sonabend *et al.*, 2007; Li and Wong, 2008; Sampson *et al.*, 2008)

Since EGFRvIII seems to be a tumor-specific marker (Wikstrand *et al.*, 1995), the mutant is currently investigated as therapeutic target in anti-cancer immunotherapy through monoclonal antibodies, i.e. mAb806 or cetuximab, and single chain antibody variable domains (scFv) (Kuan *et al.*, 2000; Shankar *et al.*, 2006; Aerts *et al.*, 2007; Yoshimoto *et al.*, 2008; Yang *et al.*, 2008). In summary, several monoclonal antibodies including the antibody cetuximab were described to recognize the mutated receptor *in vitro* (Wikstrand *et al.*, 1995; Modjtahedi *et al.*, 2003). However, *in vivo* effectivity of cetuximab was reported to be reduced in comparison with mAb806 (Li *et al.*, 2007). Cetuximab was described to bind to EGFRvIII expressed by human glioma cell lines and to trigger ADCC in a dose-dependent

manner, but not to exhibit a growth-inhibitory effect (Fukai *et al.*, 2008). Furthermore, boronated cetuximab was used for boron neutron capture therapy of rat gliomas, but showed *in vivo* reduced binding to EGFRvIII in comparison to the wild type EGFR (Yang *et al.*, 2008). A chimeric version of the mouse mAb 806 (ch806) has been engineered and has performed well in phase I trials (Scott *et al.*, 2007). The antibody was reported to accumulate in patient tumor tissue in comparison with normal tissue. This is in accordance with the observation that mAb806 binds to EGFRvIII and to wild type EGFR in cells expressing elevated levels of the receptor, but not to wild type EGFR in tissue expressing normal levels of EGFR (Jungbluth *et al.*, 2003).

In addition, combination therapy of different tyrosine kinase inhibitors with chemotherapy was described to be potentially beneficial for glioblastoma patients with high EGFRvIII expression levels (Huang *et al.*, 2007). Methods to detect EGFRvIII in tissue samples of patients are developed to enable EGFRvIII-directed therapies (Yoshimoto *et al.*, 2008).

6.2. Results

In this chapter the structure of the isolated extracellular domain of sEGFRvIII is investigated as well as its dimerization properties. In addition the binding characteristics of EGF and the monoclonal antibodies matuzumab (see 5) and cetuximab to the EGFRvIII ectodomain are analyzed.

6.2.1. Expression and purification sEGFRvIII

This section describes for the first time the expression and purification of the mutant EGFR variant III ectodomain for crystallization experiments and antibody and ligand binding studies. The soluble extracellular domain of EGFR variant III (sEGFRvIII) was expressed in a 6 L scale Sf9 cell culture (see 4.2.1 and 4.3.2). The yield was about 0.2 mg/L purified protein depending on the age and condition of the Sf9 cells. The sEGFRvIII C-terminal end was confirmed by Western blot with an anti-His₆-antibody. The N-terminal sequence and the mutation fusion junction (Fig. 3) were confirmed by Edman degradation. The purity of sEGFRvIII was confirmed both by reducing and non-reducing SDS-PAGE (Fig. 22), by dynamic light scattering (DLS) and by analytical size exclusion chromatography (SEC)/static light scattering (SLS) methods. sEGFRvIII samples showed a polydispersity of 17.2 % at 10 mg/ml measured by DLS and a defined SEC peak with a corresponding molar mass of 47 kDa. This is in accordance with a molecular weight of sEGFRvIII by sequence of 39.2 kDa plus glycosylation.

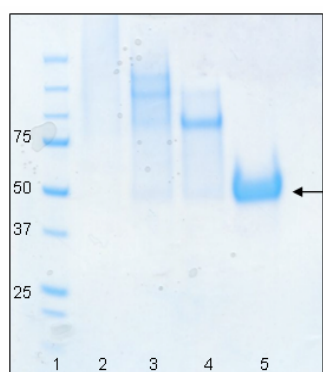


Fig. 22: SDS-PAGE sEGFRvIII purification

The non-reducing SDS-PAGE of sEGFRvIII gel filtration fractions shows a single band in lane 5 corresponding to a protein of the expected size (39.2 kDa by sequence plus glycosylation, marked with an arrow). Aggregated or misfolded protein (lanes 2-4) was separated through the gel filtration run using a HiLoad™ Superdex200 16/60 preparation grade column (GE Healthcare) pre-equilibrated with 20 mM HEPES, 100 mM NaCl (pH 7.5). The protein marker is shown in lane 1 with the sizes indicated in kDa.

6.2.2. sEGFRvIII dimerization properties

Soluble EGFR wild type (sEGFR) and mutant EGFR variant III (sEGFRvIII) ectodomains (see 4.2.1 and 4.3) were analyzed for their ligand dependent dimerization properties by analytical SEC/SLS (Fig. 23).

Addition of a 1.2 molar excess of the ligand EGF to sEGFR leads to a doubling of molecular weight of the species in the sample from 77 kDa to 133 kDa. This was not seen for sEGFRvIII samples, which showed a shift in molar mass from 45 Da to 48 kDa in the presence of excess ligand EGF.

In addition the heterodimerization properties of sEGFR and sEGFRvIII were investigated in absence and presence of excess ligand. Beside clear homodimeric sEGFR and monomeric sEGFRvIII peaks as seen in Fig. 23 no defined heterodimer peaks could be observed. However, this could be due to the resolution limit of the column.

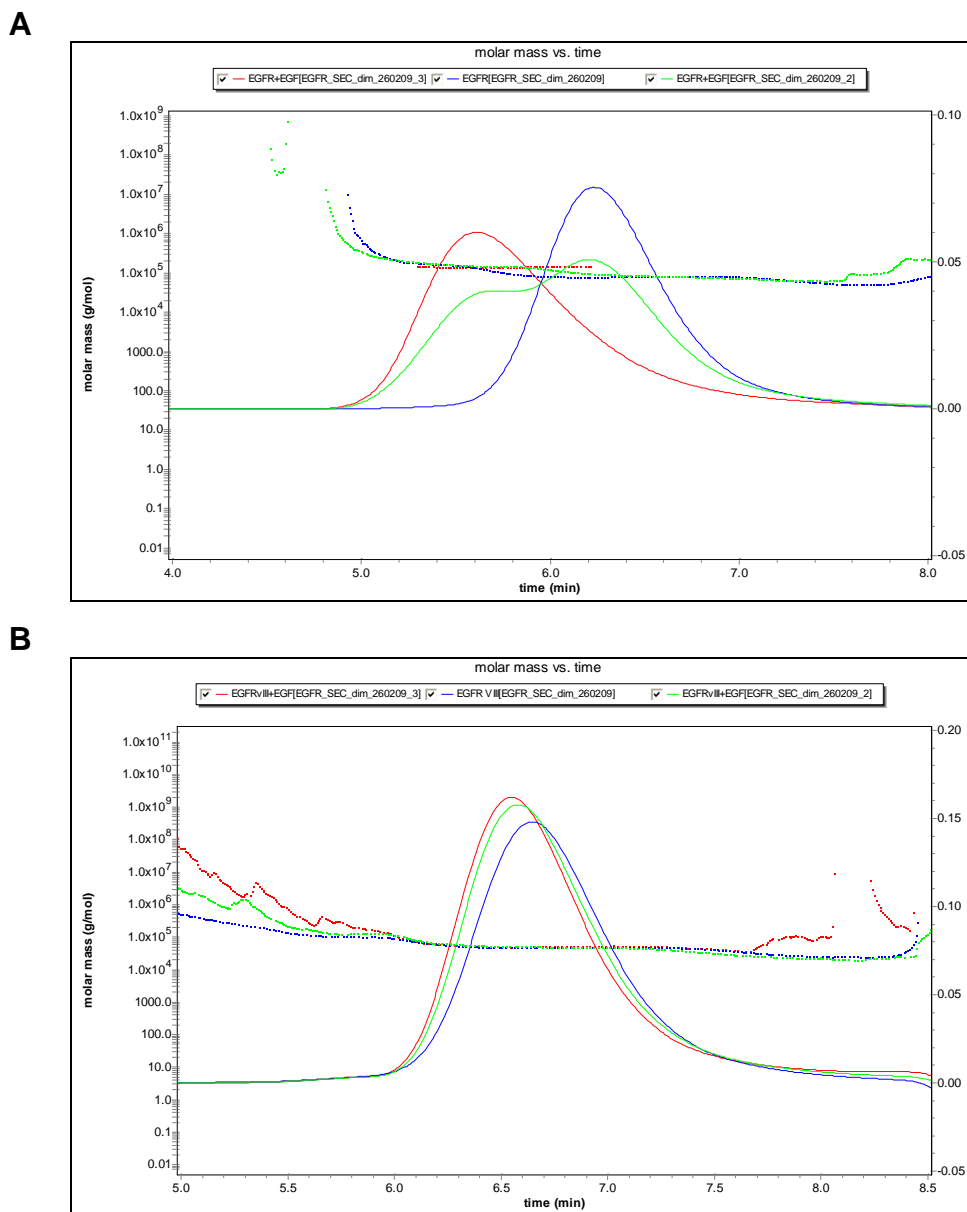


Fig. 23: sEGFR and sEGFRvIII dimerization properties analysed by static light scattering

sEGFR (A) and sEGFRvIII (B) ligand dependent dimerization was analysed by analytical SEC/static light scattering (SLS). The red line indicates a sample with a 1.2 molar excess of EGF, the green line a 0.5 molar excess of EGF and the blue line the respective receptor without added ligand. The straight lines indicate the molecular mass distribution in the sample, whereas the curves show the elution profile as determined by the refractive index. 30-40 μ l (2 mg/ml) protein solution was injected onto a Superdex75 HR analytical SEC column (GE Healthcare) and the molecular weight determined from light scattering data. The column was equilibrated with 20 mM HEPES, 100 mM NaCl (pH 7.5) using an Agilent 1200 HPLC system. SLS data for protein eluting from the SEC column were collected using a DAWN-HELEOS-II static light scattering detector coupled to an in-line refractive index meter (Wyatt Technologies). The data were analyzed using the Astra V software (Wyatt Technologies). The molar weight of sEGFR (77 kDa) doubled in the presence of EGF (133 kDa), indicating a dimerization event. This was not seen for sEGFRvIII (47 kDa) in the presence of excess ligand (48 kDa).

6.2.3. Antibody and ligand binding properties of sEGFRvIII

Surface plasmon resonance (SPR)/Biacore experiments were carried out to characterize the binding of the matuzumab Fab fragment (Fab72000) and the cetuximab Fab fragment (FabC225) to sEGFRvIII. The apparent K_D values obtained were 19.4 ± 2.4 nM and 2.2 ± 0.1 nM for matuzumab and cetuximab, respectively (Fig. 24).

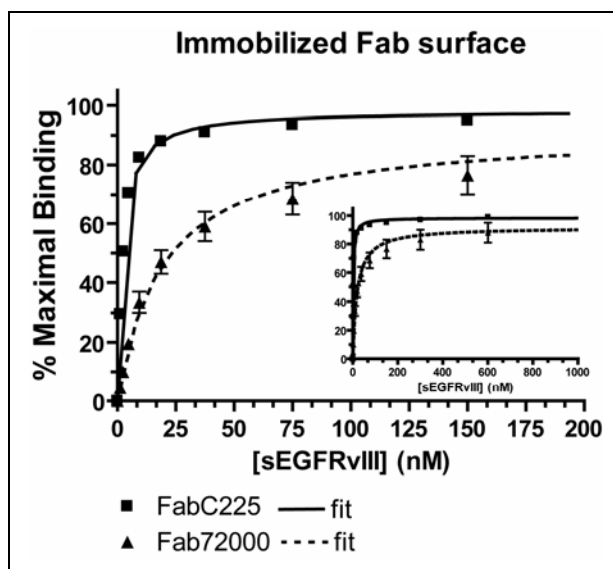


Fig. 24: Characterization of cetuximab and matuzumab binding to sEGFRvIII

Surface plasmon resonance (SPR)/Biacore analysis of the binding of sEGFRvIII to immobilized FabC225 or Fab72000. A series of sEGFRvIII samples of the indicated concentrations was passed over a biosensor surface to which FabC225 or Fab72000 had been amine coupled. Data points show the equilibrium SPR response value for a representative set of samples for FabC225 (black squares) and Fab72000 (black triangles), expressed as a percentage of the maximal SPR binding response. The curves represent the fit of these data to a simple one-site Langmuir binding equation. The inset shows that there is no additional binding at higher concentrations. K_D values, based on at least three independent binding experiments, are 19.4 ± 2.4 nM and 2.2 ± 0.1 nM for sEGFRvIII binding to Fab matuzumab and Fab cetuximab, respectively.

SPR/ Biacore experiments were carried out to characterize the binding of the ligand to sEGFRvIII. The apparent K_D value obtained was $2.4 \pm 0.3 \mu\text{M}$ (Fig. 24).

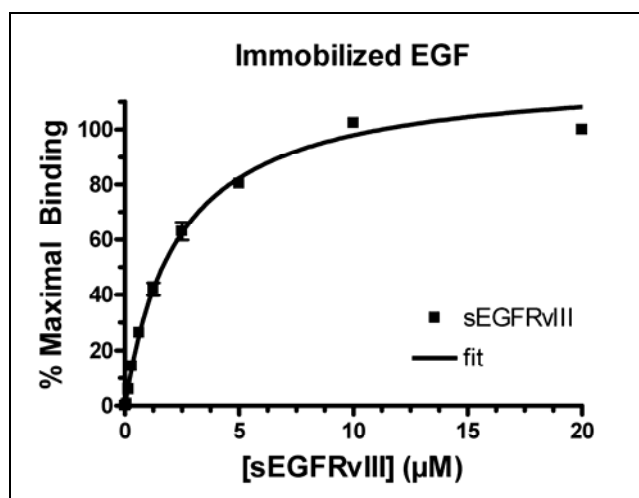


Fig. 25: Characterization of EGF binding to sEGFRvIII

Surface plasmon resonance (SPR)/Biacore analysis of the binding of sEGFRvIII to immobilized EGF. A series of sEGFRvIII samples of the indicated concentrations was passed over a biosensor surface to which EGF had been covalently coupled. Data points show the equilibrium SPR response value for a representative set of samples expressed as a percentage of the maximal SPR binding response. The curve represents the fit of these data to a simple one-site Langmuir binding equation. The K_D value, based on at least three independent binding experiments, is $2.4 \pm 0.3 \mu\text{M}$.

6.2.4. The sEGFRvIII structure

The crystal structure of sEGFRvIII was determined at 3.9 \AA resolution. It reveals the intact sEGFR wild type domain III and IV. However, for domain I and II including the deletion junction (residues 1-5 and 274-309 of wild type sEGFR) almost no electron density was visible. These domains are probably disordered in the crystal structure and are therefore not included in the model of sEGFRvIII (Fig. 26 and Fig. 27).

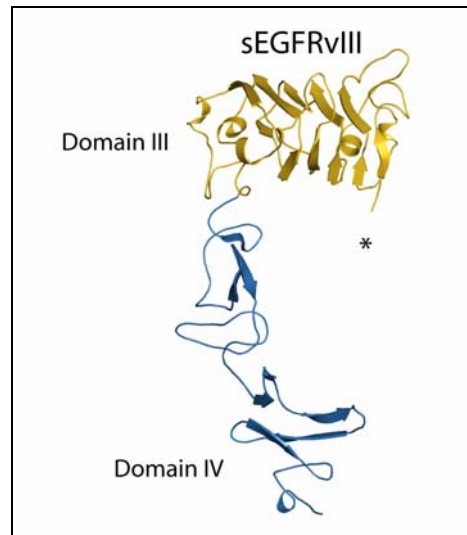


Fig. 26: Structure of sEGFRvIII

Cartoon representation of the extracellular domain of the mutant EGFR variant III (sEGFRvIII). Domain III is colored in gold and domain IV in blue. No electron density was observed for domain II and domain I including the deletion junction indicating a disordered region in the crystal (marked by an asterisk) (see Fig. 27).

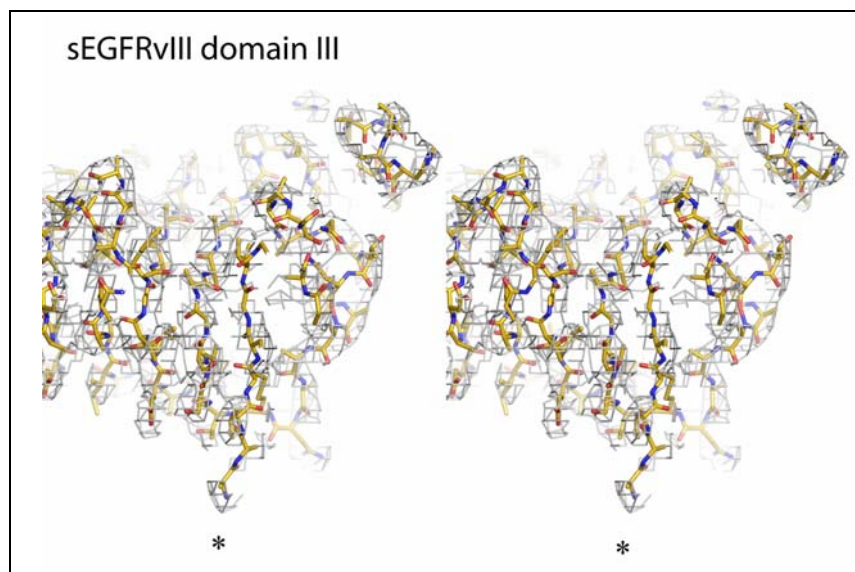


Fig. 27: Electron density of sEGFRvIII domain III

Stereo representation of a slab of the sEGFRvIII domain III electron density. Amino acids are shown in stick representation and colored in gold. The grey mesh represents the $2F_o - F_c$ electron density map contoured at 1.0σ . Oxygen atoms are colored in red, nitrogen in blue and disulfide bridges in yellow. The asterisks mark the last amino acid that is visible at the N-terminus of domain III.

6.2.5. The sEGFRvIII solution structure

Small-angle X-ray solution scattering studies were carried out to calculate a low resolution shape of sEGFRvIII in solution and to model the disordered regions in the crystal structure. An estimate of the molecular mass was assessed from the Porod volume of the particle in solution, which is equal to 1230 \AA^3 . The experimental radius of gyration R_g and maximum size D_{\max} of sEGFRvIII were estimated as $40 \pm 5 \text{ \AA}$ and $160 \pm 10 \text{ \AA}$, respectively.

The processed and merged SAXS scattering curve in the range $0.05 < s < 0.30 \text{ \AA}^{-1}$ from sEGFRvIII is displayed in Fig. 28. Overlaid are the by CRY SOL calculated scattering curves of sEGFRvIII as seen in the crystal structure and sEGFRvIII ($\chi = 9.39$) modeled by BUNCH ($\chi = 3.21$, see below) (Svergun *et al.*, 1995; Petoukhov and Svergun, 2005).

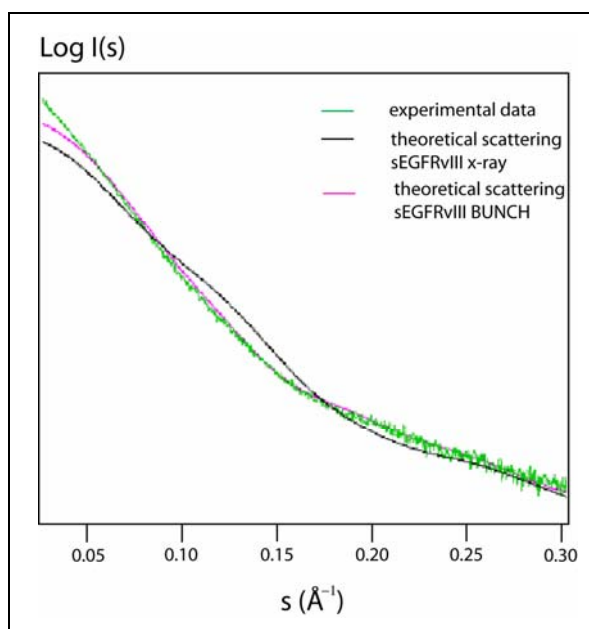


Fig. 28: Experimental and calculated SAXS scattering curves sEGFRvIII

Experimental and theoretical scattering intensities calculated by CRY SOL (relative scale) as a function of the momentum transfer $0.05 < s < 0.30 \text{ \AA}^{-1}$ ($s = 4\pi \sin\theta/\lambda$) for sEGFRvIII. Displayed are the experimental scattering data (green), the theoretical scattering curve of the sEGFRvIII fragment seen in the crystal structure (sEGFRvIII x-ray, black) and the theoretical scattering of sEGFRvIII modeled by BUNCH (sEGFRvIII BUNCH, pink). The scattering of sEGFRvIII x-ray and sEGFRvIII BUNCH fit the experimental data with discrepancies of $\chi = 9.39$ and $\chi = 3.21$, respectively.

The model of sEGFRvIII calculated by BUNCH (Petoukhov *et al.*, 2002; Petoukhov and Svergun, 2005) shows domain I and II as well as the receptor ectodomain C-terminus as dummy residues (DR) (Fig. 29). The model fits the experimental scattering with a discrepancy of $\chi = 3.21$ (Fig. 28).

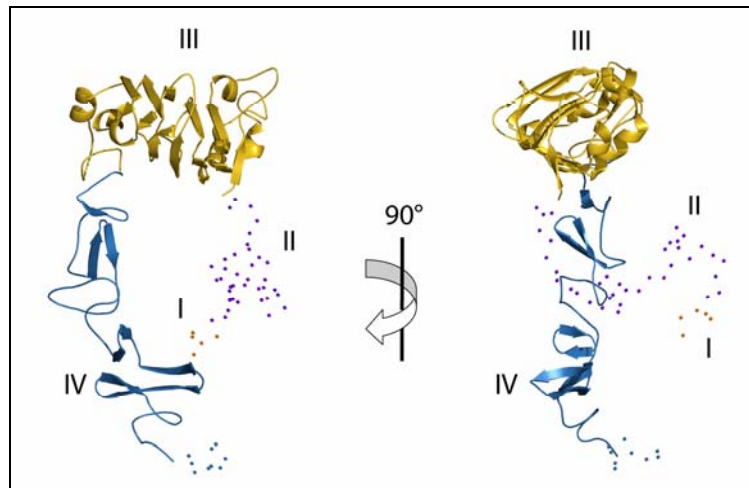


Fig. 29: Model of the disordered sEGFRvIII regions calculated by BUNCH

Cartoon representation of sEGFRvIII modeled by BUNCH (Petoukhov and Svergun, 2005) with domain III and IV colored according to Fig. 26. The model of the C-terminus (blue) as well as domain I (orange) and II (purple) are displayed as dummy residue chain. The optimal position of domain III and IV as rigid body domain and the probable conformations of the C-terminus and domain I/II were found by a simulated annealing protocol using the program BUNCH. The program combines rigid body with *ab initio* modeling.

The low resolution shape of sEGFRvIII was reconstructed *ab initio* using the bead modelling program DAMMIN (Svergun, 1999), which employs the range of scattering vectors up to $s = 0.3 \text{ \AA}^{-1}$ (resolution about 20 \AA). The most probable model averaged out of a 10 reconstructions (Fig. 30) displays a very extended structure and fits the experimental data with discrepancy $\chi = 1.69$.

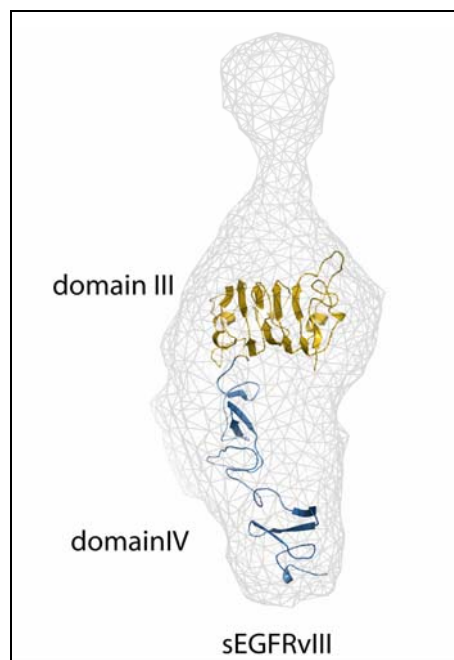


Fig. 30: *Ab initio* solution structure of sEGFRvIII calculated by DAMMIN

Cartoon representation of sEGFRvIII as seen in the crystal structure (Fig. 26) fitted into the *ab initio* shape (displayed as a grid) of solution sEGFRvIII calculated by the program DAMMIN (Svergun, 1999). 10 densely packed bead models were calculated based on simulated annealing procedures and averaged to determine common structural features using the programs DAMAVER (Volkov and Svergun, 2003) and SUPCOMB (Kozin and Svergun, 2001).

6.3. Discussion

6.3.1. Antibody and ligand binding characteristics to soluble EGFRvIII

The K_D values of 19.4 ± 2.4 nM and 2.2 ± 0.1 nM for Fab72000 and FabC225, respectively, binding to sEGFRvIII obtained by surface plasmon resonance (SPR)/Biacore studies (see 6.2.3) are in accordance with the affinity values for wild type sEGFR: the Fab72000 showed a K_D value of 43 ± 13 nM for binding to the isolated sEGFR domain III (Schmiedel *et al.*, 2008; see 5.2.1), and FabC225 was reported to have a K_D value of 2.3 ± 0.5 nM for wild type sEGFR (Li *et al.*, 2005). For Fab72000 binding to the full ectodomain of EGFR a K_D value of 113 ± 25 nM was obtained (Schmiedel *et al.*, 2008; see 5.2.1). An overview of the K_D values compared here is given in Table 5.

Table 5: Affinities of Fab72000, FabC225 and EGF to different sEGFR constructs

| K_D values | Fab72000 | FabC225 | EGF |
|------------------|-------------------|-------------------|------------------------|
| sEGFR | 113 ± 25 nM | 2.3 ± 0.5 nM* | 130 ± 3 nM* |
| sEGFRvIII | 19.4 ± 2.4 nM | 2.2 ± 0.1 nM | 2.4 ± 0.3 μ M |
| sEGFR domain III | 43 ± 13 nM | 1.7 ± 0.6 nM* | 2.3 ± 0.5 μ M* |

(*data marked with an asterisk are taken from Li *et al.*, 2005)

The reduced affinity of the Fab to the full ectodomain in comparison to the single domain could be explained by steric hindrances from the other domains of sEGFR. The similar affinities of Fab matuzumab binding to sEGFRvIII and sEGFR domain III can be explained by the same absence of steric influence in sEGFRvIII with the deleted parts of domain I and II. Cetuximab binding seems to be less impaired by the presence of the other domains in the EGFR ectodomain since its affinities for sEGFR and sEGFRvIII are the same.

The characteristics of ligand binding to sEGFRvIII obtained by SPR/Biacore studies are also in accordance with previously reported affinities (Table 5). The K_D value 2.4 ± 0.3 μ M of EGF binding to sEGFRvIII (see 6.2.3) corresponds well with the K_D value for the binding to isolated domain III: between 500 nM for the Kohda fragment (Kohda *et al.*, 1993) and 2.3 ± 0.5 μ M for insect cell expressed sEGFRd3 (Ogiso *et al.*, 2002; Dawson *et al.*, 2005; Li *et al.*, 2005). Thus, the mutation is not affecting EGF binding to the domain III binding site. However, high affinity ligand binding to EGFR requires the presence of both domain I and domain III, which explains why no ligand binding at the cell surface has been observed

(Wikstrand *et al.*, 1997). At the cell surface the concentration of EGF is well below the K_D value for the binding of EGF to domain III alone. By contrast the Biacore assay is performed at a much higher concentration of soluble ligand (in this case sEGFRvIII, which binds to immobilized EGF). Under these conditions the monovalent binding of domain III alone to EGF can be detected, which is not seen at the cell surface.

Based on the sequence of sEGFRvIII the receptor domain III is predicted to be unaffected by the deletion mutation. The unchanged affinities of ligand and of antibody binding to different epitopes on this domain indeed indicate the same overall fold of domain III in wild type sEGFR and mutant sEGFRvIII. To further investigate the structure of the EGFRvIII ectodomain and to gain insight into the activation of the mutant, its crystal and solution structure were determined by x-ray crystallography and SAXS, respectively.

6.3.2. The structure of EGFRvIII domain III and IV is unaffected by the mutation

The 3.9 Å low resolution crystal structure of sEGFRvIII (Fig. 26) shows the intact sEGFR wild type domain III and IV. The flexible N-terminus of sEGFRvIII that is not seen in the crystal structure might be one reason for the low diffraction quality of the crystals.

Superposition of the domains III of sEGFRvIII and sEGFR shows a shift of domain IV of about 20° relative to domain III (Fig. 31).

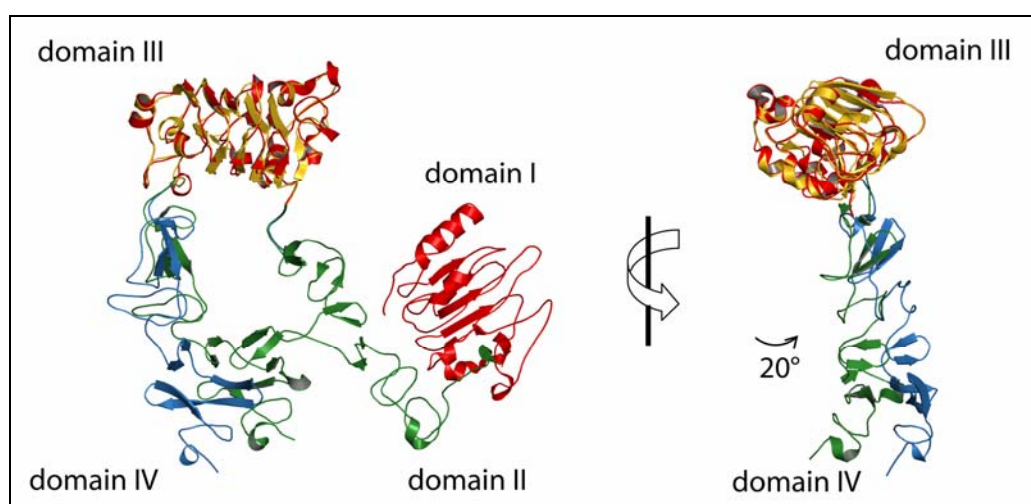


Fig. 31: sEGFRvIII and sEGFR wild type in comparison

Cartoon presentation of sEGFR wild type and sEGFRvIII aligned with their domains III. sEGFR (PDB ID 1YY9, Li *et al.*, 2005) is colored in green and red analogue to Fig. 6, sEGFRvIII is shown in yellow and blue analogue to the coloring in Fig. 26. The receptor domain IV shows a shift of about 20° in respect to domain III.

The shift of domain IV in respect to domain III in comparison to sEGFR in PDB ID 1YY9 could be induced by crystal packing or could signify a biological relevance. Crystal packing as a reason for the shift seems to be more reasonable, since the position of domain IV in 1YY9 would be impaired in the crystal of sEGFRvIII through symmetry mates. Furthermore other ErbB structures indicate a flexibility in the linker region between domain III and IV. Superposition of the domains III of other EGFR structures (PDB IDs 1NQL, 3B2V) or other ErbB family members (PDB IDs 1N8Z, 1M6B, 1S78, 2AHX) also shows slight shifts ($\sim 10^\circ$) of domain IV relative to domain III.

6.3.3. sEGFRvIII in solution

An estimate of the molecular mass of sEGFRvIII in solution was assessed from the Porod volume of the particle, which was calculated as 1230 \AA^3 . Noting that, for globular proteins, the hydrated volume in \AA^3 should be about twice the molecular mass in Da (Porod, 1982), a molecular weight estimate of 61.5 kDa is obtained. This is in line with monomeric sEGFRvIII (47 kDa by SLS/SEC). The experimental radius of gyration R_g and maximum size D_{\max} ($40 \pm 1 \text{ \AA}$ and $160 \pm 5 \text{ \AA}$, respectively) are larger than expected from the crystal structure of sEGFRvIII, where the maximum distance is 100 \AA (Fig. 26). The additional extension of the particle in solution could be due to partial receptor aggregation. This leads to the generation of a very extended molecule in the *ab initio* shape reconstitutions (Fig. 29 and Fig. 30) and to a high discrepancy ($\chi = 3.21$) of the experimental scattering and the theoretical scattering of the model calculated by BUNCH (Fig. 28 and Fig. 29). The *ab initio* models calculated by DAMMIN (Fig. 30) fit the experimental data with a lower discrepancy ($\chi = 1.69$), but is still not close to the ideal fit with a χ value 1.

The SAXS measurements need to be repeated with samples closer to monodispersity.

6.3.4. sEGFRvIII dimerization and activation

Analytical size exclusion chromatography (SEC) and static light scattering (SLS) experiments (Fig. 23) showed that the isolated extracellular domain of sEGFRvIII is unable to dimerize in the presence of ligand. This is maybe not surprising in the absence of the dimerization arm. However, this result shows that the amino acids N274 and E293 in domain II, which are unaffected by the deletion mutation, are not sufficient for soluble receptor

dimerization. These amino acids are known to participate in crucial interactions for stabilizing the dimerization competent conformation of the receptor (Dawson *et al.*, 2005).

Recently, it was argued that for a thorough analysis of EGF receptor dimerization and activation the *whole* receptor needs to be investigated beside the ectodomain (Lemmon, 2009). The ligand binding properties of wild type sEGFR can only be explained if in addition to the soluble extracellular domain also the transmembrane and juxtamembrane domains are included (Macdonald and Pike, 2008). However, studies investigating the homodimerization properties of EGFRvIII at the cell surface are controversial. On one hand it was reported that the transforming characteristics of EGFRvIII at the cell surface are independent of receptor dimerization (Chu *et al.*, 1997). On the other hand it was reported that the mutant receptor partly homodimerizes at the cell surface and induces constitutive receptor activation (Fernandes *et al.*, 2001).

Heterodimerization between the ectodomains of EGFR and EGFRvIII could not be observed in the SEC/SLS studies presented here (Fig. 23). In mouse cells transfected with EGFR and EGFRvIII heterodimerization was reported for the two receptors leading to enhanced phosphorylation of the wild type receptor (Luwor *et al.*, 2004). It is unclear if the mutant receptor is able to heterodimerize with the other ErbB family members.

The studies presented here show that the isolated extracellular domain of sEGFRvIII itself is unable to dimerize and to explain the oncogenic properties of the mutant. The results underline the importance to investigate the whole transmembrane receptor in order to understand its signaling properties. Cell surface homo- and heterodimerization properties of EGFRvIII and its influence on EGFRvIII signaling are still not fully understood.

6.3.5. Implications for a therapeutic approach against EGFRvIII driven cancers

The mutant receptor EGFRvIII was shown to be constitutively active on the cell surface independent of ligand binding (Pedersen *et al.*, 2001; Zhu *et al.*, 2009). The structure of the extracellular domain as well as the binding studies presented here show that the ligand binding site on domain III is unaffected by the mutation. However, the affinity of the ligand to domain III alone is too low to observe binding at the ligand concentration present at the cell surface. The results are in accordance with the observation that no ligand binding can be detected at the cell surface.

If EGFRvIII is indeed constitutively active independent of receptor dimerization as was argued by Chu *et al.* (Chu *et al.*, 1997), a therapeutic approach by monoclonal antibodies would be a special case in the EGFR field. Many modes of action described for therapeutic anti-EGFR antibodies such as direct steric blockage of ligand binding or inhibition of receptor dimerization (Schmitz and Ferguson, 2009) (see 5.1.5) would not be relevant for EGFRvIII. However, antibody-dependent cellular cytotoxicity (ADCC) and complement-dependent cytotoxicity (CDC) as well as antibody-mediated receptor down-regulation and augmentation of the antitumor effects of chemo- and radiotherapy (Mendelsohn and Baselga, 2006; Schmitz and Ferguson, 2009) might still be very powerful effects of antibody binding. The structure of the EGFRvIII extracellular domain and the binding studies presented here showed that the antibodies cetuximab and matuzumab are able to bind to the soluble mutant receptor with wild type affinity. Cellular studies showed efficient recognition of cell surface EGFRvIII by several monoclonal antibodies directed against EGFR, including cetuximab (Wikstrand *et al.*, 1995; Modjtahedi *et al.*, 2003; Aerts *et al.*, 2007; Yang *et al.*, 2008). However, *in vivo* effectivity of cetuximab was reported to be reduced in comparison to targeting the wild type receptor (Fukai *et al.*, 2008). On human glioma cell lines expressing EGFRvIII cetuximab was shown to bind and to trigger ADCC in a dose-dependent manner, but to exhibit no growth-inhibitory effect (Fukai *et al.*, 2008). This reduced efficacy of cetuximab in EGFRvIII expressing gliomas might be due to the missing direct effects of cetuximab observed for wild type EGFR.

6.4. Conclusion

The deletion mutation in the ectodomain of the EGFR variant III is not affecting the structure of domain III and IV as seen in the crystal structure presented here (Fig. 26). The mutant is binding ligand with its domain III binding site (Fig. 25) with an affinity comparable to wild type EGFR. This affinity is however too low to see effective ligand binding at the cell surface. The dimerization studies presented here (Fig. 23) show that the soluble ectodomain is not able to dimerize upon ligand stimulation. This result is consistent with cell surface studies of Chu *et al.*, which showed that EGFRvIII activation does not include receptor dimerization (Chu *et al.*, 1997). However, Fernandes *et al.* presented cell surface experiments with partly dimerized EGFRvIII (Fernandes *et al.*, 2001). It remains unclear what exactly happens at the cell surface, when EGFRvIII is present. Thorough cell surface studies and full length receptor experiments are needed to understand the oncogenic properties of the mutant at the cell surface.

However, a therapeutic approach against EGFRvIII driven cancers, most notably glioblastomas, with monoclonal antibodies binding to the wild type domain III or IV might be beneficial for patients. These antibodies are predicted to bind with wild type affinity to the mutant at the cell surface since the structure of the two domains is unaffected by the deletion mutation as seen in the crystal structure (Fig. 26). Binding studies with cetuximab and matuzumab presented here confirmed that prediction (Fig. 24).

The antibodies are not expected to impair receptor dimerization through block of ligand binding or steric hindrances as seen for the wild type receptor. But they might be able to elicit antibody-dependent cellular cytotoxicity and receptor down-regulation as well as to increase the susceptibility of the cells to radio- and/or chemotherapy. Effectiveness of antibody-based therapy against EGFRvIII driven cancers needs to be evaluated in clinical trials.



7. Characterization of the antibody EMD1159476 binding to the insulin-like growth factor-1 receptor (IGF-1R)

7.1. Introduction

The insulin-like growth factor-I receptor (IGF-1R) is a member of the receptor tyrosine kinase family (see 3.1) and, together with the insulin receptor (IR) and insulin-related receptor (IRR), forms a subfamily with similar structural organization (Ward and Lawrence, 2009) (Fig. 1 and Fig. 32). In normal physiology, ligand activation of IGF-1R is involved in fetal growth and linear growth of the skeleton and other organs (Ruan *et al.*, 1992; Ruan *et al.*, 1999; Sullivan *et al.*, 2008), whereas IR regulates glucose homeostasis (Kitamura *et al.*, 2003). Children with mutations in IGF-1R have been described to have poor *in utero* and postnatal growth and neurodevelopmental delay (Woods *et al.*, 1996; Abuzzahab *et al.*, 2003). The third member of the IR family IRR has no known ligand and no identified function (Ward *et al.*, 2007).

Although IGF-1R and IR are in their domain organization very similar and both receptors almost ubiquitously expressed in the organism, they perform accurately distinct cellular and physiological functions. This is achieved through a fundamentally different regulation of ligand bioavailability. The ligand of IR insulin is excreted by the pancreas depending on blood glucose levels, whereas the ligands of IGF-1R are produced under endocrine growth hormone (GH) control in the liver as well as in somatic cells. IGF-1R is bound by three different ligands: insulin-like growth factor-1 (IGF-1), IGF-2 and with a twofold lower affinity insulin (Ryan and Goss, 2008). The bioavailability of IGF-1 and IGF-2 in the tissue is regulated by a family of six binding proteins, called IGF binding proteins (IGFBPs) (Clemmons, 2007). However, gene deletion studies suggest that IGF-1R and IR are still capable of compensating the loss of the respective other receptor, with IR able to stimulate growth (Firth and Baxter, 2002) and IGF-1R capable of regulating a metabolic response (Di Cola *et al.*, 1997).

Both IGF-1R and IR are homodimers with their extracellular domains composed of two α and two β chains, which are covalently linked through disulfide bridges, a transmembrane region for each β chain and an intracellular kinase domain (Ullrich *et al.*, 1986; Denley *et al.*, 2005) (Fig. 32).

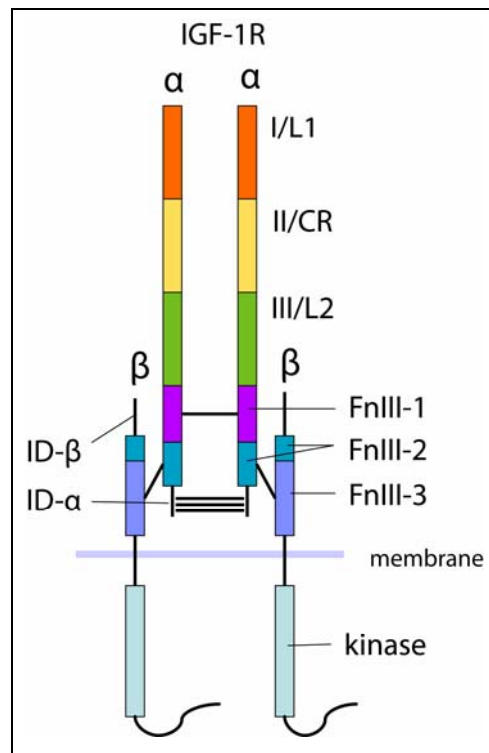


Fig. 32: Domain organization of IGF-1R

The insulin-like growth factor-1 receptor (IGF-1R) is a disulfide-linked dimer and belongs to the family of transmembrane receptor tyrosine kinases. The extracellular domain comprises two α and two β chains each with two homologous large domains I and III (or L1 and L2) in orange and green and a cysteine-rich domain II (or CR) in yellow. These domains are closely related to the EGF receptor family domains I-III. Three Fn type III domains (FnIII-1 – 3) in magenta, cyan and blue are linked by disulfide bridges with the approximate locations indicated. The second FnIII domain contains a 120-residue long insert domain (ID), which includes the cleavage site to generate the α and β chain (figure adapted from Ward *et al.*, 2007)

The α and β subunits are expressed as a single precursor polypeptide, which is then post-translationally processed by dimerization, proteolytic cleavage and glycosylation (Ward *et al.*, 2007). The amino-terminal regions of the α chain of both IGF-1R and IR are composed of three domains, which show a close resemblance to the domains I-III of the EGF receptor family (see 5.1). They comprise two structurally homologous domains, called large homologous domain L1 (domain I) and L2 (domain III), which are separated by a cysteine-rich (CR) domain (domain II) (Surinya *et al.*, 2008). Domains I to III of IGF-1R are connected to the transmembrane region through three fibronectin type-III domains (FnIII-1 - 3) (Fig. 32).

7.1.1. Structures of IGF-1R and IR extracellular domains

The first ectodomain structure of the IGF-1R/IR family was solved in 1998: the domains I-III of IGF-1R (Garrett *et al.*, 1998). This structure provided a framework to interpret mutations leading to alterations in ligand binding specificity both for IGF-1R and IR (Whittaker *et al.*, 2001; Whittaker *et al.*, 2002). Only 8 years later the structure of the same construct of IR was solved (Lou *et al.*, 2006). A comparison of the IGF-1R and IR structures showed differences in two regions that are thought to influence ligand specificity: one residue (F39 in IR and S35 in IGF-1R) in domain I and a large loop in the domain II (Lou *et al.*, 2006) (Fig. 33). This loop protrudes into the putative ligand binding site in IR, but is more flat and shows significantly less α -helix in IGF-1R. It has almost no sequence similarity and an opposite electrostatic potential in the two receptors.

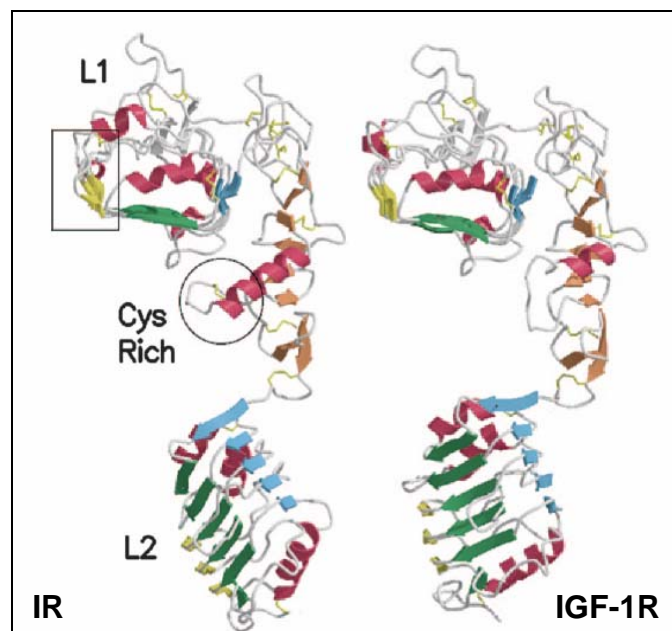


Fig. 33: Comparison of the domain I-III structures of IR and IGF-1R

Cartoon representation of the first three domains of the insulin receptor (IR) and the insulin-like growth factor 1 receptor (IGF-1R). Helices are shown in red; sheets in domain I (L1) and domain III (L3) in blue, green and yellow; sheets in domain II (Cys Rich) are shown in orange. The side chains of disulfide-linked cysteine residues are represented as yellow sticks. The two regions comprising the main structural differences between the two related receptors are indicated with a box and a circle in IR (figure adapted from Lou *et al.*, 2006).

The first full length ectodomain structure of the IGF-1R/IR family was solved in the same year (McKern *et al.*, 2006). The IR-A extracellular domain crystallized at 3.8 Å resolution as a dimer bound by four monoclonal anti-body Fabs for stabilization. Surprisingly and in contrast to previously suggested models (Ottensmeyer *et al.*, 2000; De Meyts and Whittaker, 2002), the structure showed a folded-over conformation (monomer shown in Fig. 35) that suggests a ligand binding site between the domain I, domain III and the carboxy-terminal surface of FnIII-1 (McKern *et al.*, 2006).

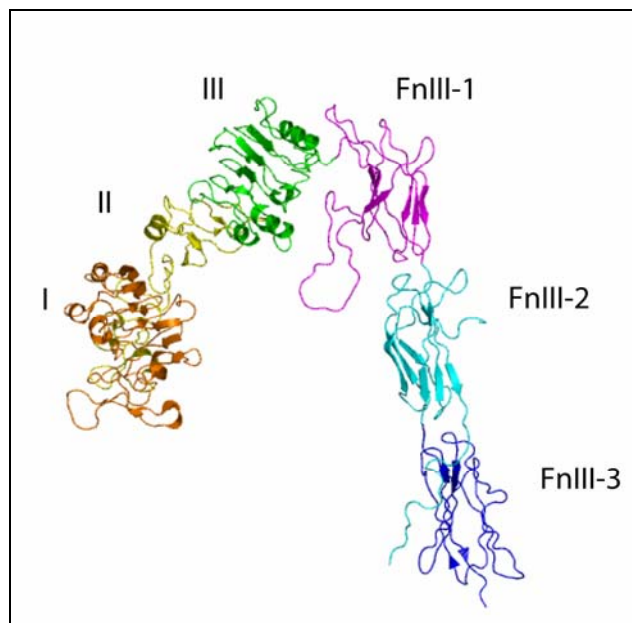


Fig. 34: Structure of the insulin receptor ectodomain monomer

Crystal structure of the insulin receptor (IR) monomer shown in cartoon representation based on protein data base (PDB) ID 2DTG (McKern *et al.*, 2006). Individual domains are colored as follows: domain I, orange; domain II, yellow; domain III, green; FnIII-1, magenta; FnIII-2, cyan; FnIII-3, blue. No convincing electron density was described for parts of the insert domain- α and - β .

A model for the ligand-induced activation of IR based on the structure of the ectodomain dimer is described in the following section. A similar mechanism is assumed for IGF-1R based on sequence similarities between the two receptors, structural similarities as seen for domain I-III and biochemical studies (Lawrence *et al.*, 2007 and references therein).

7.1.2. Ligand-induced IR/IGF-1R activation

The structure of the IR ectodomain comprises two receptor monomers as shown in Fig. 34, which are oriented to one another with a reversed mirror axis. The domains I-III (L1, CR, L2) of one monomer are packed against the three FnIII domains (FnIII-1 – 3) of the other and vice versa (McKern *et al.*, 2006) (Fig. 35). The current model for ligand binding (McKern *et al.*, 2006; Ward *et al.*, 2008) proposes that each monomer in the receptor dimer contains two different binding sites, referred to as Site 1 and Site 2 (Fig. 35). Ligand binding to Site 1 on either of the two α subunits has a low affinity and is followed by a second high-affinity binding event between the bound ligand and Site 2 of the opposite receptor.

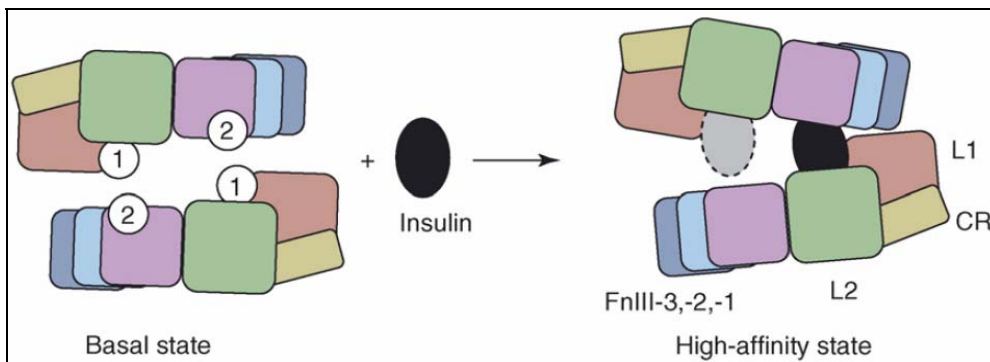


Fig. 35: Insulin receptor ligand binding model

Model of insulin binding to the insulin receptor (IR) with two ectodomains symmetrically aligned and viewed down the Y-axis. Each domain is represented as a rectangle colored the same as in Fig. 34. The approximate locations of the ligand binding Sites 1 and 2 are indicated. In the basal state, both low-affinity binding sites are equally accessible. In the high-affinity state, one insulin molecule binds to Sites 1 and 2 of opposite receptors, causing the two monomers to close up on that side and to open up on the opposite side. The simultaneous binding of two insulin molecules is not possible, thus causing negative cooperativity of ligand binding (figure taken from Ward *et al.*, 2007).

Two insulin molecules cannot bind simultaneously, which causes a ‘see-sawing’ movement of the receptors oscillating from one state into the other (De Meyts, 1994; Ward *et al.*, 2007; Kiselyov *et al.*, 2009). This model implies a negative cooperativity of ligand binding, which is indeed seen in cell surface ligand binding experiments to IGF-1R and IR (De Meyts and Whittaker, 2002; De Meyts, 2004). Interestingly, ligand binding to IGF-1R and IR reveals high and low affinity ligand binding states and a negative cooperativity exactly as observed for EGFR (see 5.1 and Lemmon, 2009).

Surprisingly, soluble ectodomains show only low affinity binding despite the fact that the dimer is already preformed through disulfide-bridges (Ward and Lawrence, 2009). This implies that the soluble constructs are unable to adopt exactly the conformation of the membrane-bound dimers. The high affinity binding of IR and IGF-1R ectodomains is restored

in the presence of a transmembrane anchor (Surinya *et al.*, 2008; Ward and Lawrence, 2009), Fc domains (Bass *et al.*, 1996) or a leucine zipper motif (Hoyne *et al.*, 2000). While soluble IR ectodomains do not show negative cooperativity as expected (De Meyts, 1994; De Meyts and Whittaker, 2002), IGF-1R soluble ectodomains do (Surinya *et al.*, 2008). This difference might be one of the factors regulating the biological activities of the two functionally different receptors.

Ligand binding induces a conformational change both in the ligand and in the receptor leading to intracellular transphosphorylation of one kinase by the other (Butler *et al.*, 1998; Ward and Lawrence, 2009). The phosphorylated tyrosine residues intracellularly recruit downstream effector proteins, including insulin receptor substrate (IRS)-1 to IRS-4, and stimulate signal cascades as described in section 3.4 (Samani and Brodt, 2001). IGF-1R signaling results in both proliferative and antiapoptotic effects (Kurmasheva and Houghton, 2006). Furthermore, IGF-1R can interact with steroid hormones and their receptors, other peptide growth factor receptors, extracellular matrix proteins, integrin receptors and cytokines, such as transforming growth factor- β (Hartog *et al.*, 2007).

7.1.3. IGF-1R and cancer

The involvement of IGF-1R in malignant transformation was first recognized in fibroblasts derived from homozygous IGF-1R null mice embryos (Sell *et al.*, 1993). These cells are normally prone to transformation; however, in the absence of IGF-1R oncogenes are unable to induce malignant transformation. Re-expression of IGF-1R in these cells restored their susceptibility to transformation. In the following years signaling from the IGF-1 system was connected to the pathogenesis of many different human cancers, including breast, colon, liver, pancreatic and prostate cancer as well as melanoma, multiple myeloma and glioblastoma (Resnicoff *et al.*, 1994; Hankinson *et al.*, 1998; Kalli *et al.*, 2002; Cardillo *et al.*, 2003; Durai *et al.*, 2005).

Studies showed that the aberrant activation of the IGF-1R signaling cascade leads to enhanced proliferation, survival and metastasis in cancer cells (DiGiovanni *et al.*, 2000; Hadsell *et al.*, 2000; Carboni *et al.*, 2005; Kurmasheva and Houghton, 2006). In addition, there also seems to be an involvement of enhanced IGF-1R activity in resistance to certain anticancer therapies, including cytotoxic chemotherapy, hormonal agents, monoclonal antibodies and radiation (Camirand *et al.*, 2002; Abe *et al.*, 2006; Desbois-Mouthon *et al.*, 2006; Allen *et al.*, 2007). IGF-1R has also be shown to be involved in the unique malignant

property of anchorage-independent growth (Baserga *et al.*, 2003) and to influence the signaling of other growth factor receptors such as the vascular endothelial growth factor receptor (VEGFR) and the epidermal growth factor receptor (EGFR) (Tao *et al.*, 2007). Amplification of the *IGF-1R* gene, however, is infrequent as shown in breast tumors (<2%) (Berns *et al.*, 1992; Almeida *et al.*, 1994) and sarcomas (Sekyi-Otu *et al.*, 1995). Activating mutants of the receptor have not been described yet.

Due to the ubiquitous presence and body-wide physiologic function of IGF-1R, serious side effects of targeting the receptor in a tumor therapy has long been a major concern. In addition cross-reactions with the IR signaling system were feared to cause diabetes. Signaling through hybrid receptors was shown to be involved in tumor promoting effects (Rose *et al.*, 2006; Avnet *et al.*, 2009). It may thus be not enough to target the IGF-1R alone.

Strategies to inhibit IGF signaling in cancer include the reduction of available ligand (Letsch *et al.*, 2003), the reduction of receptor activity (Resnicoff *et al.*, 1996; McCutcheon *et al.*, 2001; Rochester *et al.*, 2004) and receptor targeting through specific kinase inhibitors or monoclonal antibodies. Other strategies include administration of IGF binding proteins, antibodies against the ligands IGF-1 and IGF-2, and soluble decoy receptor proteins (Van Den Berg *et al.*, 1997; Samani *et al.*, 2004).

Targeted therapies include tyrosine kinase inhibitors (TKIs) against the intracellular kinase domain, e.g. cyclolignan picropodophyllin (PPP) (Vasilcanu *et al.*, 2008), and monoclonal antibodies against the IGF1-R extracellular domain.

Recent studies, which investigate the results of anti-IGF-1R antibodies given together with other mAbs and/or chemo- or radiotherapy, indicate a synergistic effect of combination therapy. Crosstalk between different receptor tyrosine kinases, e.g. the epidermal growth factor receptor (EGFR) and IGF-1R, as well as mutations or compensations in the downstream signaling cascade imply the necessity to target the transforming signaling network simultaneously at several spots (Gee *et al.*, 2005; Jones *et al.*, 2006; Knowlden *et al.*, 2008).

Several examples of combination treatment in the clinics showed advantages in therapeutic effectivity. E.g. the monoclonal antibody CP-751,871 (see 7.1.4) caused significantly greater inhibition of colorectal and breast cancer xenograft growth in combination with 5-fluorouracil or tamoxifen, respectively as compared with chemotherapy alone (Cohen *et al.*, 2005). Combination of the antibody h7C10 (see 7.1.4) with either a

chemotherapeutic agent or the anti-EGFR antibody cetuximab (see 5.1.5) was superior to either agent alone (Goetsch *et al.*, 2005). Targeting of the EGF receptor family member ErbB2 by trastuzumab (see 5.1.5) in combination with the induction of the dominant-negative IGF-1R expression resulted in enhanced growth inhibition of breast cancer cells (Camirand *et al.*, 2002). The antitumor effects of kinase inhibitors against IGF-1R and EGFR are potentiated in combination in hepatoma cells (Desbois-Mouthon *et al.*, 2006).

The following chapter summarizes the antibodies against IGF-1R that are currently under investigation.

7.1.4. Anti-IGF-1R antibodies

Several monoclonal antibodies against the IGF-1R ectodomain have been developed that block ligand binding and induce receptor internalization and degradation (Li *et al.*, 2000; Burtrum *et al.*, 2003; Maloney *et al.*, 2003; Sachdev *et al.*, 2003; Goetsch *et al.*, 2005; Wang *et al.*, 2005). Some of these are currently in phase I and phase II clinical trials for the treatment of different tumors. As side effects infrequently mild transient hyperglycaemia was observed, whereas hypoglycaemia, a potential result from increased insulin sensitivity, has so far not been reported (Hartog *et al.*, 2007).

CP-751,871. This fully human antibody (Pfizer) showed receptor down-regulation as well as inhibition of xenograft tumor growth of breast cancer, lung cancer and colorectal cancer in a dose-dependent manner (Cohen *et al.*, 2005). Antibody-dependent cellular cytotoxicity (ADCC) was not triggered by this antibody, which might be advantageous in cancer therapy due to the ubiquitous expression of IGF-1R. Phase I studies for patients with advanced solid tumors as well as multiple myeloma showed a favorable safety profile (Haluska *et al.*, 2007; Lacy *et al.*, 2008). A phase II study of CP-751,871 as first-line therapy in combination with chemotherapy for non-small cell lung cancer (NSCLC) as well as phase I/II studies in prostate, colorectal and breast cancer are still ongoing (Weroha and Haluska, 2008; Ryan and Goss, 2008).

IMC-A12. The fully human antibody IMC-A12 (ImClone) was reported to down-regulate IGF-1R and to inhibit *in vivo* breast cancer, colorectal cancer and pancreatic cancer cell growth (Burtrum *et al.*, 2003). A phase I study in solid tumors resulted in a favorable toxicity profile (Weroha and Haluska, 2008). The antibody is currently tested in phase II clinical trials in patients with prostate, breast, pancreatic and colorectal cancer in different combinations with anti-EGFR antibodies, chemotherapy and kinase inhibitors (Ryan and Goss, 2008).

h7C10/MK-0646. The humanized antibody h7C10/MK-0646 (Merck USA) showed growth inhibition for several cancer cell lines and inhibited IGF-1 induced IGF-1R phosphorylation in a dose-dependent manner. Also, h7C10 abolished IGF-1 induced activation of PI-3K/Akt and MAPK pathways, enhanced ADCC *in vitro* and stimulated receptor internalization (Wang *et al.*, 2005; Broussas *et al.*, 2009). h7C10 is currently tested in phase I and II clinical trials in patients with breast, pancreas, prostate and multiple myeloma patients (Goetsch *et al.*, 2005).

AMG 479. This fully human monoclonal antibody (Amgen) is currently in phase I and II clinical trials against bladder, breast, colorectal, gastric and head/neck cancer, as well as melanoma, non-Hodgkin's lymphoma, ovarian, pancreas, prostate and soft tissue sarcoma (Ryan and Goss, 2008). Phase I studies in solid tumors showed mild adverse events, e.g. hyperglycemia.

AVE-1642. This humanized antibody (Sanofi-Aventis) is in phase I clinical trials targeting solid tumors and multiple myeloma (Ryan and Goss, 2008; Descamps *et al.*, 2009).

R1507. The fully human recombinant antibody R1507 (Roche) is in phase I clinical trials against lymphoma, non-Hodgkin's lymphoma, soft tissue sarcoma and unspecified solid tumors (Ryan and Goss, 2008).

SCH-717454. This fully human monoclonal antibody (Schering-Plough) is currently in phase II clinical trials treating patients with sarcomas and colorectal cancer (Weroha and Haluska, 2008).

7.2. Results

In this chapter the binding characteristics of another therapeutic antibody, EMD1159476, are presented. EMD1159476 is preclinically tested as a drug which targets IGF-1R expressing tumors.

7.2.1. Expression and purification sIGF-1R

Baculovirus expression system. A yield of 40 µg/L Sf9 cell culture and of 200 µg/L Hi5 cell culture was obtained. In addition to the low protein yields, the purified proteins showed no defined gel filtration peak and appeared in non-reducing SDS-PAGEs evenly distributed over a wide range of protein sizes from ~50 kDa to 200 kDa. Due to these limitations in the protein production a mammalian expression system for sIGF-1R domain I-III and domain II was established.

Mammalian expression system. A yield of 0.5 mg/L soluble IGF-1R domain I-III (sIGF-1Rd1-3) and 1 mg/L soluble IGF-1R domain II (sIGF-1Rd2) was obtained from HEK293 cell culture. The C-terminal end of the protein was confirmed by Western blot with an anti-His₆-antibody. Purified sIGF-1Rd1-3 and d2 were analyzed both by reducing and non-reducing SDS-PAGEs (Fig. 36) and by analytical SEC/static light scattering (SLS) methods. Both constructs showed a defined SEC peak with a corresponding molar mass of 57.4 kDa for domain I-III and 28 kDa for domain II. This is in accordance with a molecular weight of 53.3 kDa and 18 kDa by sequence plus glycosylation, respectively.

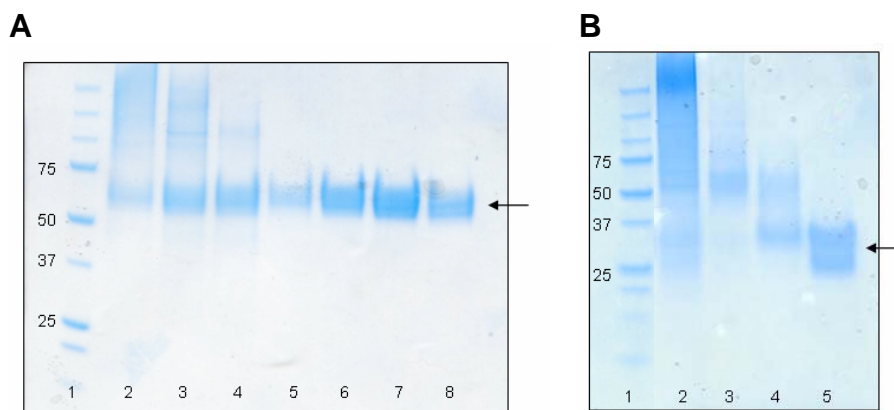


Fig. 36: SDS-PAGE sIGF-1R domain I-III and domain II purification

A: non-reducing SDS-PAGE of sIGF-1R domain I-III gel filtration fractions showing a single band (lanes 5-8) corresponding to a glycosylated protein of the expected size (53.3 kDa by sequence plus glycosylation, marked with an arrow). **B:** non-reducing SDS-PAGE of sIGF-1R domain II gel filtration fractions showing a broad band (lane 5) corresponding to a glycosylated protein of the expected size (17.3 kDa by sequence plus glycosylation, marked with an arrow). The bands appear very broad in the gel, which probably indicates inhomogeneities in the glycosylation pattern. Aggregated or misfolded protein (A and B lanes 2-4) was separated through the gel filtration run using a HiLoad™ Superdex200 16/60 preparation grade column (GE Healthcare) pre-equilibrated with 20 mM HEPES, 100 mM NaCl (pH 7.5). The protein marker is shown both in A and B in lane 1 with the sizes indicated in kDa.

7.2.2. Fab1159476 structure

The x-ray structure of the EMD1159476 Fab fragment (Fab1159476) (see 4.3.3) was determined at 1.7 Å (Fig. 37 and Fig. 38).

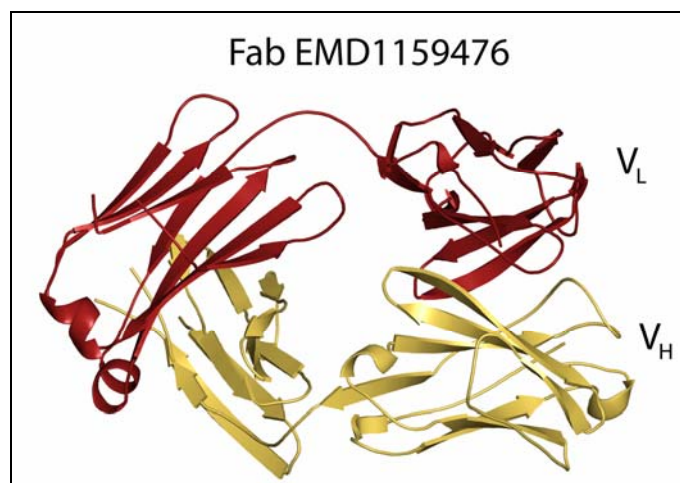


Fig. 37: Fab1159476 structure

Cartoon representation of the Fab fragment EMD1159476. The heavy chain is colored in yellow and the light chain in red.

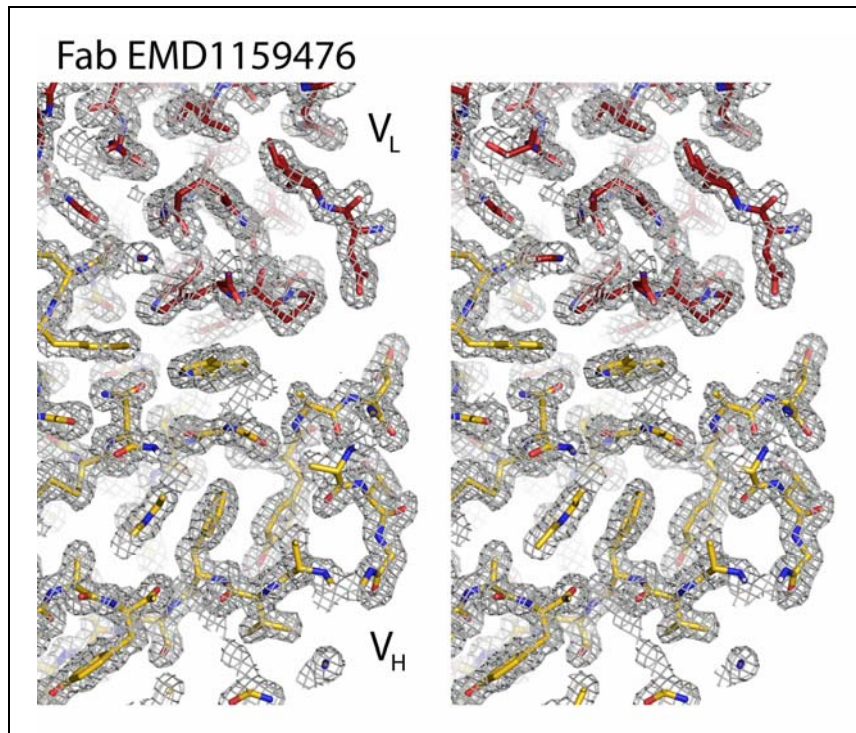


Fig. 38: Fab1159476 electron density

Stereo view of a section of the antibody Fab fragment heavy and light chain. Amino acids are shown in stick representation and are colored in red and yellow for the light and heavy chain, respectively. The gray mesh represents the final $2F_o - F_c$ electron density map contoured at 1.0σ . Oxygen atoms are colored in red, nitrogen in blue and disulfide bridges in yellow.

Crystallization conditions for the complex of sIGF-1R domain I-III:Fab1159476 and IGF-1R domain II:Fab1159476 were extensively screened, but no crystals were obtained.

7.2.3. Antibody binding to sIGF-1R domain I-III and domain II

Surface plasmon resonance (SPR)/Biacore experiments were performed to characterize the binding of Fab1159476 to the isolated soluble extracellular IGF-1 receptor domains I-III (sIGF-1Rd1-3) and domain II (sIGF-1Rd2). The apparent K_D values obtained were 61.4 ± 1.9 nM for sIGF-1Rd1-3 and 30.7 ± 1.4 nM for sIGF-1Rd2 (Fig. 39).

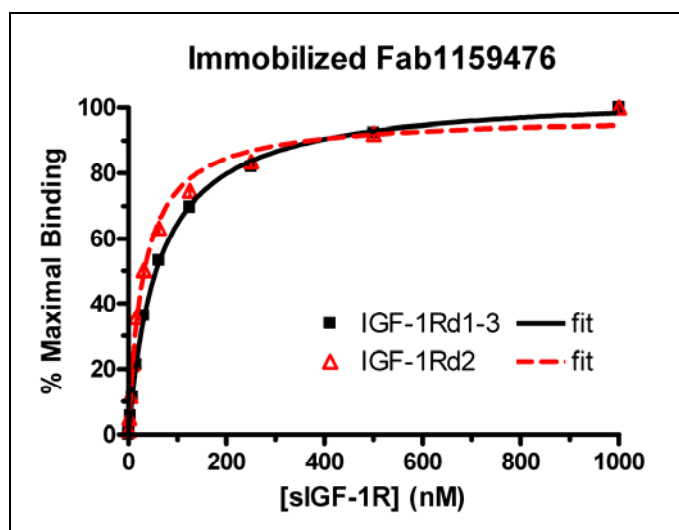


Fig. 39: Characterization of EMD1159476 binding to sIGF-1R

Surface plasmon resonance (SPR)/Biacore analysis of the binding of sIGF-1Rd1-3 and sIGF-1Rd2 to immobilized Fab1159476. A series of samples of sIGF-1Rd1-3 or sIGF-1Rd2, at the indicated concentrations, was passed over a biosensor surface to which Fab1159476 had been amine coupled. Data points show the equilibrium SPR response value for a representative set of samples of sIGF-1Rd1-3 (black squares) and of sIGF-1Rd2 (red triangles), expressed as a percentage of the maximal SPR binding response. The curves represent the fit of these data to a simple one-site Langmuir binding equation. K_D values, based on at least three independent binding experiments, are 61.4 ± 1.9 nM for sIGF-1Rd1-3 and 30.7 ± 1.4 nM for sIGF-1Rd2.

The affinity of the Fab fragment to both receptor constructs was additionally analyzed by ITC. A K_D value of 6.1 ± 1.3 nM and 4.1 ± 0.7 nM for domain I-III and domain II, respectively, was obtained (Fig. 40 and Fig. 41)

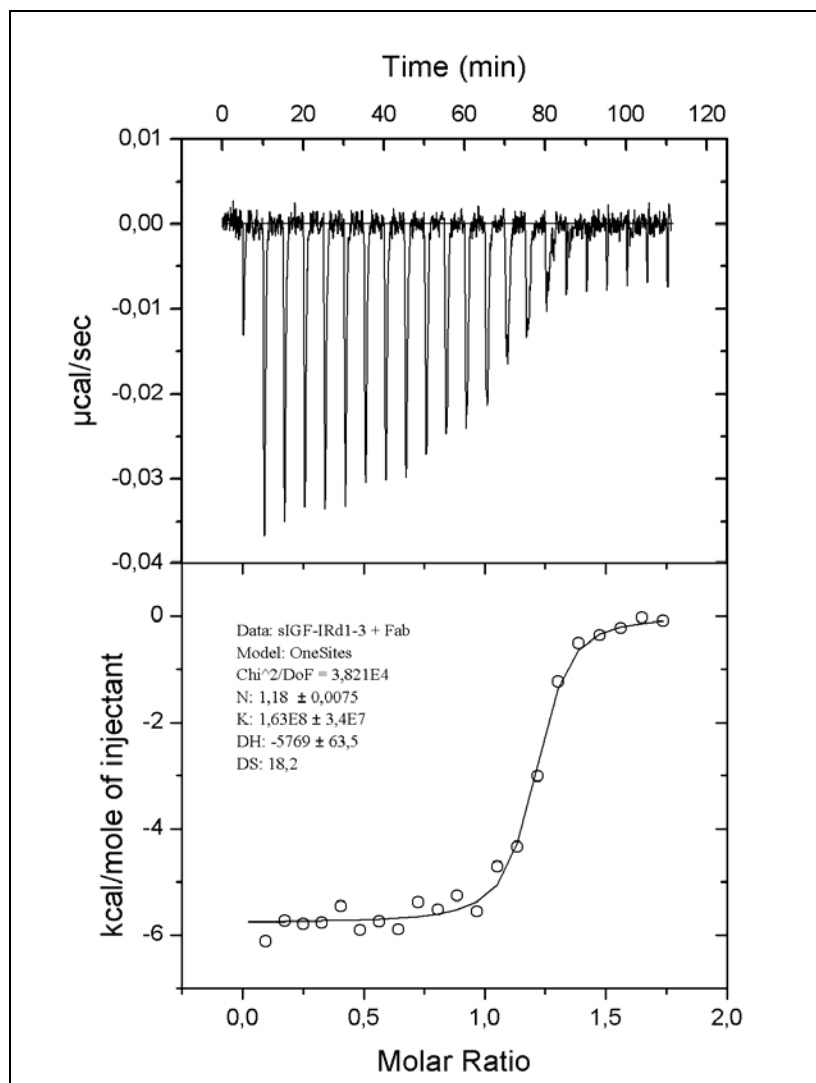


Fig. 40: ITC sIGF-1R domain I-III and Fab1159476

Fab1159476 (16.7 μM) was injected in 11 μl steps into a cell containing 1.7 μM sIGF-1R domain I-III (sIGF-1Rd1-3) at 25°C. Each peak represents the heat of binding following one injection (upper plot). The lower plot shows the integrated results, where each point represents the normalized heat change for each injection. The calculated K_D for this interaction is 6.1 ± 1.3 nM.

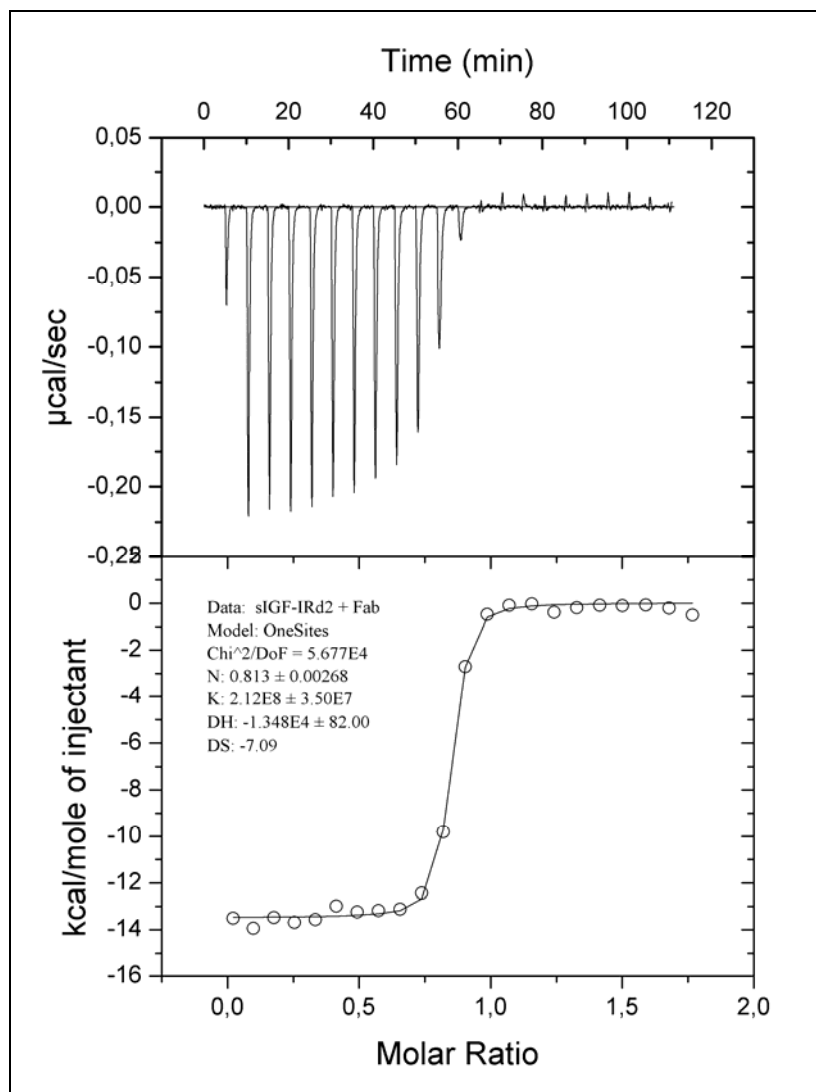


Fig. 41: ITC sIGF-1R domain II and Fab1159476

Fab1159476 (50 μ M) was injected in 11 μ l steps into a cell containing 5 μ M sIGF-1R domain II (sIGF-1Rd2) at 25°C. Each peak represents the heat of binding following one injection (upper plot). The lower plot shows the integrated results, where each point represents the normalized heat change for each injection. The calculated K_D for this interaction is 4.7 ± 0.7 nM.

Biacore competition assays. Preliminary competition assays were carried out to investigate the ability of IGF-1 to compete with Fab1159476 binding to commercial sIGF-1R (R&D Systems) and sIGF-1R domain I-III (sIGF-1Rd1-3). The commercial sIGF-1R samples consist of a mixture of the cleaved and disulfide-bridged heterodimer and the unprocessed disulfide-bridged α - β polypeptide pro-receptor. Binding of ligand requires the fully processed form of the receptor. sIGF-1Rd1-3 and the pro-receptor are not expected to bind IGF-1 since they lack crucial interacting domains and the correct folding. However, all constructs are able to bind Fab1159476 as seen in Fig. 39-Fig. 41. As shown in Fig. 42 there is no decrease in the equilibrium SPR response for sIGF-1Rd1-3 samples (square symbols) as increasing IGF-1 is

added. However, with increasing amounts of IGF-1 added to sIGF-1R samples (round symbols) the equilibrium SPR response decreases to about 40%.

Part of the remaining SPR response is caused by the unprocessed pro-receptor which is still able to bind to the Fab surface with its domain II.

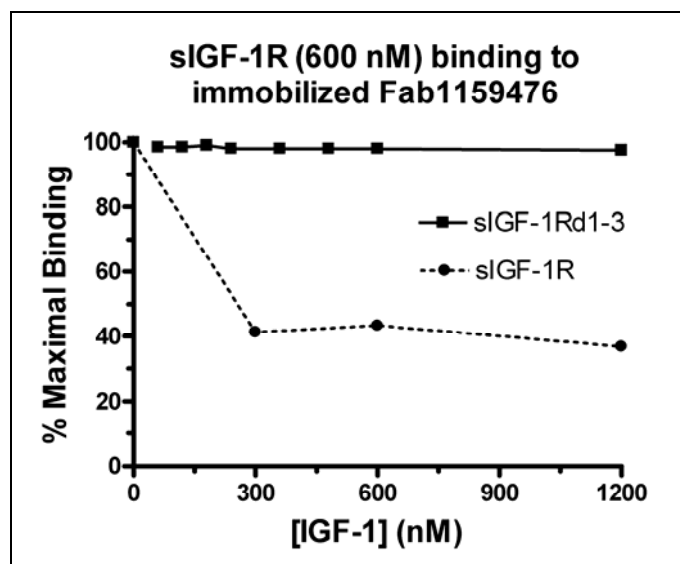


Fig. 42: Preliminary ligand competition properties of EMD1159476

A preliminary competition experiment showing the effect of addition of IGF-1 upon the binding of 600 nM sIGF-1R and sIGF-1R domain I-III (sIGF-1Rd1-3) to immobilized Fab1159476. Mixtures of 600 nM sIGF-1R and sIGF-1Rd1-3 plus the indicated concentrations of IGF-1 were passed over a biosensor surface to which Fab1159476 had been amine coupled. The equilibrium SPR responses for each mixture is shown, normalized to the response obtained with no added ligand (squares and straight line for sIGF-1Rd1-3; dots and dotted line for sIGF-1R). The lines simply connect the data points.

7.3. Discussion

The K_D value of 61.4 ± 1.9 nM for Fab1159476 binding to sIGF-1R domain I-III obtained by surface plasmon resonance (SPR)/Biacore studies is 10-fold weaker than observed for the binding of the Fab fragment determined by ITC (K_D of 6.1 ± 1.3 nM). This could be explained by hindrances induced by the immobilization of the Fab fragment or by an underestimation of the K_D value introduced by the steady-state fitting of the SPR/Biacore data.

A similar difference between Biacore and ITC results was seen for binding studies carried out with isolated sIGF-1R domain II. The K_D values of Fab1159476 binding were 30.7 ± 1.4 nM and 4.7 ± 0.7 nM for Biacore and ITC, respectively. The tighter binding of the isolated domain II in the Biacore experiments is possibly due to the absence of steric hindrance from the other domains of sIGF-1Rd1-3. The affinities for isolated domain II indicate an even a tighter binding (Biacore) or the same affinity within the error range (ITC) as compared to the domain I-III data. This suggests that the epitope of the antibody is exclusively within domain II of IGF-1R with no additional interactions from other domains.

The affinities of the Fab binding obtained by ITC are similar to affinities reported for other anti-IGF-1R antibodies. Doern *et al.* described two Biogen in-house antibodies with K_D values of 1 ± 0.2 nM and 4 ± 0.5 nM obtained by ITC for the full ectodomain (Doern *et al.*, 2009).

Surface plasmon resonance (SPR)/Biacore competition experiments (Fig. 42) showed an impaired binding of sIGF-1R to the Fab surface in the presence of IGF-1 in comparison to samples without ligand. This indicates a competitive binding of IGF-1 and EMD1159476. However, based on the experiment presented here it remains unclear if the binding of antibody and ligand is mutually exclusive or if the presence of the ligand is just impairing the binding of the receptor to the Fab. Further experiments quantifying the amounts of the different receptor species in the samples are necessary to answer this question.

The thermodynamic data for Fab binding to isolated domain II and domain I-III show differences in enthalpy (ΔH°) and entropy (ΔS°), whereas the change in Gibbs energy (ΔG°) for both constructs is similar (Fig. 43 and see 11.3 Table 6).

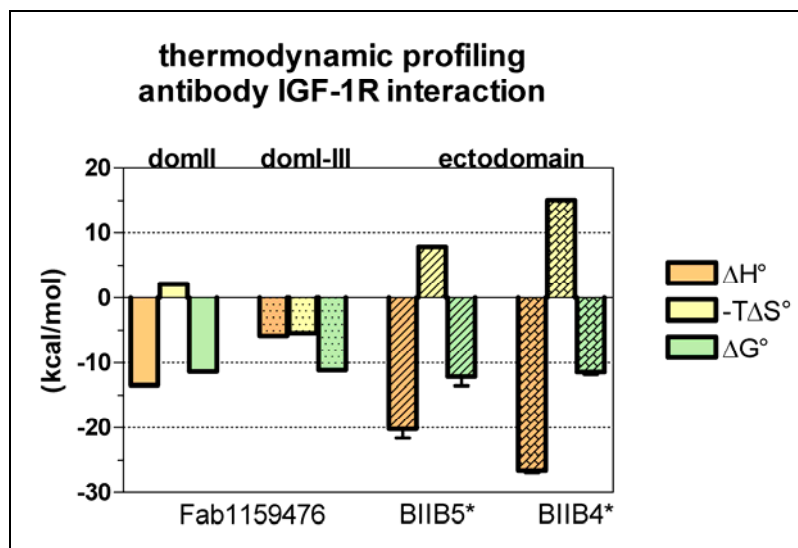


Fig. 43: Thermodynamic characteristics of Fab binding to IGF-1R

The EMD1159476 Fab binding to IGF-1R domain II (domII) and domain I-III (domI-III) was investigated by isothermal titration calorimetry (ITC) using a VP-ITC microcalorimeter (Microcal LLC) at 25°C. The data were compared to results obtained for two other antibody Fabs BIIB5 and BIIB4 binding to the full IGF-1R ectodomain (*data from Doern *et al.*, 2009). All three antibodies have similar affinities with K_D values ranging from 1-6 nM with an almost identical change in Gibbs energy (ΔG°) ranging from -11.5 – -12.3 kcal/mol. Interestingly, there is an entropic penalty for EMD1159476 Fab binding to domain II, while the Fab binding to domain I-III is connected with an entropic gain. This might indicate an increase in spatial freedom of domain I and III upon Fab binding. Exact values are given in Table 6.

In contrast to Fab binding to domain II the observed enthalpy of Fab binding to domain I-III is reduced more than half and the observed entropy of the system is increased. This may be due to differences in the rotational, conformational or solvation enthalpy upon Fab binding to the two different constructs. The entropic gain of Fab binding to domain I-III could be explained by an increase in spatial freedom of domain I and III. This may indicate an epitope for the antibody, which would remove or prevent stabilizing inter-domain interactions.

Two other antibody Fab fragments were also reported to have an entropic penalty for binding to the full length extracellular domain (Doern *et al.*, 2009) (Fig. 43). The increase in entropy indicates a conformational ordering within the receptor, the antibody, or both. An ordering of the receptor upon binding of the latter two antibodies was reported to be observed in far UV circular dichroism spectra (Doern *et al.*, 2009).

The changes in Gibbs energy and the affinities are comparable for the antibody investigated in this thesis and the antibodies described before by Doern *et al.* (2009), which are in the range of other monoclonal antibodies in preclinical studies or clinical application (Li *et al.*, 2005; Schmiedel *et al.*, 2008; Li *et al.*, 2008).

Taken together, the binding studies presented here (Fig. 39, Fig. 40 and Fig. 41) indicate that EMD1159476 is binding to domain II of the insulin-like growth factor 1 receptor IGF-1R. A K_D value of 5 ± 2.0 nM was obtained. Competition assays showed an impaired binding of the ligand IGF-1 to the receptor in the presence of the antibody Fab fragment indicating a competitive binding mode. Indeed, it was shown that domain II of IGF-1R comprises a part responsible for ligand specificity (Fig. 33).

The structure of the Fab fragment was solved at 1.7 Å resolution, but no crystals of the complex of sIGF-1R:Fab1159476 were obtained so far.



8. OUTLOOK

The outlook refers to the three different sections of this thesis (1) EGFR – antibody interactions, (2) the mutant EGFR variant III (EGFRvIII) and (3) IGF-1R – antibody interactions.

(1) EGFR – antibody interactions (chapter 5)

For the EGFR targeting monoclonal antibody matuzumab the epitope was crystallographically determined and confirmed by mutational studies (see 5.2). The results presented in this thesis indicate that both the epitope and the mechanism of inhibition by matuzumab are distinct from those for another therapeutic antibody cetuximab. It was shown that a simultaneous binding of the two antibodies on EGFR is possible, implying that a combination therapy with both antibodies could be advantageous against EGFR driven cancers. Indeed, *in vitro* studies showed a synergistic effect of matuzumab and cetuximab in combination (Dechant *et al.*, 2008; Kamat *et al.*, 2008). This has important implications for the clinical use of matuzumab and for the development of therapeutic approaches targeting the EGF receptor.

(2) The mutant EGFR variant III (chapter 6)

For the mutant EGFR variant III this thesis showed that the deletion mutation is not affecting the overall fold of the receptor domain III and IV (see 6.2). The binding sites of therapeutic antibodies on these domains remain accessible in the mutant receptor as demonstrated for matuzumab and cetuximab. In contrast to the wild type receptor, which dimerizes in the presence of the natural ligand EGF, it was shown in this thesis that sEGFRvIII is unable to dimerize in spite of ligand binding to domain III.

Further experiments clarifying the dimerization and activation characteristics of the mutant at the cell surface are needed. Homo- or heterodimerization studies could be performed using mutant and wild type specific fluorescent antibodies. A putative dependence of the constitutive activity of the sEGFRvIII kinase domain on receptor dimerization could be investigated by using antibodies that bind in the receptor dimerization interface and thus would sterically block mutant receptor dimerization or by using a dimerization incompetent sEGFR in combination with sEGFRvIII.

A large part of the excreted sEGFRvIII was misfolded indicating that this might also be the case in a cellular context. It might be important to investigate the impact of misfolded protein signaling from the inside of the cell. This could be done with phosphorylation studies using the Golgi-inhibitor Brefeldin A (Browning *et al.*, 2004).

(3) IGF-1R – antibody interactions (chapter 7)

The results presented in this thesis indicate that the epitope of the antibody EMD1159476 targeted against IGF-1R includes the receptor domain II (CR domain) and most probably is not involving other domains. Furthermore it was shown that the presence of the Fab fragment is impairing ligand binding indicating a competitive inhibition mechanism. The structure of the Fab fragment was solved; screening for crystallization conditions of the receptor-Fab fragment complex was performed but yielded no crystals so far. This might be due to inhomogeneous receptor glycosylation, which can prevent crystal packing through its flexibility. Future crystallization experiments are needed with deglycosylated complex protein.

9. REFERENCES

- Abe,S., Funato,T., Takahashi,S., Yokoyama,H., Yamamoto,J., Tomiya,Y., Yamada-Fujiwara,M., Ishizawa,K., Kameoka,J., Kaku,M., Harigae,H., and Sasaki,T. (2006). Increased expression of insulin-like growth factor I is associated with Ara-C resistance in leukemia. *Tohoku J Exp Med* **209**, 217-228.
- Abuzzahab,M.J., Schneider,A., Goddard,A., Grigorescu,F., Lautier,C., Keller,E., Kiess,W., Klammt,J., Kratzsch,J., Osgood,D., Pfaffle,R., Raile,K., Seidel,B., Smith,R.J., and Chernausk,S.D. (2003). IGF-I receptor mutations resulting in intrauterine and postnatal growth retardation. *New Engl J Med* **349**, 2211-2222.
- Aerts,H.J.W.L., Dubois,L., Hackeng,T.M., Straathof,R., Chiu,R.K., Lieuwes,N.G., Jutten,B., Wepler,S.A., Lammering,G., Wouters,B.G., and Lambin,P. (2007). Development and evaluation of a cetuximab-based imaging probe to target EGFR and EGFRvIII. *Radiother Oncol* **83**, 326-332.
- Aldape,K.D., Ballmann,K., Furth,A., Buckner,J.C., Giannini,C., Burger,P.C., Scheithauer,B.W., Jenkins,R.B., and James,C.D. (2004). Immunohistochemical detection of EGFRvIII in high malignancy grade astrocytomas and evaluation of prognostic significance. *J Neuropathol Exp Neurol* **63**, 700-707.
- Allen,G.W., Saba,C., Armstrong,E.A., Huang,S.M., Benavente,S., Ludwig,D.L., Hicklin,D.J., and Harari,P.M. (2007). Insulin-like growth factor-I receptor signaling blockade combined with radiation. *Cancer Res* **67**, 1155-1162.
- Almeida,A., Muleris,M., Dutrillaux,B., and Malfoy,B. (1994). The insulin-like growth factor I receptor gene is the target for the 15q26 amplicon in breast cancer. *Gene Chromosome Canc* **11**, 63-65.
- Arevalo,J.H., Stura,E.A., Taussig,M.J., and Wilson,I.A. (1993). Three-dimensional structure of an anti-steroid Fab' and progesterone-Fab' complex. *J Mol Biol* **231**, 103-118.
- Avnet,S., Sciacca,L., Salerno,M., Gancitano,G., Cassarino,M.F., Longhi,A., Zakikhani,M., Carboni,J.M., Gottardis,M., Giunti,A., Pollak,M., Vigneri,R., and Baldini,N. (2009). Insulin receptor isoform A and insulin-like growth factor II as additional treatment targets in human osteosarcoma. *Cancer Res* **69**, 2443-2452.
- Banfield,M.J., Naylor,R.L., Robertson,A.G.S., Allen,S.J., Dawbarn,D., and Brady,R.L. (2001). Specificity in Trk receptor:neurotrophin interactions: The crystal structure of TrkB-d5 in complex with neurotrophin-4/5. *Structure* **9**, 1191-1199.
- Barton,W.A., Tzvetkova-Robev,D., Miranda,E.P., Kolev,M.V., Rajashankar,K.R., Himanen,J.P., and Nikolov,D.B. (2006). Crystal structures of the Tie2 receptor ectodomain and the angiopoietin-2-Tie2 complex. *Nat Struct Mol Biol* **13**, 524-532.
- Baselga,J. (2008). Novel agents in the era of targeted therapy: what have we learned and how has our practice changed? *Ann Oncol* **19**, vii281-vii288.
- Baselga,J. (2002). Why the epidermal growth factor receptor? The rationale for cancer therapy. *Oncologist* **7**, 2-8.
- Baselga,R., Peruzzi,F., and Reiss,K. (2003). The IGF-1 receptor in cancer biology. *Int J Cancer* **107**, 873-877.
- Bass,J., Kurose,T., Pashmforoush,M., and Steiner,D.F. (1996). Fusion of insulin receptor ectodomains to immunoglobulin constant domains reproduces high-affinity insulin binding *in vitro*. *J Biol Chem* **271**, 19367-19375.
- Bellot,F., Moolenaar,W., Kris,R., Mirakhor,B., Verlaan,I., Ullrich,A., Schlessinger,J., and Felder,S. (1990). High-affinity epidermal growth factor binding is specifically reduced by a monoclonal antibody, and appears necessary for early responses. *J Cell Biol* **110**, 491-502.
- Benvenuti,S., Sartore-Bianchi,A., Di Nicolantonio,F., Zanon,C., Moroni,M., Veronese,S., Siena,S., and Bardelli,A. (2007). Oncogenic activation of the RAS/RAF signaling pathway impairs the response of metastatic colorectal cancers to anti-epidermal growth factor receptor antibody therapies. *Cancer Res* **67**, 2643-2648.
- Berezov,A., Chen,J., Liu,Q., Zhang,H.T., Greene,M.I., and Murali,R. (2002). Disabling receptor ensembles with rationally designed interface peptidomimetics. *J Biol Chem* **277**, 28330-28339.
- Berger,M.B., Mendrola,J.M., and Lemmon,M.A. (2004). ErbB3/HER3 does not homodimerize upon neuregulin binding at the cell surface. *FEBS Lett* **569**, 332-336.

- Berns, E.M.J.J., Klijn, J.G.M., van Staveren, I.L., Portengen, H., and Foekens, J.A. (1992). Sporadic amplification of the insulin-like growth factor 1 receptor gene in human breast tumors. *Cancer Res* **52**, 1036-1039.
- Bier, H., Hoffmann, T., Hauser, U., Wink, M., Ochler, M., Kovar, A., Müser, M., and Knecht, R. (2001). Clinical trial with escalating doses of the antiepidermal growth factor receptor humanized monoclonal antibody EMD 72 000 in patients with advanced squamous cell carcinoma of the larynx and hypopharynx. *Cancer Chemoth Pharm* **47**, 519-524.
- Blagoev, B., Ong, S.E., Kratchmarova, I., and Mann, M. (2004). Temporal analysis of phosphotyrosine-dependent signaling networks by quantitative proteomics. *Nat Biotechnol* **22**, 1139-1145.
- Blume-Jensen, P. and Hunter, T. (2001). Oncogenic kinase signalling. *Nature* **411**, 355-365.
- Bokemeyer, C., Bondarenko, I., Makhson, A., Hartmann, J.T., Aparicio, J., de Braud, F., Donea, S., Ludwig, H., Schuch, G., Stroh, C., Loos, A.H., Zubel, A., and Koralewski, P. (2009). Fluorouracil, leucovorin, and oxaliplatin with and without cetuximab in the first-line treatment of metastatic colorectal cancer. *J Clin Oncol* **27**, 663-671.
- Bouyain, S., Longo, P.A., Li, S., Ferguson, K.M., and Leahy, D.J. (2005). The extracellular region of ErbB4 adopts a tethered conformation in the absence of ligand. *P Natl Acad Sci USA* **102**, 15024-15029.
- Broussas, M., Dupont, J., Gonzalez, A., Blaecke, A., Fournier, M., Corvaia, N., and Goetsch, L. (2009). Molecular mechanisms involved in activity of h7C10, a humanized monoclonal antibody, to IGF-1 receptor. *Int J Cancer* **124**, 2281-2293.
- Browning, K.N., Kalyuzhny, A.E., and Travagli, R.A. (2004). μ -Opioid receptor trafficking on inhibitory synapses in the rat brainstem. *J Neurosci* **24**, 7344-7352.
- Brünger, A.T., Adams, P.D., Clore, G.M., DeLano, W.L., Grose, P., Grosse-Kunstleve, R.W., Jiang, J.S., Kuszewski, J., Nilges, M., Pannuh, N.S., Read, R.J., Rice, L.M., Simonson, T., and Warren, G.L. (1998). Crystallography & NMR system: A new software suite for macromolecular structure determination. *Acta Cryst D* **54**, 905-921.
- Burgess, A.W., Cho, H.S., Eigenbrot, C., Ferguson, K.M., Garrett, T.P.J., Leahy, D.J., Lemmon, M.A., Sliwkowski, M.X., Ward, C.W., and Yokoyama, S. (2003). An open-and-shut case? Recent insights into the activation of EGF/ErbB receptors. *Mol Cell* **12**, 541-552.
- Burtrum, D., Zhu, Z., Lu, D., Anderson, D.M., Prewett, M., Pereira, D.S., Bassi, R., Abdullah, R., Hooper, A.T., Koo, H., Jimenez, X., Johnson, D., Apblett, R., Kussie, P., Bohlen, P. *et al.* (2003). A fully human monoclonal antibody to the insulin-like growth factor I receptor blocks ligand-dependent signaling and inhibits human tumor growth *in vivo*. *Cancer Res* **63**, 8912-8921.
- Butler, A.A., Yakar, S., Gewolb, I.H., Karas, M., Okubo, Y., and LeRoith, D. (1998). Insulin-like growth factor-I receptor signal transduction: at the interface between physiology and cell biology. *Comp Biochem Physiol B Biochem Mol Biol* **121**, 19-26.
- Camirand, A., Lu, Y., and Pollak, M. (2002). Co-targeting HER2/ErbB2 and insulin-like growth factor-1 receptors causes synergistic inhibition of growth in HER2-overexpressing breast cancer cells. *Med Sci Monit* **8**, BR521-526.
- Carboni, J.M., Lee, A.V., Hadsell, D.L., Rowley, B.R., Lee, F.Y., Bol, D.K., Camuso, A.E., Gottardis, M., Greer, A.F., Ho, C.P., Hurlburt, W., Li, A., Saulnier, M., Velaparthi, U., Wang, C. *et al.* (2005). Tumor development by transgenic expression of a constitutively active insulin-like growth factor I receptor. *Cancer Res* **65**, 3781-3787.
- Cardillo, M.R., Monti, S., Di Silverio, F., Gentile, V., Sciarra, F., and Toscano, V. (2003). Insulin-like growth factor (IGF)-I, IGF-II and IGF type I receptor (IGFR-I) expression in prostatic cancer. *Anticancer Res* **23**, 3825-3835.
- Carpenter, G. (2003). ErbB-4: mechanism of action and biology. *Exp Cell Res* **284**, 66-77.
- Carter, P. (2001). Improving the efficacy of antibody-based cancer therapies. *Nat Rev Cancer* **1**, 118-129.
- Cavenee, W.K. (2002). Genetics and new approaches to cancer therapy. *Carcinogenesis* **23**, 683-686.
- CCP4 (1994). The CCP4 suite: Programs for protein crystallography. *Acta Cryst D* **50**, 760-763.
- Cho, H.S. and Leahy, D.J. (2002). Structure of the extracellular region of HER3 reveals an interdomain tether. *Science* **297**, 1330-1333.
- Cho, H.S., Mason, K., Ramyar, K.X., Stanley, A.M., Gabelli, S.B., Denney, D.W., and Leahy, D.J. (2003). Structure of the extracellular region of HER2 alone and in complex with the Herceptin Fab. *Nature* **421**, 756-760.

- Chrencik, J.E., Brooun, A., Kraus, M.L., Recht, M.I., Kolatkar, A.R., Han, G.W., Seifert, J.M., Widmer, H., Auer, M., and Kuhn, P. (2006). Structural and biophysical characterization of the EphB4-EphrinB2 protein-protein interaction and receptor specificity. *J Biol Chem* **281**, 28185-28192.
- Christinger, H.W., Fuh, G., de Vos, A.M., and Wiesmann, C. (2004). The crystal structure of placental growth factor in complex with domain 2 of vascular endothelial growth factor receptor-1. *J Biol Chem* **279**, 10382-10388.
- Chu, C.T., Everiss, K.D., Wikstrand, C.J., Batra, S.K., Kung, H.J., and Bigner, D.D. (1997). Receptor dimerization is not a factor in the signalling activity of a transforming variant epidermal growth factor receptor (EGFRvIII). *Biochem J* **324**, 855-861.
- Citri, A., Skaria, K.B., and Yarden, Y. (2003). The deaf and the dumb: the biology of ErbB-2 and ErbB-3. *Exp Cell Res* **284**, 54-65.
- Clayton, A.H.A., Walker, F., Orchard, S.G., Henderson, C., Fuchs, D., Rothacker, J., Nice, E.C., and Burgess, A.W. (2005). Ligand-induced dimer-tetramer transition during the activation of the cell surface epidermal growth factor receptor - A multidimensional microscopy analysis. *J Biol Chem* **280**, 30392-30399.
- Clemmons, D.R. (2007). Modifying IGF1 activity: an approach to treat endocrine disorders, atherosclerosis and cancer. *Nat Rev Drug Discov* **6**, 821-833.
- Cohen, B.D., Baker, D.A., Soderstrom, C., Tkalcevic, G., Rossi, A.M., Miller, P.E., Tengowski, M.W., Wang, F., Gualberto, A., Beebe, J.S., and Moyer, J.D. (2005). Combination therapy enhances the inhibition of tumor growth with the fully human anti-type 1 insulin-like growth factor receptor monoclonal antibody CP-751,871. *Clin Cancer Res* **11**, 2063-2073.
- Coussens, L., Yang-Feng, T.L., Liao, Y.C., Chen, E., Gray, A., McGrath, J., Seeburg, P.H., Libermann, T.A., Schlessinger, J., Francke, U., and et al. (1985). Tyrosine kinase receptor with extensive homology to EGF receptor shares chromosomal location with *neu* oncogene. *Science* **230**, 1132-1139.
- Davies, G.C., Ryan, P.E., Rahman, L., Zajac-Kaye, M., and Lipkowitz, S. (2006). EGFRvIII undergoes activation-dependent downregulation mediated by the Cbl proteins. *Oncogene* **25**, 6497-6509.
- Dawson, J.P., Berger, M.B., Lin, C.C., Schlessinger, J., Lemmon, M.A., and Ferguson, K.M. (2005). Epidermal growth factor receptor dimerization and activation require ligand-induced conformational changes in the dimer interface. *Mol Cell Biol* **25**, 7734-7742.
- Dawson, J.P., Bu, Z., and Lemmon, M.A. (2007). Ligand-induced structural transitions in ErbB receptor extracellular domains. *Structure* **15**, 942-954.
- De Larco, J.E. and Todaro, G.J. (1987). Epithelioid and fibroblastic rat kidney cell clones: epidermal growth factor (EGF) receptors and the effect of mouse sarcoma virus transformation. *J Cell Physiol* **94**, 335-342.
- De Meyts, P. (1994). The structural basis of insulin and insulin-like growth factor-I receptor binding and negative cooperativity, and its relevance to mitogenic versus metabolic signalling. *Diabetologia* **37**, S135-S148.
- De Meyts, P. (2004). Insulin and its receptor: structure, function and evolution. *Bioassays* **26**, 1351-1362.
- De Meyts, P. (2008). The insulin receptor: a prototype for dimeric, allosteric membrane receptors? *Trends Biochem Sci* **33**, 376-384.
- De Meyts, P. and Whittaker, J. (2002). Structural biology of insulin and IGF1 receptors: implications for drug design. *Nat Rev Drug Discov* **1**, 769-783.
- Dechant, M., Weisner, W., Berger, S., Peipp, M., Beyer, T., Schneider-Merck, T., Lammerts van Bueren, J.J., Bleeker, W.K., Parren, P.W.H.I., van de Winkel, J.G.J., and Valerius, T. (2008). Complement-dependent tumor cell lysis triggered by combinations of epidermal growth factor receptor antibodies. *Cancer Res* **68**, 4998-5003.
- Defize, L.H., Boonstra, J., Meisenhelder, J., Kruijjer, W., Tertoolen, L.G., Tilly, B.C., Hunter, T., van Bergen en Henegouwen, P., Moolenaar, W.H., and de Laat, S.W. (1989). Signal transduction by epidermal growth factor occurs through the subclass of high affinity receptors. *J Cell Biol* **109**, 2495-2507.
- Dempke, W.C. and Heinemann, V. (2009). Resistance to EGF-R (erbB-1) and VEGF-R modulating agents. *Eur J Cancer* **45**, 1117-1128.
- Denley, A., Cosgrove, L.J., Booker, G.W., Wallace, J.C., and Forbes, B.E. (2005). Molecular interactions of the IGF system. *Cytokine Growth Factor Rev* **16**, 421-439.

- Desbois-Mouthon,C., Cacheux,W., Blivet-Van Eggelpoël,M.J., Barbu,V., Fartoux,L., Poupon,R., Housset,C., and Rosmorduc,O. (2006). Impact of IGF-1R/EGFR cross-talks on hepatoma cell sensitivity to gefitinib. *Int J Cancer* **119**, 2557-2566.
- Descamps,G., Gomez-Bougie,P., Venot,C., Moreau,P., Bataille,R., and Amiot,M. (2009). A humanised anti-IGF-1R monoclonal antibody (AVE1642) enhances bortezomib-induced apoptosis in myeloma cells lacking CD45. *Br J Cancer* **100**, 366-369.
- Di Cola,G., Cool,M.H., and Accili,D. (1997). Hypoglycemic effect of insulin-like growth factor-1 in mice lacking insulin receptors. *J Clin Invest* **99**, 2538-2544.
- Di Fiore,P.P., Pierce,J.H., Kraus,M.H., Segatto,O., King,C.R., and Aaronson,S.A. (1987). *ErbB-2* is a potent oncogene when overexpressed in NIH/3T3 cells. *Science* **237**, 178-182.
- DiGiovanni,J., Kiguchi,K., Frijhoff,A., Wilker,E., Bol,D.K., Beltr+in,L., Moats,S., Ramirez,A., Jorcano,J., and Conti,C. (2000). Deregulated expression of insulin-like growth factor 1 in prostate epithelium leads to neoplasia in transgenic mice. *P Natl Acad Sci USA* **97**, 3455-3460.
- Doern,A., Cao,X., Sereno,A., Reyes,C.L., Altshuler,A., Huang,F., Hession,C., Flavier,A., Favis,M., Tran,H., Ailor,E., Levesque,M., Murphy,T., Berquist,L., Tamraz,S. *et al.* (2009). Characterization of inhibitory anti-IGF-1R antibodies with different epitope specificity and ligand blocking properties: Implications for mechanism of action *in vivo*. *J Biol Chem* **284**, 10254-10267.
- Domagala,T., Konstantopoulos,N., Smyth,F., Jorissen,R.N., Fabri,L., Geleick,D., Lax,I., Schlessinger,J., Sawyer,W., Howlett,G.J., Burgess,A.W., and Nice,E.C. (2000). Stoichiometry, kinetic and binding analysis of the interaction between epidermal growth factor (EGF) and the extracellular domain of the EGF receptor. *Growth Factors* **18**, 11-29.
- Downward,J., Yarden,Y., Mayes,E., Scrace,G., Totty,N., Stockwell,P., Ullrich,A., Schlessinger,J., and Waterfield,M.D. (1984). Close similarity of epidermal growth factor receptor and *v-erb-B* oncogene protein sequences. *Nature* **307**, 521-527.
- Drebin,J.A., Link,V.C., Stern,D.F., Weinberg,R.A., and Greene,M.I. (1985). Down-modulation of an oncogene protein product and reversion of the transformed phenotype by monoclonal antibodies. *Cell* **41**, 697-706.
- Duneau,J.P., Vegh,A.P., and Sturgis,J.N. (2007). A dimerization hierarchy in the transmembrane domains of the HER receptor family. *Biochemistry-US* **46**, 2010-2019.
- Durai,R., Yang,W., Gupta,S., Seifalian,A.M., and Winslet,M.C. (2005). The role of the insulin-like growth factor system in colorectal cancer: review of current knowledge. *Int J Colorectal Dis* **20**, 203-220.
- Elleman,T.C., Domagala,T., McKern,N.M., Nerrie,M., Lonqvist,B., Adams,T.E., Lewis,J., Lovrecz,G.O., Hoyne,P.A., Richards,K.M., Howlett,G.J., Rothacker,J., Jorissen,R.N., Lou,M., Garrett,T.P.J. *et al.* (2001). Identification of a determinant of epidermal growth factor receptor ligand-binding specificity using a truncated, high-affinity form of the ectodomain. *Biochemistry-US* **40**, 8930-8939.
- Emsley,P. and Cowtan,K. (2004). Coot: model-building tools for molecular graphics. *Acta Cryst D* **60**, 2126-2132.
- Falls,D.L. (2003). Neuregulins: functions, forms, and signaling strategies. *Exp Cell Res* **284**, 14-30.
- Ferguson,K.M., Darling,P.J., Mohan,M.J., Macatee,T.L., and Lemmon,M.A. (2000). Extracellular domains drive homo- but not hetero-dimerization of erbB receptors. *EMBO J* **19**, 4632-4643.
- Ferguson,K.M., Berger,M.B., Mendrola,J.M., Cho,H.S., Leahy,D.J., and Lemmon,M.A. (2003). EGF activates its receptor by removing interactions that autoinhibit ectodomain dimerization. *Mol Cell* **11**, 507-517.
- Fernandes,H., Cohen,S., and Bishayee,S. (2001). Glycosylation-induced conformational modification positively regulates receptor-receptor association. A study with an aberrant epidermal growth factor receptor (EGFRvIII/delta EGFR) expressed in cancer cells. *J Biol Chem* **276**, 5375-5383.
- Firth,S.M. and Baxter,R.C. (2002). Cellular actions of the insulin-like growth factor binding proteins. *Endocr Rev* **23**, 824-854.
- Franklin,M.C., Carey,K.D., Vajdos,F.F., Leahy,D.J., de Vos,A.M., and Sliwkowski,M.X. (2004). Insights into ErbB signaling from the structure of the ErbB2-pertuzumab complex. *Cancer Cell* **5**, 317-328.

- Frederick,L., Wang,X.Y., Eley,G., and James,C.D. (2000). Diversity and frequency of epidermal growth factor receptor mutations in human glioblastomas. *Cancer Res* **60**, 1383-1387.
- Friedman,L.M., Rinon,A., Schechter,B., Lyass,L., Lavi,S., Bacus,S.S., Sela,M., and Yarden,Y. (2005). Synergistic down-regulation of receptor tyrosine kinases by combinations of mAbs: Implications for cancer immunotherapy. *P Natl Acad Sci USA* **102**, 1915-1920.
- Fukai,J., Nishio,K., Itakura,T., and Koizumi,F. (2008). Antitumor activity of cetuximab against malignant glioma cells overexpressing EGFR deletion mutant variant III. *Cancer Sci* **99**, 2062-2069.
- Garrett,T.P.J., McKern,N.M., Lou,M., Elleman,T.C., Adams,T.E., Lovrecz,G.O., Kofler,M., Jorissen,R.N., Nice,E.C., Burgess,A.W., and Ward,C.W. (2003). The crystal structure of a truncated ErbB2 ectodomain reveals an active conformation, poised to interact with other ErbB receptors. *Mol Cell* **11**, 495-505.
- Garrett,T.P.J., McKern,N.M., Lou,M., Elleman,T.C., Adams,T.E., Lovrecz,G.O., Zhu,H.J., Walker,F., Frenkel,M.J., Hoyne,P.A., Jorissen,R.N., Nice,E.C., Burgess,A.W., and Ward,C.W. (2002). Crystal structure of a truncated epidermal growth factor receptor extracellular domain bound to transforming growth factor α . *Cell* **110**, 763-773.
- Garrett,T.P.J., McKern,N.M., Lou,M., Frenkel,M.J., Bentley,J.D., Lovrecz,G.O., Elleman,T.C., Cosgrove,L.J., and Ward,C.W. (1998). Crystal structure of the first three domains of the type-1 insulin-like growth factor receptor. *Nature* **394**, 395-399.
- Gee,J.M., Robertson,J.F., Gutteridge,E., Ellis,I.O., Pinder,S.E., Rubini,M., and Nicholson,R.I. (2005). Epidermal growth factor receptor/HER2/insulin-like growth factor receptor signalling and oestrogen receptor activity in clinical breast cancer. *Endocr-Relat Cancer* **12**, S99-111.
- Gherardi,E., Sandin,S., Petoukhov,M.V., Finch,J., Youles,M.E., +ufverstedt,L.G., Miguel,R.N., Blundell,T.L., Vande Woude,G.F., Skoglund,U., and Svergun,D.I. (2006). Structural basis of hepatocyte growth factor/scatter factor and MET signalling. *P Natl Acad Sci USA* **103**, 4046-4051.
- Gill,G.N., Kawamoto,T., Cochet,C., Le,A., Sato,J.D., Masui,H., McLeod,C., and Mendelsohn,J. (1984). Monoclonal anti-epidermal growth factor receptor antibodies which are inhibitors of epidermal growth factor binding and antagonists of epidermal growth factor binding and antagonists of epidermal growth factor-stimulated tyrosine protein kinase activity. *J Biol Chem* **259**, 7755-7760.
- Giusti,R.M., Cohen,M.H., Keegan,P., and Pazdur,R. (2009). FDA review of a panitumumab (Vectibix) clinical trial for first-line treatment of metastatic colorectal cancer. *Oncologist* **Epub**.
- Goetsch,L., Gonzalez,A., Leger,O., Beck,A., Pauwels,P.J., Haeuw,J.F., and Corvaia,N. (2005). A recombinant humanized anti-insulin-like growth factor receptor type I antibody (h7C10) enhances the antitumor activity of vinorelbine and anti-epidermal growth factor receptor therapy against human cancer xenografts. *Int J Cancer* **113**, 316-328.
- Goldgur,Y., Paavilainen,S., Nikolov,D., and Himanen,J.P. (2009). Structure of the ligand-binding domain of the EphB2 receptor at 2 Å resolution. *Acta Cryst F* **65**, 71-74.
- Graeven,U., Kremer,B., Sudhoff,T., Killing,B., Rojo,F., Weber,D., Tillner,J., Unal,C., and Schmiegel,W. (2006). Phase I study of the humanised anti-EGFR monoclonal antibody matuzumab (EMD 72000) combined with gemcitabine in advanced pancreatic cancer. *Br J Cancer* **94**, 1293-1299.
- Grandal,M.V., Zandi,R., Pedersen,M.W., Willumsen,B.M., van Deurs,B., and Poulsen,H.S. (2007). EGFRvIII escapes down-regulation due to impaired internalization and sorting to lysosomes. *Carcinogenesis* **28**, 1408-1417.
- Graus-Porta,D., Beerli,R.R., Daly,J.M., and Hynes,N.E. (1997). ErbB-2, the preferred heterodimerization partner of all ErbB receptors, is a mediator of lateral signaling. *EMBO J* **16**, 1647-1655.
- Guinier,A. (1939). Diffraction of x-rays of very small angles-application to the study of ultramicroscopic phenomenon. *Ann Phys* **12**, 161-237.
- Gureasko,J., Galush,W.J., Boykevisch,S., Sondermann,H., Bar-Sagi,D., Groves,J.T., and Kuriyan,J. (2008). Membrane-dependent signal integration by the Ras activator son of sevenless. *Nat Struct Mol Biol* **15**, 452-461.
- Hadsell,D.L., Murphy,K.L., Bonnette,S.G., Reece,N., Laucirica,R., and Rosen,J.M. (2000). Cooperative interaction between mutant p53 and des(1-3)IGF-I accelerates mammary tumorigenesis. *Oncogene* **19**, 889-898.

- Haluska,P., Shaw,H.M., Batzel,G.N., Yin,D., Molina,J.R., Molife,L.R., Yap,T.A., Roberts,M.L., Sharma,A., Gualberto,A., Adjei,A.A., and de Bono,J.S. (2007). Phase I dose escalation study of the anti insulin-like growth factor-I receptor monoclonal antibody CP-751,871 in patients with refractory solid tumors. *Clin Cancer Res* **13**, 5834-5840.
- Han,S.W., Oh,D.Y., Im,S.A., Park,S.R., Lee,K.W., Song,H.S., Lee,N.S., Lee,K.H., Choi,I.S., Lee,M.H., Kim,M.A., Kim,W.H., Bang,Y.J., and Kim,T.Y. (2009). Phase II study and biomarker analysis of cetuximab combined with modified FOLFOX6 in advanced gastric cancer. *Br J Cancer* **100**, 298-304.
- Hankinson,S.E., Willett,W.C., Colditz,G.A., Hunter,D.J., Michaud,D.S., Deroo,B., Rosner,B., Speizer,F.E., and Pollak,M. (1998). Circulating concentrations of insulin-like growth factor-I and risk of breast cancer. *Lancet* **351**, 1393-1396.
- Harris,R.C., Chung,E., and Coffey,R.J. (2003). EGF receptor ligands. *Exp Cell Res* **284**, 2-13.
- Hartog,H., Wesseling,J., Boezen,H.M., and van der Graaf,W.T.A. (2007). The insulin-like growth factor 1 receptor in cancer: Old focus, new future. *Eur J Cancer* **43**, 1895-1904.
- Heimberger,A.B., Hlatky,R., Suki,D., Yang,D., Weinberg,J., Gilbert,M., Sawaya,R., and Aldape,K. (2005). Prognostic effect of epidermal growth factor receptor and EGFRvIII in glioblastoma multiforme patients. *Clin Cancer Res* **11**, 1462-1466.
- Heiring,C., Dahlback,B., and Muller,Y.A. (2004). Ligand recognition and homophilic interactions in Tyro3: Structural insights into the Axl/Tyro3 receptor tyrosine kinase family. *J Biol Chem* **279**, 6952-6958.
- Himanen,J.P., Chumley,M.J., Lackmann,M., Li,C., Barton,W.A., Jeffrey,P.D., Vearing,C., Geleick,D., Feldheim,D.A., Boyd,A.W., Henkemeyer,M., and Nikolov,D.B. (2004). Repelling class discrimination: ephrin-A5 binds to and activates EphB2 receptor signaling. *Nat Neurosci* **7**, 501-509.
- Himanen,J.P., Rajashankar,K.R., Lackmann,M., Cowan,C.A., Henkemeyer,M., and Nikolov,D.B. (2001). Crystal structure of an Eph receptor-ephrin complex. *Nature* **414**, 933-938.
- Hirsch,F.R., Varella-Garcia,M., Cappuzzo,F., McCoy,J., Bemis,L., Xavier,A.C., Dziadziuszko,R., Gumerlock,P., Chansky,K., West,H., Gazdar,A.F., Crino,L., Gandara,D.R., Franklin,W.A., and Bunn,P.A., Jr. (2007). Combination of EGFR gene copy number and protein expression predicts outcome for advanced non-small-cell lung cancer patients treated with gefitinib. *Ann Oncol* **18**, 752-760.
- Holbro,T. and Hynes,N.E. (2004). ErbB receptors: Directing key signaling networks throughout life. *Annu Rev Pharmacol* **44**, 195-217.
- Holbrook,M.R., Slakey,L.L., and Gross,D.J. (2000). Thermodynamic mixing of molecular states of the epidermal growth factor receptor modulates macroscopic ligand binding affinity. *Biochem J* **352**, 99-108.
- Horan,T., Wen,J., Arakawa,T., Liu,N., Brankow,D., Hu,S., Ratzkin,B., and Philo,J.S. (1995). Binding of neu differentiation factor with the extracellular domain of Her2 and Her3. *J Biol Chem* **270**, 24604-24608.
- Hoyne,P.A., Cosgrove,L.J., McKern,N.M., Bentley,J.D., Ivancic,N., Elleman,T.C., and Ward,C.W. (2000). High affinity insulin binding by soluble insulin receptor extracellular domain fused to a leucine zipper. *FEBS Lett* **479**, 15-18.
- Huang,H.-J.S., Nagane,M., Klingbeil,C.K., Lin,H., Nishikawa,R., Ji,X.D., Huang,C.M., Gill,G.N., Wiley,H.S., and Cavenee,W.K. (1997). The enhanced tumorigenic activity of a mutant epidermal growth factor receptor common in human cancers is mediated by threshold levels of constitutive tyrosine phosphorylation and unattenuated signaling. *J Biol Chem* **272**, 2927-2935.
- Huang,P.H., Mukasa,A., Bonavia,R., Flynn,R.A., Brewer,Z.E., Cavenee,W.K., Furnari,F.B., and White,F.M. (2007). Quantitative analysis of EGFRvIII cellular signaling networks reveals a combinatorial therapeutic strategy for glioblastoma. *P Natl Acad Sci USA* **104**, 12867-12872.
- Hubbard,S.R. (2004). Juxtamembrane autoinhibition in receptor tyrosine kinases. *Nat Rev Mol Cell Biol* **5**, 464-471.
- Hubbard,S.R. and Miller,W.T. (2007). Receptor tyrosine kinases: mechanisms of activation and signaling. *Curr Opin Cell Biol* **19**, 117-123.
- Hubbard,S.R., Mohammadi,M., and Schlessinger,J. (1998). Autoregulatory mechanisms in protein-tyrosine kinases. *J Biol Chem* **273**, 11987-11990.

- Hudziak,R.M., Lewis,G.D., Winget,M., Fendly,B.M., Shepard,H.M., and Ullrich,A. (1989). p185HER2 monoclonal antibody has antiproliferative effects *in vitro* and sensitizes human breast tumor cells to tumor necrosis factor. *Mol Cell Biol* **9**, 1165-1172.
- Hunter,T. (1998). The Croonian lecture, 1997. The phosphorylation of proteins on tyrosine: its role in cell growth and disease. *Philos T Roy Soc B* **353**, 583-605.
- Hunter,T. (2000). Signaling - 2000 and beyond. *Cell* **100**, 113-127.
- Hunter,T., Ling,N., and Cooper,J.A. (1984). Protein kinase C phosphorylation of the EGF receptor at a threonine residue close to the cytoplasmic face of the plasma membrane. *Nature* **311**, 480-483.
- Ichikawa,O., Osawa,M., Nishida,N., Goshima,N., Nomura,N., and Shimada,I. (2007). Structural basis of the collagen-binding mode of discoidin domain receptor 2. *EMBO J* **26**, 4168-4176.
- Invitrogen. Gateway[®] Technology, Version E.
- Invitrogen. Bac-to-Bac[®] Baculovirus Expression System, Version E.
- Johns,T.G., Adams,T.E., Cochran,J.R., Hall,N.E., Hoyne,P.A., Olsen,M.J., Kim,Y.S., Rothacker,J., Nice,E.C., Walker,F., Ritter,G., Jungbluth,A.A., Old,L.J., Ward,C.W., Burgess,A.W. *et al.* (2004). Identification of the epitope for the epidermal growth factor receptor-specific monoclonal antibody 806 reveals that it preferentially recognizes an untethered form of the receptor. *J Biol Chem* **279**, 30375-30384.
- Jones,H.E., Gee,J.M.W., Hutcheson,I.R., Knowlden,J.M., Barrow,D., and Nicholson,R.I. (2006). Growth factor receptor interplay and resistance in cancer. *Endocr Relat Cancer* **13**, S45-S51.
- Jorissen,R.N., Walker,F., Pouliot,N., Garrett,T.P.J., Ward,C.W., and Burgess,A.W. (2003). Epidermal growth factor receptor: mechanisms of activation and signalling. *Exp Cell Res* **284**, 31-53.
- Jungbluth,A.A., Stockert,E., Huang,H.J., Collins,V.P., Coplan,K., Iversen,K., Kolb,D., Johns,T.J., Scott,A.M., Gullick,W.J., Ritter,G., Cohen,L., Scanlan,M.J., Cavenee,W.K., and Old,L.J. (2003). A monoclonal antibody recognizing human cancers with amplification/overexpression of the human epidermal growth factor receptor. *P Natl Acad Sci USA* **100**, 639-644.
- Kabsch,W. (1993). Automatic processing of rotation diffraction data from crystals of initially unknown symmetry and cell constants. *J Appl Cryst* **26**, 795-800.
- Kalli,K.R., Falowo,O.I., Bale,L.K., Zschunke,M.A., Roche,P.C., and Conover,C.A. (2002). Functional insulin receptors on human epithelial ovarian carcinoma cells: Implications for IGF-II mitogenic signaling. *Endocrinology* **143**, 3259-3267.
- Kamat,V., Donaldson,J.M., Kari,C., Quadros,M.R., Lelkes,P.I., Chaiken,I., Cocklin,S., Williams,J.C., Papazoglou,E., and Rodeck,U. (2008). Enhanced EGFR inhibition and distinct epitope recognition by EGFR antagonistic mAbs C225 and 425. *Cancer Biol Ther* **7**, 726-733.
- Kawamoto,T., Sato,J.D., Le,A., Polikoff,J., Sato,G.H., and Mendelsohn,J. (1983). Growth stimulation of A431 cells by epidermal growth factor: identification of high-affinity receptors for epidermal growth factor by an anti-receptor monoclonal antibody. *P Natl Acad Sci USA* **80**, 1337-1341.
- Kettleborough,C.A., Saldanha,J., Heath,V.J., Morrison,C.J., and Bendig,M.M. (1991). Humanization of a mouse monoclonal antibody by CDR-grafting: the importance of framework residues on loop conformation. *Protein Eng Design Selection* **4**, 773-783.
- Khambata-Ford,S., Garrett,C.R., Meropol,N.J., Basik,M., Harbison,C.T., Wu,S., Wong,T.W., Huang,X., Takimoto,C.H., Godwin,A.K., Tan,B.R., Krishnamurthi,S.S., Burris,H.A., III, Poplin,E.A., Hidalgo,M. *et al.* (2007). Expression of epiregulin and amphiregulin and K-ras mutation status predict disease control in metastatic colorectal cancer patients treated with cetuximab. *J Clin Oncol* **25**, 3230-3237.
- Kim,N., Stiegler,A.L., Cameron,T.O., Hallock,P.T., Gomez,A.M., Huang,J.H., Hubbard,S.R., Dustin,M.L., and Burden,S.J. (2008). Lrp4 is a receptor for Agrin and forms a complex with MuSK. *Cell* **135**, 334-342.
- Kiselyov,V.V., Versteyhe,S., Gauguin,L., and De Meyts,P. (2009). Harmonic oscillator model of the insulin and IGF1 receptors' allosteric binding and activation. *Mol Syst Biol* **5**.
- Kitamura,T., Kahn,C.R., and Accili,D. (2003). Insulin receptor knockout mice. *Annu Rev Physiol* **65**, 313-332.

- Klein,P., Mattoon,D., Lemmon,M.A., and Schlessinger,J. (2004). A structure-based model for ligand binding and dimerization of EGF receptors. *P Natl Acad Sci USA* **101**, 929-934.
- Klingler-Hoffmann,M., Bukczynska,P., and Tiganis,T. (2003). Inhibition of phosphatidylinositol 3-kinase signaling negates the growth advantage imparted by a mutant epidermal growth factor receptor on human glioblastoma cells. *Int J Cancer* **105**, 331-339.
- Knowlden,J., Jones,H., Barrow,D., Gee,J., Nicholson,R., and Hutcheson,I. (2008). Insulin receptor substrate-1 involvement in epidermal growth factor receptor and insulin-like growth factor receptor signalling: implication for gefitinib (Iressa) response and resistance. *Breast Cancer Res Tr* **111**, 79-91.
- Koch,M.H., Vachette,P., and Svergun,D.I. (2003). Small-angle scattering: a view on the properties, structures and structural changes of biological macromolecules in solution. *Q Rev Biophys* **36**, 147-227.
- Kohda,D., Odaka,M., Lax,I., Kawasaki,H., Suzuki,K., Ullrich,A., Schlessinger,J., and Inagaki,F. (1993). A 40-kDa epidermal growth factor/transforming growth factor α -binding domain produced by limited proteolysis of the extracellular domain of the epidermal growth factor receptor. *J Biol Chem* **268**, 1976-1981.
- Kollmannsberger,C., Schittenhelm,M., Honecker,F., Tillner,J., Weber,D., Oechsle,K., Kanz,L., and Bokemeyer,C. (2006). A phase I study of the humanized monoclonal anti-epidermal growth factor receptor (EGFR) antibody EMD 72000 (matuzumab) in combination with paclitaxel in patients with EGFR-positive advanced non-small-cell lung cancer (NSCLC). *Ann Oncol* **17**, 1007-1013.
- Konarev,P.V., Volkov,V.V., Sokolova,A.V., Koch,M.H., and Svergun,D.I. (2003). PRIMUS: a Windows PC-based system for small-angle scattering data analysis. *J Appl Cryst* **36**, 1277-1282.
- Kossiakoff,A.A. and de Vos,A.M. (1998). Structural basis for cytokine hormone-receptor recognition and receptor activation. *Adv Protein Chem* **52**, 67-108.
- Kozin,M.B. and Svergun,D.I. (2001). Automated matching of high- and low-resolution structural models. *J Appl Cryst* **34**, 33-41.
- Kreysch,H.G. and Schmidt,J. Pharmaceutical compositions directed to Erb-B1 receptors. Merck Patent GmbH. **032960 A1**[EP1549344].
- Kuan,C.T., Wikstrand,C., and Bigner,D. (2000). EGFRvIII as a promising target for antibody-based brain tumor therapy. *Brain Tumor Pathol* **17**, 71-78.
- Kurmasheva,R.T. and Houghton,P.J. (2006). IGF-I mediated survival pathways in normal and malignant cells. *BBA-Rev Cancer* **1766**, 1-22.
- Lacy,M.Q., Alsina,M., Fonseca,R., Paccagnella,M.L., Melvin,C.L., Yin,D., Sharma,A., Enriquez Sarano,M., Pollak,M., Jagannath,S., Richardson,P., and Gualberto,A. (2008). Phase I, pharmacokinetic and pharmacodynamic study of the anti-insulin-like growth factor type 1 receptor monoclonal antibody CP-751,871 in patients with multiple myeloma. *J Clin Oncol* **26**, 3196-3203.
- Lawrence,M.C. and Colman,P.M. (1993). Shape complementarity at protein/protein interfaces. *J Mol Biol* **234**, 946-950.
- Lawrence,M.C., McKern,N.M., and Ward,C.W. (2007). Insulin receptor structure and its implications for the IGF-1 receptor. *Curr Opin Struct Biol* **17**, 699-705.
- Le Roy,C. and Wrana,J.L. (2005). Clathrin- and non-clathrin-mediated endocytic regulation of cell signalling. *Nat Rev Mol Cell Biol* **6**, 112-126.
- Leahy,D.J. (2008). A molecular view of anti-ErbB monoclonal antibody therapy. *Cancer Cell* **13**, 291-293.
- Learn,C.A., Hartzell,T.L., Wikstrand,C.J., Archer,G.E., Rich,J.N., Friedman,A.H., Friedman,H.S., Bigner,D.D., and Sampson,J.H. (2004). Resistance to tyrosine kinase inhibition by mutant epidermal growth factor receptor variant III contributes to the neoplastic phenotype of glioblastoma multiforme. *Clin Cancer Res* **10**, 3216-3224.
- Lee,J.C., Vivanco,I., Beroukhim,R., Huang,J.H.Y., Feng,W.L., DeBiasi,R.M., Yoshimoto,K., King,J.C., Nghiemphu,P., Yuza,Y., Xu,Q., Greulich,H., Thomas,R.K., Paez,J.G., Peck,T.C. *et al.* (2006). Epidermal growth factor receptor activation in glioblastoma through novel missense mutations in the extracellular domain. *PLoS Med* **3**, e485.
- Lemmon,M.A. (2009). Ligand-induced ErbB receptor dimerization. *Exp Cell Res* **315**, 638-648.

- Lemmon, M.A., Bu, Z., Ladbury, J.E., Zhou, M., Pinchasi, D., Lax, I., Engelman, D.M., and Schlessinger, J. (1997). Two EGF molecules contribute additively to stabilization of the EGFR dimer. *EMBO J* **16**, 281-294.
- Letsch, M., Schally, A.V., Busto, R., Bajo, A.M., and Varga, J.L. (2003). Growth hormone-releasing hormone (GHRH) antagonists inhibit the proliferation of androgen-dependent and -independent prostate cancers. *P Natl Acad Sci USA* **100**, 1250-1255.
- Lewis, G.D., Figari, I., Fendly, B.M., Wong, W.L., Carter, P., Gorman, C., and Shepard, H.M. (1993). Differential responses of human tumor cell lines to anti-p185HER2 monoclonal antibodies. *Cancer Immunol Immunother* **37**, 255-263.
- Li, D., Ji, H., Zaghul, S., McNamara, K., Liang, M.-C., Shimamura, T., Kubo, S., Takahashi, M., Chiriac, L.R., Padera, R.F., Scott, A.M., Jungbluth, A.A., Cavenee, W.K., Old, L.J., Demetri, G.D. *et al.* (2007). Therapeutic anti-EGFR antibody 806 generates responses in murine de novo EGFR mutant-dependent lung carcinomas. *J Clin Invest* **117**, 346-352.
- Li, G. and Wong, A.J. (2008). EGF receptor variant III as a target antigen for tumor immunotherapy. *Exp Rev Vaccines* **7**, 977-985.
- Li, S., Kussie, P., and Ferguson, K.M. (2008). Structural basis for EGF receptor inhibition by the therapeutic antibody IMC-11F8. *Structure* **16**, 216-227.
- Li, S., Schmitz, K.R., Jeffrey, P.D., Wiltzius, J.J.W., Kussie, P., and Ferguson, K.M. (2005). Structural basis for inhibition of the epidermal growth factor receptor by cetuximab. *Cancer Cell* **7**, 301-311.
- Li, S.L., Liang, S.J., Guo, N., Wu, A.M., and Fujita-Yamaguchi, Y. (2000). Single-chain antibodies against human insulin-like growth factor I receptor: expression, purification, and effect on tumor growth. *Cancer Immunol Immunother* **49**, 243-252.
- Livneh, E., Prywes, R., Kashles, O., Reiss, N., Sasson, I., Mory, Y., Ullrich, A., and Schlessinger, J. (1986). Reconstitution of human epidermal growth factor receptors and its deletion mutants in cultured hamster cells. *J Biol Chem* **261**, 12490-12497.
- Logtenberg, T. (2007). Antibody cocktails: next-generation biopharmaceuticals with improved potency. *Trends Biotechnol* **25**, 390-394.
- Lorimer, I.A.J. and Lavioire, S.J. (2001). Activation of extracellular-regulated kinases by normal and mutant EGF receptors. *BBA-Mol Cell Res* **1538**, 1-9.
- Lou, M., Garrett, T.P.J., McKern, N.M., Hoyne, P.A., Epa, V.C., Bentley, J.D., Lovrecz, G.O., Cosgrove, L.J., Frenkel, M.J., and Ward, C.W. (2006). The first three domains of the insulin receptor differ structurally from the insulin-like growth factor 1 receptor in the regions governing ligand specificity. *P Natl Acad Sci USA* **103**, 12429-12434.
- Luwor, R.B., Zhu, H.J., Walker, F., Vitali, A.A., Perera, R.M., Burgess, A.W., Scott, A.M., and Johns, T.G. (2004). The tumor-specific de2-7 epidermal growth factor receptor (EGFR) promotes cells survival and heterodimerizes with the wild-type EGFR. *Oncogene* **23**, 6095-6104.
- Macdonald, J.L. and Pike, L.J. (2008). Heterogeneity in EGF-binding affinities arises from negative cooperativity in an aggregating system. *P Natl Acad Sci USA* **105**, 112-117.
- Magun, B.E., Matrisian, L.M., and Bowden, G.T. (1980). Epidermal growth factor. Ability of tumor promoter to alter its degradation, receptor affinity and receptor number. *J Biol Chem* **255**, 6373-6381.
- Maira, S.M., Stauffer, F., Schnell, C., and García-Echeverría, C. (2009). PI3K inhibitors for cancer treatment: where do we stand? *Biochem Soc Trans* **37**, 265-272.
- Maloney, E.K., McLaughlin, J.L., Dagdigian, N.E., Garrett, L.M., Connors, K.M., Zhou, X.M., Blattler, W.A., Chittenden, T., and Singh, R. (2003). An anti-insulin-like growth factor I receptor antibody that is a potent inhibitor of cancer cell proliferation. *Cancer Res* **63**, 5073-5083.
- Masui, H., Kawamoto, T., Sato, J.D., Wolf, B., Sato, G., and Mendelsohn, J. (1984). Growth Inhibition of Human Tumor Cells in Athymic Mice by Anti-Epidermal Growth Factor Receptor Monoclonal Antibodies. *Cancer Res* **44**, 1002-1007.
- Mayawala, K., Vlachos, D.G., and Edwards, J.S. (2005). Heterogeneities in EGF receptor density at the cell surface can lead to concave up scatchard plot of EGF binding. *FEBS Lett* **579**, 3043-3047.
- McCutcheon, I.E., Flyvbjerg, A., Hill, H., Li, J., Bennett, W.F., Scarlett, J.A., and Friend, K.E. (2001). Antitumor activity of the growth hormone receptor antagonist pegvisomant against human meningiomas in nude mice. *J Neurosurg* **94**, 487-492.

- McKern,N.M., Lawrence,M.C., Streltsov,V.A., Lou,M.Z., Adams,T.E., Lovrecz,G.O., Elleman,T.C., Richards,K.M., Bentley,J.D., Pilling,P.A., Hoyne,P.A., Cartledge,K.A., Pham,T.M., Lewis,J.L., Sankovich,S.E. *et al.* (2006). Structure of the insulin receptor ectodomain reveals a folded-over conformation. *Nature* **443**, 218-221.
- Mendelsohn,J. and Baselga,J. (2006). Epidermal growth factor receptor targeting in cancer. *Semin Oncol* **33**, 369-385.
- Mendrola,J.M., Berger,M.B., King,M.C., and Lemmon,M.A. (2002). The Single Transmembrane Domains of ErbB Receptors Self-associate in Cell Membranes. *J. Biol. Chem.* **277**, 4704-4712.
- Mi,L.Z., Grey,M.J., Nishida,N., Walz,T., Lu,C., and Springer,T.A. (2008). Functional and Structural Stability of the Epidermal Growth Factor Receptor in Detergent Micelles and Phospholipid Nanodiscs. *Biochemistry* **47**, 10314-10323.
- Modjtahedi,H., Moscatello,D.K., Box,G., Green,M., Shotton,C., Lamb,D.J., Reynolds,L.J., Wong,A.J., Dean,C., Thomas,H., and Eccles,S. (2003). Targeting of cells expressing wild-type EGFR and type-III mutant EGFR (EGFRvIII) by anti-EGFR MAb ICR62: a two-pronged attack for tumour therapy. *Int J Cancer* **105**, 273-280.
- Mohammadi,M., Olsen,S.K., and Ibrahimi,O.A. (2005). Structural basis for fibroblast growth factor receptor activation. *Cytokine Growth Factor Rev* **16**, 107-137.
- Molina,M.A., Codony-Servat,J., Albanell,J., Rojo,F., Arribas,J., and Baselga,J. (2001). Trastuzumab (Herceptin), a Humanized Anti-HER2 Receptor Monoclonal Antibody, Inhibits Basal and Activated HER2 Ectodomain Cleavage in Breast Cancer Cells. *Cancer Res* **61**, 4744-4749.
- Moscatello,D.K., Holgado-Madruga,M., Emler,D.R., Montgomery,R.B., and Wong,A.J. (1998). Constitutive Activation of Phosphatidylinositol 3-Kinase by a Naturally Occurring Mutant Epidermal Growth Factor Receptor. *J. Biol. Chem.* **273**, 200-206.
- Moscatello,D.K., Holgado-Madruga,M., Godwin,A.K., Ramirez,G., Gunn,G., Zoltick,P.W., Biegel,J.A., Hayes,R.L., and Wong,A.J. (1995). Frequent Expression of a Mutant Epidermal Growth Factor Receptor in Multiple Human Tumors. *Cancer Res* **55**, 5536-5539.
- Moscatello,D.K., Montgomery,R.B., Sundareshan,P., McDanel,H., Wong,M.Y., and Wong,A.J. (1996). Transformational and altered signal transduction by a naturally occurring mutant EGF receptor. *Oncogene* **13**, 85-96.
- Moscatello,D.K., Ramirez,G., and Wong,A.J. (1997). A naturally occurring mutant human epidermal growth factor receptor as a target for peptide vaccine immunotherapy of tumors. *Cancer Res* **57**, 1419-1424.
- Murphy,L.O. and Blenis,J. (2006). MAPK signal specificity: the right place at the right time. *Trends Biochem Sci* **31**, 268-275.
- Murthy,U., Basu,A., Rodeck,U., Herlyn,M., Ross,A.H., and Das,M. (1987). Binding of an antagonistic monoclonal antibody to an intact and fragmented EGF-receptor polypeptide. *Arch Biochem Biophys* **252**, 549-560.
- Nagata,Y., Lan,K.H., Zhou,X., Tan,M., Esteva,F.J., Sahin,A.A., Klos,K.S., Li,P., Monia,B.P., Nguyen,N.T., Hortobagyi,G.N., Hung,M.C., and Yu,D. (2004). PTEN activation contributes to tumor inhibition by trastuzumab, and loss of PTEN predicts trastuzumab resistance in patients. *Cancer Cell* **6**, 117-127.
- Narita,Y., Nagane,M., Mishima,K., Huang,H.-J.S., Furnari,F.B., and Cavenee,W.K. (2002). Mutant Epidermal Growth Factor Receptor Signaling Down-Regulates p27 through Activation of the Phosphatidylinositol 3-Kinase/Akt Pathway in Glioblastomas. *Cancer Res* **62**, 6764-6769.
- Nishikawa,R., Ji,X., Harmon,R.C., Lazar,C.S., Gill,G.N., Cavenee,W.K., and Huang,H.S. (1994). A mutant epidermal growth factor receptor common in human glioma confers enhanced tumorigenicity. *P Natl Acad Sci USA* **91**, 7727-7731.
- O'Rourke,D.M., Nute,E.J., Davis,J.G., Wu,C., Lee,A., Murali,R., Zhang,H.T., Qian,X., Kao,C.C., and Greene,M.I. (1998). Inhibition of a naturally occurring EGFR oncoprotein by the p185*neu* ectodomain: implications for subdomain contributions to receptor assembly. *Oncogene* **16**, 1197-1207.
- Oda,K., Matsuoka,Y., Funahashi,A., and Kitano,H. (2005). A comprehensive pathway map of epidermal growth factor receptor signaling. *Mol Syst Biol* **1**.
- Ogiso,H., Ishitani,R., Nureki,O., Fukai,S., Yamanaka,M., Kim,J.H., Saito,K., Sakamoto,A., Inoue,M., Shirouzu,M., and Yokoyama,S. (2002). Crystal structure of the complex of human epidermal growth factor and receptor extracellular domains. *Cell* **110**, 775-787.

- Olsen,S.K., Ibrahimi,O.A., Raucci,A., Zhang,F., Eliseenkova,A.V., Yayon,A., Basilico,C., Linhardt,R.J., Schlessinger,J., and Mohammadi,M. (2004). Insights into the molecular basis for fibroblast growth factor receptor autoinhibition and ligand-binding promiscuity. *P Natl Acad Sci USA* **101**, 935-940.
- Olsen,S.K., Li,J.Y.H., Bromleigh,C., Eliseenkova,A.V., Ibrahimi,O.A., Lao,Z., Zhang,F., Linhardt,R.J., Joyner,A.L., and Mohammadi,M. (2006). Structural basis by which alternative splicing modulates the organizer activity of FGF8 in the brain. *Gene Dev* **20**, 185-198.
- Ottensmeyer,F.P., Beniac,D.R., Luo,R.Z.T., and Yip,C.C. (2000). Mechanism of transmembrane signaling: Insulin binding and the insulin receptor. *Biochemistry-US* **39**, 12103-12112.
- Otwinowski,Z. and Minor,W. (1997). Processing of X-Ray Diffraction Data Collected in Oscillation Mode. In: *Macromolecular Crystallography*, ed. C.W.Carter and R.M.SweetNew York: Academic Press, 307-326.
- Özcan,F., Klein,P., Lemmon,M.A., Lax,I., and Schlessinger,J. (2006). On the nature of low- and high-affinity EGF receptors on living cells. *P Natl Acad Sci USA* **103**, 5735-5740.
- Papin,J.A., Hunter,T., Palsson,B.O., and Subramaniam,S. (2005). Reconstruction of cellular signalling networks and analysis of their properties. *Nat Rev Mol Cell Biol* **6**, 99-111.
- Park,J., Neve,R., Szollosi,J., and Benz,C. (2008). Unraveling the biologic and clinical complexities of HER2. *Clin Breast Cancer* **8**, 392-401.
- Pedersen,M.W., Meltorn,M., Damstrup,L., and Poulsen,H.S. (2001). The type III epidermal growth factor receptor mutation: Biological significance and potential target for anti-cancer therapy. *Ann Oncol* **12**, 745-760.
- Petoukhov,M.V., Eady,N.A.J., Brown,K.A., and Svergun,D.I. (2002). Addition of missing loops and domains to protein models by X-ray solution scattering. *Biophys J* **83**, 3113-3125.
- Petoukhov,M.V. and Svergun,D.I. (2005). Global rigid body modeling of macromolecular complexes against small-angle scattering data. *Biophys J* **89**, 1237-1250.
- Plotnikov,A.N., Schlessinger,J., Hubbard,S.R., and Mohammadi,M. (1999). Structural basis for FGF receptor dimerization and activation. *Cell* **98**, 641-650.
- Plotnikov,A.N., Hubbard,S.R., Schlessinger,J., and Mohammadi,M. (2000). Crystal structures of two FGF-FGFR complexes reveal the determinants of ligand-receptor specificity. *Cell* **101**, 413-424.
- Porod,G. (1982). General Theory. In: *Small-angle X-ray scattering*, ed. O.KratkyLondon: Academic Press, 17-51.
- Portera,C.C., Walshe,J.M., Rosing,D.R., Denduluri,N., Berman,A.W., Vatas,U., Velarde,M., Chow,C.K., Steinberg,S.M., Nguyen,D., Yang,S.X., and Swain,S.M. (2008). Cardiac toxicity and efficacy of trastuzumab combined with pertuzumab in patients with trastuzumab-insensitive human epidermal growth factor receptor 2-positive metastatic breast cancer. *Clin Cancer Res* **14**, 2710-2716.
- Pråhl,M., Nederman,T., Carlsson,J., and Sjödin,L. (1991). Binding of epidermal growth factor (EGF) to a cultured human glioma cell line. *J Recept Res* **11**, 791-812.
- Qin,H., Shi,J., Noberini,R., Pasquale,E.B., and Song,J. (2008). Crystal structure and NMR binding reveal that two small molecule antagonists target the high affinity ephrin-binding channel of the EphA4 receptor. *J Biol Chem* **283**, 29473-29484.
- Rao,S., Starling,N., Cunningham,D., Benson,M., Wotherspoon,A., Lüpfer,C., Kurek,R., Oates,J., Baselga,J., and Hill,A. (2008). Phase I study of epirubicin, cisplatin and capecitabine plus matuzumab in previously untreated patients with advanced oesophagogastric cancer. *Br J Cancer* **99**, 868-874.
- Resnicoff,M., Coppola,D., Sell,C., Rubin,R., Ferrone,S., and Baserga,R. (1994). Growth inhibition of human melanoma cells in nude mice by antisense strategies to the type 1 insulin-like growth factor receptor. *Cancer Res* **54**, 4848-4850.
- Resnicoff,M., Li,W., Basak,S., Herlyn,D., Baserga,R., and Rubin,R. (1996). Inhibition of rat C6 glioblastoma tumor growth by expression of insulin-like growth factor I receptor antisense mRNA. *Cancer Immunol Immunother* **42**, 64-68.
- Robertson,A.G.S., Banfield,M.J., Allen,S.J., Dando,J.A., Mason,G.G.F., Tyler,S.J., Bennett,G.S., Brain,S.D., Clarke,A.R., Naylor,R.L., Wilcock,G.K., Brady,R.L., and Dawbarn,D. (2001). Identification and structure of the nerve growth factor binding site on TrkA. *Biochem Biophys Res Co* **282**, 131-141.

- Robinson,D.R., Wu,Y.M., and Lin,S.F. (2000). The protein tyrosine kinase family of the human genome. *Oncogene* **19**, 5548-5557.
- Rochester,M.A., Riedemann,J., Hellowell,G.O., Brewster,S.F., and Macaulay,V.M. (2004). Silencing of the IGF1R gene enhances sensitivity to DNA-damaging agents in both PTEN wild-type and mutant human prostate cancer. *Cancer Gene Ther* **12**, 90-100.
- Rose,P.P., Carroll,J.M., Carroll,P.A., DeFilippis,V.R., Lagunoff,M., Moses,A.V., Roberts,C.T., Jr., and Fruh,K. (2006). The insulin receptor is essential for virus-induced tumorigenesis of Kaposi's sarcoma. *Oncogene* **26**, 1995-2005.
- Ruan,W., Newman,C.B., and Kleinberg,D.L. (1992). Intact and amino-terminally shortened forms of insulin-like growth factor I induce mammary gland differentiation and development. *P Natl Acad Sci USA* **89**, 10872-10876.
- Ruan,W., Powell-Braxton,L., Kopchick,J.J., and Kleinberg,D.L. (1999). Evidence that insulin-like growth factor I and growth hormone are required for prostate gland development. *Endocrinology* **140**, 1984-1989.
- Ryan,P.D. and Goss,P.E. (2008). The emerging role of the insulin-like growth factor pathway as a therapeutic target in cancer. *Oncologist* **13**, 16-24.
- Sachdev,D., Li,S.L., Hartell,J.S., Fujita-Yamaguchi,Y., Miller,J.S., and Yee,D. (2003). A chimeric humanized single-chain antibody against the type I insulin-like growth factor (IGF) receptor renders breast cancer cells refractory to the mitogenic effects of IGF-I. *Cancer Res* **63**, 627-635.
- Saffarian,S., Li,Y., Elson,E.L., and Pike,L.J. (2007). Oligomerization of the EGF receptor investigated by live cell fluorescence intensity distribution analysis. *Biophys J* **93**, 1021-1031.
- Samani,A.A. and Brodt,P. (2001). The receptor for the type I insulin-like growth factor and its ligands regulate multiple cellular functions that impact on metastasis. *Surg Oncol Clin N Am* **10**, 289-312, viii.
- Samani,A.A., Chevet,E., Fallavollita,L., Galipeau,J., and Brodt,P. (2004). Loss of tumorigenicity and metastatic potential in carcinoma cells expressing the extracellular domain of the type 1 insulin-like growth factor receptor. *Cancer Res* **64**, 3380-3385.
- Sampson,J.H., Archer,G.E., Mitchell,D.A., Heimberger,A.B., and Bigner,D.D. (2008). Tumor-specific immunotherapy targeting the EGFRvIII mutation in patients with malignant glioma. *Semin Immunol* **20**, 267-275.
- Sasaki,T., Knyazev,P.G., Clout,N.J., Cheburkin,Y., Göhring,W., Ullrich,A., Timpl,R., and Hohenester,E. (2006). Structural basis for Gas6-Axl signalling. *EMBO J* **25**, 80-87.
- Sato,J.D., Kawamoto,T., Le,A., Mendelsohn,J., Polikoff,J., and Sato,G.H. (1983). Biological effects *in vitro* of monoclonal antibodies to human epidermal growth factor receptors. *Mol Biol Med* **1**, 511-529.
- Schechter,A.L., Stern,D.F., Vaidyanathan,L., Decker,S.J., Drebin,J.A., Greene,M.I., and Weinberg,R.A. (1984). The *neu* oncogene: an *erb*-B-related gene encoding a 185,000-Mr tumour antigen. *Nature* **312**, 513-516.
- Schlee,S., Carmillo,P., and Whitty,A. (2006). Quantitative analysis of the activation mechanism of the multicomponent growth-factor receptor Ret. *Nat Chem Biol* **2**, 636-644.
- Schlessinger,J. (2000). Cell signaling by receptor tyrosine kinases. *Cell* **103**, 211-225.
- Schmiedel,J., Blaukat,A., Li,S., Knöchel,T., and Ferguson,K.M. (2008). Matuzumab binding to EGFR prevents the conformational rearrangement required for dimerization. *Cancer Cell* **13**, 365-373.
- Schmitz,K.R. and Ferguson,K.M. (2009). Interaction of antibodies with ErbB receptor extracellular regions. *Exp Cell Res* **315**, 659-670.
- Schreiber,A.B., Lax,I., Yarden,Y., Eshhar,Z., and Schlessinger,J. (1981). Monoclonal antibodies against receptor for epidermal growth factor induce early and delayed effects of epidermal growth factor. *P Natl Acad Sci USA* **78**, 7535-7539.
- Schreiber,A.B., Libermann,T.A., Lax,I., Yarden,Y., and Schlessinger,J. (1983). Biological role of epidermal growth factor-receptor clustering. Investigation with monoclonal anti-receptor antibodies. *J Biol Chem* **258**, 846-853.
- Scott,A.M., Lee,F.T., Tebbutt,N., Herbertson,R., Gill,S.S., Liu,Z., Skrinos,E., Murone,C., Saunder,T.H., Chappell,B., Papenfuss,A.T., Poon,A.M., Hopkins,W., Smyth,F.E., MacGregor,D. *et al.* (2007). A phase I clinical trial with monoclonal

- antibody ch806 targeting transitional state and mutant epidermal growth factor receptors. *P Natl Acad Sci USA* **104**, 4071-4076.
- Sebastian,S., Settleman,J., Reshkin,S.J., Azzariti,A., Bellizzi,A., and Paradiso,A. (2006). The complexity of targeting EGFR signalling in cancer: From expression to turnover. *BBA-Rev Cancer* **1766**, 120-139.
- Seiden,M.V., Burris,H.A., Matulonis,U., Hall,J.B., Armstrong,D.K., Speyer,J., Weber,J.D.A., and Muggia,F. (2007). A phase II trial of EMD72000 (matuzumab), a humanized anti-EGFR monoclonal antibody, in patients with platinum-resistant ovarian and primary peritoneal malignancies. *Gynecol Oncol* **104**, 727-731.
- Sekyi-Otu,A., Bell,R.S., Ohashi,C., Pollak,M., and Andrulis,I.L. (1995). Insulin-like growth factor 1 (IGF-1) receptors, IGF-1, and IGF-2 are expressed in primary human sarcomas. *Cancer Res* **55**, 129-134.
- Sell,C., Rubini,M., Rubin,R., Liu,J.P., Efstratiadis,A., and Baserga,R. (1993). Simian virus 40 large tumor antigen is unable to transform mouse embryonic fibroblasts lacking type 1 insulin-like growth factor receptor. *P Natl Acad Sci USA* **90**, 11217-11221.
- Shankar,S., Vaidyanathan,G., Kuan,C.T., Bigner,D.D., and Zalutsky,M.R. (2006). Antiepidermal growth factor variant III scFv fragment: effect of radioiodination method on tumor targeting and normal tissue clearance. *Nucl Med Biol* **33**, 101-110.
- Shepherd,F.A., Rodrigues Pereira,J., Ciuleanu,T., Tan,E.H., Hirsh,V., Thongprasert,S., Campos,D., Maoleekoonpiroj,S., Smylie,M., Martins,R., van Kooten,M., Dediu,M., Findlay,B., Tu,D., Johnston,D. *et al.* (2005). Erlotinib in previously treated non-small-cell lung cancer. *N Engl J Med* **353**, 123-132.
- Shoyab,M., De Larco,J.E., and Todaro,G.J. (1979). Biologically active phorbol esters specifically alter affinity of epidermal growth factor membrane receptors. *Nature* **279**, 387-391.
- Singer,E. (2005). Iressa's fall from grace points to need for better clinical trials. *Nat Med* **11**, 107.
- Slamon,D.J., Leyland-Jones,B., Shak,S., Fuchs,H., Paton,V., Bajamonde,A., Fleming,T., Eiermann,W., Wolter,J., Pegram,M., Baselga,J., and Norton,L. (2001). Use of chemotherapy plus a monoclonal antibody against HER2 for metastatic breast cancer that overexpresses HER2. *New Engl J Med* **344**, 783-792.
- Socinski,M.A. (2007). Antibodies to the epidermal growth factor receptor in non small cell lung cancer: Current status of matuzumab and panitumumab. *Clin Cancer Res* **13**, 4597s-4601.
- Sonabend,A.M., Dana,K., and Lesniak,M.S. (2007). Targeting epidermal growth factor receptor variant III: a novel strategy for the therapy of malignant glioma. *Exp Rev Anticancer Ther* **7**, S45-S50.
- Spiridon,C.I., Ghetie,M.A., Uhr,J., Marches,R., Li,J.L., Shen,G.L., and Vitetta,E.S. (2002). Targeting multiple HER-2 epitopes with monoclonal antibodies results in improved antigrowth activity of a human breast cancer cell line *in vitro* and *in vivo*. *Clin Cancer Res* **8**, 1720-1730.
- Stamos,J., Lazarus,R.A., Yao,X., Kirchhofer,D., and Wiesmann,C. (2004). Crystal structure of the HGF beta-chain in complex with the Sema domain of the Met receptor. *EMBO J* **23**, 2325-2335.
- Stanfield,R.L., Zemla,A., Wilson,I.A., and Rupp,B. (2006). Antibody elbow angles are influenced by their light chain class. *J Mol Biol* **357**, 1566-1574.
- Stauber,D.J., DiGabriele,A.D., and Hendrickson,W.A. (2000). Structural interactions of fibroblast growth factor receptor with its ligands. *P Natl Acad Sci USA* **97**, 49-54.
- Stephenson,J., Gregory,C., Burris,H., Larson,T., Verma,U., Cohn,A., Crawford,J., Cohen,R., Martin,J., Lum,P., Yang,X., and Amado,R. (2008). An open-label clinical trial evaluating safety and pharmacokinetics of two dosing schedules of panitumumab in patients with solid tumors. *Clin Colorect Cancer* **8**, 29-37.
- Stiegler,A.L., Burden,S.J., and Hubbard,S.R. (2006). Crystal structure of the agrin-responsive immunoglobulin-like domains 1 and 2 of the receptor tyrosine kinase MuSK. *J Mol Biol* **364**, 424-433.
- Stutz,M.A., Shattuck,D.L., Laederich,M.B., Carraway,K.L., III, and Sweeney,C. (2008). LRIG1 negatively regulates the oncogenic EGF receptor mutant EGFRvIII. *Oncogene* **27**, 5741-5752.
- Sullivan,K.A., Kim,B., and Feldman,E.L. (2008). Insulin-like growth factors in the peripheral nervous system. *Endocrinology* **149**, 5963-5971.

- Sundberg, E.J. and Mariuzza, R.A. (2002). Molecular recognition in antibody-antigen complexes. *Adv Protein Chem* **61**, 119-160.
- Surinya, K.H., Forbes, B.E., Occhiodoro, F., Booker, G.W., Francis, G.L., Siddle, K., Wallace, J.C., and Cosgrove, L.J. (2008). An investigation of the ligand binding properties and negative cooperativity of soluble insulin-like growth factor receptors. *J Biol Chem* **283**, 5355-5363.
- Svergun, D.I. (1992). Determination of the regularization parameter in indirect-transform methods using perceptual criteria. *J Appl Cryst* **25**, 495-503.
- Svergun, D.I. (1999). Restoring low resolution structure of biological macromolecules from solution scattering using simulated annealing. *Biophys J* **76**, 2879-2886.
- Svergun, D.I., Barberato, C., and Koch, M.H. (1995). CRY SOL - a program to evaluate X-ray solution scattering of biological macromolecules from atomic coordinates. *J Appl Cryst* **28**, 768-773.
- Tao, Y., Pinzi, V., Bourhis, J., and Deutsch, E. (2007). Mechanisms of disease: signaling of the insulin-like growth factor 1 receptor pathway - therapeutic perspectives in cancer. *Nat Clin Pract Oncol* **4**, 591-602.
- Thatcher, N., Chang, A., Parikh, P., Rodrigues Pereira, J., Ciuleanu, T., von Pawel, J., Thongprasert, S., Tan, E.H., Pemberton, K., Archer, V., and Carroll, K. (2005). Gefitinib plus best supportive care in previously treated patients with refractory advanced non-small-cell lung cancer: results from a randomised, placebo-controlled, multicentre study (Iressa Survival Evaluation in Lung Cancer). *Lancet* **366**, 1527-1537.
- Ullrich, A., Gray, A., Tam, A.W., Yang-Feng, T., Tsubokawa, M., Collins, C., Henzel, W., Le Bon, T., Kathuria, S., Chen, E., and et al. (1986). Insulin-like growth factor I receptor primary structure: comparison with insulin receptor suggests structural determinants that define functional specificity. *EMBO J* **5**, 2503-2512.
- Ullrich, A. and Schlessinger, J. (1990). Signal transduction by receptors with tyrosine kinase activity. *Cell* **61**, 203-212.
- Ultsch, M.H., Wiesmann, C., Simmons, L.C., Henrich, J., Yang, M., Reilly, D., Bass, S.H., and de Vos, A.M. (1999). Crystal structures of the neurotrophin-binding domain of TrkA, TrkB and TrkC. *J Mol Biol* **290**, 149-159.
- Vajdos, F.F., Adams, C.W., Breece, T.N., Presta, L.G., de Vos, A.M., and Sidhu, S.S. (2002). Comprehensive functional maps of the antigen-binding site of an anti-ErbB2 antibody obtained with shotgun scanning mutagenesis. *J Mol Biol* **320**, 415-428.
- Van Den Berg, C.L., Cox, G.N., Stroh, C.A., Hilsenbeck, S.G., Weng, C.-N., Mcdermott, M.J., Pratt, D., Osborne, C.K., Coronado-Heinsohn, E.B., and Yee, D. (1997). Polyethylene glycol conjugated insulin-like growth factor binding protein-1 (IGFBP-1) inhibits growth of breast cancer in athymic mice. *Eur J Cancer* **33**, 1108-1113.
- Vanhoefer, U., Tewes, M., Rojo, F., Dirsch, O., Schleucher, N., Rosen, O., Tillner, J., Kovar, A., Braun, A.H., Trarbach, T., Seeber, S., Harstick, A., and Baselga, J. (2004). Phase I study of the humanized anti-epidermal growth factor receptor monoclonal antibody EMD72000 in patients with advanced solid tumors that express the epidermal growth factor receptor. *J Clin Oncol* **22**, 175-184.
- Vasilcanu, R., Vasilcanu, D., Sehat, B., Yin, S., Girmita, A., Axelson, M., and Girmita, L. (2008). Insulin-like growth factor type-I receptor-dependent phosphorylation of extracellular signal-regulated kinase 1/2 but not Akt (protein kinase B) can be induced by picropodophyllin. *Mol Pharmacol* **73**, 930-939.
- Volkov, V.V. and Svergun, D.I. (2003). Uniqueness of *ab initio* shape determination in small-angle scattering. *J Appl Cryst* **36**, 860-864.
- Wada, T., Qian, X., and Greene, M.I. (1990). Intermolecular association of the p185neu protein and EGF receptor modulates EGF receptor function. *Cell* **61**, 1339-1347.
- Wang, H., Jiang, H., Zhou, M., Xu, Z., Liu, S., Shi, B., Yao, X., Yao, M., Gu, J., and Li, Z. (2009). Epidermal growth factor receptor vIII enhances tumorigenicity and resistance to 5-fluorouracil in human hepatocellular carcinoma. *Cancer Lett* **in press**.
- Wang, W. and Malcolm, B.A. (2002). Two-stage polymerase chain reaction protocol allowing introduction of multiple mutations, deletions, and insertions, using QuikChange site-directed mutagenesis. *Method Mol Biol* **182**, 37-43.
- Wang, Y., Hailey, J., Williams, D., Wang, Y., Lipari, P., Malkowski, M., Wang, X., Xie, L., Li, G., Saha, D., Ling, W.L., Cannon-Carlson, S., Greenberg, R., Ramos, R.A., Shields, R. et al. (2005). Inhibition of insulin-like growth factor-I receptor (IGF-IR) signaling and tumor cell growth by a fully human neutralizing anti-IGF-IR antibody. *Mol Cancer Ther* **4**, 1214-1221.

- Ward,C., Lawrence,M., Streltsov,V., Garrett,T., McKern,N.M., Lou,M., Lovrecz,G.O., and Adams,T.E. (2008). Structural insights into ligand-induced activation of the insulin receptor. *Acta Physiol* **192**, 3-9.
- Ward,C.W., Hoyne,P.A., and Flegg,R.H. (1995). Insulin and epidermal growth factor receptors contain the cysteine repeat motif found in the tumor necrosis factor receptor. *Proteins* **22**, 141-153.
- Ward,C.W. and Lawrence,M.C. (2009). Ligand-induced activation of the insulin receptor: a multi-step process involving structural changes in both the ligand and the receptor. *Bioassays* **31**, 422-434.
- Ward,C.W., Lawrence,M.C., Streltsov,V.A., Adams,T.E., and McKern,N.M. (2007). The insulin and EGF receptor structures: new insights into ligand-induced receptor activation. *Trends Biochem Sci* **32**, 129-137.
- Wehrman,T.S., Raab,W.J., Casipit,C.L., Doyonnas,R., Pomerantz,J.H., and Blau,H.M. (2006). A system for quantifying dynamic protein interactions defines a role for Herceptin in modulating ErbB2 interactions. *P Natl Acad Sci USA* **103**, 19063-19068.
- Wehrman,T., He,X., Raab,B., Dukipatti,A., Blau,H., and Garcia,K.C. (2007). Structural and mechanistic insights into nerve growth factor interactions with the TrkA and p75 receptors. *Neuron* **53**, 25-38.
- Weinberg,R.A. (2007). *The Biology of Cancer*, New York: Garland Science, Taylor & Francis Group.
- Weppler,S.A., Li,Y., Dubois,L., Lieuwes,N., Jutten,B., Lambin,P., Wouters,B.G., and Lammering,G. (2007). Expression of EGFR variant vIII promotes both radiation resistance and hypoxia tolerance. *Radiother Oncol* **83**, 333-339.
- Weroha,S. and Haluska,P. (2008). IGF-1 receptor inhibitors in clinical trials – early lessons. *J Mammary Gland Biol* **13**, 471-483.
- Whittaker,J., Groth,A.V., Mynarcik,D.C., Pluzek,L., Gadsboll,V.L., and Whittaker,L.J. (2001). Alanine scanning mutagenesis of a type 1 insulin-like growth factor receptor ligand binding site. *J Biol Chem* **276**, 43980-43986.
- Whittaker,J., Sorensen,H., Gadsboll,V.L., and Hinrichsen,J. (2002). Comparison of the functional insulin binding epitopes of the A and B isoforms of the insulin receptor. *J Biol Chem* **277**, 47380-47384.
- Wiesmann,C., Fuh,G., Christinger,H.W., Eigenbrot,C., Wells,J.A., and de Vos,A.M. (1997). Crystal structure at 1.7 Å resolution of VEGF in complex with domain 2 of the Flt-1 receptor. *Cell* **91**, 695-704.
- Wiesmann,C., Ultsch,M.H., Bass,S.H., and de Vos,A.M. (1999). Crystal structure of nerve growth factor in complex with the ligand-binding domain of the TrkA receptor. *Nature* **401**, 184-188.
- Wikstrand,C.J., Hale,L.P., Batra,S.K., Hill,M.L., Humphrey,P.A., Kurpad,S.N., McLendon,R.E., Moscatello,D., Pegram,C.N., Reist,C.J., Traweek,S.T., Wong,A.J., Zalutsky,M.R., and Bigner,D.D. (1995). Monoclonal antibodies against EGFRvIII are tumor specific and react with breast and lung carcinomas and malignant gliomas. *Cancer Res* **55**, 3140-3148.
- Wikstrand,C.J., McLendon,R.E., Friedman,A.H., and Bigner,D.D. (1997). Cell surface localization and density of the tumor-associated variant of the epidermal growth factor receptor, EGFRvIII. *Cancer Res* **57**, 4130-4140.
- Wofsy,C., Goldstein,B., Lund,K., and Wiley,H.S. (1992). Implications of epidermal growth factor (EGF) induced EGF receptor aggregation. *Biophys J* **63**, 98-110.
- Woods,K.A., Camacho-Hubner,C., Savage,M.O., and Clark,A.J.L. (1996). Intrauterine growth retardation and postnatal growth failure associated with deletion of the insulin-like growth factor I gene. *N Engl J Med* **335**, 1363-1367.
- Wu,C.J., Qian,X., and O'Rourke,D.M. (1999). Sustained mitogen-activated protein kinase activation is induced by transforming erbB receptor complexes. *DNA Cell Biol* **18**, 731-741.
- Yang,W., Wu,G., Barth,R.F., Swindall,M.R., Bandyopadhyaya,A.K., Tjarks,W., Tordoff,K., Moeschberger,M., Sferra,T.J., Binns,P.J., Riley,K.J., Ciesielski,M.J., Fenstermaker,R.A., and Wikstrand,C.J. (2008). Molecular targeting and treatment of composite EGFR and EGFRvIII-positive gliomas using boronated monoclonal antibodies. *Clin Cancer Res* **14**, 883-891.
- Yang,X.D., Jia,X.C., Corvalan,J.R., Wang,P., and Davis,C.G. (2001). Development of ABX-EGF, a fully human anti-EGF receptor monoclonal antibody, for cancer therapy. *Crit Rev Oncol Hematol* **38**, 17-23.
- Yarden,Y. and Schlessinger,J. (1987a). Epidermal growth factor induces rapid, reversible aggregation of the purified epidermal growth factor receptor. *Biochemistry-US* **26**, 1443-1451.

- Yarden, Y. and Schlessinger, J. (1987b). Self-phosphorylation of epidermal growth factor receptor: evidence for a model of intermolecular allosteric activation. *Biochemistry-US* **26**, 1434-1442.
- Ye, D., Mendelsohn, J., and Fan, Z. (1999). Augmentation of a humanized anti-HER2 mAb 4D5 induced growth inhibition by a human-mouse chimeric anti-EGF receptor mAb C225. *Oncogene* **18**, 731.
- Yeh, B.K., Igarashi, M., Eliseenkova, A.V., Plotnikov, A.N., Sher, I., Ron, D., Aaronson, S.A., and Mohammadi, M. (2003). Structural basis by which alternative splicing confers specificity in fibroblast growth factor receptors. *P Natl Acad Sci USA* **100**, 2266-2271.
- Yoshimoto, K., Dang, J., Zhu, S., Nathanson, D., Huang, T., Dumont, R., Seligson, D.B., Yong, W.H., Xiong, Z., Rao, N., Winther, H., Chakravarti, A., Bigner, D.D., Mellinghoff, I.K., Horvath, S. *et al.* (2008). Development of a real-time RT-PCR assay for detecting EGFRvIII in glioblastoma samples. *Clin Cancer Res* **14**, 488-493.
- Yuzawa, S., Opatowsky, Y., Zhang, Z., Mandiyan, V., Lax, I., and Schlessinger, J. (2007). Structural Basis for Activation of the Receptor Tyrosine Kinase KIT by Stem Cell Factor. *Cell* **130**, 323-334.
- Zhang, H., Berezov, A., Wang, Q., Zhang, G., Drebin, J.A., Murali, R., and Greene, M.I. (2007). ErbB receptors: from oncogenes to targeted cancer therapies. *J Clin Invest* **117**, 2051-2058.
- Zhang, X., Gureasko, J., Shen, K., Cole, P.A., and Kuriyan, J. (2006b). An Allosteric Mechanism for Activation of the Kinase Domain of Epidermal Growth Factor Receptor. *Cell* **125**, 1137-1149.
- Zhang, X., Gureasko, J., Shen, K., Cole, P.A., and Kuriyan, J. (2006a). An Allosteric Mechanism for Activation of the Kinase Domain of Epidermal Growth Factor Receptor. *Cell* **125**, 1137-1149.
- Zhang, Y., Wolf-Yadlin, A., Ross, P.L., Pappin, D.J., Rush, J., Lauffenburger, D.A., and White, F.M. (2005). Time-resolved Mass Spectrometry of Tyrosine Phosphorylation Sites in the Epidermal Growth Factor Receptor Signaling Network Reveals Dynamic Modules. *Mol Cell Proteomics* **4**, 1240-1250.
- Zhu, H., Acquaviva, J., Ramachandran, P., Boskovitz, A., Woolfenden, S., Pfannl, R., Bronson, R.T., Chen, J.W., Weissleder, R., Housman, D.E., and Charest, A. (2009). Oncogenic EGFR signaling cooperates with loss of tumor suppressor gene functions in gliomagenesis. *P Natl Acad Sci USA*.

10. GLOSSARY

| | |
|-----------------|--|
| AB | acidic box |
| ADCC | antibody-dependent cellular cytotoxicity |
| ATP | adenosine-5'-triphosphate |
| AUC SE | analytical ultracentrifugation sedimentation equilibrium |
| Axl | Tyros3 protein tyrosine kinase |
| C225 | cetuximab |
| Cadhd | cadherin-like domain |
| CDC | complement-dependent cytotoxicity |
| CDR | complementarity determining region |
| CR | cysteine-rich |
| CRC | colorectal cancer |
| CRD | cysteine-rich domain |
| CV | column volume |
| DDR | discoidin domain receptor |
| DiscD | discoidin-like domain |
| DLS | dynamic light scattering |
| DMEM | Dulbecco's modified Eagle medium |
| EDC | <i>N</i> -ethyl- <i>N'</i> -(dimethylaminopropyl)-carbodiimide hydrochloride |
| EDTA | ethylenediaminetetraacetic acid |
| EGFD | epidermal growth factor-like domain |
| EGFR | epidermal growth factor receptor |
| EMD72000 | matuzumab |
| EphR | ephrin receptors |
| Fab | fragment antigen binding |
| Fab1159476 | fragment antigen binding of EMD1159476 |
| Fab72000 | fragment antigen binding of matuzumab |
| FabC225 | fragment antigen binding of cetuximab |
| FDA | US American Food and Drug administration |
| FGFR | fibroblast growth factor receptors |
| FnIII | fibronectin type-III domain |
| GAP | guanine exchange factors (Ras-GAP) |
| GBM | glioblastoma |
| GH | growth hormone |
| GHR | growth hormone receptor |
| h | hours |
| HB-EGF | heparin binding EGF-like growth factor (|
| HEPES | 2-(4-(2-Hydroxyethyl)-1-piperazinyl)-ethansulfonsäure |
| HER2 | human epidermal growth factor receptor 2 |
| HGFR | hepatocyte growth factor receptor, Met |
| ID | insert domain |
| IgD | immunoglobulin-like domain |
| IGF-1R | insulin-like growth factor-1 receptor |
| IGFBP | insulin-like growth factor binding proteins |
| IMAC | immobilized metal-ion affinity chromatography |
| IP ₃ | inositol-3,4,5-trisphosphate |
| IR | insulin receptor |
| IRR | insulin-related receptor |
| ITC | isothermal titration calorimetry |
| KinD | kringle-like domain |
| KLK/CCK | colon carcinoma kinase |
| LMR | lemur |
| LRD | leucine-rich domain |

| | |
|-----------------------------|--|
| LRIG1 | leucine rich repeat and immunoglobulin-like domain-1 protein |
| LTK | leukocyte tyrosine kinase |
| mAb | monoclonal antibody |
| MAPK | mitogen-activated protein kinase (ERK) |
| MAPKK | MAP-kinase-kinase (MEK1) |
| min | minutes |
| MOI | multiplicity of infection |
| mSOS | mammalian son of sevenless |
| mTOR | mammalian target of rapamycin |
| MuSK | muscle-specific kinase |
| NaCl | sodium chloride |
| NGFR | nerve growth factor receptor |
| NHS | <i>N</i> -hydroxysuccinimide |
| NRG | neuregulin |
| NSCLC | non-small cell lung cancer |
| PBS | phosphate-buffered saline |
| PCR | polymerase chain reaction |
| PDB | protein data base |
| PDGFR | platelet-derived growth factor receptor |
| PDK1 | pyruvate dehydrogenase kinase 1 |
| PEI | polyethylenimin |
| PI-3K | phosphoinositidyl-3 kinase |
| PKB | protein kinase B (Akt) |
| PKC | protein kinase C |
| PTB | phosphotyrosine-binding |
| PtdIns(3,4)P ₂ | phosphatidylinositol-3,4-bisphosphate |
| PtdIns(3,4,5)P ₃ | phosphatidylinositol-3,4,5-trisphosphate |
| Ret | rearranged during transfection |
| ROR | receptor orphan |
| ROS | receptor tyrosine kinase expressed in some epithelial cell types |
| RTK | receptor tyrosine kinase |
| RU | response units |
| RYK | receptor related to tyrosine kinases |
| SC | shape complementarity |
| sec | seconds |
| SEC | size exclusion chromatography |
| sEGFR | soluble ectodomain of EGFR |
| sEGFRd3 | soluble ectodomain EGFR domain III |
| SH2 | SRC homology-2 |
| SHC | SH2 domain-containing enzymes |
| sIGF-1R | soluble ectodomain of IGF-1R |
| SLS | static light scattering |
| SPR | surface plasmon resonance |
| TGF- α | transforming growth factor α |
| TIE | tyrosine kinase receptor in endothelial cells |
| TKI | tyrosine kinase inhibitor |
| VEGF | vascular endothelial growth factor |
| VEGFR | vascular endothelial growth factor receptors |

11. APPENDIX

11.1. Primer sequences

| | |
|---------------------|---|
| K454 up | 5' AATACAATAAACTGGGCAAAACTGTTTGGGACC 3' |
| K454 rev | 5' GGTCCCAAACAGTTTTGCCAGTTTATTGTATT 3' |
| K463 up | 5' GGGACCTCCGGTCAGGCAACCAAAATTATAAGC 3' |
| K463 rev | 5' GCTTATAATTTTGGTTGCCTGACCGGAGGTCCC 3' |
| T459A/S460A up | 5' AAAAAACTGTTTGGGGCCGCCGGTCAGAAAACCAAA 3' |
| T459A/S460A rev | 5' TTTGGTTTTCTGACCGGCGGCCCAAACAGTTTTTTT 3' |
| tripleK454A up | 5' AATACAATAAACTGGGCAAAACTGTTTGGGGCC 3' |
| tripleK454A rev | 5' GGCCCAAACAGTTTTGCCAGTTTATTGTATT 3' |
| tripleK463A up | 5' GGGGCCGCCGGTCAGGCAACCAAAATTATAAGC 3' |
| tripleK463A rev | 5' GCTTATAATTTTGGTTGCCTGACCGGCGGCCCC 3' |
| sEGFRvIII f1 up | 5' GGCTTCGAAGGAGATAGAACCATGCGACCCTCCGGGACGGCC GGG 3' |
| sEGFRvIII f1 rev | 5'GTGATCTGTCACCACATAATTACCTTTCTTTTCCTCCAGAGCCCC ACT3' |
| sEGFRvIII f2 up | 5' AGTCGGGCTCTGGAGGAAAAGAAAGGTAATTATGTGGTGACAGAT CAC 3' |
| sEGFRvIII f2 rev | 5' GTCCTATTAATGGTGATGGTGATGGTGCTTAGGCCCATTCGTTGGA CAG 3' |
| sIGF-1Rd1-3 up | 5' GGCTTCGAAGGAGATAGAACCATGAAGTCTGGCTCCGGAG 3' |
| sIGF-1Rd1-3 rev | 5' GTCCTATTAATGGTGATGGTGATGGTGGACGTCACCTTCACAGG AGG 3' |
| sIGF-1Rd2 blunt up | 5' TCCACTCGTCGGCCAGAGCGAGA 3' |
| sIGF-1Rd2 blunt rev | 5' GACCTGTGTCCAGGGACCATGGAG 3' |
| sIGF-1Rd2 up | 5' GGCTTCGAAGGAGATAGAACCATGAAGTCTGGCTCCGGAG 3' |
| sIGF-1Rd2 rev | 5' CAAGAAAGCTGGGTCTTATTACGGGCAAGGACCTTCACAAGG GAT 3' |

11.2. Protein constructs

Amino acid sequence *sEGFR_His₆* (signal peptide in bold)

MRPSGTAGAALLALLAALCPASRALEEKKVCQGTSSNKLTQLGTFEDHFSLQRMFNCEVVL
GNLEITYVQRNYDLSFLKTIQEVAGYVLIALNTVERIPLLENLQIIRGNMYEENSIALAVLSN
YDANKTGLKELPMRNLQEILHGAVRFSNNPALCNVESIQWRDIVSSDFLSNMSMDFQNLHGS
CQKCDPSCPNWSCWGAGEENCQKLTKIICAQQCSGRCRGKSPSDCCHNQCAAGCTGPRESDC
LVCRKFRDEATCKDTCPLMLYNPTTYQMDVNPEGKYSFGATCVKKCPRNYVVTDHGSCVRA
CGADSYEMEEDGVRKCKKCEGPCRKVCNGIGIGEFKDSLSINATNIKHFKNCTSSISGDLHIL
PVAFRGDSFTHTPPLDPQELDILKTVKEITGFLLIQAWPENRTDLHAFENLEIIRGRKQHG
QFSLAVVSLNITSLGLRSLKEISDGDVILISGNKNLCYANTINWKKLFGTSGQKTKIISNRGE
NSCKATGQVCHALCSPEGCWGPEDRDCVSCRNVSRGRECVDKCKLLEGEPPREFVENSECIQC
HPECLPQAMNITCTGRGPDNCIQCAHYIDGPHCVKTCPAGVMGENNTLVWKYADAGHVCHLC
HPNCTYGCTGPGLEGCPNTPKHHHHHH.

Nucleotide sequence *sEGFR_His₆*

ATGCGACCCTCCGGGACGGCCGGGGCAGCGCTCCTGGCGCTGCTGGCTGCGCTCTGCCCGGC
GAGTCGGGCTCTGGAGGAAAAGAAAGTTTGCCAAGGCACGAGTAACAAGCTCACGCAGTTGG
GCACTTTTGAAGATCATTTTCTCAGCCTCCAGAGGATGTTCAATAACTGTGAGGTGGTCTTT
GGGAATTTGGAAATTACCTATGTGCAGAGGAATTATGATCTTTCCTTCTTAAAGACCATCCA
GGAGGTGGCTGGTTATGTCCTCATTGCCCTCAACACAGTGGAGCGAATTCCTTTGGAAAACC
TGCAGATCATCAGAGGAAATATGTAACGAAAATTCCTATGCCTTAGCAGTCTTATCTAAC
TATGATGCAAATAAAACCGGACTGAAGGAGCTGCCCATGAGAAAATTTACAGGAAATCCTGCA
TGGCGCCGTGCGGTTACAGCAACAACCTGCCCCGTGCAACGTGGAGAGCATCCAGTGGCGGG
ACATAGTCAGCAGTGACTTTTCTCAGCAACATGTCGATGGACTTCCAGAACCACCTGGGCAGC
TGCCAAAAGTGTGATCCAAGCTGTCCCAATGGGAGCTGCTGGGGTGCAGGAGAGGAGAACTG
CCAGAACTGACCAAAATCATCTGTGCCCAGCAGTGTCTCCGGGCGCTGCCGTGGCAAGTCCC
CCAGTGACTGCTGCCACAACCAGTGTGCTGCAGGCTGCACAGGCCCCCGGAGAGCGACTGC
CTGGTCTGCCGCAAATTCGAGACGAAGCCACGTGCAAGGACACCTGCCCCCACTCATGCT
CTACAACCCACCACGTACCAGATGGATGTGAACCCCGAGGGCAAATACAGCTTTGGTGCCA
CCTGCGTGAAGAAGTGTCCCCGTAATTATGTGGTGACAGATCACGGCTCGTGCGTCCGAGCC
TGTGGGGCCGACAGCTATGAGATGGAGGAAGACGGCGTCCGCAAGTGTAAGAAGTGCAGAGG
GCCTTGCCGCAAAGTGTGTAACGGAATAGGTATTGGTGAATTTAAAGACTCACTCTCCATAA
ATGCTACGAATATTAACACTTCAAAAACACTGCACCTCCATCAGTGGCGATCTCCACATCCTG
CCGTTGGCATTTAGGGGTGACTCCTTACACATACTCCTCCTCTGGATCCACAGGAACTGGA
TATTCTGAAAACCGTAAAGGAAATCACAGGGTTTTTGTGATTCAGGCTTGGCCTGAAAACA
GGACGGACCTCCATGCCTTTGAGAACCTAGAAATCATAACGCGGCAGGACCAAGCAACATGGT
CAGTTTTCTCTTGCAGTCGTGACCTGAACATAACATCCTTGGGATTACGCTCCCTCAAGGA
GATAAGTGATGGAGATGTGATAATTTAGGAAACAAAATTTGTGCTATGCAAATACAATAA
ACTGGAAAAAACTGTTTGGGACCTCCGGTACAGAAAACAAAATTTATAAGCAACAGAGGTGAA
AACAGCTGCAAGGCCACAGGCCAGGTCTGCCATGCCTTGTGCTCCCCGAGGGCTGCTGGGG
CCCGGAGCCAGGGACTGCGTCTTTGCCGGAATGTCAGCCGAGGCAGGGAATGCGTGGACA
AGTGCAAGCTTCTGGAGGGTGAGCCAAGGGAGTTTGTGGAGAACTCTGAGTGCATACAGTGC
CACCCAGAGTGCCTGCCTCAGGCCATGAACATCACCTGCACAGGACGGGGACCAGACAACCTG
TATCCAGTGTGCCACTACATTGACGGCCCCACTGCGTCAAGACCTGCCCGGCAGGAGTCA
TGGGAGAAAACAACACCCTGGTCTGGAAGTACGCAGACGCCGGCCATGTGTGCCACCTGTGC
CATCAAACCTGCACCTACGGATGCACTGGGCCAGGTCTTGAAGGCTGTCCAACGAATGGGCC
TAAGCACCATCACCATCACCATTGA

Amino acid sequence sEGFRd3_His₆ (signal peptide in bold)

MRPSGTAGAALLALLAALCPASRALEEKVKVNGIGIGEFKDSLSINATNIKHFKNCTSIISGD
LHILPVAFRGDSFTHTPPLDPQELDILKTVKEITGFLLIQAWPENRTDLHAFENLEIIRGRT
KQHGQFSLAVVSLNITSLGLRSLKEISDGDVIIISGNKNLCYANTINWKKLFGTSGQKTKIIS
NRGENSCKATGQVCHALCSPEGCWGPEPRDCVSCRNVSRGRECVDKHHHHHH

Nucleotide sequence *sEGFRd3_His₆*

ATGCGACCCTCCGGGACGGCCGGGGCAGCGCTCCTGGCGCTGCTGGCTGCGCTCTGCCCGGC
GAGTCCGGGCTCTGGAGGAAAAGAAAGTTTGAACCGAATAGGTATTGGTGAATTTAAAGACT
CACTCTCATAAATGCTACGAATATTAACACTTCAAAAACCTGCACCTCCATCAGTGGCGAT
CTCCACATCCTGCCGGTGGCATTAGGGGTGACTCCTTCACACATACTCCTCCTCTGGATCC
ACAGGAACTGGATATTCTGAAAACCGTAAAGGAAATCACAGGGTTTTTGTGCTGATTCAGGCTT
GGCCTGAAAACAGGACGGACCTCCATGCCTTTGAGAACCCTAGAAATCATAACGCGGCAGGACC
AAGCAACATGGTCAGTTTTCTCTTGCAGTCGTCAGCCTGAACATAACATCCTTGGGATTACG
CTCCCTCAAGGAGATAAGTGATGGAGATGTGATAATTTAGGAAACAAAAATTTGTGCTATG
CAAATAACAATAAACTGGAAAAAACTGTTTGGGACCTCCGGTCAGAAAACCAAATTTATAAGC
AACAGAGGTGAAAACAGCTGCAAGGCCACAGGCCAGGTCTGCCATGCCTTGTGCTCCCCGA
GGGCTGCTGGGGCCCGGAGCCCAGGGACTGCGTCTCTTGCCGGAATGTCAGCCGAGGCAGGG
AATGCGTGGACAAGTGAAGCTTCTGGAGGGTGAAGCAAGGGAGTTTGTGGAGAACTCTGAG
TGCATACAGTGCCACCCAGAGTGCCTGCCTCAGGCCATGAACATCACCTGCACAGGACGGGG
ACCAGACAACCTGTATCCAGTGTGCCACTACATTGACGGCCCCACTGCGTCAAGACCTGCC
CGGCAGGAGTCATGGGAGAAAACAACACCCTGGTCTGGAAGTACGCAGACGCCGGCCATGTG
TGCCACCTGTGCCATCCAACTGCACCTACGGATGCACTGGGCCAGGTCTTGAAGGCTGTCC
AACGAATGGGCCTAAGCACCATCACCATCACCATTGA

Amino acid sequence sEGFRvIII_His₆ (signal peptide in bold)

MRPSGTAGAALLALLAALCPASRALEEKKNYVVTDHGSCVRACGADSYEMEEDGVKCKKC
EGPCRKVCNGIGIGEFKDSLSINATNIKHFKNCTSIISGDLHILPVAFRGDSFTHTPPLDPQE
LDILKTVKEITGFLLIQAWPENRTDLHAFENLEIIRGRTKQHGQFSLAVVSLNITSLGLRSL
KEISDGDVIIISGNKNLCYANTINWKKLFGTSGQKTKIISNRGENSCKATGQVCHALCSPEGC
WGPEPRDCVSCRNVSRGRECVDKCKLLEGEPEFVENSEC IQCHPECLPQAMNITCTGRGPD
NCIQCAHYIDGPHCVKTCPAGVMGENNTLVWKYADAGHVCHLCHPNCTYGCTGPGLEGCPN
GPKHHHHHH.

Nucleotide sequence *sEGFRvIII_His₆*

ATGCGACCCTCCGGGACGGCCGGGGCAGCGCTCCTGGCGCTGCTGGCTGCGCTCTGCCCGGC
GAGTCCGGGCTCTGGAGGAAAAGAAAGTAAATTATGTGGTGACAGATCACGGCTCGTGCGTCC
GAGCCTGTGGGGCCGACAGCTATGAGATGGAGGAAGACGGCGTCCGCAAGTGTAAAGAAGTGC
GAAGGGCCTTGCCGCAAAGTGTGTAACCGAATAGGTATTGGTGAATTTAAAGACTCACTCTC
CATAAATGCTACGAATATTAACACTTCAAAAACCTGCACCTCCATCAGTGGCGATCTCCACA
TCCTGCCGGTGGCATTAGGGGTGACTCCTTCACACATACTCCTCCTCTGGATCCACAGGAA
CTGGATATTCTGAAAACCGTAAAGGAAATCACAGGGTTTTTGTGCTGATTCAGGCTTGGCCTGA
AAACAGGACGGACCTCCATGCCTTTGAGAACCCTAGAAATCATAACGCGGCAGGACCAAGCAAC
ATGGTCAGTTTTCTCTTGCAGTCGTCAGCCTGAACATAACATCCTTGGGATTACGCTCCCTC
AAGGAGATAAGTGATGGAGATGTGATAATTTAGGAAACAAAAATTTGTGCTATGCAAATAC
AATAAACTGGAAAAAACTGTTTGGGACCTCCGGTCAGAAAACCAAATTTATAAGCAACAGAG
GTGAAAACAGCTGCAAGGCCACAGGCCAGGTCTGCCATGCCTTGTGCTCCCCGAGGGCTGC
TGGGGCCCGGAGCCCAGGGACTGCGTCTCTTGCCGGAATGTCAGCCGAGGCAGGGAATGCGT

GGACAAGTGCAAGCTTCTGGAGGGTGGAGCCAAGGGAGTTTGTGGAGAAGCTCTGAGTGCATAC
 AGTGCCACCCAGAGTGCCTGCCTCAGGCCATGAACATCACCTGCACAGGACGGGGACCAGAC
 AACTGTATCCAGTGTGCCCACTACATTGACGGCCCCACTGCGTCAAGACCTGCCCGGCAGG
 AGTCATGGGAGAAAACAACACCCTGGTCTGGAAGTACGCAGACGCCGGCCATGTGTGCCACC
 TGTGCCATCCAACTGCACCTACGGATGCACTGGGCCAGGTCTTGAAGGCTGTCCAACGAAT
 GGGCCTAAGCACCATCACCATCACCATTGA

Amino acid sequence sIGF-1Rd1-3_His₆ (signal peptide in bold)

MKSGSGGGSPTSLWGLLFLSAALSLWPTSGEICGPGIDIRNDYQQLKRLNCTVIEGYLHIL
 LISKAEYRSYRFPKLTVITEYLLLFRVAGLESGLDFPNLTVIRGWKLFYNYALVIFEMTN
 LKDIGLYNLRNITRGAIRIEKNADLCYLSTVDWSLILDVSNNYIVGNKPPKECGDLCPGTM
 EEKPMCEKTTINNEYNYRCWTTNRCQKMC PSTCGKRACTENNECCHPECLGSCSAPDNDTAC
 VACRHYYYAGVCPACPPNTYRFEGRVDRDFCANILSAESSDSEGFVIHDGECMQECP
 FIRNGSQSMYCI PCEGPCPKVCEEKKTIDSVTSAQMLQGCTIFKGNLLINIRRGNNIAS
 ELENFMGLIEVVTGYVKIRHSHALVSL SFLKLNRLILGEEQLEGNYSFYVLDNQNQLQ
 LDWD
 DHRNLTIKAGKMYFAFNPKLCVSEIYRMEEVGTGKGRQSKGDINTRNNGERASCESDVH
 HHH
 HH .

Nucleotide sequence *sIGF-1Rd1-3_His₆*

ATGAAGTCTGGCTCCGGAGGAGGGTCCCCGACCTCGCTGTGGGGGCTCCTGTTTCTCTCCGC
 CGCGCTCTCGCTCTGGCCGACGAGTGGAGAAATCTGCGGGCCAGGCATCGACATCCGCAACG
 ACTATCAGCAGCTGAAGCGCCTGGAGAAGTGCACGGTGATCGAGGGCTACCTCCACATCCTG
 CTCATCTCCAAGCCGAGGACTACCGCAGCTACCGCTTCCCCAAGCTCACGGTCATTACCGA
 GTACTTGCTGCTGTTCCGAGTGGCTGGCCTCGAGAGCCTCGGAGACCTCTTCCCCAACCTCA
 CGGTCATCCGCGGCTGGAAACTCTTCTACAAC TACGCCCTGGTCATCTTCGAGATGACCAAT
 CTCAAGGATATTGGGCTTTACAACCTGAGGAACATTACTCGGGGGCCATCAGGATTGAGAA
 AAATGCTGACCTCTGTTACCTCTCCACTGTGGACTGGTCCCTGATCCTGGATGCGGTGTCCA
 ATA ACTACATTGTGGGAATAAAGCCCCAAAGGAATGTGGGGACCTGTGTCCAGGGACCATG
 GAGGAGAAGCCGATGTGTGAGAAGACCACCATCAACAATGAGTACAAC TACCGCTGCTGGAC
 CACAAACCGCTGCCAGAAAATGTGCCCAAGCACGTGTGGGAAGCGGGCGTGCACCGAGAACA
 ATGAGTGCTGCCACCCCGAGTGCCTGGGCAGCTGCAGCGCGCCTGACAACGACACGGCCTGT
 GTAGCTTGCCGCCACTACTACTATGCCGGTGTCTGTGTGCCTGCCTGCCCGCCAACACCTA
 CAGGTTTGAGGGCTGGCGCTGTGTGGACCGTGACTTCTGCGCCAACATCCTCAGCGCCGAGA
 GCAGCGACTCCGAGGGGTTTGTGATCCACGACGGCGAGTGCATGCAGGAGTGCCCCCTCGGGC
 TTCATCCGCAACGGCAGCCAGAGCATGTACTGCATCCCTTGTGAAGTCCCTTGCCCGAAGGT
 CTGTGAGGAAGAAAAGAAAACAAAGACCATTGATTCTGTTACTTCTGCTCAGATGCTCCAAG
 GATGCACCATCTTCAAGGGCAATTTGCTCATTAACATCCGACGGGGGAATAACATTGCTTCA
 GAGCTGGAGAAGTTCATGGGGCTCATCGAGGTGGTGACGGGCTACGTGAAGATCCGCCATTC
 TCATGCCTTGGTCTCCTTGTCTTCTTAAAAACCTTCGCCTCATCCTAGGAGAGGAGCAGC
 TAGAAGGGAATTACTCCTTCTACGTCTCGACAACCAGAACTTGCAGCAACTGTGGGACTGG
 GACCACCGCAACCTGACCATCAAAGCAGGGAAAATGTACTTTGCTTTCAATCCCAAATTATG
 TGTTCGAAATTTACCGCATGGAGGAAGTGACGGGGACTAAAGGGCGCCAAAGCAAAGGGG
 ACATAAACACCAGGAACAACGGGGAGAGAGCCTCCTGTGAAAGTGACGTCCACCATCACCAT
 CACCATTAA

Amino acid sequence sIGF-1Rd2_His₆ (signal peptide in bold)

MKSGSGGGSPTSLWGLLFLSAALSLWPTSGDLCPGTMEEKPMCEKTTINNEYNYRCWTTNRC
QKMCPSTCGKRACTENNECCHPECLGSCSAPDNDTACVACRHYYYAGVCPACPPNTYRFEG
WRCVDRDFCANILSAESSDSEGFVIHDGECMQECPSGFIRNGSQSMYCIPEGPCPHHHHHH

Nucleotide sequence *sIGF-1Rd2_His₆*

ACCATGAAGTCTGGCTCCGGAGGAGGGTCCCCGACCTCGCTGTGGGGGCTCCTGTTTCTCTC
CGCCGCGCTCTCGCTCTGGCCGACGAGTGGAGACCTGTGTCCAGGGACCATGGAGGAGAAGC
CGATGTGTGAGAAGACCACCATCAACAATGAGTACAACCTACCGCTGCTGGACCACAAACCGC
TGCCAGAAAATGTGCCCAAGCACGTGTGGGAAGCGGGCGTGCACCGAGAACAAATGAGTGCTG
CCACCCCGAGTGCCTGGGCAGCTGCAGCGCGCCTGACAACGACACGGCCTGTGTAGCTTGCC
GCCACTACTACTATGCCGGTGTCTGTGTGCCTGCCTGCCCGCCAACACCTACAGGTTTGAG
GGCTGGCGCTGTGTGGACCGTGACTTCTGCGCCAACATCCTCAGCGCCGAGAGCAGCGACTC
CGAGGGGTTTGTGATCCACGACGGCGAGTGCATGCAGGAGTGCCCCCTCGGGCTTCATCCGCA
ACGGCAGCCAGAGCATGTACTGCATCCCTTGTGAAGGTCCTTGCCCGCACCATCACCATCAC
CATTAA

11.3. Supplementary data

Table 6: ITC-derived characteristics of antibody binding to IGF-1R at 25°C

| Construct | ΔH° (kcal/mol) | $-T\Delta S^\circ$ (kcal/mol) | ΔG° (kcal/mol) | K_D (nM) | Stoichiometry of binding (n) |
|------------|--------------------------------|----------------------------------|--------------------------------|---------------|---------------------------------|
| IGF-1Rd2 | -13.5±0.1 | 2.1 | -11.4 | 4.1 ± 0.7 | 0.81 |
| IGF-1Rd1-3 | -5.8±0.1 | -5.4 | -11.2 | 6.1 ± 1.3 | 1.18 |
| BIIB5* | -20.2±2.5 | 7.8 | -12.3 | 1 ± 0.2 | 0.98 |
| BIIB4* | -26.6±0.6 | 15.1 | -11.5 | 4 ± 0.5 | 0.91 |

(*data from Doern *et al.*, 2009)

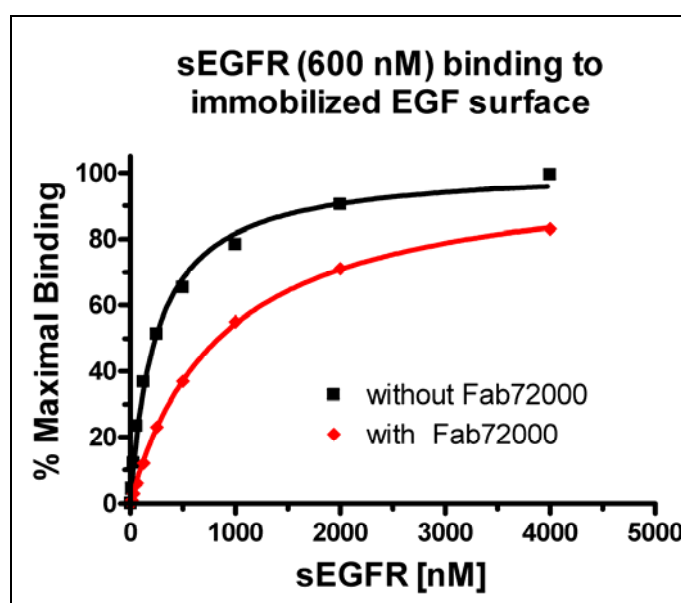


Fig. 44: sEGFR in complex with matuzumab binding to EGF

Surface plasmon resonance (SPR)/Biacore analysis of the binding of sEGFR and sEGFR in complex with a 10fold excess of Fab72000 to immobilized EGF. A series of samples of sEGFR or sEGFR:Fab72000, at the indicated concentrations, was passed over a biosensor surface to which EGF had been amine coupled. Data points show the equilibrium SPR response value for a representative set of samples of sEGFR (black squares) and sEGFR:Fab72000 (red diamonds), expressed as a percentage of maximal SPR binding response. The curves represent a fit of these data to a simple one-site Langmuir binding equation. K_D values, based on at least three independent binding experiments, are 248 ± 11.2 nM for sEGFR and 868 ± 26.1 nM for sEGFR:Fab72000.

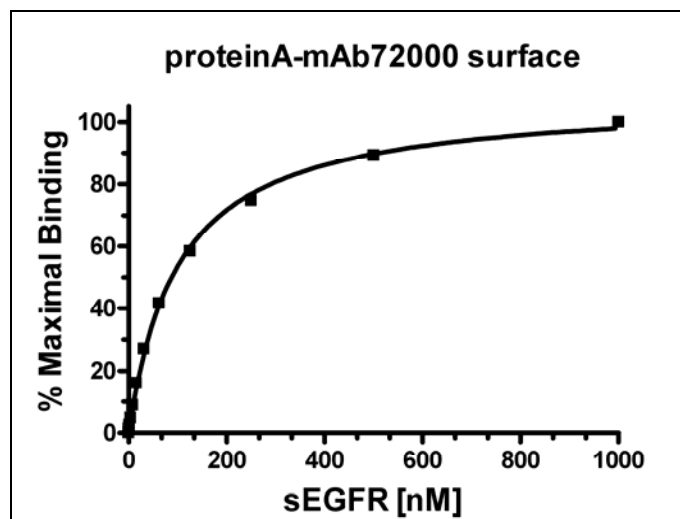


Fig. 45: sEGFR binding to mAb72000 immobilized by protein A

The binding of sEGFR (0.5 nM – 1 μ M) to whole length antibody EMD72000 on a protein A surface was investigated by Surface plasmon resonance (SPR)/Biacore. The preliminary K_D value (101.1 ± 3.9 nM) is in the range of the affinity of the receptor to a surface with immobilized Fab72000 (113 ± 25 nM). For exact measurement of the affinity a surface regeneration is required.

Previous Biacore binding studies of sEGFR flown over a Fab72000 surface showed an affinity of 113 ± 25 nM (Fig. 9). This is lower than the value observed for cetuximab, which binds with an affinity of 2.3 ± 0.5 nM. It is possible that this K_D value is anomalously low due to some steric effect of the direct amine coupling of the Fab on the chip surface. To test this, a different immobilization strategy was employed. Protein A was amine coupled to a Biosensor chip and mAb72000 bound to this protein A surface through interaction with the Fc region of the mAb, leaving the Fv regions fully accessible to sEGFR binding.

8.3 μ g protein A in NaAc pH 4.5 were immobilized on an activated CM5 chip surface at a flow rate of 5 μ l/min. After blocking the activated surface an immobilization level of 2275 RU was reached. Subsequently 0.1 μ g mAb72000 was flown over the protein A surface at 5 μ l/min. This yielded a immobilization level of 3510 RU (total 5780 RU). This preliminary sEGFR binding analysis gives a K_D value of 101.1 ± 3.9 nM, which is in the range of the affinity obtained for the receptor binding to directly immobilized Fab72000.

Matuzumab Binding to EGFR Prevents the Conformational Rearrangement Required for Dimerization

Judith Schmiedel,^{1,2} Andree Blaukat,³ Shiqing Li,¹ Thorsten Knöchel,^{2,*} and Kathryn M. Ferguson^{1,*}

¹Department of Physiology, University of Pennsylvania School of Medicine, Philadelphia, PA 19104, USA

²NCE Lead Discovery Technologies

³TA Oncology

Merck Serono Research, Merck KGaA, 64293 Darmstadt, Germany

*Correspondence: ferguso2@mail.med.upenn.edu (K.M.F.), thorsten.knoechel@merck.de (T.K.)

DOI 10.1016/j.ccr.2008.02.019

SUMMARY

An increasing number of therapeutic antibodies targeting tumors that express the epidermal growth factor receptor (EGFR) are in clinical use or late stages of clinical development. Here we investigate the molecular basis for inhibition of EGFR activation by the therapeutic antibody matuzumab (EMD72000). We describe the X-ray crystal structure of the Fab fragment of matuzumab (Fab72000) in complex with isolated domain III from the extracellular region of EGFR. Fab72000 interacts with an epitope on EGFR that is distinct from the ligand-binding region on domain III and from the cetuximab/Erbitux epitope. Matuzumab blocks ligand-induced receptor activation indirectly by sterically preventing the domain rearrangement and local conformational changes that must occur for high-affinity ligand binding and receptor dimerization.

INTRODUCTION

The epidermal growth factor receptor (EGFR) is aberrantly activated in a variety of epithelial tumors and has been the focus of much interest as a target in anticancer therapy. EGFR is one of a family of four receptor tyrosine kinases (collectively known as the ErbB or HER receptors) that are involved in critical cellular processes such as proliferation, differentiation, and apoptosis (Hubbard and Miller, 2007; Schlessinger, 2000). Misregulation of EGFR, through overexpression or mutation, leads to constitutive activity or impaired receptor downregulation and can cause malignant transformation of the cell (Mendelsohn and Baselga, 2006).

Based on structural studies over the past 5 years of the ErbB receptors, a model has been proposed for ligand-dependent dimerization and activation of EGFR (Figure 1) (Burgess et al., 2003; Ferguson et al., 2003; Zhang et al., 2006). Dimerization of the EGFR extracellular region is entirely receptor mediated,

with the majority of interactions contributed by domain II of EGFR (Garrett et al., 2002; Ogiso et al., 2002). In the unliganded state, the receptor adopts a very different conformation that occludes much of the domain II dimerization interface in an intramolecular interaction or tether with domain IV (Bouyain et al., 2005; Cho and Leahy, 2002; Ferguson et al., 2003). Upon ligand binding, the extracellular region of EGFR must undergo a dramatic domain rearrangement, which exposes the domain II dimerization interface. Additional localized ligand-induced changes stabilize the precise conformation of domain II that is required for dimerization (Dawson et al., 2005). Receptor dimerization brings the intracellular regions into close proximity, promoting the allosteric activation of the kinase domains (Zhang et al., 2006).

This mechanism suggests a number of ways to inhibit EGFR activation through interaction with the extracellular region of the receptor (Ferguson, 2004). X-ray crystallographic and biochemical analysis of receptor-antibody complexes have indicated several modes of binding that lead to effective inhibition of

SIGNIFICANCE

Antibodies targeting the EGF receptor family are proven anticancer drugs. The anti-ErbB2 antibody trastuzumab/Herceptin is established as a treatment of ErbB2-positive breast cancer, and therapeutic protocols are in clinical use for two EGFR-targeting antibodies, cetuximab/Erbitux and panitumumab/Vectibix. Matuzumab, a humanized form of the mouse anti-EGFR mAb425, is in phase II clinical trials. Our studies show that both the epitope for and the mechanism of inhibition by matuzumab are distinct from those for cetuximab. We show that matuzumab and cetuximab can both simultaneously bind to EGFR, implying that combination therapy with both antibodies could be advantageous. This has important implications for the clinical use of matuzumab and in moving forward with the development of therapeutic approaches targeting the EGF receptor.

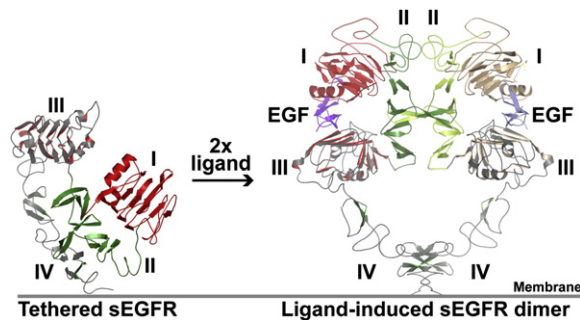


Figure 1. Ligand-Induced EGF Receptor Dimerization

The extracellular region of the EGF receptor (sEGFR) is shown in cartoon representation with domain I in red, domain II in green, and domains III and IV in gray, with the secondary structure elements highlighted in red and green, respectively. The inactive receptor (left-hand view) exists in a tethered, autoinhibited conformation with an intramolecular interaction between domains II and IV. Upon ligand binding, the receptor adopts a very different domain arrangement (right-hand view). Ligand (here EGF, shown in purple cartoon) binds between domains I and III of a single EGFR molecule, stabilizing the precise, extended configuration of EGFR that can dimerize. All contacts between the two molecules in the dimer are receptor mediated, with domain II providing the primary dimerization contacts. EGF receptor dimerization is ligand induced, but entirely receptor mediated. The colors on the right-hand molecule in the sEGFR dimer have been muted for contrast. Coordinates from PDB IDs 1IVO and 1NQL were used to generate this figure. Domain IV in the sEGFR dimer was modeled as previously described (Ferguson et al., 2003).

ErbB receptor signaling. The chimeric antibody cetuximab/Erbbitux (Imclone/BMS and Merck KGaA) binds to domain III of EGFR, directly blocking ligand binding (Li et al., 2005). Another anti-EGFR antibody, mAb806, binds to domain II close to the receptor dimerization site (Johns et al., 2004). The anti-ErbB2 antibody pertuzumab/Omnitarg (Genentech) binds to the domain II dimerization arm and prevents ligand-induced ErbB2 heterodimerization (Franklin et al., 2004), while trastuzumab/Herceptin (Genentech) binds to the membrane-proximal domain IV of ErbB2 (Cho et al., 2003) and likely modulates a cleavage event that leads to ectodomain shedding and kinase activation (Molina et al., 2001).

We were interested to establish the mode of inhibition of EGFR by another therapeutic antibody, matuzumab (EMD72000), which targets EGFR-expressing tumors. Matuzumab is the humanized form of the murine mAb 425 (EMD55900) that was produced by immunization of BALB/c mice with human A431 epidermoid carcinoma cells (Kettleborough et al., 1991; Murthy et al., 1987). Monoclonal antibody 425 (EMD55900) blocks ligand-dependent activation of EGFR in tumor cell lines (Rodeck et al., 1990) and has been demonstrated to inhibit growth of EGFR-dependent tumors in preclinical studies (Rodeck et al., 1987). Matuzumab has performed well in phase I clinical trials against a number of cancers, both alone and in combination with chemotherapy (Bier et al., 2001; Graeven et al., 2006; Kollmannsberger et al., 2006; Vanhoefer et al., 2004), and is being actively pursued in multiple ongoing phase II trials (Seiden et al., 2007; Socinski, 2007).

Here we describe the crystal structure of the Fab fragment of matuzumab (Fab72000) bound to a truncated form of the extracellular region of EGFR that comprises all of domain III plus the first 24 amino acids from domain IV. Matuzumab binds to an epitope on domain III of EGFR that is distinct from both the

ligand-binding site and the cetuximab epitope on that domain. Matuzumab does not directly block the access of ligand to the domain III-binding site, and thus does not share the primary mechanism for inhibition of ligand-induced EGFR activation employed by cetuximab. Rather, the binding of matuzumab to domain III sterically blocks the domain rearrangement that is required for high-affinity ligand binding and receptor dimerization. Further, binding to this epitope places the antigen-binding domains of matuzumab such as to impede the formation of the critical contacts between domains II and III that are required to stabilize the dimerization competent conformation of domain II. This noncompetitive mechanism of inhibition of EGFR activation has implications for both the application of current drugs and the development of anti-EGFR therapeutics.

RESULTS AND DISCUSSION

Binding Characteristics of Matuzumab to Cell Surface and Soluble EGFR

To determine the mode of binding of matuzumab to EGFR, and to elucidate the mechanism of inhibition of EGFR by this therapeutic antibody, we sought to determine the X-ray crystal structure of the complex between the Fab fragment of the antibody and the extracellular region of EGFR. We first characterized the binding of matuzumab to the soluble extracellular domain of EGFR (sEGFR) and compared the results to the behavior of this antibody in cell surface binding assays.

Soluble EGFR was produced by secretion from baculovirus-infected Sf9 cells and purified exactly as described (Ferguson et al., 2000). The Fab fragment of matuzumab (Fab72000), produced by papain cleavage of the antibody, was immobilized on a CM5 biosensor chip (see Experimental Procedures). Using surface plasmon resonance (SPR/Biacore), we established that sEGFR binds to this immobilized Fab72000 with a K_D value of 113 ± 25 nM (Figure 2A). This value is weaker than that observed for the binding of 125 I-labeled intact matuzumab to cell surface EGFR (about 1–10 nM, depending on the cell line employed; data not shown), although these binding assays are not directly comparable. It has previously been shown that the epitope for cetuximab lies exclusively on domain III of sEGFR (Li et al., 2005). To address whether this is also true for matuzumab, we produced and purified isolated domain III of sEGFR (sEGFRd3; amino acids 311–514 of mature EGFR) exactly as described (Li et al., 2005). As shown in Figure 2A, sEGFRd3 binds to immobilized Fab72000 with a K_D value of 43.0 ± 12.9 nM. The antigen-binding domain of matuzumab, like that of cetuximab, binds more tightly to sEGFRd3, possibly due to the absence of steric hindrance from the other domains of sEGFR.

We next used both SPR and cell surface binding analysis to investigate the ability of matuzumab to compete with ligand binding to EGFR. As shown in Figure 2B, matuzumab, like cetuximab, competes efficiently for the binding of 3 nM 125 I-labeled EGF to the surface of A431 epidermoid carcinoma cells. It has previously been shown that, in the context of an SPR/Biacore assay, the Fab fragment of cetuximab (FabC225) is able to block all binding of soluble sEGFR to immobilize EGF (Li et al., 2005). We asked if this is also true for the Fab fragment of matuzumab. Samples of 600 nM sEGFR containing increasing excesses of Fab72000 were passed over a biosensor surface to which EGF

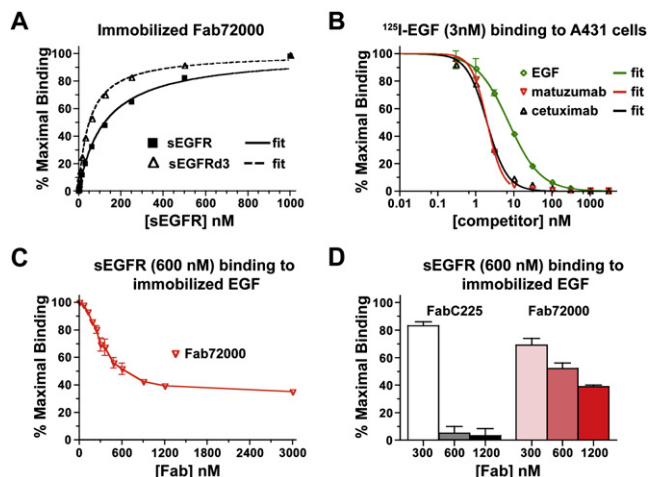


Figure 2. Characterization of the EGFR-Binding and Ligand Competition Properties of Matuzumab

(A) Surface Plasmon Resonance (SPR) analysis of the binding of sEGFR and sEGFRd3 to immobilized Fab72000 (the antigen-binding domain of matuzumab). A series of samples of sEGFR or sEGFRd3, at the indicated concentrations, was passed over a biosensor surface to which Fab72000 had been amine coupled. Data points show the equilibrium SPR response value for a representative set of samples of sEGFR (black squares) and of sEGFRd3 (open triangles), expressed as a percentage of the maximal SPR-binding response. The curves represent the fit of these data to a simple one-site Langmuir binding equation. K_D values, based on at least three independent binding experiments, are 113 ± 25 nM for sEGFR and 43 ± 13 nM for sEGFRd3.

(B) Competition of EGF (green diamonds), matuzumab (red triangles), or cetuximab (black triangles) for the binding of ^{125}I -labeled EGF to A431 cells. Cells were incubated with media containing 3 nM ^{125}I -labeled EGF plus the indicated concentration of cold matuzumab, cetuximab, or EGF for 6 hr at 4°C. Following washing to remove unbound material, cells were lysed and liquid scintillation counting was used to determine the amount of bound ^{125}I -labeled EGF. The counts per minute (CPM) for each sample are shown, expressed as a percentage of the CPM value obtained for no added competitor. Error bars indicate the standard deviation on three independent experiments. The line indicates the fit to a sigmoidal dose-response model. IC_{50} values from this analysis are 2.0 nM for matuzumab and cetuximab and 7.3 nM for EGF.

(C) A competition experiment showing the effect of addition of Fab72000 upon the binding of 600 nM sEGFR to immobilized EGF. Mixtures of 600 nM sEGFR plus the indicated concentrations of Fab72000 were passed over a biosensor surface to which EGF had been amine coupled. The equilibrium SPR responses for each mixture is shown, normalized to the response obtained with no added Fab. Error bars indicate the standard deviation on at least three independent measurements. The line simply connects the data points.

(D) The ability of FabC225 (the antigen-binding domain of cetuximab; gray shades) and Fab72000 (red shades) to compete for the binding of 600 nM sEGFR to immobilized EGF, determined exactly as described in (C). Samples of each Fab alone show no binding to the immobilized EGF (data not shown). Data for FabC225 taken from Li et al. (2005). Error bars indicate the standard deviation on at least three independent measurements.

had been immobilized. As shown in Figure 2C, there is an initial decrease in the equilibrium SPR response as increasing Fab72000 is added. At a 1:1 molar ratio of Fab72000:sEGFR, the SPR response is about 45% of that obtained with no added Fab. Addition of increasing excesses of Fab72000 does not further reduce this binding level. Even at a higher concentration of sEGFR and with up to a 50-fold excess of Fab72000 (data not shown), the equilibrium SPR response does not fall below 40% of the value in the absence of added Fab. One possible explana-

tion for the observed SPR responses in Figure 2C is that both unbound sEGFR and the Fab72000/sEGFR complex can interact with the immobilized EGF, but that the complex binds with substantially weaker affinity. Equilibrium binding analysis to immobilized EGF for samples of sEGFR containing a 10-fold molar excess of Fab72000 indicates an apparent K_D value that is approximately 5-fold weaker than that for sEGFR alone (data not shown). Certainly these data suggest that there must be something quite different about the mode of binding to sEGFR of the Fab fragment of matuzumab compared to that of cetuximab. Both antibodies are able to compete for binding of low concentrations of EGF to cell surface EGFR, yet the Fab fragments from the two antibodies have very different effects on the ability of soluble EGFR to bind to immobilized EGF in the Biacore assay (Figure 2D and Li et al., 2005).

To gain further insight into the precise mode of binding of matuzumab to EGFR, and to understand how this leads to inhibition of cell surface ligand binding and of ligand-stimulated EGFR activation, we crystallized and solved the structures of Fab72000 alone and in complex with the sEGFRd3 (see Experimental Procedures and Table 1).

The Structure of the Fab72000/sEGFRd3 Complex

Crystals of the isolated Fab72000 that diffract to 2.15 Å resolution were obtained, and the structure was solved by molecular replacement (MR) methods using as search model the coordinates of an Fab fragment selected by degree of sequence similarity (Protein Data Bank [PDB] ID 1L7I). A complex of sEGFRd3 and Fab72000 was purified by size exclusion chromatography (SEC), and crystals that diffract to 3.2 Å resolution were obtained using streak seeding techniques. To solve this structure, MR search models based on the coordinates for domain III of sEGFR (PDB ID 1YY9) and the coordinates of the refined Fab72000 were used to locate the two Fab72000/sEGFRd3 complexes in the asymmetric unit. Data collection and refinement statistics are given in Table 1.

Fab72000 binds primarily to the loop that precedes the most C-terminal strand of the domain III β -helix (amino acids 454–464; highlighted in red in Figure 3A). This loop penetrates into a cleft between the V_L and V_H domains of the Fab. The tip of this loop forms a type I beta turn, with T459 and S460 in this turn protruding the farthest into the cleft. This mode of binding is unusual for the recognition of a large protein antigen, where it is more common for the epitope to comprise a large flat surface on the antigen (Sundberg and Mariuzza, 2002), as was observed for the binding of cetuximab to EGFR (Li et al., 2005). All of the key interactions made by the Fab are from the complementarity-determining regions (CDRs), with the major specificity-determining contacts coming from CDRs H3 and L3. All of the CDRs contribute to binding to domain III, also an unusual feature compared to most antigen-antibody complexes (Sundberg and Mariuzza, 2002).

The tip of the buried loop from sEGFR makes interactions with both the heavy- and light-chain CDRs (Figure 3B); the side chain of T459 interacts with that of H93 from the Fab light chain, while the side chain of S460 contacts the CDR H2 side chain E50. Two lysines, one on either end of the sEGFRd3 epitope loop, form salt bridge interactions with aspartic acids on the Fab (K454 with D100 from CDR H3 and K463 with CDR L2 D49). Additional

Table 1. Data Collection and Refinement Statistics

| | Fab72000 | Fab72000/sEGFRd3 |
|--|--|---|
| Data Collection Statistics ^a | | |
| Space group | P2 ₁ 2 ₁ 2 ₁ | C2 |
| Unique cell dimensions | a = 56.8 Å, b = 61.4 Å, c = 102.7 Å | a = 141.1 Å, b = 205.0 Å, c = 81.6 Å, β = 117.5° |
| X-ray source | CHESS F1 | SLS X06SA |
| Resolution limit | 2.15 Å | 3.2 Å |
| Observed/unique | 107,297/ 20,191 | 120,206/33,886 |
| Completeness (%) | 99.9 (99.9) | 99.7 (98.7) |
| R _{sym} ^b | 0.10 (0.42) | 0.12 (0.35) |
| <I/σ> | 20.7 (3.6) | 11.4 (3.4) |
| Refinement Statistics | | |
| Resolution limits | 50–2.15 Å | 50–3.2 Å |
| No. of reflections/no. test set | 19,098/1029 | 32,028/1709 |
| R factor (R _{free}) ^c | 0.22 (0.26) | 0.24 (0.29) |
| Model | one Fab72000 molecule | two Fab72000/sEGFRd3 complexes |
| Protein | aa 4–211 of light chain; aa 1–224 of heavy chain | aa 310–500 of mature sEGFR with 13 saccharide units; aa 1–211 of Fab light chain; aa 1–135, 142–222 of Fab heavy chain ^d |
| Water/ions | 99 water molecules; 2 sulfates | — |
| Total number of atoms | 3209 | 8517 |
| RMSD bond length (Å) | 0.012 | 0.015 |
| RMSD bond angles (°) | 1.35 | 1.6 |

^a Numbers in parentheses refer to last resolution shell.

^b $R_{sym} = \sum |I_h - \langle I_h \rangle| / \sum I_h$, where $\langle I_h \rangle$ is the average intensity over symmetry equivalent measurements.

^c R factor = $\sum |F_o - F_c| / \sum F_o$, where summation is over data used in the refinement; R_{free} includes 5% of the data excluded from the refinement.

^d Number of missing amino acids in the heavy and light chains differs in the two complexes.

interactions with the buried epitope loop are contributed by side chains in CDRs H1, H2, and L1 that are within hydrogen-bonding distance of the main chain of sEGFRd3 (Figure 3B and Figure S1 available online). Two important direct interactions are made between the Fab and regions of domain III outside the loop between amino acids 454–464. A histidine from CDR L3 (H93) interacts with D434 on the adjacent loop of the sEGFRd3 β-helix, while on the other side of the binding site Y103 from the apex of CDR H3 extends to interact with N449. These two interactions anchor the Fab over the central binding loop and expand the epitope substantially beyond the single peptide loop.

A total of two salt bridges and 11 predicted hydrogen bonds are involved in the interaction between Fab72000 and sEGFRd3, in an interface that buries 758 Å² of solvent-accessible surface on domain III (a total of 1516 Å² of surface is occluded from solvent in the complex). The shape complementarity (sc) parameter for the interface of the Fab72000/sEGFRd3 complex is 0.62,

slightly lower than is typically observed for antigen-antibody interfaces (0.64 to 0.68) (Lawrence and Colman, 1993). The sc values reported for cetuximab bound to EGFR (Li et al., 2005) and for the pertuzumab and trastuzumab complexes with the extracellular region ErbB2 (Cho et al., 2003; Franklin et al., 2004) are all somewhat higher, in the range from 0.70 to 0.75, perhaps reflecting the more convex shape of the matuzumab epitope compared to those of these other antibody drugs.

Neither the conformation of sEGFRd3 nor that of Fab72000 is significantly altered upon formation of the complex. There are very minor differences in the side chain positions in both the domain III epitope and in the CDRs of the Fab. Most notably, Y103 in the V_H domain is disordered in the unbound Fab and becomes ordered on interacting with sEGFR. The elbow angle changes by only 4° between the bound and unbound Fab72000, which is within the range expected due to dynamic elbow flexibility (Stanfield et al., 2006).

Not only is the conformation of domain III unaltered by Fab72000 binding, but also the location of the bound Fab72000 would not be expected to disrupt the tethered configuration of sEGFR (Figure 1, left panel), the preferred solution conformation of the receptor (Dawson et al., 2007), and the likely conformation of the unliganded receptor at the cell surface. Fab72000 can readily be docked onto its epitope on either of the two known structures of tethered sEGFR (PDB IDs 1NQL and 1YY9) without hindrance from any of the other domains of sEGFR.

The Matuzumab Epitope Is Distinct from the Ligand-Binding Site on Domain III of sEGFR

To confirm that the crystallographically defined epitope for matuzumab precisely represents what is seen in solution, we generated site-specific alterations in sEGFR at key amino acids in the domain III matuzumab epitope (Figures 3B and 4A). Each alteration was introduced in the context of the full-length extracellular domain and these altered sEGFR proteins expressed and purified using appropriately baculovirus infected Sf9 cells. Each purified, altered sEGFR was analyzed for binding to immobilized Fab72000 and to immobilized EGF, exactly as described (Li et al., 2005). Alteration to alanine of either of the two lysines on the epitope loop (K454A or K463A) leads to an approximate 100-fold reduction in the affinity of sEGFR for Fab72000 (Figure 4B). Substitution of alanines at T459 and S460 (T459A/T460A) also dramatically reduces the binding affinity. The combination of either lysine to alanine substitution with T459A/T460A abolishes all detectable interaction between sEGFR and the immobilized Fab72000.

As shown in Figure 4A, the binding sites for matuzumab and for EGF on domain III do not overlap. As would be predicted based upon this observation, the sEGFR proteins with alterations in the Fab72000 epitope bind to immobilized EGF with near wild-type affinity (Figure 4B). This also confirms that the striking reduction in binding affinity of these altered sEGFR proteins for Fab72000 is not due to a global disruption of the structure of domain III of sEGFR. Finally, substitution of two amino acids that are known to be critical for EGF binding (D355T/F357A) have negligible effect on binding of sEGFR to Fab72000.

Not only is there no overlap of the epitope for matuzumab and the ligand binding region on domain III, but a bound Fab72000 would impose no steric hindrance to the binding of EGF or of

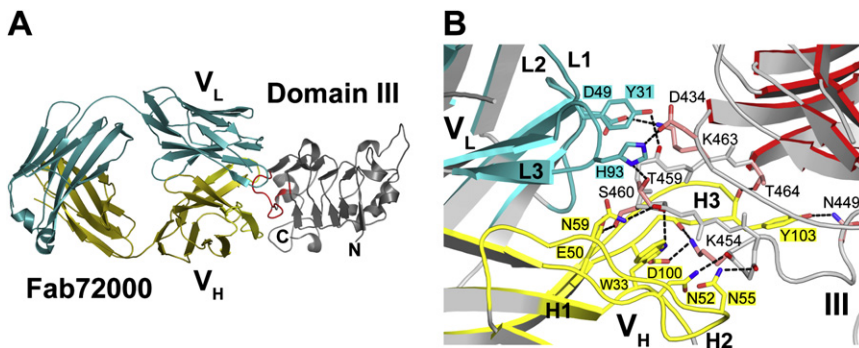


Figure 3. Structure of the Complex between the Matuzumab Fab Fragment and Domain III of sEGFR

(A) Cartoon of the Fab72000/sEGFRd3 complex. Domain III is colored in gray with the epitope highlighted in red. The orientation of domain III is the same as for the tethered sEGFR (left-hand view) in Figure 1. Fab72000 is colored cyan for the light chain and yellow for the heavy chain.

(B) A closeup view of the interactions between Fab72000 and domain III of sEGFR. Domain III is in gray with the secondary structure elements highlighted in red. The V_L and V_H domains of Fab72000 are in gray with cyan and yellow highlights, respectively. The CDRs of Fab72000 are

shown in cyan for L1, L2, and L3 of the V_L domain, and in yellow for H1, H2, and H3 of the V_H domain. The side chains of the amino acids participating in key interactions are shown, colored as for the CDRs for the Fab and in pink for domain III. The amino acids are labeled on a cyan background for those from V_L , on a yellow background for V_H , and in black for sEGFRd3. Distances consistent with hydrogen bonds are shown with dashed black lines.

TGF α to domain III. With domain III from the Fab72000/sEGFRd3 complex overlaid on domain III from the sEGFR/EGF complex (PDB ID 1IVO) the closest approach of the Fab and EGF is 9 Å. This is in stark contrast to the situation for cetuximab binding. There is a high degree of overlap between the cetuximab and EGF-binding sites on domain III (Figure 4C). The steric block of this ligand-binding site is the primary mechanism of cetuximab-mediated inhibition of ligand-induced dimerization and activation of EGFR (Li et al., 2005). Clearly the mechanism of inhibition of EGFR activation by matuzumab must be different.

Implications for the Mechanism of Inhibition of EGFR Activation by Matuzumab

If matuzumab does not directly block access of the ligand to the domain III ligand-binding site, how does it prevent high-affinity ligand binding, receptor dimerization, and activation? To understand this, we consider the effect of the binding of Fab72000 upon the formation of the ligand-induced dimeric form of the receptor. As shown in Figure 1, sEGFR undergoes a dramatic domain rearrangement in going from the tethered inactive state to the ligand-bound dimeric state (Burgess et al., 2003). Additional local structural changes in domain II are known to be key for high-affinity ligand binding, receptor dimerization, and activation (Dawson et al., 2005; Ogiso et al., 2002). As shown in Figure 5, and discussed in detail below, when domain III from the Fab72000/sEGFRd3 complex is overlaid on domain III from the receptor in its extended, dimerization-competent conformation (PDB ID 1MOX), there are direct clashes between the bound Fab72000 and both domains I and II of the extended receptor. With matuzumab bound to domain III of EGFR, the receptor cannot undergo the large-scale domain rearrangement that is required for dimerization. Further, the binding of Fab72000 blocks the critical local conformational changes in domain II.

With the receptor in the extended conformation, the N-terminal region of the domain I clashes with the light chain of Fab72000, preventing domain I from reaching the position that is required for high-affinity ligand binding (indicated with an arrow in Figure 5A). This is reminiscent in nature and extent to clashes between the antigen-binding fragment of cetuximab (FabC225) and domain I that were previously implicated as part of the mechanism of inhibition of EGFR dimerization by that antibody (Li et al., 2005). In that case, the different orientation of FabC225 on domain III positions the V_H domain such as to occlude the N-terminal portion of domain I from its required position in the receptor dimer.

Clashes between domain II of the extended receptor and the Fab were not seen in the cetuximab complex, and are significant. With Fab72000 bound to domain III of EGFR, it would not be possible for the C-terminal portion of domain II to adopt the conformation observed in the ligand-bound dimeric form of the receptor. As shown in Figure 5B, if Fab72000 is docked onto its epitope on domain III of an sEGFR molecule in the extended conformation, there are clashes along the C-terminal half of

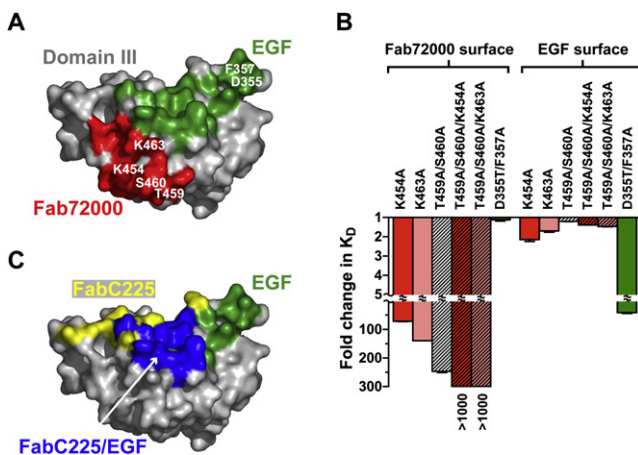


Figure 4. The Matuzumab Epitope Is Distinct from the Ligand-Binding Site on Domain III

(A) A surface representation of domain III is shown in gray viewed in approximately the same orientation as in Figure 3. Amino acids on domain III that are within 4 Å of Fab72000 (red) or of EGF (green) are indicated on this surface. The amino acids that were altered (see [B]) are labeled in white.

(B) Surface Plasmon Resonance (SPR) analysis of the binding of altered sEGFR proteins to immobilized Fab72000 or EGF. The equilibrium binding K_D values for each protein were determined exactly as described in the legend to Figure 2A. The fold change in this K_D value for each altered protein relative to that for the binding of wild-type sEGFR to each immobilized ligand is plotted. Error bars indicate the standard deviation on at least three independent sets of measurements.

(C) The same surface representation of domain III as in (A) is shown with the contacting amino acids for FabC225 in yellow, for EGF in green, and for the region of overlap between FabC225 and EGF in blue.

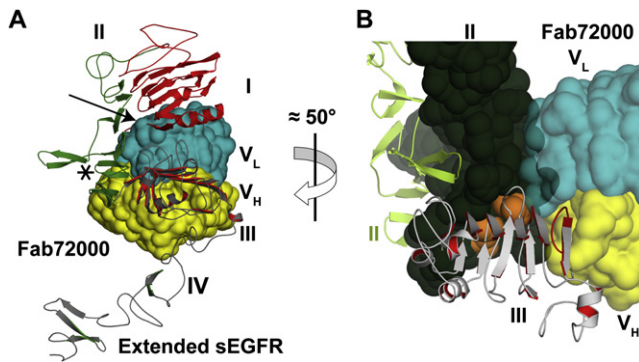


Figure 5. Implications for the Mechanism of Inhibition of EGFR by Matuzumab

(A) Cartoon of the extended sEGFR with Fab72000, in surface representation, docked onto its domain III epitope. The orientation of the receptor is the same as for the right-hand protomer in the sEGFR dimer shown in Figure 1 (with domains colored as for the left-hand protomer; EGF is omitted for clarity). The Fab72000 is colored as in Figure 3. The N-terminal region of domain I clashes with the V_L domain (indicated with an arrow). Additional clashes occur along the C-terminal half of domain II (see [B]). The C-terminal loop on domain II (D278, H280) that makes critical contacts across the dimer interface is marked with an asterisk.

(B) In this view, an approximate 50° rotation about the vertical axis relative to (A), domain II is shown in sphere representation in dark green. A cartoon of domain II of the other molecule in the dimer is shown (light green) for reference. Domain I has been omitted for clarity. The V_L domain of the Fab clashes with domain II in the critical C-terminal region that forms the binding pocket for the dimerization arm and makes important contacts with domain III (from N274 and E293 in domain II, colored orange). These interactions are known to be crucial for stabilizing the dimerization competent conformation of domain II. The Fab72000 epitope loop on domain III is colored in red.

domain II, predominantly with the V_L domain of the Fab. This C-terminal half of domain II forms the binding pocket for the dimerization arm from the other molecule in the receptor dimer. Additional interactions across the dimer interface from a C-terminal loop on domain II (D279 and H280, marked with an asterisk in Figure 5A) contribute substantially to the stability of the EGFR dimer. The conformation of domain II in this region is stabilized by interactions with domain III that have been demonstrated to be critical for EGFR dimerization and activation (Dawson et al., 2005; Ogiso et al., 2002). The binding of Fab72000 to domain III would disrupt all of these interactions. Thus, Fab72000 binding to domain III of EGFR blocks the global domain rearrangement of EGFR and the local conformational changes in domain II. We propose that blocking both of these key elements in formation of the productive EGFR dimer is critical for the effective inhibition of EGFR activation by matuzumab.

The steric restriction on EGFR conformation imposed by the binding of matuzumab offers a structural framework to explain the competition data presented in Figure 2. When matuzumab (or just its antigen-binding domain, Fab72000) binds to the extracellular region of EGFR, the receptor cannot adopt the conformation required for both domains I and III to engage in ligand binding. However, the ligand-binding site on domain III is completely exposed. EGF can bind to this site with low affinity (approximately $1 \mu\text{M}$; Kohda et al., 1993; Lemmon et al., 1997; Li et al., 2005). Under the conditions of the cell-based assay, weak binding of EGF to only domain III of EGFR is not detected.

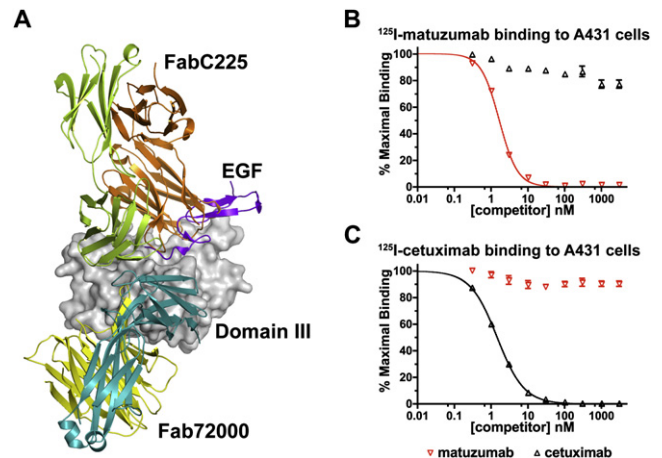


Figure 6. The Matuzumab and Cetuximab Epitopes Do Not Overlap

(A) A surface representation of the domain III as in Figure 4 is shown. Cartoons of Fab72000, FabC225 (PDB ID 1YY9), and EGF (PDB ID 1YV0) are shown docked onto their respective binding sites on domain III. Fab72000 is colored as in Figure 3A, FabC225 is shown with the heavy chain in orange and the light chain in light green, and EGF is in purple.

(B and C) Competition of matuzumab (red triangles) or cetuximab (black triangles) for binding of ^{125}I -labeled matuzumab (B) or ^{125}I -labeled cetuximab (C) to A431 cells, performed and analyzed as described in Figure 2B.

By preventing the receptor from adopting the conformation required for the bipartite binding of EGF between domains I and III, matuzumab blocks all detectable binding of EGF to cell surface EGFR in this assay. By contrast, the Biacore assay is performed at a much higher concentration of soluble ligand (in this case 600 nM sEGFR, which binds to immobilized EGF). Under these conditions, the monovalent binding of domain III alone to EGF can be detected. In the Biacore assay, the residual binding to immobilized EGF observed for sEGFR in the presence of excess Fab72000 is due, at least in part, to binding to EGF of the exposed domain III in an Fab72000/sEGFR complex.

Implications for the Therapeutic Application of Matuzumab

As discussed above, the mechanism of inhibition of matuzumab is different from that previously described for cetuximab. Both antibodies effectively block productive binding of EGF to cell surface EGFR (Figure 2B) but do so by interacting with distinct epitopes on domain III. Not only are the epitopes nonoverlapping, but the structures suggest that both antibodies could simultaneously bind to EGFR. As shown in Figure 6A, when FabC225 and Fab72000 are simultaneously docked onto their respective epitopes on domain III the two Fab fragments occupy different positions and do not clash. This observation is consistent with cellular competition assays. Excess cetuximab is unable to compete with the binding of ^{125}I -labeled matuzumab to the cell surface EGFR on A431 cells (Figure 6B). Similarly matuzumab cannot compete for ^{125}I -labeled cetuximab binding (Figure 6C). Further, it has been reported that there are an increased number of cell surface antibody-binding sites for a mixture of matuzumab and cetuximab compared to either antibody alone (Kreysch and Schmidt, 2004). This suggests that both matuzumab and cetuximab can bind to a single receptor molecule at the cell surface.

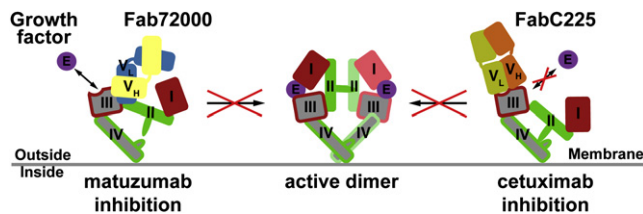


Figure 7. Matuzumab and Cetuximab Use Different Mechanisms to Block Ligand-Induced EGFR Dimerization and Activation

In the center of the scheme, the ligand-induced sEGFR dimer is represented, with domain I in red, domain II in green, domain III in gray with red border, domain IV in gray with green border, and the ligand (E) in violet. The colors for one protomer are lightened for contrast. On the left-hand side a scheme is shown to illustrate the mechanism of inhibition of ligand-induced dimerization by matuzumab. Fab72000 binds to domain III of sEGFR and sterically prevents the receptor from adopting the conformation required for dimerization. Importantly, Fab72000 blocks the local conformational changes in domain II that are critical for both high-affinity ligand binding and dimerization. The inhibition is noncompetitive; the ligand-binding site on domain III is not blocked. This contrasts with the mechanism of inhibition previously reported for cetuximab (Li et al., 2005). FabC225 (right side) is a competitive inhibitor that blocks the ligand-binding site on domain III. This is the primary mechanism of inhibition of ligand-mediated dimerization by cetuximab.

Treatment of cells with combinations of antibodies against distinct epitopes on the extracellular domain of EGFR, and on the related family member ErbB2, leads to enhanced receptor internalization and degradation (Friedman et al., 2005), a factor that contributes to the antitumor activity of many therapeutic antibodies. Matuzumab and cetuximab can both bind simultaneously to EGFR, and this has the potential to lead to synergistic antitumor effects. Combination of matuzumab and cetuximab could thus be beneficial in cancer therapy.

Conclusion

EGFR dimerization requires a conformational reorganization of the receptor extracellular region that is promoted by ligand binding to domains I and III (Figures 1 and 7). As shown schematically in Figure 7, cetuximab acts as a competitive inhibitor, preventing ligand-induced dimerization by directly blocking access of ligand to the domain III ligand-binding site. By contrast, matuzumab does not occlude the ligand-binding site on domain III. Rather, matuzumab exploits a noncompetitive mechanism to inhibit sEGFR dimerization and activation. Inhibition of ligand-induced EGFR activation by matuzumab is entirely dependent on sterically blocking the receptor from adopting the conformation that is required for high-affinity ligand binding and dimerization. These different mechanisms of inhibition suggest opportunities to exploit multiple EGFR-targeting drugs to act synergistically for optimal therapeutic gain.

EXPERIMENTAL PROCEDURES

Protein Expression and Purification

sEGFR and sEGFRd3 were expressed in baculovirus-infected Sf9 cells, purified as described (Ferguson et al., 2000; Li et al., 2005) and used without modification of their glycosylation state. Matuzumab (EMD72000) was provided by Merck KGaA. The Fab fragment of matuzumab (Fab72000) was generated by papain cleavage using the ImmunoPure Fab Preparation Kit (Pierce) and used without additional purification. Fab72000/sEGFR complex was generated exactly as described (Li et al., 2005). To generate the complex with sEGFRd3, Fab was mixed

with a 1.2-fold molar excess of sEGFRd3 and excess sEGFRd3 separated from Fab72000/sEGFRd3 complex by SEC using a Bio-Silect SEC250 column (Bio-Rad), equilibrated with 20 mM HEPES and 100 mM NaCl (pH 7.5).

Crystallization and Data Collection

Proteins were concentrated and buffer exchanged into 10 mM HEPES and 50 mM NaCl (pH 7.5) and crystallized using the hanging drop vapor diffusion method. Large single crystals of Fab72000 were obtained by mixing equal volumes (1 μ l) of the Fab (13 mg/ml) with a solution containing 1.8 M ammonium sulfate and 0.1 M MES (pH 6.5) and equilibrating over a reservoir of this buffer at 20°C. Crystals were flash frozen in reservoir solution that was supplemented with 9% sucrose, 2% glucose, 8% glycerol, and 8% ethylene glycol. X-ray diffraction data were collected at the Cornell High Energy Synchrotron Source (CHESS) beamline F1, using an ADSC Quantum-210 CCD detector. Fab72000/sEGFRd3 was crystallized by mixing equal parts (1 μ l) of the SEC purified complex (14 mg/ml) with 1 M NaCl, 16% PEG 3350, and 50 mM MES (pH 6.0) and equilibrating over a reservoir of the same buffer at 20°C. Streak seeding was used to produce large single crystals (0.5 \times 0.1 \times 0.15 mm) that were cryostabilized by serial transfer to solutions of reservoir containing increasing concentrations of ethylene glycol. Following transfer to the final cryostabilizer of reservoir plus 15% ethylene glycol, crystals were flash frozen in liquid nitrogen. Data were collected at the Swiss Light Source (SLS) beamline X06SA, using a Mar225 CCD detector. All data were processed in HKL2000 (Otwinowski and Minor, 1997). Data collection statistics are summarized in Table 1.

Structure Determination and Refinement

The structures of the Fab72000 and Fab72000/sEGFRd3 were solved by the method of MR using the program PHASER (CCP4, 1994). To solve the Fab structure, the coordinates for Fab2C4 (PDB ID 1L7I) (Vajdos et al., 2002) were selected as the initial search model based on the sequence identity between Fab2C4 and Fab72000. To solve the Fab72000/sEGFRd3 structure, one of the two Fab fragments in the asymmetric unit was first located using the refined Fab72000 coordinates as search model. With the position of this Fab fragment fixed, a second search using the coordinates of domain III of sEGFR (amino acids 310–500 from PDB ID 1YY9) located one of the sEGFRd3 molecules. Subsequently, the second Fab72000/sEGFRd3 complex in the asymmetric unit was found. Coordinates were manually rebuilt in COOT (Emsley and Cowtan, 2004) and refined using CNS (Brünger et al., 1998) and Refmac (CCP4, 1994). New maps were calculated following each iteration of refinement, including solvent flattened maps with minimized model bias calculated using the program DM (CCP4, 1994). Refinement statistics are summarized in Table 1.

SPR/Biacore-Binding Studies

Surface Plasmon Resonance (SPR)/Biacore studies were carried out using a Biacore 3000 instrument at 25°C in 10 mM Tris, 150 mM NaCl, 3 mM EDTA, and 0.005% Tween-20 (pH 8.0). Fab72000 was immobilized on a Biacore CM5 biosensor chip as follows: the CM-dextran matrix was activated with *N*-ethyl-*N'*-(dimethylaminopropyl)-carbodiimide hydrochloride (EDC) and *N*-hydroxysuccinimide (NHS). Fab72000 (500 ng) was flowed over this activated surface at a concentration of 5 μ g/ml in 10 mM sodium acetate (pH 5.0) at 5 μ l per minute for 20 min. The remaining reactive sites were blocked with 1 M ethanolamine-HCl (pH 8.5). Immobilized Fab fragment contributed a signal of 1436 response units (RU). The surface was regenerated between sEGFR injections with two 5 μ l injections of 10 mM glycine and 1 M NaCl (pH 2.5) to remove remaining bound sEGFR. EGF immobilization and sEGFR-binding analysis were performed exactly as described (Ferguson et al., 2000). Data were analyzed using Prism 4 (GraphPad Software, Inc.).

Cell-Based Binding Studies

¹²⁵I-labeled EGF, matuzumab, and cetuximab were generated with specific activities of 1750 Ci/mmol, 273 Ci/mmol, and 238 Ci/mmol, respectively. A431 epidermoid carcinoma cells were plated in 96-well dishes and grown to 75%–90% confluence. Cells were washed twice with ice-cold DMEM containing 1% BSA (incubation medium) and incubated in this medium containing 3 nM radio-labeled ligand plus the relevant cold competitor (200 μ l/well) for 6 hr at 4°C. Cells were washed three times with ice-cold incubation medium and were lysed with

1 M NaOH (200 μ l/well). The wells were washed with 200 μ l of water, and liquid scintillation counting was used to determine the counts of bound 125 I-labeled species. Data were analyzed using Prism 4 (GraphPad Software, Inc.).

Generation of sEGFR Epitope Mutations

Standard PCR-directed site-directed mutagenesis strategies were used to produce the appropriate DNA in the pFastBac vector. The following mutations were made: K454A, K463A, T459A/S460A, K454A/T459A/S460A, and T459A/S460A/K463A. The generation of recombinant baculovirus, overexpression in Sf9 cells, and protein purification were exactly as described before for wild-type sEGFR (Ferguson et al., 2000).

ACCESSION NUMBERS

Coordinates of the Fab72000 and Fab72000/sEGFRd3 structures have been deposited, with PDB ID codes 3C08 and 3C09, respectively.

SUPPLEMENTAL DATA

The Supplemental Data include one supplemental figure and can be found with this article online at <http://www.cancer-cell.org/cgi/content/full/13/4/365/DC1>.

ACKNOWLEDGMENTS

We thank Karl Schmitz, Steve Stayrook, Per Hillertz, and Djordje Musil for assistance with data collection; Jens Oliver Funk for support of this collaboration; Volker Doetsch (Johann Wolfgang Goethe Universität, Frankfurt, Germany) for assuming the role of dissertation supervisor to J.S.; Christof Reusch and Jürgen Schmidt for performing the radiolabeled binding experiments; and Mark Lemmon and members of the Ferguson and Lemmon laboratories at the University of Pennsylvania for valuable discussions and critical comments on the manuscript. J.S. conducted all other experiments in the laboratory of K.M.F., under direct daily detailed guidance from K.M.F. and valuable periodic supervision of T.K. J.S. solved the structures described in this manuscript at the University of Pennsylvania, with assistance from S.L., Karl Schmitz, and K.M.F. T.K. established the University of Pennsylvania /Merck KGaA collaboration and provided scientific advice to J.S. The research of K.M.F. is supported by a Career Award in the Biomedical Sciences from the Burroughs Wellcome Fund, and by NIH grant R01-CA112552. K.M.F. is also the Dennis and Marsha Dammerman Scholar supported by the Damon Runyon Cancer Research Foundation (DRS-52-06). This work is based upon research conducted at (1) the Cornell High Energy Synchrotron Source (CHESS), which is supported by the National Science Foundation under award DMR 97-13424, using the Macromolecular Diffraction at CHESS (MacCHESS) facility, which is supported by award RR-01646 from the National Institutes of Health, through its National Center for Research Resources, and (2) the Swiss Light Source (SLS), Villigen. The Biacore instrument utilized in this study was funded by grants from the NIH and the University of Pennsylvania to the Ferguson and Lemmon laboratories. T.K. and A.B. are employees of Merck KGaA, the manufacturer of the drug matuzumab. J.S. is a Ph.D. student at Merck KGaA under supervision of T.K. J.S. conducted this work as a Visiting Research Scholar in the laboratory of K.M.F. at the University of Pennsylvania. This collaboration is governed by a Supported Research Agreement between Merck KGaA and the Trustees of the University of Pennsylvania and is financially supported in part by Merck KGaA.

Received: November 19, 2007

Revised: January 21, 2008

Accepted: February 27, 2008

Published: April 7, 2008

REFERENCES

Bier, H., Hoffmann, T., Hauser, U., Wink, M., Ochler, M., Kovar, A., Müser, M., and Knecht, R. (2001). Clinical trial with escalating doses of the antiepidermal growth factor receptor humanized monoclonal antibody EMD 72 000 in patients with advanced squamous cell carcinoma of the larynx and hypopharynx. *Cancer Chemother. Pharmacol.* 47, 519–524.

Bouyain, S., Longo, P.A., Li, S., Ferguson, K.M., and Leahy, D.J. (2005). The extracellular region of ErbB4 adopts a tethered conformation in the absence of ligand. *Proc. Natl. Acad. Sci. USA* 102, 15024–15029.

Brünger, A.T., Adams, P.D., Clore, G.M., DeLano, W.L., Gros, P., Grosse-Kunstleve, R.W., Jiang, J.S., Kuszewski, J., Nilges, M., Pannu, N.S., et al. (1998). Crystallography & NMR system: A new software suite for macromolecular structure determination. *Acta Crystallogr. D* 54, 905–921.

Burgess, A.W., Cho, H.S., Eigenbrot, C., Ferguson, K.M., Garrett, T.P.J., Leahy, D.J., Lemmon, M.A., Sliwkowski, M.X., Ward, C.W., and Yokoyama, S. (2003). An open-and-shut case? Recent insights into the activation of EGF/ErbB receptors. *Mol. Cell* 12, 541–552.

CCP4 (Collaborative Computational Project, Number 4). (1994). The CCP4 suite: Programs for protein crystallography. *Acta Crystallogr. D Biol. Crystallogr.* 50, 760–763.

Cho, H.S., and Leahy, D.J. (2002). Structure of the extracellular region of HER3 reveals an interdomain tether. *Science* 297, 1330–1333.

Cho, H.S., Mason, K., Ramyar, K.X., Stanley, A.M., Gabelli, S.B., Denney, D.W., and Leahy, D.J. (2003). Structure of the extracellular region of HER2 alone and in complex with the Herceptin Fab. *Nature* 421, 756–760.

Dawson, J.P., Berger, M.B., Lin, C.C., Schlessinger, J., Lemmon, M.A., and Ferguson, K.M. (2005). Epidermal growth factor receptor dimerization and activation require ligand-induced conformational changes in the dimer interface. *Mol. Cell Biol.* 25, 7734–7742.

Dawson, J.P., Bu, Z., and Lemmon, M.A. (2007). Ligand-induced structural transitions in ErbB receptor extracellular domains. *Structure* 15, 942–954.

Emsley, P., and Cowtan, K. (2004). Coot: Model-building tools for molecular graphics. *Acta Crystallogr. D* 60, 2126–2132.

Ferguson, K.M. (2004). Active and inactive conformations of the epidermal growth factor receptor. *Biochem. Soc. Trans.* 32, 742–745.

Ferguson, K.M., Darling, P.J., Mohan, M.J., Macatee, T.L., and Lemmon, M.A. (2000). Extracellular domains drive homo- but not hetero-dimerization of ErbB receptors. *EMBO J.* 19, 4632–4643.

Ferguson, K.M., Berger, M.B., Mendrola, J.M., Cho, H.S., Leahy, D.J., and Lemmon, M.A. (2003). EGF activates its receptor by removing interactions that autoinhibit ectodomain dimerization. *Mol. Cell* 11, 507–517.

Franklin, M.C., Carey, K.D., Vajdos, F.F., Leahy, D.J., de Vos, A.M., and Sliwkowski, M.X. (2004). Insights into ErbB signaling from the structure of the ErbB2-pertuzumab complex. *Cancer Cell* 5, 317–328.

Friedman, L.M., Rinon, A., Schechter, B., Lyass, L., Lavi, S., Bacus, S.S., Sela, M., and Yarden, Y. (2005). Synergistic down-regulation of receptor tyrosine kinases by combinations of mAbs: Implications for cancer immunotherapy. *Proc. Natl. Acad. Sci. USA* 102, 1915–1920.

Garrett, T.P.J., McKern, N.M., Lou, M., Elleman, T.C., Adams, T.E., Lovrecz, G.O., Zhu, H.J., Walker, F., Frenkel, M.J., Hoyne, P.A., et al. (2002). Crystal structure of a truncated epidermal growth factor receptor extracellular domain bound to transforming growth factor alpha. *Cell* 110, 763–773.

Graeven, U., Kremer, B., Südhoff, T., Killing, B., Rojo, F., Weber, D., Tillner, J., Unal, C., and Schmiegel, W. (2006). Phase I study of the humanised anti-EGFR monoclonal antibody matuzumab (EMD 72000) combined with gemcitabine in advanced pancreatic cancer. *Br. J. Cancer* 94, 1293–1299.

Hubbard, S.R., and Miller, W.T. (2007). Receptor tyrosine kinases: Mechanisms of activation and signaling. *Curr. Opin. Cell Biol.* 19, 117–123.

Johns, T.G., Adams, T.E., Cochran, J.R., Hall, N.E., Hoyne, P.A., Olsen, M.J., Kim, Y.S., Rothacker, J., Nice, E.C., Walker, F., et al. (2004). Identification of the epitope for the epidermal growth factor receptor-specific monoclonal antibody 806 reveals that it preferentially recognizes an untethered form of the receptor. *J. Biol. Chem.* 279, 30375–30384.

Kettleborough, C.A., Saldanha, J., Heath, V.J., Morrison, C.J., and Bendig, M.M. (1991). Humanization of a mouse monoclonal antibody by CDR-grafting: The importance of framework residues on loop conformation. *Protein Eng.* 4, 773–783.

Kohda, D., Odaka, M., Lax, I., Kawasaki, H., Suzuki, K., Ullrich, A., Schlessinger, J., and Inagaki, F. (1993). A 40-kDa epidermal growth factor/transforming growth factor alpha-binding domain produced by limited proteolysis of the

- extracellular domain of the epidermal growth factor receptor. *J. Biol. Chem.* 268, 1976–1981.
- Kreysch, H.G., and Schmidt, J. (2004). Pharmaceutical compositions directed to Erb-B1 receptors. Merck Patent GMBH (DE), EP1549344. April 2004. WO 2004/032960 A1.
- Kollmannsberger, C., Schittenhelm, M., Honecker, F., Tillner, J., Weber, D., Oechsle, K., Kanz, L., and Bokemeyer, C. (2006). A phase I study of the humanized monoclonal anti-epidermal growth factor receptor (EGFR) antibody EMD 72000 (matuzumab) in combination with paclitaxel in patients with EGFR-positive advanced non-small-cell lung cancer (NSCLC). *Ann. Oncol.* 17, 1007–1013.
- Lawrence, M.C., and Colman, P.M. (1993). Shape complementarity at protein/protein interfaces. *J. Mol. Biol.* 234, 946–950.
- Lemmon, M.A., Bu, Z., Ladbury, J.E., Zhou, M., Pinchasi, D., Lax, I., Engelman, D.M., and Schlessinger, J. (1997). Two EGF molecules contribute additively to stabilization of the EGFR dimer. *EMBO J.* 16, 281–294.
- Li, S., Schmitz, K.R., Jeffrey, P.D., Wiltzius, J.J.W., Kussie, P., and Ferguson, K.M. (2005). Structural basis for inhibition of the epidermal growth factor receptor by cetuximab. *Cancer Cell* 7, 301–311.
- Mendelsohn, J., and Baselga, J. (2006). Epidermal growth factor receptor targeting in cancer. *Semin. Oncol.* 33, 369–385.
- Molina, M.A., Codony-Servat, J., Albanell, J., Rojo, F., Arribas, J., and Baselga, J. (2001). Trastuzumab (herceptin), a humanized anti-Her2 receptor monoclonal antibody, inhibits basal and activated Her2 ectodomain cleavage in breast cancer cells. *Cancer Res.* 61, 4744–4749.
- Murthy, U., Basu, A., Rodeck, U., Herlyn, M., Ross, A.H., and Das, M. (1987). Binding of an antagonistic monoclonal antibody to an intact and fragmented EGF-receptor polypeptide. *Arch. Biochem. Biophys.* 252, 549–560.
- Ogiso, H., Ishitani, R., Nureki, O., Fukai, S., Yamanaka, M., Kim, J.H., Saito, K., Sakamoto, A., Inoue, M., Shirouzu, M., et al. (2002). Crystal structure of the complex of human epidermal growth factor and receptor extracellular domains. *Cell* 110, 775–787.
- Otwinowski, Z., and Minor, W. (1997). Processing of X-ray diffraction data collected in oscillation mode. In *Macromolecular Crystallography, Volume 276*, C.W. Carter and R.M. Sweet, eds. (New York: Academic Press), pp. 307–326.
- Rodeck, U., Herlyn, M., Herlyn, D., Molthoff, C., Atkinson, B., Varello, M., Stepkowski, Z., and Koprowski, H. (1987). Tumor growth modulation by a monoclonal antibody to the epidermal growth factor receptor: Immunologically mediated and effector cell-independent effects. *Cancer Res.* 47, 3692–3696.
- Rodeck, U., Williams, N., Murthy, U., and Herlyn, M. (1990). Monoclonal antibody 425 inhibits growth stimulation of carcinoma cells by exogenous EGF and tumor-derived EGF/TGF- α . *J. Cell Biol.* 44, 69–79.
- Schlessinger, J. (2000). Cell signaling by receptor tyrosine kinases. *Cell* 103, 211–225.
- Seiden, M.V., Burris, H.A., Matulonis, U., Hall, J.B., Armstrong, D.K., Speyer, J., Weber, J.D.A., and Muggia, F. (2007). A phase II trial of EMD72000 (matuzumab), a humanized anti-EGFR monoclonal antibody, in patients with platinum-resistant ovarian and primary peritoneal malignancies. *Gynecol. Oncol.* 104, 727–731.
- Socinski, M.A. (2007). Antibodies to the epidermal growth factor receptor in non small cell lung cancer: Current status of matuzumab and panitumumab. *Clin. Cancer Res.* 13, 4597–4601.
- Stanfield, R.L., Zemla, A., Wilson, I.A., and Rupp, B. (2006). Antibody elbow angles are influenced by their light chain class. *J. Mol. Biol.* 31, 1566–1574.
- Sundberg, E.J., and Mariuzza, R.A. (2002). Molecular recognition in antibody-antigen complexes. *Adv. Protein Chem.* 61, 119–160.
- Vajdos, F.F., Adams, C.W., Breece, T.N., Presta, L.G., de Vos, A.M., and Sidhu, S.S. (2002). Comprehensive functional maps of the antigen-binding site of an anti-ErbB2 antibody obtained with shotgun scanning mutagenesis. *J. Mol. Biol.* 320, 415–428.
- Vanhoefer, U., Tewes, M., Rojo, F., Dirsch, O., Schleucher, N., Rosen, O., Tillner, J., Kovar, A., Braun, A.H., Trarbach, T., et al. (2004). Phase I study of the humanized antiepidermal growth factor receptor monoclonal antibody EMD72000 in patients with advanced solid tumors that express the epidermal growth factor receptor. *J. Clin. Oncol.* 22, 175–184.
- Zhang, X., Gureasko, J., Shen, K., Cole, P.A., and Kuriyan, J. (2006). An allosteric mechanism for activation of the kinase domain of epidermal growth factor receptor. *Cell* 125, 1137–1149.

Supplemental Data

Matuzumab Binding to EGFR Prevents the Conformational Rearrangement

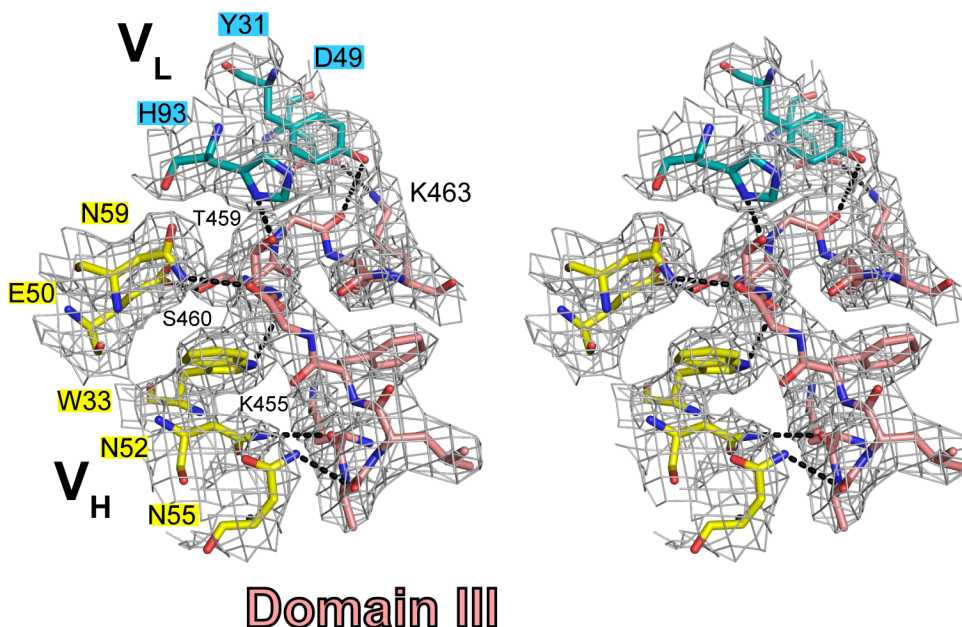
Required for Dimerization

Judith Schmiedel, Andree Blaukat, Shiqing Li, Thorsten Knöchel, and Kathryn M. Ferguson

Figure S1. Electron Density at the sEGFRd3/Fab72000 Interface

Stereo view of select interactions between domain III of sEGFR and Fab72000. Amino acids are shown in stick representation and are colored in pink for domain III, and in yellow or cyan for the Fab72000 V_H and V_L domains, respectively. Side chain labels for the Fab are on yellow or cyan background (V_H and V_L, respectively). The gray mesh represents the final 2F_o-F_c electron density map contoured at 1.0 σ . Distances consistent with hydrogen bond formation are indicated with dashed black lines.

Fab72000



REFERENCES

- Cozzio, A., Passegue, E., Ayton, P.M., Karsunky, H., Cleary, M.L., and Weissman, I.L. (2003). *Genes Dev.* **17**, 3029–3035.
- Heath, V., Suh, H.C., Holman, M., Renn, K., Gooya, J.M., Parkin, S., Klarmann, K.D., Ortiz, M., Johnson, P., and Keller, J. (2004). *Blood* **104**, 1639–1647.
- Huntly, B.J., Shigematsu, H., Deguchi, K., Lee, B.H., Mizuno, S., Duclos, N., Rowan, R., Amaral, S., Curley, D., Williams, I.R., et al. (2004). *Cancer Cell* **6**, 587–596.
- Kirstetter, P., Schuster, M.B., Bereshchenko, O., Moore, S., Dvinge, H., Kurz, E., Theilgaard-Monch, K., Mansson, R., Pedersen, T.A., Pabst, T., et al. (2008). *Cancer Cell*, this issue.
- Krivtsov, A.V., Twomey, D., Feng, Z., Stubbs, M.C., Wang, Y., Faber, J., Levine, J.E., Wang, J., Hahn, W.C., Gilliland, D.G., et al. (2006). *Nature* **442**, 818–822.
- Nerlov, C. (2004). *Nat. Rev. Cancer* **4**, 394–400.
- Passegue, E., Jamieson, C.H., Ailles, L.E., and Weissman, I.L. (2003). *Proc. Natl. Acad. Sci. USA* **100** (Suppl 1), 11842–11849.
- Porse, B.T., Bryder, D., Theilgaard-Monch, K., Hasemann, M.S., Anderson, K., Damgaard, I., Jacobsen, S.E., and Nerlov, C. (2005). *J. Exp. Med.* **202**, 85–96.
- Wagner, K., Zhang, P., Rosenbauer, F., Drescher, B., Kobayashi, S., Radomska, H.S., Kutok, J.L., Gilliland, D.G., Krauter, J., and Tenen, D.G. (2006). *Proc. Natl. Acad. Sci. USA* **103**, 6338–6343.
- Wechsler, J., Greene, M., McDevitt, M.A., Anastasi, J., Karp, J.E., Le Beau, M.M., and Crispino, J.D. (2002). *Nat. Genet.* **32**, 148–152.
- Zhang, P., Iwasaki-Arai, J., Iwasaki, H., Fenyus, M.L., Dayaram, T., Owens, B.M., Shigematsu, H., Levantini, E., Huettner, C.S., Lekstrom-Himes, J.A., et al. (2004). *Immunity* **21**, 853–863.

A Molecular View of Anti-ErbB Monoclonal Antibody Therapy

Daniel J. Leahy^{1,*}

¹Department of Biophysics and Biophysical Chemistry, Johns Hopkins University School of Medicine, Baltimore, MD 21205, USA

*Correspondence: dleahy@jhmi.edu

DOI 10.1016/j.ccr.2008.03.010

Abnormal activation of the epidermal growth factor receptor (EGFR) and its homolog HER2 (Neu/ErbB2) has been associated with many human cancers, and monoclonal antibodies targeting EGFR and HER2 are effective anticancer therapies. Structural studies of these receptors and antibodies have revealed much about how they function. In this issue of *Cancer Cell*, Schmiedel et al. report structural and functional studies of the anti-EGFR monoclonal antibody Matuzumab. They show that Matuzumab binds and inhibits EGFR in a manner distinctive from that of other therapeutic anti-EGFR antibodies and suggest that combination therapies with Matuzumab and other antibodies may prove beneficial.

The epidermal growth factor receptor (EGFR/ErbB1/HER1) consists of an extracellular ligand binding region followed by a single membrane-spanning helix, a cytoplasmic tyrosine kinase domain, and a C-terminal tail of ~230 amino acids (Burgess et al., 2003). Ligand binding to the extracellular region promotes receptor dimerization, which in turn leads to activation of the cytoplasmic tyrosine kinase (Holbro and Hynes, 2004). When activated, the EGFR kinase phosphorylates several tyrosines in the EGFR C-terminal tail that then serve as docking sites for downstream signaling effectors that initiate signaling cascades and stimulate cell growth and differentiation (Holbro and Hynes, 2004). Three EGFR homologs, HER2 (Neu/ErbB2), HER3 (ErbB3), and HER4 (ErbB4) are found in humans and,

together with EGFR, make up the EGFR/ErbB family of receptors. HER2 is an atypical member of this family in that it is not directly activated by ligand but rather serves as a universal heterodimeric partner for each of the other ErbB family members (Holbro and Hynes, 2004).

EGFR was the first cell-surface receptor to be associated with cancer, and abnormal EGFR or HER2 function has subsequently been found to contribute to the severity of many human tumors (Hynes and Lane, 2005). For this reason, agents targeting EGFR or HER2 have been actively pursued as cancer therapies. These agents fall into two general classes: monoclonal antibodies, which bind to receptor extracellular regions and will be discussed here, and small-molecule kinase inhibitors that target the

cytoplasmic kinase activity. To date, two monoclonal antibodies against EGFR, Cetuximab (Erbix) and Panitumumab (Vectibix), have been approved by the FDA for treatment of colorectal and/or head-and-neck cancer, and two EGFR kinase inhibitors, erlotinib (Tarceva) and gefitinib (Iressa), have been approved for the treatment of lung cancer. A monoclonal antibody targeting HER2, Trastuzumab (Herceptin), and a pan-ErbB kinase inhibitor, lapatinib (Tykerb), have also been approved for treatment of HER2-overexpressing breast cancers. Many other ErbB-targeted therapies are under development.

Beginning ~5 years ago, X-ray crystallographic studies of the extracellular regions of ErbB family members uncovered the basic mechanism by which ligand binding

regulates receptor dimerization and activity (Burgess et al., 2003) (Figure 1A). The extracellular regions of ErbB family members are composed of four subdomains. Domains I and III are homologous, and both contribute to ligand binding. Domains II and IV are homologous and form extended, cysteine-rich structures (Burgess et al., 2003). In the absence of ligand, an extended loop from domain II contacts a pocket at the C terminus of domain IV and constrains the extracellular region to a compact, “tethered” conformation in which domains I and III are held far apart (Figure 1A, left panel). To bind ligand with high affinity, a domain rearrangement occurs in which the domain II/IV contact is broken and domains I and II rotate as a pair and domains I and III rotate as a pair to bring domains I and III into proximity and allow them to bind ligand simultaneously in a clamp-like interaction (Figure 1A, middle panel). In this ligand-bound, extended structure, the domain II loop that contacted domain IV in the absence of ligand becomes exposed and mediates receptor dimerization (Figure 1A, middle and right panels). This loop is, thus, frequently referred to as the “dimerization arm.”

It came as a pleasing surprise when crystal structures of the HER2 extracellular region showed that it does not adopt the tethered conformation. Instead, HER2 is fixed in an active-like conformation characterized by an interaction between domains I and III and a constitutively exposed dimerization arm (Cho et al., 2003; Garrett et al., 2003) (Figure 1B). This domain I/III interaction occludes the canonical ErbB ligand-binding surface and appears to mimic the effects of ligand binding, which rationalizes the absence of a HER2 ligand and the role of HER2 as a universal partner for other ErbB family members.

Given the long time scale of clinical trials, many ErbB-targeted therapies entered development long before the molecular

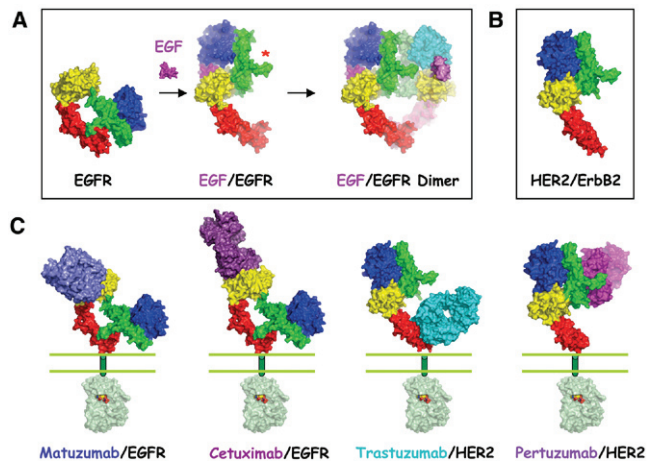


Figure 1. Surface Representations of EGFR and HER2 in Active, Inactive, and Antibody-Bound Conformations

(A) A surface representation of the extracellular region of EGFR in the absence of ligand is shown with domains I (blue), II (green), III (yellow), and IV (red) colored as indicated (left panel). Ligand (EGF, purple) binding stabilizes a domain rearrangement in which domains I and II rotate as a pair and break the domain II/IV contact, bringing domain I (blue) and III (yellow) into proximity to bind ligand. This rearrangement exposes the previously buried domain II dimerization arm, which is marked with a red asterisk (middle panel). The exposed dimerization arm then mediates receptor dimerization and activation (right panel).

(B) The HER2/ErbB2 extracellular region adopts a constitutively “active-like” structure in which domains I and III contact each other directly and the domain II dimerization arm is exposed.

(C) The Fab fragments of Matuzumab (slate blue) bound to EGFR (far left), Cetuximab (purple) bound to EGFR (second from left), Trastuzumab (cyan) bound to HER2 (second from right), and Pertuzumab (magenta) bound to HER2 (far right) are shown. The plasma membrane is indicated with two green lines, and a membrane-spanning region is represented with a green cylinder. A surface representation of the EGFR kinase is shown in light green with a space-filling representation of a bound nucleotide.

underpinnings of ErbB activation and HER2 behavior became apparent. It has, thus, been particularly satisfying that as structural and biochemical studies of therapeutic anti-ErbB antibodies progress, a consistent picture of ErbB function is emerging. For example, Trastuzumab (Herceptin) binds to the juxtamembrane region of HER2 (Figure 1C) at a site that would not obviously interfere with HER2 dimerization or activation (Cho et al., 2003). Indeed, biochemical studies show that Trastuzumab does not block either dimerization or activation of HER2 (Agus et al., 2002). Trastuzumab does block proteolytic cleavage of the HER2 ectodomain, however, which occurs adjacent to the cell membrane and leaves behind an active kinase, and this effect may contribute to its antiproliferative activity (Baselga et al., 2001). Antibody-dependent cellular cytotoxicity also appears to contribute significantly to Trastuzumab activity (Clynes et al., 2000). In contrast,

the anti-HER2 antibody Pertuzumab, currently in phase III clinical trials for ovarian cancer, binds directly to the HER2 dimerization arm and blocks both dimerization and activation in response to stimulation of a HER2 partner (Agus et al., 2002) (Figure 1C). This difference appears to explain why Pertuzumab is more effective than Trastuzumab in cancers where HER2 is activated, but not overexpressed.

Unlike HER2, targeting the dimerization arm of EGFR does not appear to be an effective strategy as it is generally buried at either an intra- or intermolecular interface. Indeed, the first anti-EGFR antibody to be approved by the FDA for cancer therapy, Cetuximab (Erbix), competes with ligand for binding to EGFR and was shown by Ferguson and colleagues to bind and block the ligand binding site on EGFR domain III (Li et al., 2005) (Figure 1C). These authors also noted that Cetuximab binding to EGFR would sterically prohibit EGFR

adopting the extended, active-like conformation (Figure 1), providing a dual mechanism of EGFR inhibition. The humanized anti-EGFR antibody IMC-11F8 binds at this same site and also works by this dual mechanism (Li et al., 2008).

In this issue of *Cancer Cell*, Schmiedel et al. now show that a third anti-EGFR mAb, Matuzumab, binds at a nearby but distinct site on EGFR and displays a different constellation of biochemical and inhibitory properties (Schmiedel et al., 2008). Matuzumab, which is currently in phase II trials for treatment of lung and stomach cancer, is like Cetuximab in that it binds to domain III of EGFR (Figure 1C). Unlike Cetuximab, however, the Matuzumab binding site does not overlap with the EGF binding site, and Matuzumab does not completely compete with EGF for binding to EGFR. Matuzumab does reduce the apparent affinity of EGF for EGFR. How to explain this behavior? Schmiedel et al. point out that although Matuzumab and EGF could simultane-

ously bind to EGFR domain III, the binding of Matuzumab would interfere with formation of the active-like EGFR conformation (Figure 1A, middle panel). Thus, in the presence of Matuzumab, EGF could only contact domain III (or domain I), and its affinity for EGFR would be reduced—exactly what is observed. Schmiedel et al. also show that Cetuximab and Matuzumab do not compete for binding to EGFR, as predicted from comparison of crystal structures of their complexes with EGFR, and suggest that combination therapy with Cetuximab (or IMC-11F8) and Matuzumab may result in added clinical benefit.

It is clear that basic and clinical studies of the ErbB family of receptors have come a long way in the last few years. The results

from each type of inquiry has informed the other, and together, they are leading to a deeper understanding of ErbB function and how to treat ErbB-involved diseases. It is also clear that much remains to be learned, and exciting times are ahead.

REFERENCES

Agus, D.B., Akita, R.W., Fox, W.D., Lewis, G.D., Higgins, B., Pisacane, P.I., Lofgren, J.A., Tindell, C., Evans, D.P., Maiese, K., et al. (2002). *Cancer Cell* 2, 127–137.

Baselga, J., Albanell, J., Molina, M.A., and Arribas, J. (2001). *Semin. Oncol.* 28, 4–11.

Burgess, A.W., Cho, H.S., Eigenbrot, C., Ferguson, K.M., Garrett, T.P., Leahy, D.J., Lemmon, M.A., Sliwkowski, M.X., Ward, C.W., and Yokoyama, S. (2003). *Mol. Cell* 12, 541–552.

Cho, H.S., Mason, K., Ramyar, K.X., Stanley, A.M.,

Gabelli, S.B., Denney, D.W., Jr., and Leahy, D.J. (2003). *Nature* 421, 756–760.

Clynes, R.A., Towers, T.L., Presta, L.G., and Ravetch, J.V. (2000). *Nat. Med.* 6, 443–446.

Garrett, T.P., McKern, N.M., Lou, M., Elleman, T.C., Adams, T.E., Lovrecz, G.O., Kofler, M., Jorissen, R.N., Nice, E.C., Burgess, A.W., and Ward, C.W. (2003). *Mol. Cell* 11, 495–505.

Holbro, T., and Hynes, N.E. (2004). *Annu. Rev. Pharmacol. Toxicol.* 44, 195–217.

Hynes, N.E., and Lane, H.A. (2005). *Nat. Rev. Cancer* 5, 341–354.

Li, S., Kussie, P., and Ferguson, K.M. (2008). *Structure* 16, 216–227.

Li, S., Schmitz, K.R., Jeffrey, P.D., Wiltzius, J.J., Kussie, P., and Ferguson, K.M. (2005). *Cancer Cell* 7, 301–311.

Schmiedel, J., Blaukat, A., Li, S., Knoechel, T., and Ferguson, K.M. (2008). *Cancer Cell*, this issue.

RanBP2: A Tumor Suppressor with a New Twist on Topoll, SUMO, and Centromeres

Michelle S. Navarro¹ and Jeff Bachant^{1,*}

¹Department of Cell Biology and Neuroscience, University of California, Riverside, Riverside, CA 92521, USA

*Correspondence: jeffbach@citrus.ucr.edu

DOI 10.1016/j.ccr.2008.03.011

In vertebrate cells, the small ubiquitin-like modifier SUMO plays a poorly defined role in targeting DNA topoisomerase II (Topoll) to centromeres (CENs) during mitosis, presumably to facilitate the untangling of sister chromatids as cells transition into anaphase. A new study by Dawlaty in the April 4 issue of *Cell* identifies the nucleoporin RanBP2 as a novel tumor suppressor that acts as a SUMO ligase for Topoll. Analysis of this interaction reveals Topoll recruitment to CENs is likely to play an important role in preventing chromosome segregation errors that lead to cancer.

RanBP2 is a remarkably large (350 kD!) protein that contains, as its only enzymatic function, an unusual SUMO E3 ligase domain (Pichler et al., 2002). In the final step of SUMO modification, the E2 conjugating enzyme Ubc9 transfers activated SUMO moieties to lysines on substrate proteins. This reaction typically requires, or is greatly stimulated by, SUMO E3 ligases. The best understood SUMO E3s are the PIAS family of proteins, which contain a RING finger motif and promote sumoylation by recruiting

substrates to the E2 enzyme (Jackson, 2001). The RanBP2 E3 domain, in contrast, fits tidily within a ~300 amino acid segment that is structurally unrelated to PIAS proteins. Rather than binding substrates, this E3 acts more like a cofactor for Ubc9, possibly serving to directly stimulate E2 catalysis (Reverter and Lima, 2005).

The cell biology of RanBP2 has also provided surprises. In addition to binding Ubc9, the RanBP2 E3 domain interacts specifically with SUMO-modified

forms of RanGAP1. During interphase, this complex localizes to the cytoplasmic face of the nuclear pore. But once mitosis is underway, the entire RanBP2-SUMO-RanGAP1-Ubc9 complex partners with the nuclear export receptor Crm1 and moonlights as a component of the kinetochore (K; Arnaoutov et al., 2005). This is arguably even more important than RanBP2's day job, as RanBP2 depletion produces severe mitotic defects, including perturbations to K-microtubule (MT) attachment, mis-

ACKNOWLEDGEMENT

Special thanks go to my supervisors Thorsten Knöchel and Andree Blaukat at Merck Serono for giving me the opportunity to work as PhD student in industry and for their support during the last three years. Thank you very much for the helpful discussions in spite of very busy times.

Also a lot of thanks go to Volker Dötsch to support me at the University of Frankfurt Main. It was great to join your lab meetings and to try to follow the NMR experiment descriptions.

Sincere thanks go to Kathryn Ferguson and her lab at the University of Pennsylvania for a very exciting year in Philadelphia. I think I never learned so much before in such a short time and I enjoyed it enormously. Thank you very much for the great time together with you, Shawn Li and Karl Schmitz!

Great thanks to Matthias Frech and the MIB-groups at Merck Serono for the very friendly working atmosphere and the support from everyone. Many thanks to Djordje Musil and the x-ray team Verena Dresing, Martin Lehmann, Ulrich Grädler and Per Hillertz; I really appreciated the open discussions, the humorous spirit and Djordje's great ability during times of stress to always keep his warm attitude towards us. A lot of thanks also to Ansgar Wegener and the ITC group for letting me use the ITC and for the great interest in my experiments. Your comments helped a lot. Also many thanks to Jörg Bomke and the Biacore group for letting me use the A3000 so many times. Thank you for teaching me to be more patient with control samples!

Also a lot of thanks to Detlef Güssow and the molecular biology group for their support with the cloning and mutational work and to Björn Hock and the Baculo expression group for letting me do my expression trials in the middle of their own busy schedules.

Special thanks to Thomas Rysiok and the protein fermentation group for their help with the Baculo and mammalian expression! You really helped a lot and I especially appreciated to touch some philosophical questions about science in between the tubes and valves.

Sincere thanks to Dirk Müller-Pompalla, Jens Hannewald and the protein purification group. I don't know what I would have done without you. Thank you very much for very patiently letting me use the Äkta systems and always to be there in case of trouble or questions!

Huge thanks to the other PhD students at Merck Serono in the x-ray, pharma department, oncology and the aptamer group, especially to Per Hillertz and Maria Leonor Alvarenga! Thank you very much for the great time together (midsummer in Sweden!) and the discussions about work in detail and life in general.

LEBENS LAUF

Name: Schmiedel
Vorname: Judith
Adresse: Gabelweihstr. 6a, 13505 Berlin, Deutschland
Email: Judith.Schmiedel@googlemail.com
Geburtstag: 27.12.1980
Geburtsort: Berlin

AUSBILDUNG

1993 – 2000 Humboldt-Gymnasium, Berlin
2000 – 2001 Freiwilliges Ökologisches Jahr, Fachamt für Umweltuntersuchungen,
Hamburg
2001 – 2003 Universität Hamburg, Deutschland
2003 – 2006 Rheinisch-Westfälische Technische Hochschule Aachen, Deutschland
Diplomarbeit bei Prof. Lothar Elling, Insitut für Biomaterialien, Helmholtz-
Institut für Biomedizinische Technik
2006 Abschluss: Diplom-Biologin (Note: sehr gut)
2006 – 2008 Promotion „Struktur und molekulare Interaktionsanalyse von monoklonalen
Antikörpern in Komplex mit Rezeptor-Tyrosinkinasen“ bei Prof. Kathryn
Ferguson, School of Medicine, University of Pennsylvania, USA und
2008 – 2009 bei Dr. Thorsten Knöchel, Merck KGaA, Darmstadt, Deutschland/ Prof.
Volker Dötsch, Insitut für Biophysikalische Chemie, Johann-Wolfgang Goethe
Universität, Frankfurt/Main, Deutschland

PUBLIKATIONEN & PATENTE

J. Schmiedel, A. Blaukat, S. Li, T. Knöchel, K.M. Ferguson (2008) Matuzumab binding to EGFR prevents the conformational rearrangement required for dimerization. *Cancer Cell*, 13(4), 365-373.

Patent I 07/137 Crystalline EGFR-matuzumab complex and matuzumab mimetics obtained thereof.

B. Sauerzapfe, K. Křenek, J. Schmiedel, W. Wakarchuk, H. Pelantová, V. Křen, L. Elling (2008) Chemo-enzymatic synthesis of poly-N-acetyllactosamine (poly-LacNAc) structures and their characterization for CGL2-galectin-mediated binding of ECM glycoproteins to biomaterial surfaces. *Glycoconj J.*, 26(2), 141-159.

D.-J. Namdjou, B. Sauerzapfe, J. Schmiedel, G. Dräger, S. Bernatchez, W. Wakarchuk, L. Elling (2007) Combination of UDP-Glc(NAc) 4'-Epimerase and Galactose Oxidase in a One-Pot Synthesis of Biotinylated Nucleotide Sugars. *Adv. Synth. Catal.*, 349, 314-318.

PRÄSENTATIONEN & KURSE

- 2007 American Crystallographic Association ACA annual meeting 2007, Salt Lake City, Utah, USA
SHELX workshop, George Sheldrick
- 2007 Anti-Cancer Drug Discovery & Development Retreat, University of Pennsylvania, School of Medicine, USA
- 2008 Biophysical Society Annual Meeting & IUPAB International Biophysics Congress, Long Beach, California, USA
Poster "Structural insight into mechanisms of antibody mediated inhibition of EGFR" J. Schmiedel, A. Blaukat, S. Li, T. Knoechel, K.M. Ferguson
- 2008 EMBO Practical Course on Solution Scattering from Biological Macromolecules, EMBL Hamburg, Deutschland
- 2008 Wyatt Static Light Scattering University, Dernbach, Deutschland

BETEILIGUNG AN DER LEHRE

- 2002 - 2003 Praktikum „Grundlagen der Zoologie“, Prof. Bernhard Hausdorf, Institut für Zoologie, Universität Hamburg, Deutschland
- 2004 - 2006 Vorlesung „Zellbiologie“, Prof. Margrit Frentzen, Institut für Zellbiologie, Rheinisch-Westfälische Technische Hochschule Aachen, Deutschland

AKADEMISCHE LEHRER

- Prof. Dr. Ferguson (Rezeptor-Tyrosinkinasen)
Prof. Dr. Elling (Glykobiotechnologie und Biomaterialien)
Prof. Dr. Hartmeier (Biotechnologie)
Prof. Dr. Frentzen (Zellbiologie)
Prof. Dr. Kreuzaler (Zellbiologie, Molekulargenetik)
Prof. Dr. Möller (Makromolekulare Chemie)
Prof. Dr. Slusarenko (Pflanzenphysiologie)
Prof. Dr. Schuphan (Ökotoxikologie)
PD Dr. Tiemann (Zoologie)
Prof. Dr. Mühlbach (Botanik)
PD Dr. Fretwurst (Physik)
Prof. Dr. Meyer (Chemie)
-

